ANALYSIS OF REINFORCED CONCRETE BRIDGE WITH CIRCULAR PIER SUBJECTED TO EARTHQUAKE

By

Mohd Ritzman Bin Abdul Karim

A Thesis Submitted in Partial Fulfilment of the Requirements for the Degree of Doctor of Philosophy

Department of Civil and Environmental Engineering

College of Engineering, Design and Physical Sciences

Brunel University London

DECEMBER 2019

Abstract

Structural engineers and designers have a great responsibility for incorporating seismic design into reinforced concrete (RC) structures, particular RC bridges, in order to minimise damages and loss of life during an earthquake event. Extensive research has been conducted to develop robust seismic design procedures for RC bridges. Recent research has indicated that among several displacement-based design methods developed, the direct displacement-based design (DDBD) method has become one of the most reliable methods for designing the RC bridge under earthquake conditions. Due to the uncertainty in the estimation of the yield displacement and target displacement, further developments are needed to fill those gaps in the development of the robust DDBD method. Therefore, those research gaps are addressed in this PhD research.

In this PhD research, a comprehensive 3D FEM for analysis of RC bridge with circular pier subjected to the earthquake has been developed. The FEM can be used for the full-scale modelling of RC bridge and assess the earthquake resistance of RC bridge with a circular pier. The 3D FEM considers the full interaction between circular RC bridge pier, deck, and steel reinforcement. The developed FEM can accurately predict the structural responses of the RC bridge with circular pier subjected to an earthquake in terms of displacement, strain, and damage. In this 3D FEM, the concrete damage plasticity (CDP) material model is considered to capture the nonlinear behaviour of concrete. A bilinear stress-strain relationship is adopted for reinforcing steel. Also, a full implementation of damage parameters is considered where compressive and tensile damage parameters for unconfined and confined concrete are taken into account to accurately capture the damage of the circular RC bridge pier and bridge subjected to an earthquake.

Also, an analytical model has been developed for predicting the yield displacement of circular RC bridge piers for the DDBD method in this PhD project. The model is based on the improved yield curvature estimation by introducing new essential parameters, including concrete strength, longitudinal reinforcement ratio, and axial load ratio. The model incorporates a modified plastic hinge region with equivalent curvature distribution for strain penetration length to predict the yield displacement of the RC bridge pier. A series of RC bridge piers previously tested under cyclic loading (pushover tests) are selected to validate the proposed model. The yield displacement is estimated through the force–displacement response and is compared with the proposed model. A series of

validation subjected to a seismic loading are conducted to evaluate the proposed model of yield displacement. Extensive parametric studies are conducted to evaluate the influence of several parameters on the prediction of the yield displacement of RC bridge pier.

In this PhD research, a new model has been developed for predicting the damage-control target displacement of circular RC bridge piers for the DDBD method. The proposed model is based on the damage-control limit states, where new expressions are introduced in the model. Existing damage-control concrete compression strain and new expressions of damage-control reinforcement tensile strain are considered in this model, along with the modified plastic hinge length, modified strain penetration length, and yield displacement. The model improves the estimation of damage-control target displacement, mainly for the circular RC bridge pier. Also, the FEM is employed to validate the proposed model. The developed model has been validated using a series of RC bridge piers tested under cyclic loading (pushover tests). A series of validations are conducted using the RC bridge pier, which it is subjected to different earthquake conditions and simulated by the validated FEM. A parametric study is conducted to evaluate the influences of concrete strength and reinforcement ratio on the prediction of damage-control target displacement of the RC bridge pier.

Finally, a comprehensive study to assess the behaviour of multi-span RC bridge with a circular pier (designed based on EC8 and DDBD methods) under different earthquake conditions is conducted. Therefore, the 3D FEM developed is used to predict the behaviour of two RC bridges designed using EC8 and DDBD methods. The FE modelling results are used to investigate the seismic performance of the two RC bridges under five different earthquakes. The results indicated that the bridge designed based on EC8 suffered higher maximum displacement and more significant damages compared to the bridge designed by the DDBD method under different earthquakes. This reveals some weaknesses of the current EC8 design method.

DEDICATION

This thesis is dedicated to my family, especially my mother and father,

Khatijah Bee & Abdul Karim,

my wonderful wife and daughter,

Siti Shazirah & Siti Raisha Umaira

and my family member.

ACKNOWLEDGEMENTS

The author would like to express his sincere thanks and gratitude to the following:

- Praise, and thankful to Almighty Allah, for giving me the opportunity, strength, the ability to think, good health and patience to finish this PhD research.
- My wonderful wife, Siti Shazirah, my lovely daughter, Siti Raisha Umaira, my parents, my family, and my family-in-law for their love, supports, encouragement and patience.
- My principal supervisor, Dr. Zhaohui Huang, who always gives me strong support, guidance, encouragement, and patience throughout the completion of this research over the course of the past four years. I personally thank Dr. Zhaohui Huang for his generosity in sharing his idea and knowledge to me.
- My friends for their support and continuous encouragement.

AUTHOR'S DECLARATION

The work in this thesis is based upon the research carried out at the Department of Civil and Environmental Engineering, Brunel University London. Except where specific references have been made to the work of others, this thesis is the result of my own work. No part of this thesis has been submitted elsewhere for any other degree or qualification.

Mohd Ritzman Bin Abdul Karim

PUBLICATIONS

Published Papers

1. Abdul Karim, M. R. & Huang, Z. (2019). 'A new damage-control target displacement procedure for direct displacement-based design of circular reinforced concrete bridge pier'. *International Journal of Safety and Security Engineering*, **9**(3), pp. 249-260.

2. Abdul Karim, M. R. & Huang, Z. (2018). 'Estimation of yield displacement for seismic based design of circular RC bridge piers', *7th Asia Conference on Earthquake Engineering*. Bangkok, Thailand. 22-25 November.

3. Abdul Karim, M. R. & Huang, Z. (2019). 'A new damage-control target displacement procedure for direct displacement-based design of circular reinforced concrete bridge pier', *12th International Conference on Earthquake Resistant Engineering Structures*. Seville, Spain. 5-7 June.

Papers Under Review

1. Abdul Karim, M. R. & Huang, Z. 'The seismic design and assessment of multi-span reinforced concrete bridge by using FE analysis'. Engineering Structures.

2. Abdul Karim, M. R. & Huang, Z. 'A yield displacement model of a circular RC bridge pier for direct displacement-based design'. Advances in Structural Engineering.

Contents

Figures

xiv

Tables

Chapter 1

Introduction

1.1   Structural earthquake engineering

The earthquake can cause a significant impact that will lead to extreme damage to the structures. Ground shaking, movement of soil, and fail in the surface of ground condition are the possible results from earthquake events that result in several damages to the bridges, and buildings, which will cost high mortality. Earthquake does not only lead to injury to the human but will be the cause of damage to the structures. Normally reinforced concrete (RC) structures are designed based on current design codes and guidelines to withstand different types of natural disasters, such as an earthquake. Therefore, it is assumed that during an earthquake event, the structures can withstand and resist the impact of earthquakes. However, interestingly, this is contrary to a study conducted by Adhikari *et al.* (2015), which indicated that many RC structures were suffered severe damage from earthquake events.

In recent earthquakes events including the 2012 Emilia earthquake (Italy), 2011 Tohoku earthquake (Japan), and 2011 Christchurch earthquake (New Zealand), it was highlighted that many RC bridges which were designed according to current seismic design codes were experienced severe damage and collapse (Parghi, 2016). Many RC bridges collapsed and experienced failure of service due to severe damage to RC bridge piers. During the Wenchuan earthquake event in China in 2008, approximately 1600 bridges suffered extreme damage. Kawashima *et al.* (2009) and Yen *et al.* (2011) reported that the extreme damage of RC bridge caused obstacles and disruption to the transportation system. Previous research has shown that the further development of seismic design codes is needed in order to protect the bridges and buildings. According to Kawashima *et al.* (2009), modifications were done to the bridge seismic design code to meet the current conditions for different types of seismic design specifications. Figures 1.1 and 1.2 show that the typical circular RC bridge pier suffered extensive damage and collapse during the 2008 Wenchuan earthquake.

Figure 1.1 Collapsed RC bridge pier during the Wenchuan Earthquake in 2008 (Yen *et al.* 2011)

Figure 1.2 Damaged RC bridge pier during the Wenchuan Earthquake in 2008 (Yen *et al.* 2011)

Extensive research has been conducted in the area of the seismic analysis and design of RC structures for "seismic-ready". Up to now, several studies attempted to evaluate the seismic impact on RC structures. Nonetheless, Lee *et al.* (2005) pointed out that it is

important for the researchers to understand further the behaviour of RC structures subjected to an earthquake.

1.2   The seismic design of RC bridge

The seismic design of RC bridges is currently under critical review and going through a transitional period. RC bridge is always known as important structures that play an essential role in the global transportation system. The aim of the seismic design of RC bridges is to design the RC bridge structures which can withstand multiple types of earthquakes with no or minimal damage. Currently, the design of RC bridge structures is based on the seismic design codes and guidelines, such as Eurocode 8 (EC8).

Many approaches and guidelines have been developed in order to provide a seismic design procedure for buildings and structures (Priestley and Kowalsky, 2000; Aschheim, 2002; Fardis, 2007; Tjhin *et al.*, 2007; CEN, 2008; Suarez, 2014). However, moderate attention has been paid to RC bridges in terms of seismic design (Nguyen, 2006). As earthquake is unpredictable, the consideration of seismic design for the RC bridge, particularly RC bridge pier, is essential. In the current seismic design practice, the most RC bridge structures are required to meet current seismic requirements of the codes. One of them is to resist lateral load (seismic forces) on the bridges. Previous researches indicated that the current seismic design method and codes can be questionable due to the poor performance of the structures in the past earthquake events (Dwairi, 2004; Restrepo, 2006; Calvi *et al.*, 2013; Khan, 2015).

Based on the present seismic design method, the RC bridges and its members were designed to sustain seismic forces. Those bridges were shown some negative responses during the previous earthquakes, such as Kobe (Japan, 1995) and Chi-Chi (Taiwan, 1999) (Lee *et al.*, 2005; Calvi *et al.*, 2006; Prakash and Belarbi, 2010; Darwash, 2017). This unsatisfactory performance is due to the poor design philosophy employed in the current design codes. As a result, failure in one structural member of RC bridge structure, such as RC bridge pier, can cause extensive damage and collapse of the whole bridge. It is well known that RC bridge pier is one of the most critical structural elements of an RC bridge. Billah and Alam (2015) discussed that failure in providing better seismic design, the capabilities, and strength of the RC bridge pier to resist an earthquake could be in question. Thus, the RC bridge may experience significant damage during an earthquake. In recent years, many methods have been developed in order to provide a better seismic

design for the RC bridge. However, those design methods still need further improvements to become more reliable design standards.

Currently, available seismic design codes, such as Eurocode 8, CALTRANS, and AASHTO are all based on the force-based design (FBD) method in which force is used as a design indicator (Suarez, 2008; Suarez and Kowalsky, 2011; Massena *et al.*, 2012; Kappos, 2015). However, previous studies highlighted that the force is a poor indicator of the damage of RC bridges under seismic loading conditions and the RC bridges designed based on the FBD method demonstrated poor response during the previous earthquakes (Cardone *et al.*, 2008; Suarez, 2008; Kappos, 2015).

To overcome the limitations of FBD method, a performance-based seismic design (PBSD) method has been developed in order to prevent the structure from collapse, loss of life, and extensive economic losses (Fischinger *et al.*, 1997; Kappos, 2015). The philosophy of PBSD method is to ensure a structure is designed for achieving at least one performance level (damage levels) under earthquake intensities. In recent years, a number of PBSD methods have been developed in order to overcome the limitations of the FBD method (Restrepo, 2006; Kappos, 2015). Among them, the direct displacement-based design (DDBD) method developed by Priestley *et al.* (2007) is known as one of the reliable methods in the PBSD method. DDBD method aims to design the structure for achieving the recommended level of performance and limit state under predefined seismic conditions. The structural performance is described in terms of displacement. The current research shows that displacement is a better indicator of damage compared to force (Suarez, 2008; Suarez and Kowalsky, 2011; Wang and Padgett, 2014). Recent research shows that the DDBD method becomes one of the most promising methods for structural seismic design (Kowalsky, 2002; Suarez and Kowalsky, 2007, 2011; Suarez, 2008). In the earlier stage of development, the DDBD method was developed for buildings. However, these methods were improved and modified for the seismic design of RC bridge (Khan *et al.*, 2014; Khan, 2015). Therefore, as to date, DDBD method has reached the stage to be adopted in the design codes (Calvi and Sullivan, 2009b; Tecchio, 2013). However, certain aspects of the method still need further clarification and development for the structural seismic design in the future.

A good design should make sure the RC bridge on a safe side to use and also to prevent damage during an earthquake. During an earthquake, the RC bridge is subjected to

displacement, which can cause damage to the RC bridge pier. By controlling the displacement of the RC bridge pier, damage and losses can be reduced to a minimum (Suarez and Kowalsky, 2011). The safe RC bridge design can be achieved by selecting the right method of designing the RC bridge pier. Previous research (Suarez, 2008; Kappos, 2015) shows that the current design method and codes are no longer suitable to be used due to the poor performance of the RC bridge during an earthquake. New codes and guidelines are required in order to produce a better seismic design for the RC bridge.

DDBD method is a right design method for RC bridge to fulfil multiple numbers of performance objectives, such as to resist the structure within yield limit state, serviceability limit state, and damage-control limit state (Kowalsky, 2000; Priestley *et al.*, 2007; Montoya, 2008; Suarez, 2008, 2014; Kappos, 2015; Muljati *et al.*, 2015). For the DDBD method, the RC bridge design depends on yield displacement which occurs at critical locations of the RC bridge pier (Aschheim, 2002; Hernández-Montes and Aschleim, 2003; Tjhin *et al.*, 2004, 2007; Hernández-Montes and Aschheim, 2017). In the current context of the DDBD method, the effective yield displacement becomes a vital parameter which needs to be evaluated critically as this affects the predictions of target displacement and ductility displacement demand for the RC bridge system. However, the current approximation of yield displacement has some uncertainties. It may lead to inaccurate prediction of target displacement (mainly damage-control target displacement) for the DDBD method. As the DDBD method depends on the target displacement to design an RC bridge, this inaccurate prediction will cause the RC bridge not able to achieve the required design strength, and failure of the bridge may occur.

Currently, the DDBD method for RC bridges is still undergoing several improvements. Although the DDBD method has been considerably improved for the past ten years, further development is needed to ensure the DDBD method can be used to design a circular RC bridge pier subjected to an earthquake. As aforementioned, the DDBD method depends on the yield displacement at the critical location, which is plastic-hinge region. Due to the uncertainty and recent advancements in the plastic-hinge region concept (Goodnight *et al.*, 2016a), further research is needed to improve the calculation of yield displacement of the RC bridge pier subjected to earthquakes. Currently, the estimation of yield displacement depends on the yield strain of reinforcement and the diameter of the cross-section of the circular RC bridge pier (Kowalsky, 2000; Priestley *et al.*, 2007; Sheikh *et al.*, 2010).

As highlighted previously, several limits states may be considered to assess the performance of the structures under seismic loading conditions. In general, structural performance is focused on restrictive limit states such as damage-control and serviceability. In order to address the ductile structures' performance level, the damage-control is highly essential for the structures located in the moderate and high seismic regions (Priestley *et al.*, 2007; Suarez, 2008; Mackie *et al.*, 2010). If the damage-control limit states are not met, the damage of a circular RC bridge pier is no longer repairable due to higher cost. Presently, the damage-control limit states are governed by material strain limits such as concrete compression strain limit and reinforcement tensile strain limit. However, at present, the research on the prediction of the reinforcement tensile strain limit for damage-control limit states is still very limited (Kowalsky, 2000).

On the other note, the conventional approach for the design of RC bridge pier relies on the plastic-hinge region, where the formation of the plastic hinge is to dissipate the energy during seismic events (Suarez, 2008). In the moderate and higher magnitude of the earthquake, enormous damage to the plastic hinge of the RC bridge pier can lead to higher substantial repair cost or unrepairable. A lot of research has been conducted recently for further understanding of structural response subjected to earthquakes. In recent years, many studies have been carried out for developing damage indicators to measure the level of damage caused by the earthquake (Hindi and Sexsmith, 2001; Kim *et al.*, 2005; Malekpour and Dashti, 2013; Mahboubi and Shiravand, 2019). Damage indicator has played an essential role in helping engineers to determine the level of damage to the structures. By doing so, the damage indicator will provide the guidelines for the design methods to ensure that future development and improvement on design methods and codes will reduce and eliminate the potential of damage. According to Kowalsky (2000), it is a crucial decision to design a structure that can retain its structural strength and characteristics with slight damage after a substantial earthquake event.

Structural seismic design is one of the essential considerations in RC bridge design, as highlighted before. The conventional approach of evaluating the seismic experiments through shake table tests and constructing a full-scale model for experiments are expensive, time-consuming, and limited to different parameters. Also, it is difficult to perform a full-scale seismic test for the whole RC bridge structure with multiple types of earthquakes. Therefore, an alternative to the seismic experimental test is by using the numerical modelling approach for evaluating the seismic response of RC bridge and RC

bridge pier. The numerical approach allows considering several parameters in an efficient and cost-effective way (Zhao *et al.*, 2018). The experimental data obtained from the experimental test can be used to validate the proposed model before proceeding with the actual applications. Many Finite Element Models (FEM) have been developed in previous studies. However, those models were mainly two-dimensional (2D) and a half-scale three-dimensional (3D) models. Some of the FEM did not consider the different parameters, such as damage parameters, transverse reinforcement, RC bridge deck and so on. Therefore, the development of a comprehensive 3D FEM is required to fully analyse the RC bridge subjected to multiple earthquakes.

1.3   Research gaps

As mentioned above, for design and analysis of RC bridge with circular pier under seismic conditions, the following research gaps need to be addressed:

1) Currently, a comprehensive 3D FEM for analysis of RC bridge with circular pier subjected to the earthquake is needed. FEM should consider different parameters such as material damage parameters, details of transverse reinforcement. Also, the FEM can be used for the full-scale modelling of RC bridge and assess the earthquake resistance of RC bridge with a circular pier.

2) At present, for DDBD method, the estimation of the yield displacement of the circular RC bridge pier solely depends on the yield curvature and strain penetration of the pier. Also, the yield curvature of the pier is independent of the reinforcement and axial load contributions (Kowalsky, 2000; Priestley *et al.*, 2007). The yield curvature solely depends on the yield strain of longitudinal reinforcement and the sectional diameter of the pier. The strain penetration length of the pier depends on the diameter of the longitudinal reinforcement and the yield strength of the reinforcement (Priestley *et al.*, 1996). However, recent research highlighted that strain penetration of RC bridge pier was also depended on concrete material properties. Therefore, the estimation of yield displacement of circular RC bridge pier should consider the influences of concrete strength, longitudinal reinforcement ratio and axial load ratio of the pier.

3) At present, for DDBD method, the damage-control target displacement of the pier was based on the design damage-control limit states, which is governed by the

material's strain. However, the prediction of the reinforcement tensile strain limit for damage-control limit states is still very limited (Kowalsky, 2000; Goodnight *et al.*, 2016b). Besides, to estimate the damage-control target displacement, it is essential to have more accurate estimations of the yield displacement, strain penetration length, and the plastic hinge region.

4) A comprehensive study to assess the behaviour of multi-span RC bridge with a circular pier (designed based on EC8-2 and DDBD methods) under different earthquake conditions is needed.

All research gaps presented here will be addressed in this PhD research.

1.4   Research aims and objectives

The primary aims of this research are to improve the seismic design with DDBD method for the RC bridge with a circular pier and assess the behaviour of multi-span RC bridges with a circular pier (designed based on EC8-2 and DDBD methods) under different earthquake conditions. The detail objectives of the research are:

1) Develop a comprehensive full-scale 3D FEM by using ABAQUS for modelling of RC bridge with circular piers subjected to different earthquakes. FEM consider the different parameters such as material damage parameters, details of transverse reinforcement and concrete damaged plasticity material model.

2) Develop a new analytical model to calculate the yield displacement of circular RC bridge piers more accurately. The model is based on the improved yield curvature estimation by introducing new essential parameters, including concrete strength, longitudinal reinforcement ratio, and axial load ratio. Also, the model incorporates a modified plastic hinge region with equivalent curvature distribution for strain penetration length to predict the yield displacement of the RC bridge pier.

3) Develop a new procedure to calculate the damage-control target displacement of a circular RC bridge pier. The proposed procedure is based on the damage-control limit state (DCLS). This model incorporates a refined model of reinforcement tensile strain., yield displacement, strain penetration and plastic hinge.

4) Conduct a comprehensive parametric study to investigate the influences of concrete strength, axial load ratio, and longitudinal reinforcement ratio on the yield displacement of a circular RC bridge piers and investigate the influence of

concrete strength and reinforcement ratio on the damage-control target displacement of the RC pier.

5) Conduct a comprehensive study to assess the behaviour of multi-span RC bridge with a circular pier (designed based on EC8-2 and DDBD methods) under different earthquake conditions using developed full-scale 3D FEM.

1.5   Outline of the thesis

This PhD thesis consists of seven chapters. The organisation of the thesis is presented in Figure 1.3. The overall content of the PhD thesis is organised into the following chapters:

Chapter 1 provides an introduction to the structural earthquake engineering and seismic design of RC bridge. The research background, research gaps, and main aims and objectives of this PhD project are presented in this chapter.

Chapter 2 presents a comprehensive literature review on seismic design and assessment of RC bridge with a circular pier. This chapter starts with highlighted the performance-based seismic design (PBSD) of the RC bridge. Then, the fundamental of direct displacement-based design (DDBD) of a circular RC bridge pier is highlighted. Also, the performance levels, yield and target displacement of the circular RC bridge pier, and general procedure of DDBD are presented. The design codes related to the seismic design for circular RC bridge pier are also explained in this chapter. Finally, a brief introduction of the finite element model (FEM) and ABAQUS software for 3D FEM of circular RC bridge pier subjected to the earthquake are presented.

Chapter 3 presents the development of a comprehensive 3D FEM for modelling RC bridge with circular pier using ABAQUS software. This model incorporated concrete damaged plasticity model. The validation of the developed 3D FEM is conducted and compared with the previous experimental results.

Chapter 4 presents the development of an analytical model to predict the yield displacement of the circular RC bridge pier for direct displacement-based design. This model is incorporated effective yield curvature and modified plastic-hinge region. Then, the validation of the proposed model is performed using a 3D FEM subjected to pushover and nonlinear time-history analysis and compare with the previous experimental test results.

Chapter 5 presents the development of a procedure for prediction of damage-control target displacement in support of direct displacement-based design method. The proposed procedure is based on the damage-control limit states. The proposed procedure is validated using a 3D FEM nonlinear time-history analysis subjected to seven randomly earthquakes and compare with the previous test results available.

Chapter 6 presents the assessment of two RC bridges (designed according to EC8-2 and the improved DDBD method) under different earthquakes. The assessments are based on the maximum displacement and damage levels of the bridges. Based on the assessment results, some recommendations for improvements of EC8-2 and improved DDBD method are proposed.

Chapter 7 provides the conclusions based on the research outcomes reported in this PhD thesis and proposes some recommendations for future research works on the seismic design and assessment of RC bridge with a circular pier.

Title

Analysis of Reinforced Concrete Bridge with Circular Pier Subjected to Earthquake

Chapter 1:
Introduction

Review

Chapter 2:
Literature Review of Current Seismic Design and Assessment of RC Bridge Pier

Contributions

Chapter 3:
The Development of a Comprehensive Full-Scale 3D FEM

Chapter 4:
An Analytical Model to Predict the Yield Displacement of Circular RC Bridge Pier for DDBD Method

Chapter 5:
A New Model to Predict the Damage-Control Target Displacement of RC Bridge Pier for DDBD Method

Chapter 6:
The Seismic Design and Assessment of Multi-Span RC Bridge by using FE Analysis.

Conclusions

Chapter 7:
Conclusions and Recommendation for Future Works

Figure 1.3 Organisation of the thesis

11

Chapter 2

Literature Review of Current Seismic Design and Assessment of RC Bridge Pier

As mentioned in Chapter 1, RC bridge structural earthquake engineering is one of the most important subjects directly related to human lives and transportation networks. Therefore, it is vital to ensure that the designed RC bridge has a good resistance to an earthquake event. Although it is commonly known that seismic design has considerably improved in the past decades. However, the limitation and uncertainty in the current design codes can cause extensive damage to the structures. Hence, this chapter focuses on the most relevant literature covering the topics related to this PhD research. Through the critical reviews for design and analysis of RC bridge with circular pier under seismic conditions, some research gaps are identified. Those research gaps will be addressed in this PhD research.

2.1 Lessons learned from the previous earthquakes

Bridges are one of the critical elements in the transportation system. They are essential to humanity and have been known for their structural simplicity compared with other structures. However, in the past 30 years, various RC bridge piers have suffered minor, significant, and extensive damage caused by different levels of earthquakes. These damages were investigated by numerous researchers to understand the limitation in current design codes. The failure and damage of RC bridges, particularly RC bridge pier during and after earthquake cost a human life, economic losses in the form replacement costs, and also a disaster to the transportation system. In the traditional method, seismic structural design is based on forces. Many RC bridges suffered extensive damage was designed based on a general design philosophy which is to sustain seismic forces. The poor performance of several bridges can be seen in previous earthquakes such as San Francisco (USA, 1989), Kobe (Japan, 1995) (Calvi *et al.*, 2006; Priestley *et al.*, 2007; Prakash and Belarbi, 2010), Chi-Chi (Taiwan, 1999) and Wenchuan (China, 2008) (Kawashima *et al.*, 2009; Sun *et al.*, 2012), where RC bridges were collapsed and experienced severe damages.

One of the main objectives of the current Eurocodes for seismic design, such as Eurocode 8 (EC8) (CEN, 2004b, 2004c), is to ensure that essential structures for a human remain protected and limited damage in the event of earthquakes. The conventional procedure currently adopted in EC8 is based on "Force-Based Design" (FBD), where seismic forces govern the damage to the structures. This method is straightforward. However, specific limitation arises after numbers of structures show poor performance in the past earthquake. FBD approach relies on the force-reduction factors, to reduce the elastic force demand to a design level requirements. Therefore, to overcome this limitation, a significant number of researches has been conducted for the past 30 years for developing an improved seismic design method for RC bridges and bridge piers.

2.2 Fundamental of Direct Displacement-Based Design (DDBD)

Numerous "Displacement-Based Design" (DBD) methods have been developed and proposed to overcome the limitations of the FBD approach. In the last two decades, the DBD method has established widely. DBD method uses strain and displacement to quantify the structural damages related to an earthquake. DBD method is known as a simple approach that relies on single-degree-of-freedom (SDOF) substitute structures to predict seismic response. DBD method uses the target displacement as a reference point to determine the level of damage at a specific performance level. Direct displacement-based design (DDBD) method, one of the DBD methods, has been recognised to be valid for performance-based seismic design (PBSD) of bridges. The main objective of PBSD is to design structures to achieve specific target performance (level of damage) under specific seismic or earthquakes intensities level. Thus, the main goals of DDBD proposed by Priestley (1993) are to design a structure that will achieve a specific performance (expressed in terms of target displacement) limit state under prescribed seismic hazard (Tecchio, 2013).

DDBD method has been implemented to design for structures which will have better resistance and less damage to the structure during an earthquake event. Even though displacement-based design procedures have been used for designing the buildings, the method for bridges is still undergone modification and has limited use (Kappos, 2015). As firstly proposed by Priestley (1993), DDBD method aims to mitigate the limitations and shortcomings in the FBD approach. The main difference between DDBD and FBD methods is that DDBD uses displacement as a damage indicator in the RC bridge structure

and to measure different seismic demand (Suarez, 2014). DDBD method uses target displacement to determine the required strength for the RC bridge. The DDBD method employs the effective secant stiffness and equivalent damping method to define the structure as an equivalent linear SDOF structure. The fundamental of DDBD method is described below.
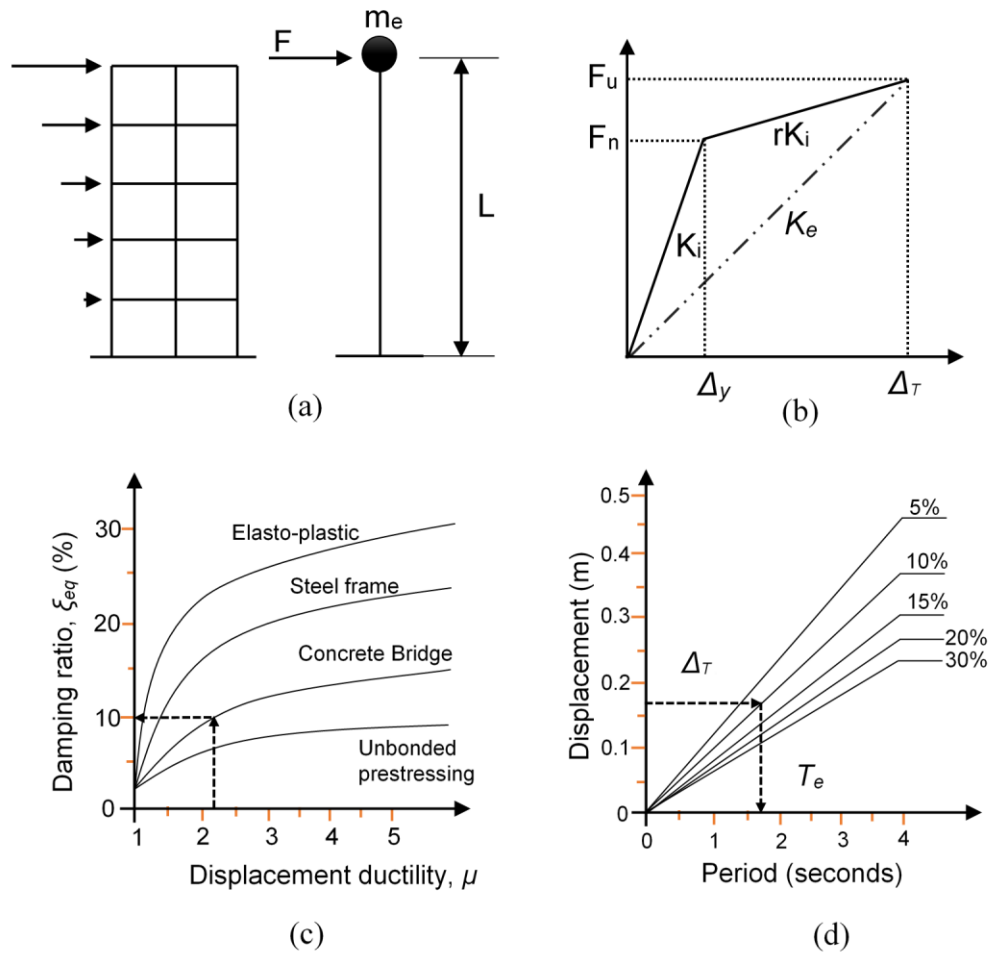
Figure 2.1 Fundamentals of direct displacement-based design (Priestley *et al.* 2007)

The equivalent SDOF structure is determined based on the real inelastic system through an effective mass, m_e, effective secant stiffness, K_e and equivalent viscous damping ξ_{eq}. In the case of multi-degree-of-freedom (MDOF) RC bridge, the DDBD characterise RC bridge by an equivalent SDOF structure with effective mass, m_e, and seismic lateral force, F as shown in Figure 2.1(a), where all individual mass and force will be imposed as system effective mass and system seismic lateral force. This equivalent concept is based substitute structure approach proposed by Shibata and Sozen (1976). This approach considers an SDOF representation of the RC bridge pier. The effective secant stiffness,

K_e is based on the system target displacement, and equivalent viscous damping, ξ_{eq} which represents the hysteretic energy dissipated and elastic damping during an earthquake. Equivalent viscous damping is a way to take into account the effects of dissipating energy on the nonlinear response of the structure. The DDBD method is started by determining the yield displacement, Δ_y and system target displacement, Δ_T. DDBD method characterises the structures by using effective secant stiffness, K_e at system target displacement based on the bi-linear envelope of the lateral force-displacement response of SDOF, as shown in Figure 2.1(b). Then, the displacement ductility demand μ_Δ is used to determine the equivalent viscous damping (damping ratio) for a different type of structure (in this case, RC bridge), as shown in Figure 2.1(c).

With the design target displacement and corresponding damping are estimated, the effective time period, T_e at design target displacement, can be read from damped displacement spectra shown in Figure 2.1(d). Finally, the base shear demand, V (seismic lateral force, F) is determined by multiplying the effective stiffness and the system target displacement. There is an increasing amount of researches has been conducted in the last 20 years to provide the better method to design RC bridge pier for achieving a high level of performance during earthquake events and preventing severe damage (Suarez and Kowalsky, 2007). However, there still have the needs for modification and extension of the DDBD method for RC bridges to improve their responses under different earthquakes (Paraskeva and Kappos, 2010).

2.2.1 Performance levels: section and structure limit states

Many studies have been conducted in order to enhance the level of understanding towards displacement-based design and also to develop a definite objective towards defining accurate seismic performance levels under specific earthquake conditions for different types of structures. As discussed in Priestley *et al.* (2007) and other sources (Hose *et al.*, 2000; Lehman *et al.*, 2004; Tecchio, 2013), DDDB method employs the performance levels which focuses on section and structure limit states for design purposes. The relationship of seismic performance level with a predicted level of earthquake ground motions is vital for seismic design guidelines. The performance levels can be classified into four categories:

i.   Level 1: **Fully operational**, where the damage on the structure is negligible, and the structures can be used.

ii.   Level 2: **Operational**, where the structures face minor damage but still can be used with minor repairs.

iii.   Level 3: **Life safe**, in which the life safety of occupants is fundamentally protected, and the structures require attention, where the damage is moderate to extensive and irreparable.

iv.   Level 4: **Near collapse**, the life safety of the occupants is in danger, and the structures require replacement.

However, the performance levels described above are incomplete and need further development. Recent research has shown that it is essential to include damage-control performance levels for economic reasons (Priestley *et al.*, 2007; Suarez, 2008; Mackie *et al.*, 2011; Suarez and Kowalsky, 2011). Based on the 1995 Kobe earthquake, the structures which were designed based on "Life Safe" performance level, were experienced excessive damage, and repairing cost was uneconomical (Priestley *et al.*, 2007). This reflects that consideration of performance level is vital in seismic design guidelines to ensure the damage can be controlled, and the cost of repair is minimal and less than replacing new structures. These performance levels were presented in some design codes in terms of material strains, such as concrete compressive and steel reinforcement tensile strain limits.

To further understand the performance level and structural response, the relationship between section and structure limit states is vital to be considered. As discussed in Priestley *et al.* (2007), the performance objectives and aims need to be more challenging and demanding in order to ensure the damage on the structures can be controlled or minimal regardless of the high intensity or lower intensity earthquake regions. As mentioned previously, to relate the structural response with the performance level, it is compulsory to define the sectional member and structure's component limit states. Section or member limit state can be defined as the limit state for the components such as the RC bridge pier. Meanwhile, structure limit state can be defined as the limit state of RC bridge structures, as one structure, subjected to an earthquake. As highlighted in the DDBD method, the damage is one of the critical aspects of seismic design. Damage is directly related to the displacement, where the damage estimation can be determined

based on the displacement response of the structures during and after earthquake events. However, up until now, the classification of damage on the structures mainly for RC bridge section is still subjective and challenging (Kowalsky *et al.*, 1995; Priestley *et al.*, 2007; Calvi *et al.*, 2013; Cao *et al.*, 2014; Su *et al.*, 2017; Liu *et al.*, 2018; Mahboubi and Shiravand, 2019).

2.2.1.1 Section limit states

Performance requirements in major seismic RC bridge design codes require the definition of section limit states (Priestley *et al.*, 2007). To highlight, five-section limit states related to the damage and the performance level of the RC bridge pier are listed as:

i. **Cracking limit state**: This limit state is under fully operational condition, where no damage or minor damage is expected to occur. For the RC bridge pier, cracking occurs due to a change in stiffness. This limit state is vital for the structures that expected to behave in the elastic region to the earthquake excitation.

ii. **First-yield limit state**: This limit state is fully operational, where minor damage is expected to occur on main longitudinal reinforcement. Significant change stiffness of concrete at the onset of yield in the extreme condition. This limit state is useful to determine the yield displacement for the RC bridge pier.

iii. **Spalling limit state**: Spalling of concrete cover on the unconfined concrete would be a significant limit state that needs attention. RC bridges components such as piers subjected to high axial load ratio would experience the loss of strength and spalling of concrete cover, associated with negative stiffness. Beyond this limit state, further attention is required, such as repairing to avoid further spalling on core concrete. In this limit state, the concrete compression strain is expected to be around 0.004 (Kowalsky, 2000). However, based on research conducted by Babazadeh *et al.* (2015), in this limit state, the concrete strain is expected to be less than or equal to 0.005. This limit state will cause delayed operational (limited service) or Level 2 performance level.

iv. **Buckling limit state**: For concrete structures such as RC bridge pier, this limit state is crucial. Beyond this limit states, further action is required, where advanced repair and replacement of a new structure's member is needed to ensure the whole

RC bridge can be used and fully operational. At this limit state, the RC bridge is closed for users, and reconstruction will take place.

v. **Ultimate limit state**: Ultimate limit state is vital towards performance level. This limit state indicates that the RC bridge pier required replacement due to loss of strength and inability to carry any load subjected to seismic excitation. Due to the RC bridge pier have potentially reduced the stiffness, the RC bridge might collapse.

2.2.1.2 Structure limit state

As discussed before, the performance level is related to section and structure limit state. Structure limit states are crucial and can be categorised into three categories. Details of structure limit states were highlighted in the DBD09 Model code (Calvi and Sullivan, 2009a) and the displacement-based design book (Priestley *et al.*, 2007). Summary of structure limit states with recent advancements is highlighted below:

i. **Serviceability Limit State**: Structure limit state not only focused to avoid collapse behaviour, but also serviceability limit state (Ghobarah, 2001). This limit state is critical, where minimal damage is expected to occur (Tecchio, 2013). However, in displacement-based design guidelines (Priestley *et al.*, 2007), the serviceability should be in the "fully operational" performance level, where no significant repairs are needed. No spalling of concrete cover should occur. The yield of reinforcement might occur in this limit state, but should be within the acceptable limit. This avoids any problem and traffic delays to any users. In this limit state, the design of the RC bridge is completed when predicted RC bridge damage and losses are acceptable.

Serviceability can be defined using concrete crack width and steel reinforcement strains. As suggested by Priestley *et al.* (1996) and Kowalsky (2000), concrete crack widths should less or equal to 1 mm, in order to ensure no repair is required. In terms of the material strains, concrete compression strain must not exceed 0.004, and reinforcement tensile strain must not exceed 0.015. This limit state also can be defined based on structural drift (Maximum lateral or target displacement divided by RC bridge pier height). Ghobarah (2001) suggests that, for the serviceability limit state, the drift should be less than 0.2%, where no damage is

expected to occur. Meanwhile, Billah and Alam (2016) suggest that drift is within 0.25%.

ii. **Damage-Control Limit State**: This limit state is one of the vital components for performance level and DDBD method. At this limit state, minimum repairable damage is acceptable, or the damage is repairable after an earthquake event. Limited service can be provided for the traffic users and fall within the "delayed operational" performance level. However, the cost of repair should be economical and must be less than the cost of replacement and build a new structure's components, such as building a new RC bridge pier or deck. In this range of limit state, type of damage can include spalling of concrete cover and minimal cracks (1-3mm) that require grouting injection. Bar buckling of longitudinal and transverse reinforcement must not occur. For core concrete, not damage is expected to occur, and no repair is needed.

As to date, damage-control can be defined using a material strain of concrete and steel reinforcement. As proposed by Priestley *et al.* (1996) and Kowalsky (2000), the concrete compression strain of 0.018 was assumed for columns with 0.8-1% transverse reinforcement with a transverse reinforcement yield stress of 450 MPa and allowable strain of 0.10. RC bridge pier with transverse reinforcement details within this range of parameters that facing damage; the damage is repairable. In terms of steel reinforcement strain, Kowalsky (2000) suggested a strain limit of 0.06. At the current stage, insufficient data exist to confirm this limit of 0.06. Therefore, a refined steel reinforcement strain is required in order to estimate the damage-control subjected to reinforcement. The strain must also be lower to avoid any rupture or bar buckling under cyclic loading. Once the bar buckling occurs, the repair is no longer feasible, and the structural members need replacement (Goodnight, 2015; Goodnight *et al.*, 2016b). Hwang *et al.* (2001) suggest that moderate damage can be used to determine the damage-control limit state. The moderate damage should be within global yields where spalling of concrete cover and shear cracking are acceptable. At this stage, the damage requires minimal repairs such as epoxy injection and concrete patching (Lehman *et al.*, 2004). Ghobarah (2001) proposed that, for the damage-control limit state, the drift should be less than 0.5%, where repairable damage is expected to occur. For well-designed structures such as RC bridges, the damage-control limit state can be

determined based on displacement ductility factors or equivalent viscous damping (target displacement divided by yield displacement), within the range of $3 \leq \mu_\Delta \leq 6$.

iii. **Survival Limit State**: Once the RC bridge components such as piers exceed the damage-control limit state; the survival limit state should reserve the capacity to ensure the RC bridge pier would not collapse during and after higher ground excitation. Safety to the users and protection against loss of life is vital in this limit state. No collapse is required. However, extensive damage may occur and accepted, but the cost of repairs is uneconomical. Therefore, for this limit state, the replacement new components of structures are required. This limit state will occur when the RC bridge pier no longer can withhold the load, including gravity loads. At this stage, ultimate displacement will represent the limit state.

Similar to serviceability and damage-control, a survival limit state can be defined using the material strains of concrete and steel reinforcement. As suggested by Calvi and Sullivan (2009), the concrete compression strain should be less than 1.5x of concrete compression strain for damage-control. For steel reinforcement tensile strain, the strain limit should be less than 0.08. Figure 2.2 shows the section and structure limit states. In Figure 2.2(b), Δ_y is yield displacement, Δ_s is serviceability displacement, Δ_d is damage-control displacement, and Δ_u is ultimate displacement.

2.2.1.3 Design selection

Different performance levels, section limit state, and structure limit state have been discussed in the previous section. For design purposes, one limit state usually would be considered, such as the damage-control limit state. However, if there is a requirement that the serviceability limit state needs to be considered, the final required strength for the structures needs to be based on both limit state, and the highest will be chosen for the final design.
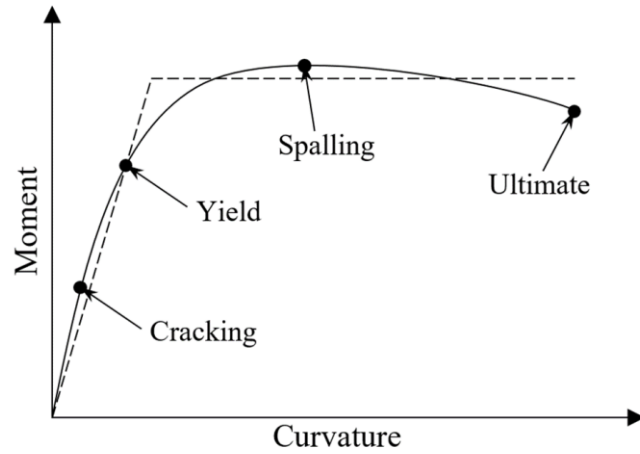
(a) Section limit states
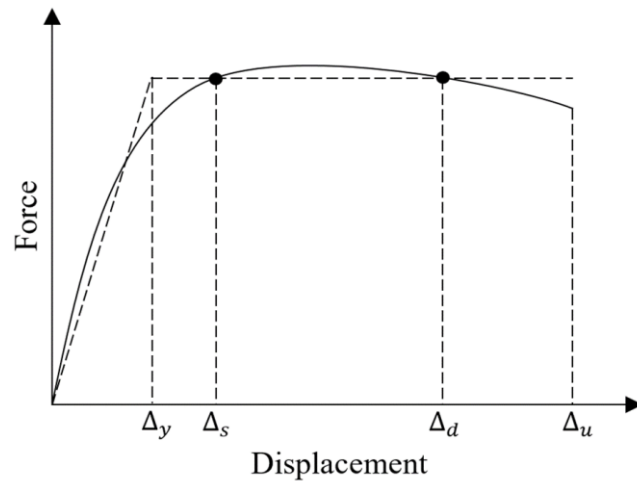
(b) Structure limit states

Figure 2.2 Section and structure limit state

2.2.2 The yield displacement of circular RC bridge pier

Yield displacement Δ_y is the one main component that needs to be defined for the DDBD method. Yield displacement becomes vital and more stable parameters that need to be defined accurately (Aschheim, 2002; Tjhin *et al.*, 2004; Safar and Ghobarah, 2006). As for SDOF, the determination of yield displacement is required for two purposes: first is to determine the limit displacement or target displacement Δ_T for circular RC bridge pier (Priestley *et al.*, 2007; Kappos *et al.*, 2011; Hernández-Montes and Aschheim, 2017) and second is to determine the equivalent viscous damping or displacement ductility

(Aschheim, 2002; Tjhin *et al.*, 2004; Fardis, 2007; Priestley *et al.*, 2007; Kappos *et al.*, 2011; Hernández-Montes and Aschheim, 2017), which is given by Eqn. (2.1).

$$\mu = \frac{\Delta_T}{\Delta_y} \tag{2.1}$$

Yield displacement can be defined based on two different approaches. First, if the target displacement and ductility are known, then yield displacement can be estimated. The second approach is that yield displacement is needed to be defined from the beginning of the design process. The estimation of yield displacement for the second approach is depended on the yield curvature and strain penetration length. Numbers of expressions for predicting yield displacement of a structure have been proposed since the beginning of the displacement-based method. The models have been developed based on different types of structure. Previous research indicates that the yield displacement depends on the fundamental property of the yield curvature: sectional depth, and the yield strain of a longitudinal reinforcement (Kowalsky *et al.*, 1995; Sullivan *et al.*, 2004; Sheikh *et al.*, 2010; Bardakis and Fardis, 2011; Wang and Padgett, 2014). For circular RC bridge piers, previous models for determining the yield displacement were based on the yield curvature that is mainly based on sectional diameter and the yield strain of the longitudinal reinforcement (Calvi *et al.*, 2013) without considering any other factors.

The estimation of the yield displacement is derived by using the direct application of the moment area method for deflections. The yield displacement can be determined when the yield curvature is established. There are many yield displacement equations; however, to suits the circular RC bridge piers, the yield displacement used in the DDBD method can be expressed based on Eqn. (2.2) (Kowalsky *et al.*, 1995; Sullivan *et al.*, 2004; Priestley *et al.*, 2007; Calvi *et al.*, 2008). In Eqn. (2.2), the strain penetration length is considered.

$$\Delta_y = \frac{\phi_y \left(L_{pier} + L_{sp} \right)^2}{3} \tag{2.2}$$

Where L_{pier} is the RC bridge pier height, L_{sp} is the strain penetration length, and ϕ_y is the equivalent yield curvature of the structure. Eqn. (2.2) is derived from the integration of the curvature through the height of the circular RC bridge piers when the yield curvature is established. In Eqn. (2.2), L_{sp} is the strain penetration length, which is a function of

the diameter of the longitudinal reinforcement, d_{bl} and the yield strength of the reinforcement, f_{ye}, as shown in Eqn. (2.3) (Priestley *et al.*, 1996; Botero, 2004).

$$L_{sp} = 0.022 f_{ye} d_{bl} \qquad (2.3)$$

In the earlier research, the calculation of yield displacement is based on initial guesses through the height of the piers. However, this formula ignores the structural stiffness, longitudinal reinforcement ratio, and axial load ratio. Only circular RC bridge pier height is considered. In recent years, the yield displacement concept has been improved by considering the refined strain penetration length based on the plastic hinge concept. In the research (Wang *et al.*, 2008), the yield displacement is calculated using Eqn. (2.2). However, the effective strain penetration is employed, given by:

$$L_{sp} = 0.08L + 0.022 f_{ye} d_{bl} \qquad (2.4)$$

Where, L_{sp} is the effective strain penetration length, f_{ye} is the yield strength of the longitudinal reinforcement and d_{bl} is the diameter of the longitudinal reinforcement. In the different studies conducted by Elwood and Eberhard (2009), the yield displacement of a circular RC bridge pier was represented as the sum of the deformations resulted from bar slip, shear, and flexure. In contrast, a recent work (Goodnight *et al.*, 2016a) indicated that bar slip displacement, shear displacement, and elastic flexure displacement needed to be considered to determine the target displacement of RC bridge piers.

2.2.2.1 Yield curvature

For a single circular RC bridge pier, the yield displacement of the pier critically depends on the yield curvature of the pier. Recent developments in the field of DDBD method reveal that it is vital to critically estimate the yield curvature of circular RC bridge piers. In the early stage, Priestley *et al.* (1996, 2007) developed an equation to determine the yield displacement of circular RC bridge pier, which depends on the strain penetration length (into the RC bridge pier foundation) of the longitudinal reinforcement and yield curvature. Traditionally, many literatures proposed that the approximation of the yield curvature of circular RC bridge piers depends mainly on the yield strain of longitudinal reinforcement, ε_y and sectional diameter, D and the independent of axial load ratio (Kowalsky, 2000; Priestley *et al.*, 2007). Table 2.1 shows some typical models for

calculating the yield curvature of circular RC bridge piers. In Table 2.1, ε_y is the yield strain of the longitudinal reinforcement, D is the diameter of the circular RC bridge pier and f_y is the yield strength of longitudinal reinforcement. From Table 2.1 (Kowalsky *et al.*, 1995; Kowalsky, 2000; Hernández-Montes and Aschleim, 2003; Priestley and Calvi, 2007; Priestley *et al.*, 2007; Tecchio, 2013), the effective yield curvature used to determine the yield displacement of circular RC bridge piers depends on the yield strain of the longitudinal reinforcement and the sectional depth of circular RC bridge piers for circular section. However, none of these equations has considered additional parameters such as concrete strength, axial load ratio and longitudinal reinforcement ratio.

Table 2.1 Some typical models for calculating the yield curvature, ϕ_y of RC bridge pier

References	Circular section
Kowalsky *et al.* (1995)	$\phi_y = \dfrac{2.25\varepsilon_y}{D}$
Kowalsky (2000)	$\varphi_y = \dfrac{2.45\varepsilon_y}{D}$
Hernández Montes and Aschleim (2003)	$\phi_y = \dfrac{2.4\varepsilon_y}{D}$ *for $f_y = 400$ MPa* *(no axial load ratio considered)* $\phi_y = \dfrac{2.3\varepsilon_y}{D}$ *for $f_y = 500$ MPa* *(no axial load ratio considered)*
Priestley and Calvi (2007)	$\phi_y = \dfrac{2.25\varepsilon_y}{D}$
Priestley *et al.* (2007)	$\varphi_y = \dfrac{2.25\varepsilon_y}{D}$
Tecchio (2013)	$\phi_y = \dfrac{2.25\varepsilon_y}{D}$

A study conducted by Hernández-Montes and Aschleim (2003) indicated that, at the beginning of the development DDBD method, the yield displacement were depended on the yield curvature. In these developed expressions, the yield curvature was depended only on the yield strain of the reinforcement and the sectional diameter of the circular RC bridge pier. An investigation was conducted in that study to investigate the influence of

the axial load ratio on the estimation of the yield curvature. The results indicated that the axial load ratio has a significant impact on the estimation of the yield curvature. The proposed equations developed by Hernández-Montes and Aschleim (2003) to account for the axial load ratio is highlighted in Eqns. (2.5) and (2.6).

$$\varphi_y = \frac{\varepsilon_y}{D}\left[2.5 - \left((a-b) \times \frac{P}{A_g f_c'}\right)^2\right] \text{ For } f_y = 400 \text{ MPa} \tag{2.5}$$

$$\varphi_y = \frac{\varepsilon_y}{D}\left[2.4 - \left((a-b) \times \frac{P}{A_g f_c'}\right)^2\right] \text{ For } f_y = 500 \text{ MPa} \tag{2.6}$$

where P is the axial load of the RC bridge pier, f_c' is the concrete compressive strength, A_g are the gross cross-sectional area of the circular RC bridge pier, and a and b are related to the diameter of the RC bridge pier. However, these equations have not been used to improve the calculation of the yield displacement of the circular RC bridge pier.

2.2.2.2 Strain penetration length

The plastic hinge region is needed to be considered to predict the yield displacement of RC bridge pier. This region is an important parameter that indicates the potential damage location for circular RC bridge piers. Many types of research have been conducted to quantify the more refined plastic hinge length of circular RC bridge piers. One of the essential components to quantify the plastic hinge length is strain penetration. Strain penetration (bond-slip) is the effective additional height that represents the longitudinal reinforcement bar penetrating into the RC bridge pier foundation. Priestley *et al.* (2007) suggested that to calculate the plastic hinge length, the effects of strain penetration length should be included by using Eqns. (2.3) and (2.4). In recent research conducted by Billah and Alam (2016b), a model to calculate the plastic hinge length was developed for circular RC bridge piers. Several parameters were introduced, including aspect ratio, axial load, and shape memory alloy (SMA). However, this model is not suitable for conventional RC bridge piers.

As to date, the current models for estimation of the yield displacement depend on the yield curvature and strain penetration length. The models do not reflect the actual behaviour of a circular RC bridge pier subjected to an earthquake. This is due to several

parameters are ignored for estimating the yield displacement. Therefore, further research is needed to take into account all the material and characteristics parameters of a circular RC bridge pier. The typical parameters include concrete strength, longitudinal reinforcement ratio, and axial load ratio. Furthermore, a little research has been conducted to investigate the influences of those parameters along with refined strain penetration on the estimation of yield displacement of the circular RC bridge pier. Therefore, in this PhD research, these parameters will be considered to improve the estimation of the yield displacement of a RC bridge pier.

2.2.3 The target displacement of circular RC bridge pier

The main objective of the DDBD method is to design a structure, such as the RC bridge, to achieve specific target displacement under specified performance limit subjected to seismic intensity. Therefore, it is essential to accurately calculate the target displacement of the RC bridge piers in DDBD method. The target displacement for the SDOF structure (such as RC bridge pier) mainly depends on the limit state, as discussed in Section 2.2.1. The target displacement of the RC bridge pier is determined in the early stage of the design. Then the target displacement profile of the RC bridge needs to be computed to evaluate the final design displacement for the RC bridge (MDOF). Dwairi and Kowalsky (2006) and Tecchio (2013) highlight that the DDBD method for the RC bridge pier starts by selecting target displacement that corresponds to the structure limit state and determines the strength required to achieve the preferable target displacement. For the case of the RC bridge structure, the target displacement profile is required rather than a single RC bridge pier target displacement. Utilising the target displacement and yield displacement, the individual ductility level for the RC bridge pier can be estimated. Then the effective stiffness and base shear demand are determined (Dwairi and Kowalsky, 2004). Several researchers have developed different methods to estimate target displacement. Suarez and Kowalsky (2011) proposed a stability-based model for determining the target displacement for RC bridge piers. In this study, $P - \Delta$ effects were included in the process of estimating target displacement at the early stage of the design process. Generally, based on the DDBD method, $P - \Delta$ effects were determined at the end of the design process to avoid instability and iteration.

In the 1995 Kobe earthquake, it was evident that the structures designed based on the "Life Safe" performance level had experienced extensive damage, where the repair cost

was uneconomical (Priestley *et al.*, 2007). For the seismic design of the RC bridge, the RC bridge piers are generally designed as ductile elements. In the event of an earthquake, the RC bridge piers will form plastic hinges to dissipate energy. To restrain the structures from extensive damage, the damage-control limit state is required in the design stage (Priestley *et al.*, 2007). It is assumed that beyond the damage-control limit state, the repair of the bridge pier is no longer cost-effective. Traditionally, the serviceability limit state of structures is commonly considered in the design stage (Priestley *et al.*, 2007; Suarez, 2008; Suarez and Kowalsky, 2011). However, for the seismic design of RC bridge piers, a stricter requirement is needed for the limit state; for instance, the damage-control limit state is needed for RC bridges located in the moderate and high seismic regions. Figure 2.3 shows an example of a typical force-displacement relationship for an RC bridge pier.
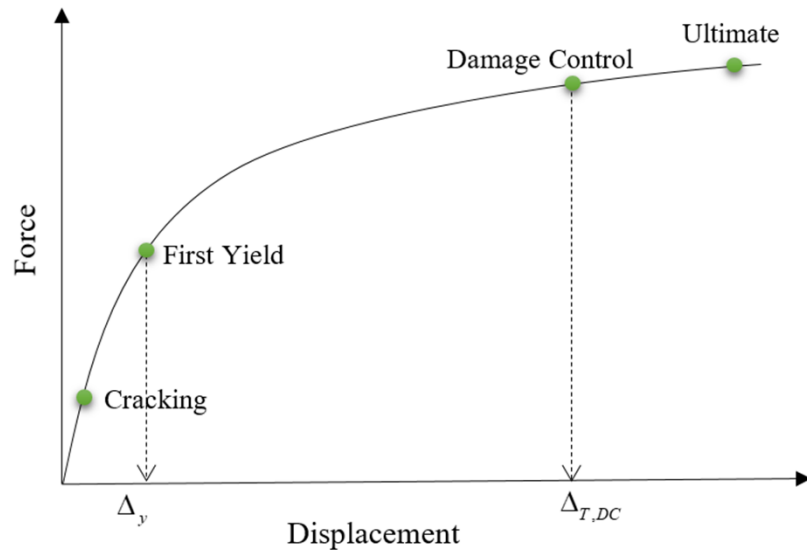
Figure 2.3 Force-displacement relationship

In Figure 2.3, $\Delta_{T,DC}$ is the damage-control target displacement and Δ_y is the yield displacement. As aforementioned, the damage-control limit state ensures that the damaged structures can be repaired cost-effectively. In DDBD method for circular RC bridge piers, damage-control limit state is based on the damage-control concrete compression strain limit, $\varepsilon_{c,dc}$, and the damage-control reinforcement tensile strain limit. $\varepsilon_{s,dc}$. $\varepsilon_{c,dc}$ can be defined as the compression strain that represents a significant damage to concrete (e.g., spalling of concrete cover, minor crack), but the structures are still repairable. The experimental research shows that $\varepsilon_{c,dc}$ depends on the transverse reinforcement details provided in the RC bridge pier. In the previous research (Kowalsky,

2000), $\varepsilon_{c,dc}$ was assumed to be 0.018 based on typical transverse reinforcement ratio (0.8%−1%) provided in the circular RC bridge pier.

The damage-control reinforcement tensile strain limit, $\varepsilon_{s,dc}$, is defined as the strain at the peak tension strain during the loading cycle, in which the buckling of the reinforcement starts to develop. However, the quantification of $\varepsilon_{s,dc}$ is still challenging due to the insufficient data at damage-control level (Goodnight *et al.*, 2016b). In the previous research (Kowalsky, 2000), $\varepsilon_{s,dc}$ was assumed to be 0.06. Later, other researchers (Priestley and Kowalsky, 2000) suggest that $\varepsilon_{s,dc}$ should be less than the ultimate strain at maximum stress in transverse reinforcement, ε_{su}, based on a specific condition, where $\varepsilon_{s,dc} = 0.6\varepsilon_{su}$. However, the strain condition relatively depends on the volumetric ratio and longitudinal spacing for transverse reinforcement. This is to ensure that the transverse reinforcement can avoid extreme buckling and rupture of the longitudinal bars of the RC bridge piers during earthquake events.

2.2.3.1 The procedure to determine damage-control target displacement

As shown in Figure 2.4, for a single circular RC bridge pier, one of the most important procedures in the DDBD method is to determine the target displacement. Based on the plastic hinge method (Priestley *et al.*, 2007), strain-based target displacement can be determined along the transverse axis of the bridge pier (Suarez, 2008).

The strain-based target displacement, Δ_{Ts}, is given as (Priestley *et al.*, 2007; Suarez, 2008; Suarez and Kowalsky, 2011):

$$\Delta_{Ts} = \Delta_y + \left(\phi_t - \phi_y\right) L_p \, L_{pier} \tag{2.7}$$

where, Δ_y is the yield displacement of the circular RC bridge pier; ϕ_t and ϕ_y are the target and yield curvature, respectively; L_{pier} is the pier height, and L_p is the plastic hinge length. Recent studies (Suarez, 2008; Kong, 2017) show that Eqn. (2.7) was used to determine the target displacement for serviceability limit state and damage-control limit state. The DDBD method highlighted in (Kong, 2017) was based on the circular RC bridge pier geometry and reinforcement detailing. As shown in Figure 2.5, the limit states can be defined based on the moment-curvature analysis of a circular RC bridge pier.
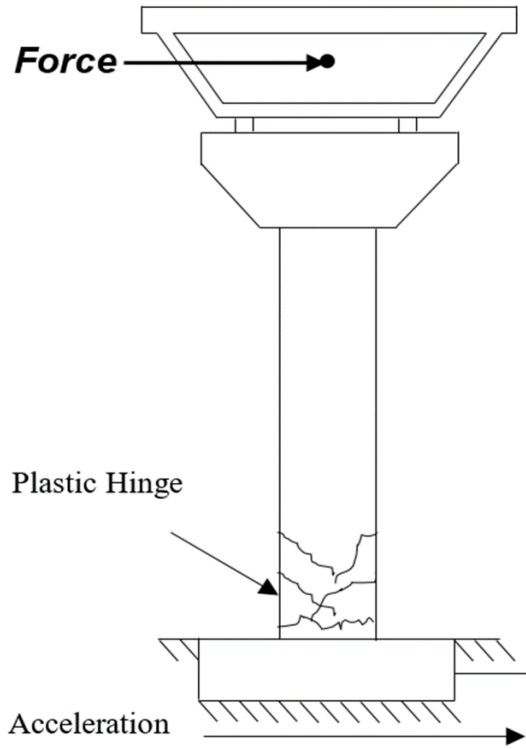
Figure 2.4 Single RC bridge pier
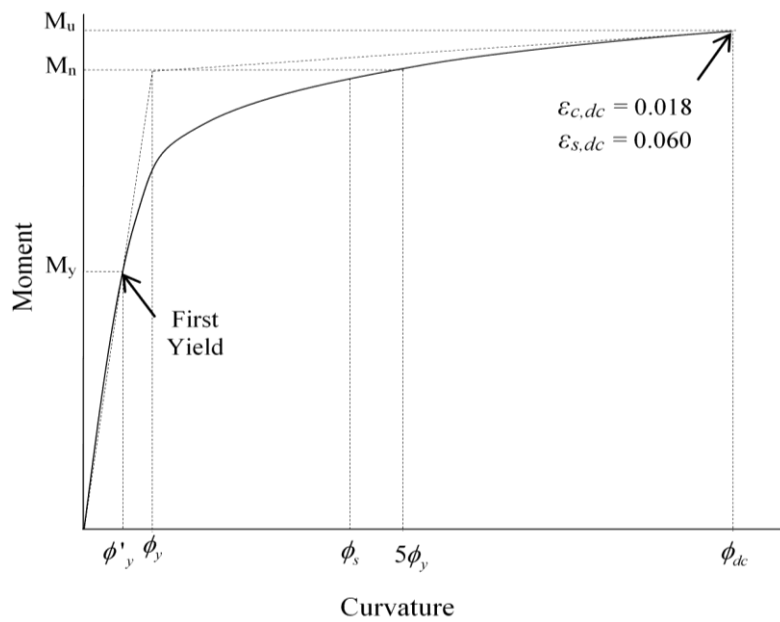
Figure 2.5 Limit states definition based on the moment-curvature analysis

In Figure 2.5, the yield curvature, ϕ_y, is determined by extrapolating the first yield curvature, ϕ'_y, at the nominal flexural moment, M_n, and ϕ_s is the serviceability target curvature. Damage-control target curvature, ϕ_{dc}, is able to be determined when the

damage-control concrete compression strain limit $\varepsilon_{c,dc}$ reached 0.018 or when the damage-control reinforcement tensile strain limit $\varepsilon_{s,dc}$ reached 0.06. This position indicates the ultimate moment, M_u. The damage-control target displacement, $\Delta_{T,DC}$, can be estimated as (Priestley $et\ al.$, 2007; Suarez, 2008; Suarez and Kowalsky, 2011):

$$\Delta_{T,DC} = \Delta_y + \left(\phi_{dc} - \phi_y\right) L_p\ L_{pier} \tag{2.8}$$

Kowalsky (2000) also suggested that ϕ_{dc} can be defined as:

$$\phi_{dc} = \frac{1}{D}\left(0.068 - 0.068\frac{P}{f'_c A_g}\right) \tag{2.9}$$

However, Eqn. (2.9) is used if the axial load and longitudinal reinforcement ratios are within the limits of 0.1–0.4 for axial load ratio, and 1%–4% for reinforcement ratio.

The yield curvature, ϕ_y, is represented as (Priestley $et\ al.$, 2007; Sheikh $et\ al.$, 2010; Calvi $et\ al.$, 2013; Hernández-Montes and Aschheim, 2017):

$$\phi_y = 2.25\frac{\varepsilon_y}{D} \tag{2.10}$$

where, ε_y is the yield strain of the longitudinal reinforcement. The yield displacement, Δ_y is given as highlighted in Eqn. (2.2).

As aforementioned, the estimation of damage-control target displacement depends on the damage-control limit states. However, the shortcoming is that the estimation of damage-control limit states is based on damage-control concrete compression strain and uncertainty damage-control reinforcement tensile strain. Therefore, further improvement is needed to estimate the damage-control target displacement based on the refined material strain limit. As highlighted previously, the damage-control target displacement depends on the yield displacement. More importantly, by improving the yield displacement, it is worth to investigate the impact of yield displacement on the damage-control target displacement. This will be addressed in this PhD research.

2.2.4 General DDBD method for RC bridges

As aforementioned, the MDOF system is characterised by the equivalent SDOF substituted structure that has similar mass, system target displacement, and effective damping. Once the yield displacement and target displacement are determined for the SDOF circular RC bridge pier, the process continues to determine the equivalent properties for the MDOF RC bridge. The main steps of the design procedure are highlighted as follows.

The RC bridge is previously designed for non-seismic loads and configuration, with all the details such RC bridge deck and foundation are known. Then the displacement profile for transverse response is required. Due to several challenges in determined the displacement profile in previous research, Kong (2017) proposed a simplified equation to determine the displacement profile under transverse response. Having established the procedure for determining the displacement profile under transverse response, the next step is the characterisation of the equivalent SDOF system. In order to characterise the MDOF as an equivalent SDOF system, two components must be established (Kowalsky, 2002). These are system target displacement and system damping.

The system target displacement depends on the limit state (Section 2.2.1.2), based on the critical circular RC bridge pier and the displacement profile. The system target displacement is based on the individual circular RC bridge pier mass and displacement determined using Eqn. (2.11) (Priestley *et al.*, 2007; Calvi *et al.*, 2013).

$$\Delta_{T,sys} = \sum_{i=1}^{n} \left(m_i \Delta_{T,i}^2 \right) \Big/ \sum_{i=1}^{n} \left(m_i \Delta_{T,i} \right) \tag{2.11}$$

where m_i is mass from bridge deck acting on individual circular RC bridge pier, $\Delta_{T,i}$ is the displacement subjected to displacement profile under transverse response (displaced shape), and μ_i is displacement ductility for each circular RC bridge pier. Once the displacement ductility has been determined, individual circular RC bridge pier equivalent damping $\xi_{eq,i}$ is determined.

Now, the equivalent SDOF system has been determined. The next step is to determine the effective time period for a substitute structure. The time period can be determined from Figure 2.1(d). Once the system damping is calculated, the effective time period T_e is

determined from the displacement spectra. Then, the effective secant stiffness is determined for the RC bridge system.

$$K_e = \frac{4\pi^2 m_e}{T_e^2}$$ (2.12)

where m_e is the system effective mass. Total base shear demand, V is calculated by multiplying the effective stiffness and the system target displacement using Eqn. (2.13).

$$F = V = K_e \Delta_{T,sys}$$ (2.13)

The base shear is distributed to each RC bridge pier in inverse proportion to the height of the circular RC bridge pier. Therefore, the circular RC bridge piers have equal bending moments and subjected to an equal longitudinal reinforcement ratio.

2.3 Design codes

The seismic design of economical and reliable RC bridges depends on the improvement of design codes. The codes are developed based on on-going research. Generally, the codes are provided that applicable for general types of structures and widely applicable for different types of conditions. In terms of seismic design in the Europe, Eurocode 8 (EC8) is one of the codes that provide the detail of design guidelines and procedures for different types of structures, such as buildings and bridges. As suggested in EC8, the seismic design of earthquake-resistant RC structures, mainly RC bridge, shall provide an adequate capacity to dissipate energy without reduction of its strength and resistance against different loading conditions.

Eurocode 8 – Part 1 (EC8-1) (CEN, 2004b) provides general rules regarding seismic design, while Eurocode 8 – Part 2 (EC8-2) (CEN, 2004c) provides details of design procedure focused on bridges. RC bridge shall be designed to meet different types of requirements, highlighted in EC8-1. Two requirements need to fulfil when designing the RC bridge subjected to an earthquake, as highlighted in Clause 2.2 EC8-2 basic requirements. The first requirement is "no collapse" or the ultimate limit state. In this requirement, the RC bridge shall be designed to withstand an earthquake with no collapses, either locally or globally. After the incident of design seismic action, the RC bridge shall retain its structural integrity, and some slight damage maybe consider. However, if the design seismic action causes the RC bridges to reduce its structural

integrity or exceedance the life span of the RC bridge, then the design should aim to design the RC bridge to meet other requirements that allow acceptable damage to occur.

The second requirement is "damage limitation" or serviceability limit state. In this requirement, the RC bridge shall be designed to withstand the seismic action that having more significant probability than design seismic action. Also, in this requirement, minor damage to secondary components and parts that contribute to energy dissipation are acceptable. However, all other parts should remain undamaged.

Traditionally, the RC bridge is designed using a force-based design (FBD) method, adopted by most of the seismic design codes, including EC8. However, as described in previous research, EC8 has many weaknesses. FBD method failed to minimise damage to the RC bridges in the major earthquakes (Ghobarah, 2001). In previous research, Bardakis and Fardis (2011) identified that EC8-2 design is less cost-effective and less rational compared with the other seismic design method. This is also supported by recent research that highlights RC bridges design using other seismic design methods, such as the DDBD method, performed much better than the bridges designed by EC8-2 (Davi, 2015).

2.4 Finite element method

Generally, the numerical analysis is carried out using the finite element (FE) method to investigate the behaviour and response of the RC bridge structures subjected to an earthquake. FE method is one of the powerful computational tools and numerical techniques that allows complex analysis such as the nonlinear response of RC bridge structures under an earthquake. In finite element models (FEM), the RC bridge pier and bridge are modelled as an assembly of 3D solid elements of finite size. The geometric and material nonlinearities of the RC bridge pier are taken into account using FE methods. By using 3D solid elements, it provides more detailed insight into the behaviour of the RC bridge pier than experimental-based investigations. As to date, the FE method has become the prevalent technique to analyse structures subjected to different loading conditions. For the past few decades, many researchers have shown interest in developing a FEM to represent the real behaviour of the RC bridge with a different type of FEM.

2.4.1 Modelling RC bridge pier and bridges subjected to earthquake

The experimental method to evaluate the response of RC bridge pier to seismic loading conditions is time-consuming and expensive. As an alternative, numerical modelling is used to evaluate the response of the RC bridge pier and the whole bridge system subjected to earthquakes. Numerical modelling allows multiple earthquakes to be applied to the FEM cost-effectively and efficiently. Numerical modelling also allows the incorporation number of parameters in the analysis. Hence, experimental test results can be served to validating the FEM. As to date, many FE software has been developed to simulate the RC bridge subjected to earthquakes, such as SAP2000, RUAUMOKO, ANSYS, OpenSees, SeismoBuild, and ABAQUS. All these FE softwares adopt the FE method to model the structural behaviour subjected to earthquakes.

Tecchio (2013) developed a FEM using OpenSees to assess the current seismic design method (direct displacement-based design) for multi-span RC bridges. In this research, Tecchio (2013) proposed a simplified method to improve the accuracy of the direct displacement-based design method subjected to earthquakes. Calibration of the simplified method was assessed for existing RC bridges, aiming to understand the collapse mechanism due to brittle ruptures of RC bridge components. Good agreements were obtained between the OpenSees simulations and experimental results. However, in this research, the RC bridge pier was developed based on a two-dimensional (2D) model without consideration damage parameters. No transverse reinforcement specified in the 2D FEM.

Reza *et al.* (2014) analysed the multi-span RC bridge with irregular pier height subjected to multiple earthquakes, using SeismoStruct software. Two types of RC bridge seismic design were investigated: force-based design and direct displacement-based design. The simulation results indicate that RC bridge design, according to direct displacement-based design, performed well and did not collapse in any of the earthquakes, based on the nonlinear time-history analysis. However, in this research, the RC bridge was modelled based on a two-dimensional (2D) fibre-model, without consideration damage parameters. In this 2D model, unconfined concrete is not taken into account. Recent research reveals that 2D models are not suitable to predict the damage that occurred on the RC bridge pier. Also, the RC bridge deck was not considered in this FEM.

Babazadeh *et al.* (2015) developed a 3D FEM using ABAQUS to estimate the intermediate damage limit states for the RC bridge pier. The results from the 3D model have been validated and compared against the experimental results from four large-scale tests. The validated model was used to estimate the intermediate damage limit states for three components: first yield of longitudinal reinforcement bar, initial spalling of concrete cover, and significant spalling of concrete cover. Good agreements were obtained between the ABAQUS simulation results and experimental test results. However, in this research, the RC bridge pier was modelled based on the half-scale RC bridge pier tested for experimental studies. Also, a two-node beam element (B31) was utilised to represent the reinforcement bar. However, these elements are numerically stable under lateral loading but not under seismic loading. Furthermore, this model can be further developed by using full implementation of damage analysis by developing an accurate damage model to investigate damage progression throughout the analysis and to estimate accurate damage on the RC bridge pier, using a full-scale model.

Simao (2017) established a FEM to conduct a seismic performance evaluation of RC structures using a 3D lattice model subjected to an earthquake. The 3D lattice model was developed, enhance from the 2D lattice model to assess performance damage of RC structures based on actual structures. Damage evaluation was conducted using a damage index to evaluate the RC structures subjected to earthquakes. The structural behaviour of structures was assessed by material behaviour. The results reveal that the reliability of the 3D lattice model manages to capture the damage conditions on the structures and more accurate than the 2D model. However, in this research, the RC bridge was developed based on the 3D lattice model (stick model) without consideration of the solid section and damage parameters. Also, the RC bridge deck has not been modelled. The RC bridge deck was considered as a mass acting on the RC bridge pier for full RC bridge FEM.

From the review presented above, it is evident that FEM is capable of providing detailed and accurate results of the performance of RC bridge pier and bridges subjected to earthquakes. The FEM considers a complex interaction between material and geometric nonlinearities. Therefore, it is suitable to use FEM to evaluate the performance of the RC bridge pier and bridges subjected to an earthquake. However, it was revealed that some of the previous FEM do not take into account a few considerations such as damage parameters, full-scale model, details of transverse reinforcement, and solid section.

Therefore, a more comprehensive 3D FEM is needed for profoundly understanding the structural response and damage mechanism of the circular RC bridge under different earthquake conditions. This issue will be addressed in this PhD research.

2.4.2 Introduction to ABAQUS software

In general, many software has been developed for practical industry to solve the structural analysis problem. ABAQUS (Simulia, 2016) is one of the commercialise software that specialised in FE analysis for different types of linear and nonlinear analysis. ABAQUS is used for different types of analysis, such as static, dynamic, seismic, computation fluid dynamics, and thermal analysis. Previous research has shown the capability of ABAQUS software to analyse many 2D and 3D FEM of structures subjected to earthquakes. ABAQUS software has been validated against experimental results for several types of analysis.

Many material models have been developed for concrete and steel reinforcement in ABAQUS software. For concrete material, the concrete damaged plasticity (CDP) model has been employed in the software. The CDP model uses the concept isotropic damaged elasticity in combination with isotropic tensile and compressive plasticity model to represent the inelastic behaviour of concrete. The CDP model also uses a combination of multi-hardening plasticity and isotropic damage elasticity to describe the irreversible damage that occurs during nonlinear analysis. CDP model enables a proper definition of the failure mechanism in concrete elements.

In this software, the RC bridge can be modelled as an assembly of a combination of 3D solid element for RC bridge pier, shell element for RC bridge deck and truss elements for reinforcement bar. The 3D solid element can be employed for the RC bridge pier even though it is computationally expensive. The material models highlight the proper damages in the material and the relationship between reinforcement and concrete material subjected to earthquakes. The embedded command can be used in order to input the reinforcement inside the RC bridge pier (Florides and Cashell, 2017). Proper interaction can be used to ensure the RC bridge and reinforcement works as one structure. For the RC bridge deck, the shell elements are employed, where it is divided into several plain concrete and reinforcement layer bars. By using different types of elements, the material properties for each element can be specified independently.

At present, this software has been validated extensively against available experimental results subjected to an earthquake. This software has been employed for many research for a structural seismic response for buildings and bridges. Therefore, this software provides a solid foundation for the research conducted in this PhD research. In this research, a comprehensive 3D FEM using ABAQUS software will be developed for the analysis of RC bridge with circular pier subjected to different earthquakes.

2.5 Conclusion

In this chapter, a comprehensive literature review on the current seismic design and assessment of RC bridge has been presented. It is clear that the yield displacement and damage-control target displacement are the key factors for the seismic design using the DDBD method. It is evident from the review conducted in this chapter that 3D FEM is an essential tool for the analysis of RC bridges with circular pier under different earthquakes conditions.

Based on the comprehensive literature review, four research gaps, as presented in Chapter 1, are identified. Five objectives of this PhD research presented in Chapter 1 are also proposed to address these research gaps. The development of a comprehensive full-scale 3D FEM by using ABAQUS for modelling of RC bridge with circular piers subjected to different earthquakes is presented in Chapter 3. A new analytical model to more accurately calculate the yield displacement of circular RC bridge piers is described in Chapter 4. The model considers the influences of concrete strength, longitudinal reinforcement ratio, and axial load ratio for the improved yield curvature estimation along with modified strain penetration length. Chapter 5 presents a new procedure to calculate the damage-control target displacement of a circular RC bridge pier. The model incorporates a refined model of reinforcement tensile strain. Also, a comprehensive parametric study is carried out to investigate the influence of concrete strength and reinforcement ratio on the damage-control target displacement of the circular RC pier. Finally, a comprehensive study to assess the behaviour of multi-span RC bridge with a circular pier (designed based on EC8-2 and DDBD methods) under different earthquake conditions using developed full-scale 3D FEM is presented in Chapter 6.

Chapter 3

The Development of a Comprehensive Full-Scale 3D FEM

3.1   Introduction

As critically review presented in Chapter 2, a comprehensive 3D FEM for analysis of RC bridge with circular pier subjected to an earthquake is needed. Hence, in this chapter, the details of the development of a comprehensive 3D FEM using ABAQUS software are described. The developed FEM can be used for the full-scale modelling of RC bridge and assess the earthquake resistance of RC bridge with a circular pier. Therefore, the detail insights of 3D FEM are highlighted as below:

1) Full-scale 3D FEM is developed to consider full interaction between circular RC bridge pier, deck, and steel reinforcement. The developed FEM can accurately predict the structural responses of the RC bridge with circular pier subjected to an earthquake in terms of displacement, strain, and damage.

2) Concrete damage plasticity (CDP) material model is considered to capture the nonlinear behaviour of concrete. A bilinear stress-strain relationship is adopted for reinforcing steel.

3) Full implementation of damage parameters is considered where compressive and tensile damage parameters for unconfined and confined concrete are taken into account to accurately capture the damage of the circular RC bridge pier and bridge subjected to an earthquake. By considering this parameter, the actual progress of damage can be captured by the model.

3.2   The development of a comprehensive 3D FEM using ABAQUS

In order to simulate the circular RC bridge pier subjected to earthquake loading, a three-dimensional (3D) finite element model (FEM) is developed using the advanced structural analysis and commercial FE software, ABAQUS (Simulia, 2016). The ABAQUS software is selected because it has good numerical convergence regardless of geometric and material nonlinearities of the structure (Florides and Cashell, 2017).

In this model, the circular RC bridge is divided into two components: the circular RC bridge pier and the RC bridge deck. Figure 3.1 shows a general schematic of a circular RC bridge pier and deck. As shown in Figure 3.2(a), the circular RC bridge pier is modelled as an assembly of eight-node 3D brick elements (C3D8R) for confined and unconfined concrete. The 3D FEM is selected to represent the actual structural dimension and behaviour. The element type of C3D8R with full integration is selected to avoid shear interlocking; also, the stress and strain are most accurate in the integration points.
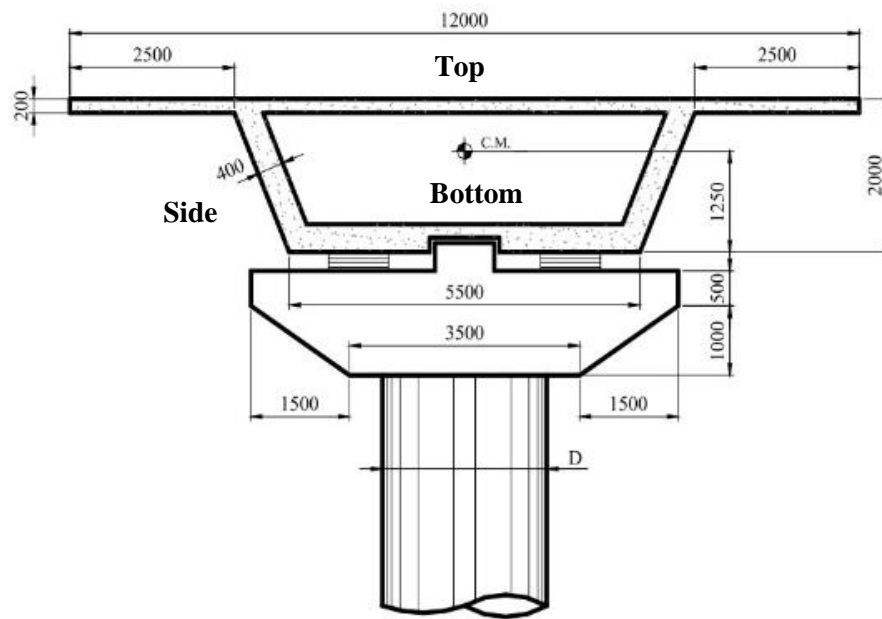
Figure 3.1 General schematic of circular RC bridge pier and deck (Botero, 2004)

For reinforcement bars, including the longitudinal and transverse bar, two-node steel truss elements (T3D2) are employed (see Figure 3.2(b)). The reinforcement is embedded in the concrete using an embedded option, which is available in ABAQUS to ensure the perfect interaction between reinforcement and concrete (Belarbi *et al.*, 1996; Cashell *et al.*, 2010). The transverse reinforcement is modelled along the height of the circular RC bridge pier and foundation using individual spiral reinforcement. A radial mesh configuration for the circular RC bridge pier is employed to ensure the rotational symmetry of the circular RC bridge pier. As highlighted in Figure 3.2(b), confined concrete is where the region of RC bridge pier having a transverse reinforcement such as spiral or circular hoops to strengthen the concrete. On the other hand, unconfined concrete is the region where concrete does not have transverse reinforcement.

As mentioned previously, to bridge the gap between previous and current research, this research consider a full implementation of damage parameters is where compressive and tensile damage parameters for unconfined and confined concrete are taken into account to accurately capture the damage of the circular RC bridge pier and bridge subjected to an earthquake. By considering this parameter, the actual progress of damage can be captured by the model.

(a)   (b)

(c)
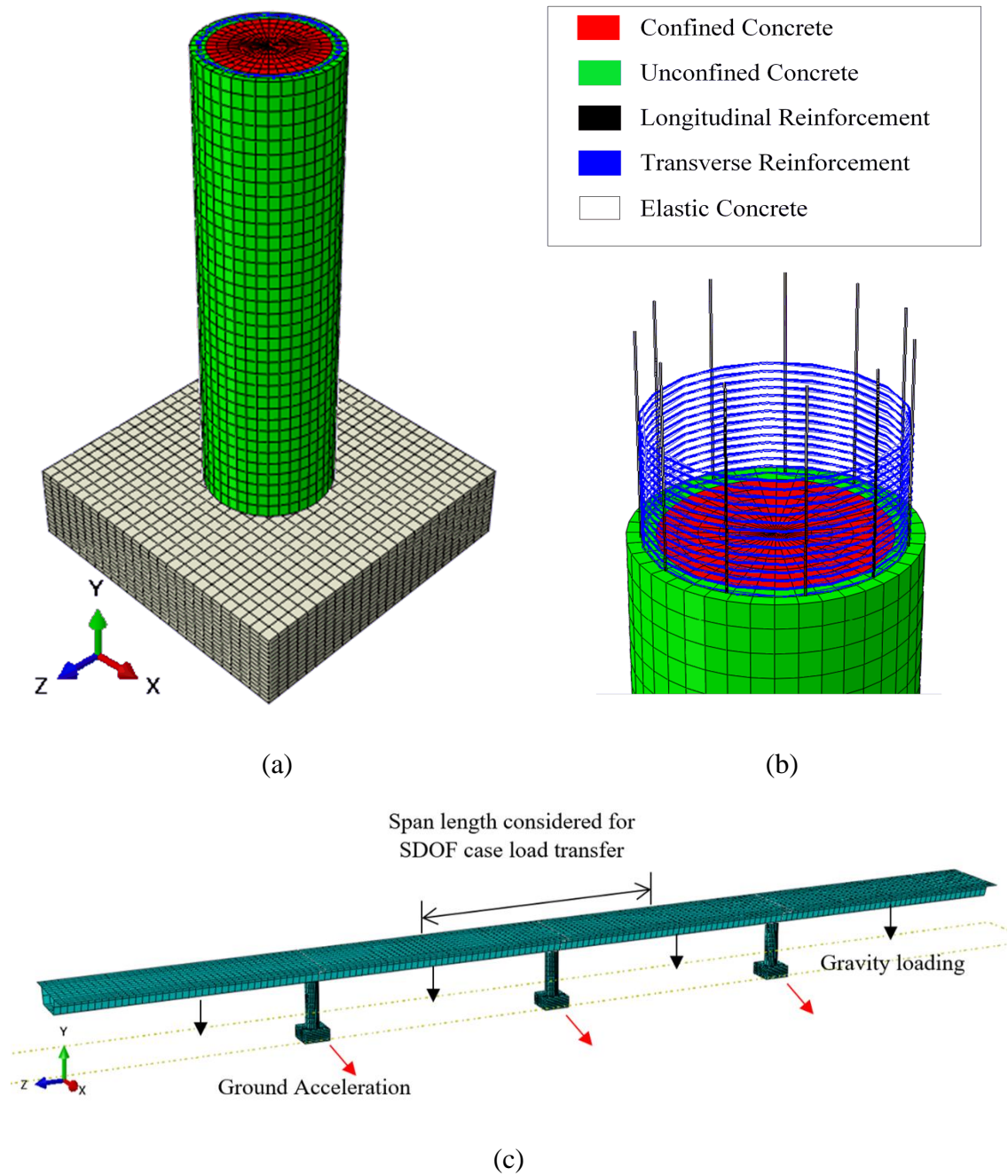
Figure 3.2 Finite element model (FEM) for a RC bridge: (a) Circular RC bridge pier; (b) Cross-section of the pier; (c) Four-span RC bridge

As shown in Figure 3.2(c), the RC bridge deck is modelled as four-node shell concrete elements with one integration point (S4R). S4R is employed in order to make a computational less expensive and reduces the simulation time compared with four-node shell elements with four integration points (S4). Due to hourglass stabilization mode through hourglass control parameters, the S4R element performed slightly better than S4 when refined mesh was used (Laulusa *et al.*, 2006). In some conditions, the S4R element converges to the reference solution for refined meshes and provides excellent accuracy for the results.

As suggested by the DDBD design method, it is assumed that the RC bridge deck remains elastic during seismic events. Therefore, for this research, the RC bridge decks are modelled as elastic members, and bridge piers are represented as inelastic members. It is assumed that bridge piers and decks are based on pinned connections. Hence, the rigid based or fixed connection at the foundation and pinned connection at the top is applied for a circular RC bridge pier in this research. It is assumed that the RC bridge is located on stiff soil. Therefore, soil-structure interaction is not considered in this research. Both ends of the abutments are fixed.

Figures 3.3 and 3.4 show the boundary condition applied to the FEMs used in Chapters 4, 5, and 6. For Figure 3.3, two different setups are considered in this research. In the first setup, the axial load is applied on the top of the circular RC bridge pier in the vertical direction. Lateral acceleration is modelled as amplitude to match the condition of acceleration time-history in a real seismic condition. Lateral acceleration is applied to the model by imposing acceleration time-history at the bottom surface of the foundation for NLTH-FE analysis. In the second setup, the constraint condition is modelled as a fixed boundary condition at the bottom of the foundation to replicate the experimental setup in the previous study. For pushover analysis, the lateral imposed displacement is applied at the top of the circular RC bridge piers to replicate the cyclic loading analysis for the experimental setup in the previous study (Lehman *et al.*, 2004).

For Figure 3.4, the axial load is applied to the top of the circular RC bridge pier in the vertical direction. Lateral acceleration is then modelled as amplitude to match the condition of acceleration time-history in a real seismic condition. Lateral acceleration is applied to the model by imposing acceleration time-history at the bottom surface of the foundation for NLTH-FE analysis. The axial load is assigned to the RC bridge deck.
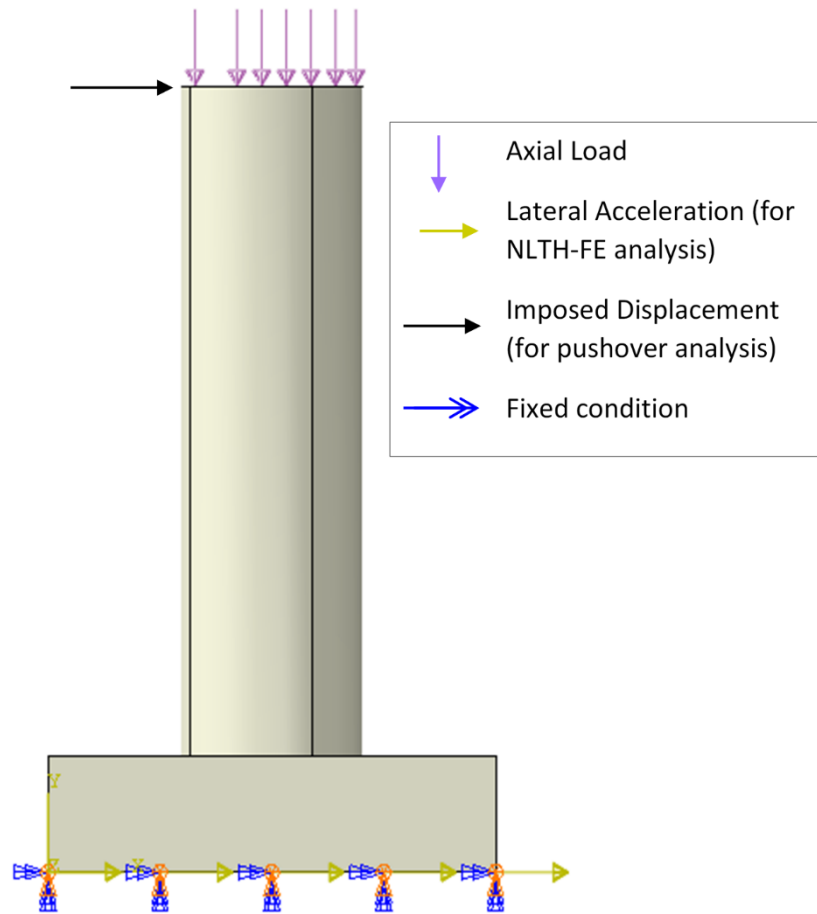
Figure 3.3 Boundary condition of FEM
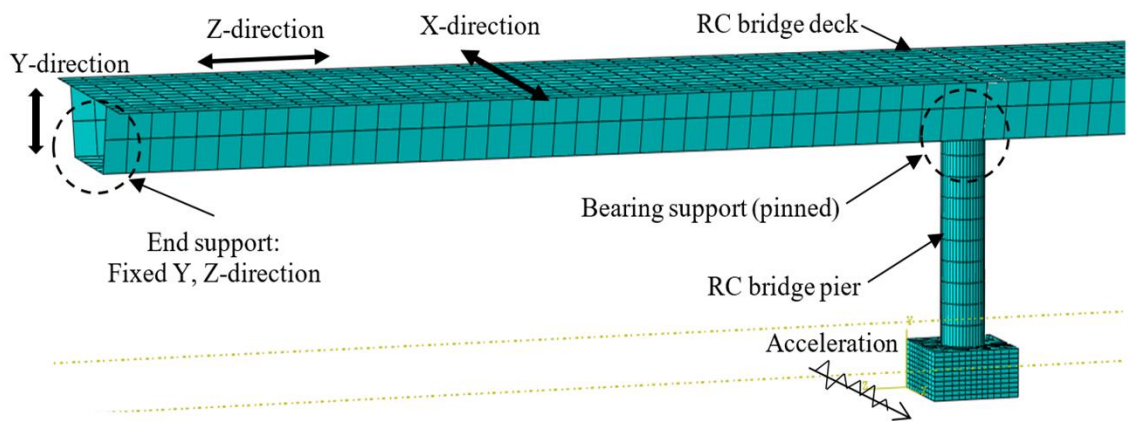
Figure 3.4 The details of boundary condition, earthquake acceleration and support for the FEM

3.2.1 The concrete damage plasticity model

ABAQUS software provides several constitutive models to simulate the elastic-plastic behaviour of concrete under dynamic loading conditions. In this research, a concrete damaged plasticity (CDP) model is chosen for simulating the nonlinear behaviour of concrete subjected to seismic loading. As suggested by ABAQUS (Simulia, 2016), the CDP model can capture the effects of irreversible damage associated with failure modes that occur in concrete by using the concept of a combination of non-associated multi-hardening plasticity and scalar damaged elasticity. The CDP model allows the consideration of inelastic behaviour of concrete in tension and compression, including damage indication in tension and compression. The CDP model is capable of considering the concrete subjected to monotonic, cyclic, and dynamic loading.

3.2.1.1 Initial parameters

The CDP model uses a yield function proposed by Lubliner *et al.* (1989) and further modification by Lee and Fenves (1998) to account for different strengths under compression and tension. The compressive and tension damage parameters for concrete are calculated based on the method suggested by Jankowiak and Lodygowski (2005). The stress-strain is based on the scalar damage elasticity, where the scalar stiffness degradation ranges from zero (undamaged) to one (fully damaged). By using the ratio of unloading stiffness to the initial damaged stiffness, the damage parameter for compression can be determined. Eleven input parameters govern the CDP model. Seven parameters is determined based on experimental studies conducted by previous researchers (Lubliner *et al.*, 1989; Lee and Fenves, 1998; and Jankowiak and Lodygowski, 2005). These parameters are dilation angle ψ, eccentricity value $\in$, the ratio between initial equibiaxial and uniaxial compressive yield stress (Lubliner *et al.*, 1989), f_{b0}/f_{c0}, K value, viscosity parameter, compressive damage parameter, and tensile damage parameter. While other four parameters is depends on selection of concrete model. In this research, two concrete model were selected for confined (Mander et al., 1988) and unconfined (CEN, 2004a) concrete model. These parameters are tensile yield stress, tensile cracking strain, compressive yield stress and compressive inelastic strain. All this parameters are highlighted in Table 3.1 until Table 3.5.

Table 3.1 Material input for CDP model

Material Parameters	Typical values	Reference
Dilation angle	30°	Jankowiak and Lodygowski (2005)
Eccentricity	0.1	ABAQUS default (Simulia, 2016)
Ratio of second stress invariant on tensile meridian to compressive meridian	0.6667	ABAQUS default (Simulia, 2016)
The ratio of initial equibiaxial to the uniaxial compressive yield stress	1.16	Lubliner *et al.* (1989)
Viscosity	0.0001	ABAQUS default (Simulia, 2016)

3.2.1.2 Plastic parameters

The concept of isotropic damage elasticity with combinations of plasticity is used to represent the inelastic behaviour of concrete for the CDP model, where the parameters are required, such as tensile yield stress, tensile cracking strain, compressive yield stress, and compressive inelastic strain. CDP also uses the concept of scalar damaged elasticity in order to represent the inelastic characteristics of concrete and the damage that would occur during the process of breaking or cracking.

As shown in Figure 3.2(a), the circular RC bridge pier is divided into three different regions to represent the confined concrete, unconfined concrete, and reinforcement. The compressive strength for confined concrete is based on Mander *et al.* (1988), and for unconfined concrete is based on Eurocode 2 (EC2) (CEN, 2004a). The stress-strain curve proposed by EC2 for unconfined concrete is given by the following equations:

$$\sigma_c = \left(\frac{k\eta - \eta^2}{1 + [k-2]\eta} \right) f_{cm} \tag{3.1}$$

where

$$\eta = \frac{\varepsilon_c}{\varepsilon_{c1}} \qquad\qquad (3.2)$$

$$k = 1.05 \, E_{cm} \frac{\varepsilon_{c1}}{f_{cm}} \qquad\qquad (3.3)$$

$$\varepsilon_{c1} \left(\%_{00} \right) = 0.7 \left(f_{cm} \right)^{0.31} \leq 2.8 \qquad\qquad (3.4)$$

$$E_{cm} = 22 \left(0.1 f_{cm} \right)^{0.3} \qquad\qquad (3.5)$$

where E_{cm} is the elastic modulus of concrete (GPa), f_{cm} is the ultimate strength of concrete and ε_{c1} is the strain at peak stress. Figure 3.5 shows the stress-strain curve of concrete in compression (Figure 3.5(a)) and tension (Figure 3.5(b)). For concrete in compression ultimate strain ε_{cu1} is taken as 0.0035 (EC2 (CEN, 2004a)).
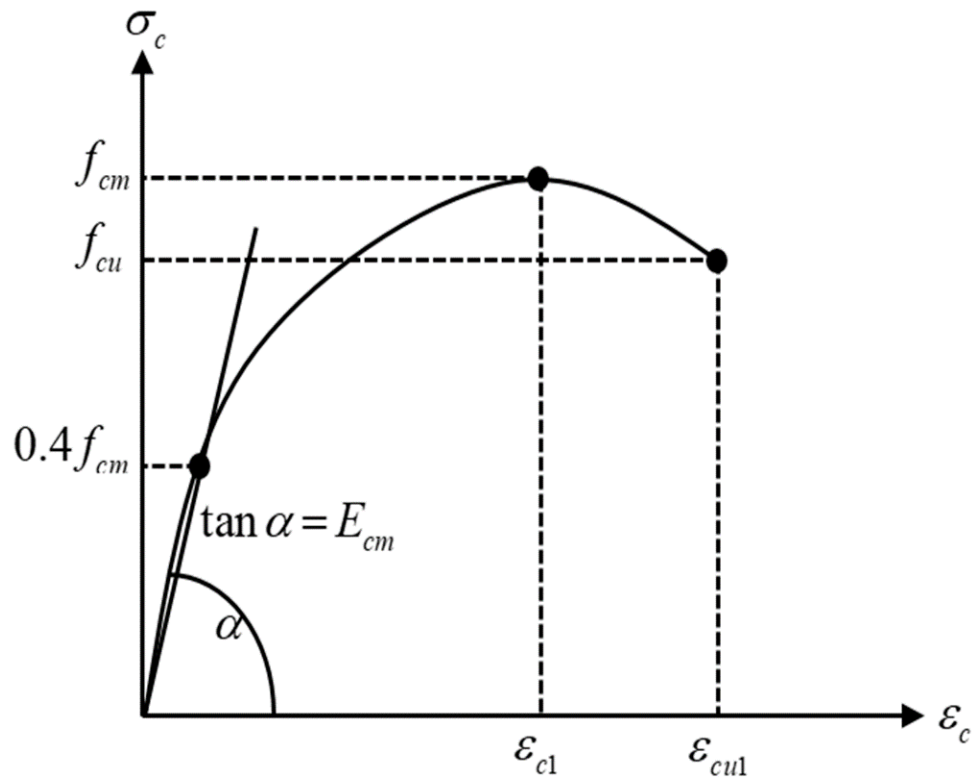
(a) Concrete in compression
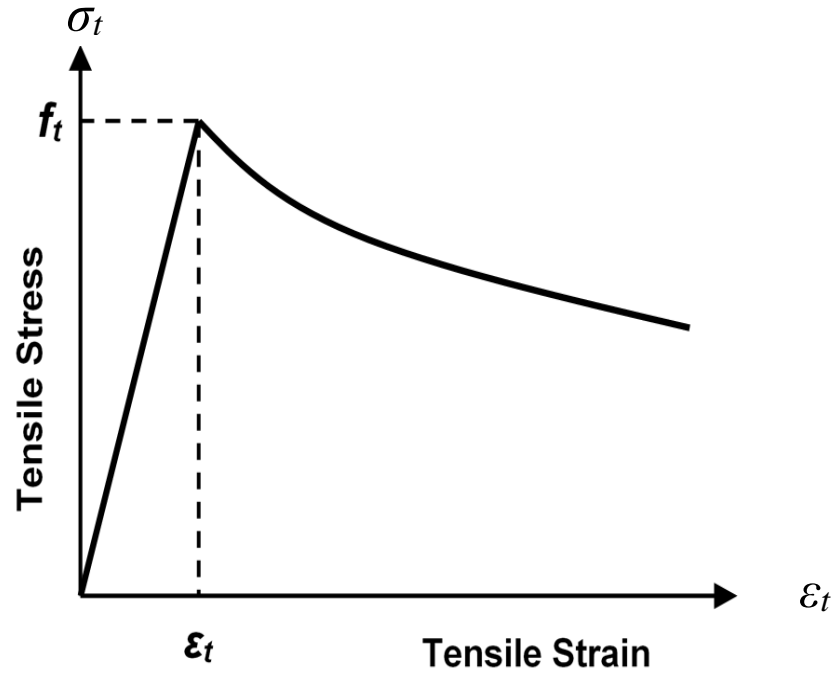
(b) Concrete in tension

Figure 3.5 Stress-strain curves of concrete in compression and tension based on

Eurocode 2 (CEN, 2004a)

In order to consider the confinement effect due to transverse reinforcement confining the core concrete, Mander *et al.* (1988) suggested that the compression of confined concrete can be estimated using the dissipation energy balance approach, as shown in Figure 3.6. Hence, for the determination of compression of confined concrete that served as damage-control concrete compression strain, $\varepsilon_{c,dc}$, the model developed by Mander *et al.* (1988) is adopted in the current study and can be expressed as:

$$\varepsilon_{c,dc} = 0.004 + 1.4 \frac{\rho_s f_{yh} \varepsilon_{su}}{f'_{cc}} \tag{3.6}$$

where ε_{su} is the ultimate strain of steel reinforcement in the transverse direction, f_{yh} is the yield stress of transverse steel reinforcement. f'_{cc} is the compressive strength of confined concrete and can be calculated as:

$$f'_{cc} = f'_{cun} \left(2.254 \sqrt{1 + \frac{7.94 f_1}{f'_{cun}}} - 2 \frac{f_1}{f'_{cun}} - 1.254 \right) \tag{3.7}$$

where f'_{cun} is the compressive strength of unconfined concrete, f_1 is confinement stress and can be expressed as:

$$f_1 = 0.5 \rho_s f_{yh} \tag{3.8}$$

where ρ_s is the transverse reinforcement ratio.

As aforementioned, the compressive strength for confined concrete is determined based on Mander *et al.* (1988) stress-strain curve, and unconfined concrete is based on EC2 (CEN, 2004a) stress-strain curve for compressive and tensile behaviours of concrete. Using Eqn. (3.1) to Eqn. (3.8), the stress-strain can be calculated and used for the CDP model in ABAQUS. Tables 3.2 and 3.3 provide typical plastic parameters for 30 MPa of concrete strength, including compressive and tensile behaviour for unconfined and confined concrete used in this research.
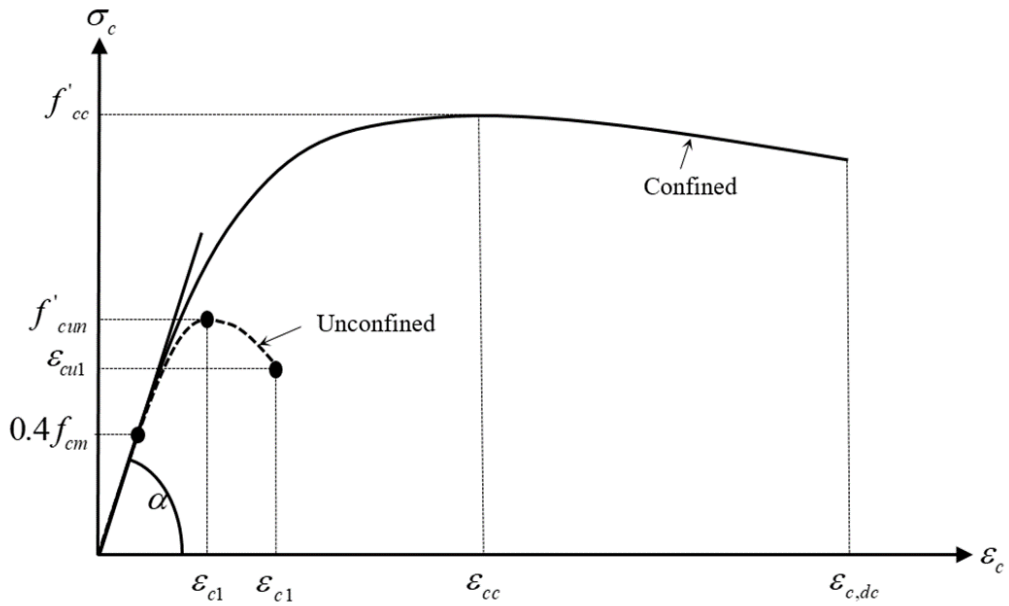
Figure 3.6 Stress-strain curve of confined and unconfined concrete of Mander's model

Table 3.2 Compressive and tensile behaviour for unconfined concrete (CEN, 2004a)

Compressive Behaviour		Tensile Behaviour	
Stress (MPa)	Crushing Strain	Stress (MPa)	Cracking Strain
10.98	0	2.91	0
21.32	0.00049	2.08	0.00017
23.77	0.00065	1.55	0.00030
25.76	0.00082	1.25	0.00042
27.35	0.00098	1.06	0.00054
29.36	0.00131	0.93	0.00066
29.84	0.00148	0.83	0.00077
30	0.00164	0.76	0.00089
29.91	0.00176	0.70	0.00100
29.25	0.00201	0.65	0.00112
28.68	0.00214	0.60	0.00123
22.44	0.00288		
20.97	0.00301		
19.39	0.00313		
14.04	0.00350		

Table 3.3 Compressive and tensile behaviour for confined concrete (Mander *et al*., 1988)

Compressive Behaviour		Tensile Behaviour	
Stress (MPa)	Crushing Strain	Stress (MPa)	Cracking Strain
15.17	0	3.52	0
27.54	0.00051	2.38	0.00021
30.77	0.00068	1.71	0.00037
35.83	0.00102	1.35	0.00052
37.63	0.00119	1.13	0.00066
39.73	0.00154	0.98	0.00080
40	0.00171	0.88	0.00094
39.89	0.00182	0.79	0.00108
38.22	0.00214	0.73	0.00122
35.97	0.00236	0.67	0.00136
30.78	0.00268	0.63	0.00150
28.55	0.00279		
26.07	0.00290		
23.33	0.00301		
20.32	0.00312		

3.2.2 Damage parameters

The concept of isotropic damage elasticity with combinations of plasticity is used to represent the inelastic behaviour of concrete for the CDP model. The parameters used in the model are compressive damage parameter and tensile damage parameter. CDP also uses the concept of scalar damaged elasticity in order to represent the inelastic characteristics of concrete and damage (Jankowiak and Lodygowski, 2005).

In the CDP model, the material damage is taken into consideration. In order to determine the inelastic strain, the compressive elastic strain ε_{0c}^{el} of undamaged material is required. Crushing (inelastic) strain, $\widetilde{\varepsilon_c^{in}}$ corresponding to the compressive stress of concrete, σ_{c0} is employed in the CDP model and can be expressed as:

$$\widetilde{\varepsilon_c^{in}} = \varepsilon_c - \varepsilon_{0c}^{el} \tag{3.9}$$

where ε_c is the total compressive strain of the element. The compressive elastic strain, ε_{0c}^{el} of undamaged material, is given by:

$$\varepsilon_{0c}^{el} = \frac{\sigma_{c0}}{E_{cm}} \tag{3.10}$$

where E_{cm} is the young modulus and σ_{c0} is compressive stress of undamaged concrete. In order to highlight the process of the stiffness degradation of concrete material, two parameters are considered: compressive damage variable (DAMAGEC), d_c and tensile damage variable (DAMAGET), d_t. The d_c needs to be defined at every level of inelastic strain and range from 0 (undamaged material) to 1 (fully damaged material). The d_c corresponding to the ultimate strength of concrete shown in Figure 3.7 and can be expressed as:

$$d_c = 1 - \frac{\sigma_{ci}}{f_{cm}} \tag{3.11}$$

where f_{cm} is the concrete compressive strength and σ_{ci} is the compressive stress of concrete corresponding to compressive damage parameter. The tensile damage variable (DAMAGET) d_t needs to be defined at every level of cracking strain. The d_t value, as shown in Figure 3.8, can be expressed as:

$$d_t = 1 - \frac{\sigma_{ti}}{\sigma_{t0}} \qquad (3.12)$$

$$\varepsilon_{cr} = \frac{\sigma_{t0}}{E_{cm}} \qquad (3.13)$$

where ε_t the total tensile strain of the element, ε_{cr} is the tensile cracking strain, σ_{ti} is the tensile stress of the concrete subjected to tensile behaviour and σ_{t0} is the tensile stress of concrete corresponding to tensile damage parameter. Details of the damage parameters used in this study are given in Tables 3.4 and 3.5.
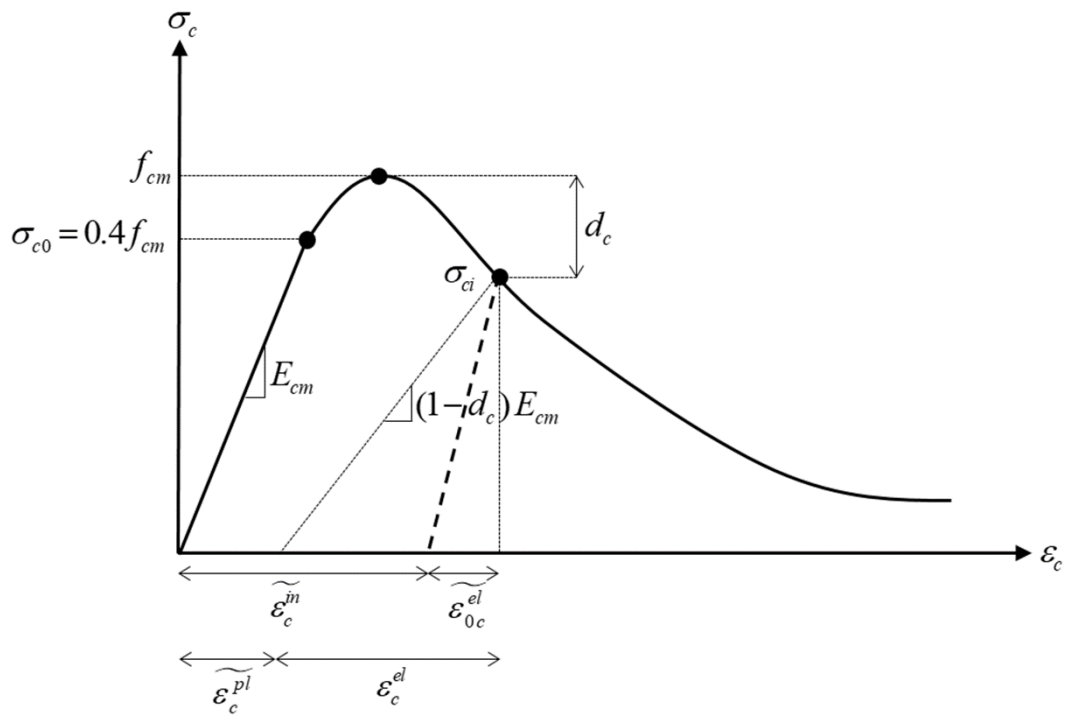
Figure 3.7 CDP model in compression (Jankowiak and Lodygowski, 2005; Simulia, 2016)
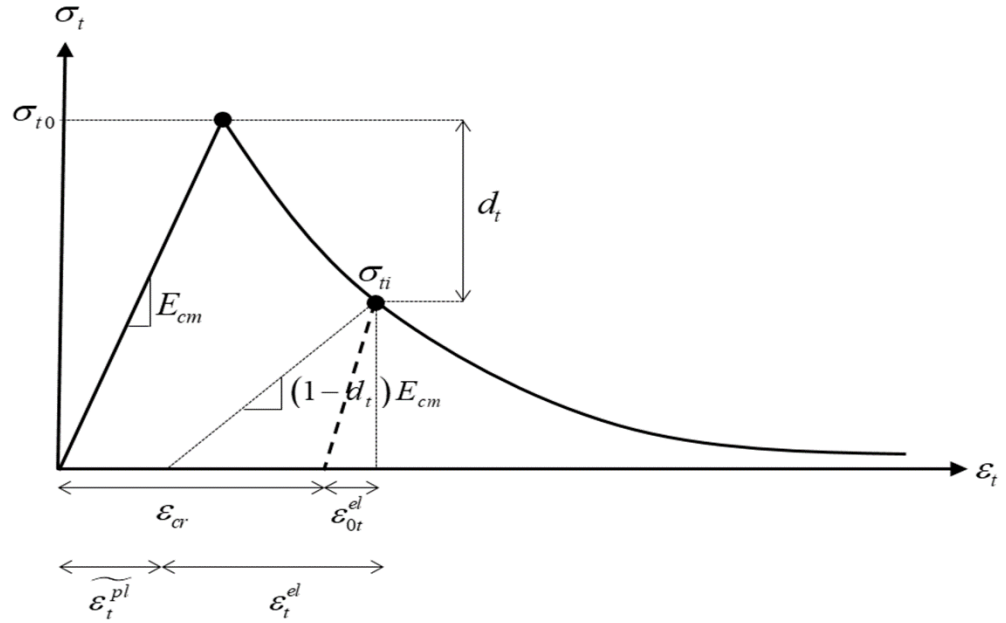
Figure 3.8 CDP model in tension (Jankowiak and Lodygowski, 2005; Simulia, 2016)

Table 3.4 Scalar damage parameter for unconfined concrete

Compressive Damage		Tensile Damage	
Damage Parameter (d_c)	Crushing Strain	Damage Parameter (d_t)	Cracking Strain
0.00	0.00000	0.00	0.00000
0.00	0.00177	0.28	0.00018
0.01	0.00189	0.47	0.00030
0.02	0.00202	0.57	0.00043
0.04	0.00214	0.63	0.00055
0.07	0.00227	0.68	0.00066
0.10	0.00239	0.71	0.00078
0.13	0.00252	0.74	0.00089
0.17	0.00264	0.76	0.00101
0.21	0.00276	0.78	0.00112
0.25	0.00289	0.79	0.00124
0.30	0.00301		
0.35	0.00314		
0.41	0.00326		
0.53	0.00351		

Table 3.5 Scalar damage parameter for confined concrete

Compressive Damage		Tensile Damage	
Damage Parameter (d_c)	Crushing Strain	Damage Parameter (d_t)	Cracking Strain
0.00	0.00000	0.00	0.00000
0.00	0.00182	0.32	0.00022
0.04	0.00215	0.51	0.00037
0.07	0.00225	0.62	0.00052
0.10	0.00236	0.68	0.00067
0.14	0.00247	0.72	0.00081
0.18	0.00258	0.75	0.00095
0.23	0.00269	0.77	0.00109
0.29	0.00280	0.79	0.00122
0.35	0.00291	0.81	0.00136
0.42	0.00302	0.82	0.00150
0.49	0.00312		

3.2.3 Steel reinforcement properties

In this study, a bilinear stress-strain relationship suggested in Eurocode 2 (EC2) (CEN, 2004a) is used for tension and compression for the steel reinforcement bar. The Young's modulus and Poisson's ratio used for the reinforcement are 200 kN/mm^2 and 0.3, respectively.

3.3 Validation of the developed FEM

In order to validate the FEM developed in this study, two experimental tests on the circular RC column subjected to cyclic loading conditions (Saatcioglu and Bingo, 1999; Lehman *et al.*, 2004) were modelled. Figs. 3.9(a) and 3.9(b) show the details of the circular RC bridge piers tested by Lehman *et al.* (2004) and Saatcioglu and Bingo (1999). The material parameters for both specimens are highlighted in Table 3.6. In the tests done by Lehman *et al.* (2004), a pier with 610 mm diameter, 22 reinforcement bars of 16 mm diameter (H16), and 32 spiral reinforcements of 6 mm diameter with 32 mm spacing c/c was used. The concrete strength and axial load considered on the pier were 30 MPa and 654 kN (axial load ratio = 0.07), respectively. Then, a horizontal displacement with a controlled increment was applied at the free end of the pier. In the tests done by Saatcioglu

and Bingo (1999), a pier with 250 mm diameter, 8 H16 longitudinal reinforcement, and a spiral reinforcement of 8 mm diameter with 50 mm equal spacing were employed. The concrete strength and axial load considered on the pier were 30 MPa and 1000 kN (axial load ratio = 0.313), respectively. The selection of this two experimental tests is to indicate different in diameter size, axial load ratio, and longitudinal reinforcement ratio. The data and results for this experimental test is available on open access data.

(a)   (b)
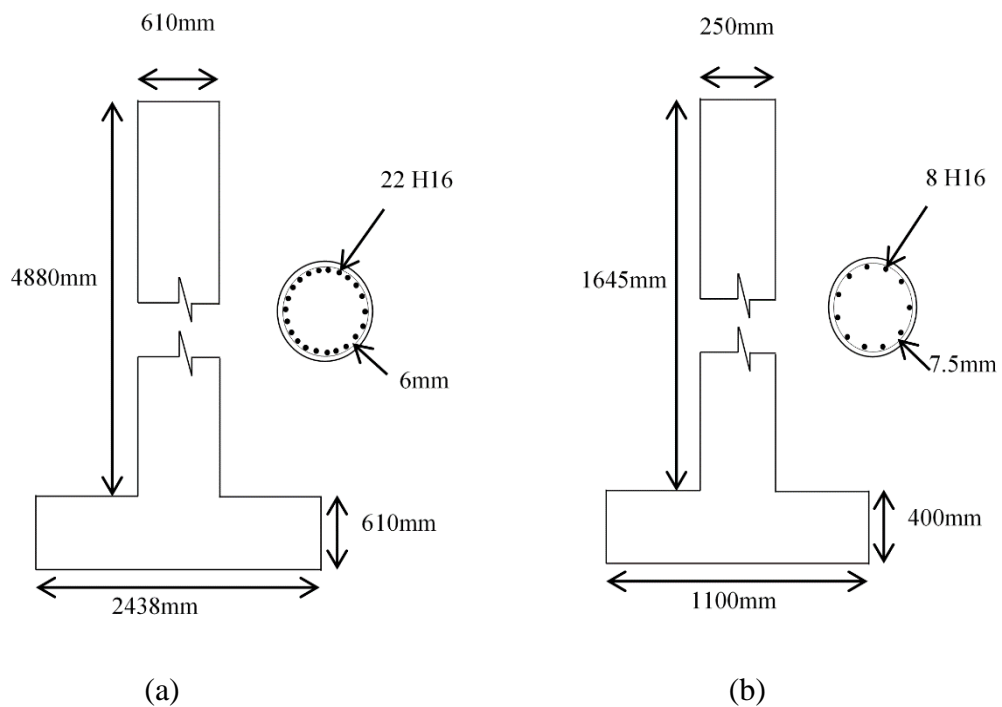
Figure 3.9 The details of tested specimens: (a) Lehmann et al.'s test and (b) Saatcioglu and Baingo's test

A horizontal displacement with controlled increment was applied at the free end of the column. Both experimental tests were modelled to validate the 3D FEM developed in this study. Figure 3.10 shows the comparisons of the force-displacement response predicted by the current FEM, together with the test results. It is evident that excellent agreements between the FEM's predictions and experimental results were achieved. Hence, the proposed FEM can be used to conduct the Nonlinear Time-History Finite Element (NLTH-FE) analysis of RC bridges under different earthquake conditions.

Table 3.6 Material parameters for experimental verification

Parameter	Lehman *et al.* (2004)	Saatcioglu and Bingo (1999)
Pier diameter (m)	0.610	0.250
Pier height (m)	4.880	1.645
Strain penetration length [L_{sp} (m)]	0.101	0.073
Longitudinal Reinforcement (mm)	22 H16	8 H16
Transverse Reinforcement (mm)	32 H6 32mm c/c	H7.5 50mm c/c
Axial load (kN)	654	1000
Concrete strength [$f_c^{'}$ (MPa)]	34	65
Longitudinal reinforcement yield strength [f_{ye} (MPa)]	497	419
Longitudinal reinforcement ultimate strength [f_{ye} (MPa)]	662	-
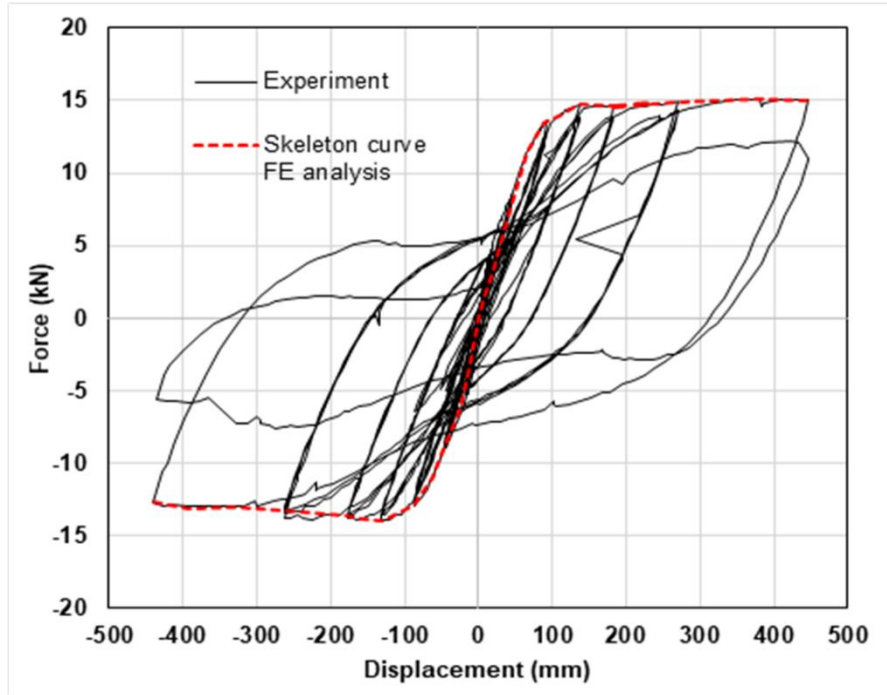
(a)
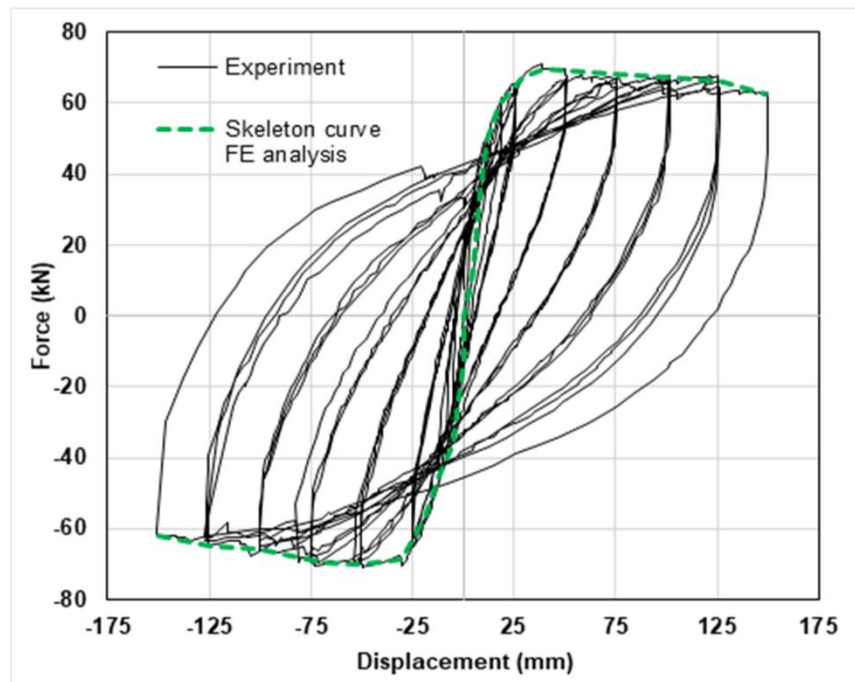
(b)

Figure 3.10 Comparison of FE model's results with experimental results: (a) Lehmann et al.'s test (Lehman *et al.*, 2004) (b) Saatcioglu and Baingo's test (Saatcioglu and Bingo, 1999)

3.4 Mesh Sensitivity Analysis

In this research, the mesh sensitivity analysis was carried out to determine the best and accurate elements mesh size for the circular RC bridge pier. Several mesh sizes were considered, and the final selection of the mesh size was based on consideration of the result's accuracy and computational time, as explained before. The data for mesh sensitivity analysis were based on Figure 3.9(b).

The 3D FEM Circular RC bridge pier (Figure 3.2(a)) was selected for the mesh sensitivity analysis. To determine the possible mesh size for the analysis, three different mesh sizes of 75 mm, 50 mm and 25 mm for the circular RC bridge pier, were studied. A coarser mesh of 100 mm and 50 mm was selected for the deck and foundation, respectively, since they were modelled with elastic material properties.

The 3D FEM was analysed under increasing lateral loads. Figure 3.11 shows that the 50 mm mesh size provide a better force-displacement distribution compared with other mesh size and experimental results. Also, a 25 mm mesh size provides 1.5 times longer for analysis that provides almost similar results.
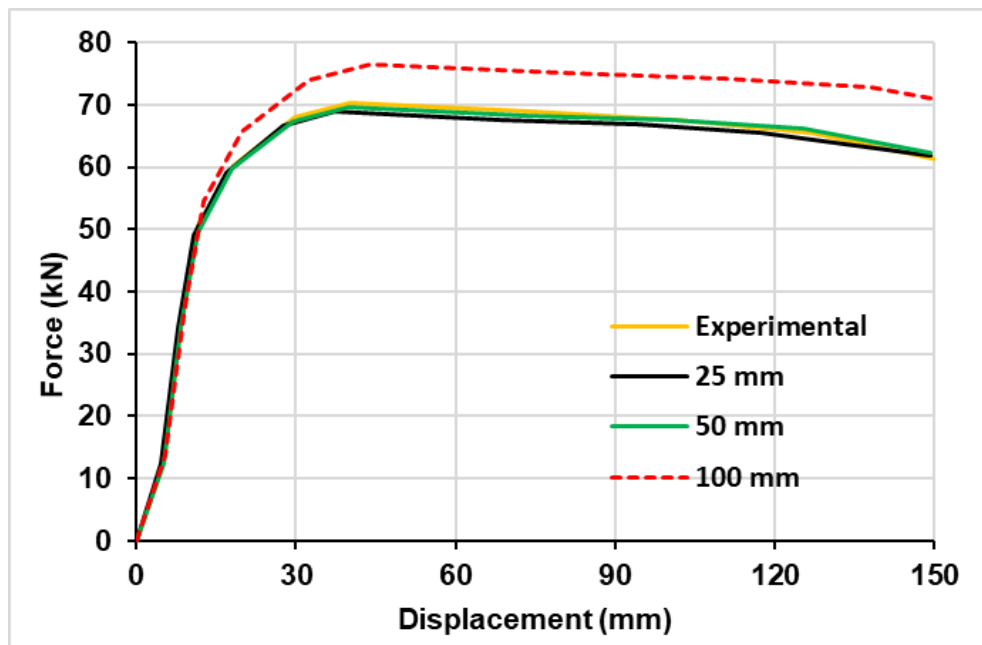
Figure 3.11 Force-displacement for different mesh size

3.5　Conclusion

In this chapter, a comprehensive full-scale 3D FEM has been developed using ABAQUS for the analysis of circular RC bridge pier and bridge subjected to earthquakes. In this FEM, the concrete damage plasticity (CDP) model is adopted for simulating the nonlinear behaviour of concrete subjected to seismic loading. The CDP model allows the consideration of inelastic behaviour of concrete in tension and compression, including damage indication in tension and compression. The CDP model is capable of considering the concrete subjected to monotonic, cyclic, and dynamic loading.

The 3D FEM has been validated against the experimental results with good agreements between the FEM and experimental results. Therefore, this developed FEM can be used to validate the proposed models which predict the yield displacement and damage-control target displacement of the circular RC bridge pier (presented in Chapters 4 and 5). Also, the FEM will be used to conduct a comprehensive study for assessing the behaviour of multi-span RC bridge with a circular pier (designed based on EC8-2 and DDBD methods) under different earthquake conditions (see Chapter 6).

Chapter 4

An Analytical Model to Predict the Yield Displacement of Circular RC Bridge Pier for DDBD Method

4.1   Introduction

The seismic design of reinforced concrete (RC) bridge pier is needed to provide better response and stability for the RC bridge structure to withstand earthquake events. Failure to provide a good design may affect the capabilities and strength of the RC bridge. Thus, the whole system of the RC bridge might experience extreme damage during earthquake events (Billah and Alam, 2015).

Traditionally, the force-based design (FBD) method has been used in many design codes, such as Eurocode 8 – Part 1 (EC8-1) (CEN, 2004b) and Eurocode 8 – Part 2 (EC8-2) (CEN, 2004c) to estimate the response of the structure when subjected to a seismic condition. The FBD method uses the seismic force coefficient as a design indicator. However, force is a poor indicator of the damage of a structure. Hence, this method provides inaccurate results in determining the structure's displacement and the base shear at the bottom of the RC bridge piers. Moreover, fundamental assumptions in FBD have shown some uncertainties which do not reflect the actual structural behaviour. Referring to the moment-curvature response of a structural cross-section, the FBD method assumes that the curvature response would be inconsistent based on the structural member's section with different moment capacities, as shown in Figure 4.1(a) (Priestley *et al.*, 2007). On the contrary, the real response characterisation of structures is as shown in Figure 4.1(b), where the section curvature remains constant with changing strength.

In order to overcome the limitations of the FBD approach, the displacement-based design has been developed, which focuses more on the structural strength, displacement ductility, secant stiffness, and the displacement profile of structures (Tecchio *et al.*, 2015). More recently, the direct displacement-based design (DDBD) method has been developed in which the yield curvature, displacement ductility, equivalent secant stiffness at system target displacement, equivalent viscous damping and base shear demand are considered. Unlike the FBD method, the DDBD method has set the displacement as the main criterion for design purposes.
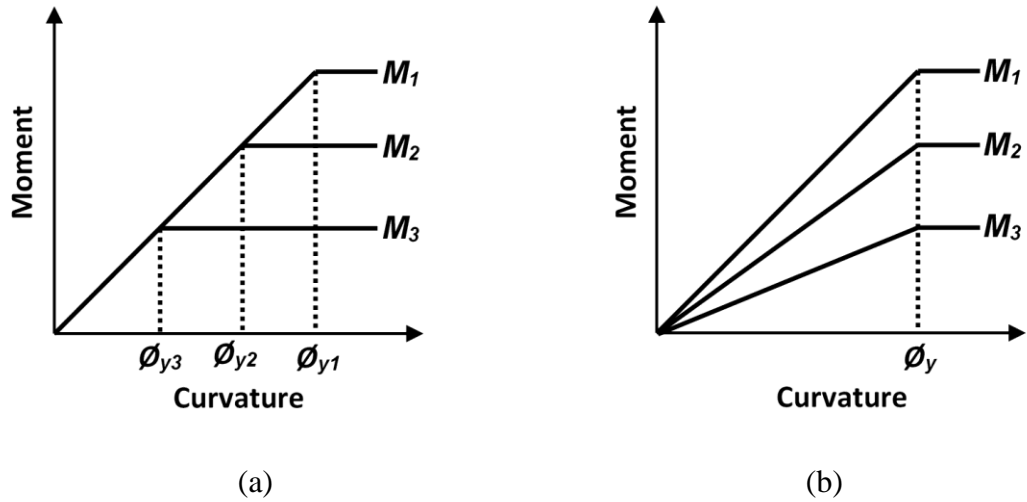
Figure 4.1 Strength influence on the moment-curvature relationship

In the RC bridge seismic design, the RC bridge pier is designed as a ductile element that forms plastic hinges at the bottom of the pier. Despite using the DDBD approach, the RC bridge pier depends on yield displacement, which occurs at a critical location. Hence, the yield displacement becomes a vital parameter that needs to be evaluated critically, as it affects the predictions of target displacement and ductility displacement demanded for a bridge system. For estimating yield displacement, it is needed to define the strain limits of materials for the RC bridge pier and determine the equivalent viscount damping and displacement ductility. The prediction of yield displacement needs to consider the yield curvature at the plastic hinge region and effective distribution length, or effective penetration plastic length. The importance of RC bridge pier stability for seismic designs has brought many researchers' attention to develop better expressions and formulas to calculate the yield displacement (Hernández-Montes and Aschheim, 2017). However, in the previous studies, the yield displacement of an RC bridge pier was obtained only based on the reinforcement strain and the sectional diameter of the pier.

Based on the literature review conducted in Chapter 2, it is clear that at present, for DDBD method, the estimation of the yield displacement of the circular RC bridge pier solely depends on the yield curvature and strain penetration of the pier. Also, the yield curvature of the pier is independent of the reinforcement and axial load contributions (Kowalsky, 2000; Priestley *et al.*, 2007). Therefore, the estimation of yield displacement of circular RC bridge pier should consider the influences of concrete strength, longitudinal reinforcement ratio and axial load ratio of the pier. Hence, a new analytical model to more accurately calculate the yield displacement of circular RC bridge piers is needed. The

model should be based on the improved yield curvature estimation by introducing new essential parameters, including concrete strength, longitudinal reinforcement ratio, and axial load ratio. Also, the model incorporates a modified plastic hinge region with equivalent curvature distribution for strain penetration length to predict the yield displacement of the RC bridge pier. Hence, the main objectives of this chapter are:

1) Develop a new analytical model to calculate the yield displacement of circular RC bridge piers. The model is based on the introduction of yield curvature modifications to estimate yield displacement by introducing new essential parameters, including concrete strength, longitudinal reinforcement ratio, and axial load ratio.

2) Incorporate a modified plastic hinge region with equivalent curvature distribution into the model for predicting the yield displacement of RC bridge piers.

3) Validate the proposed model using a 3D FEM developed in Chapter 3 for the circular RC bridge piers subjected to seismic loading conditions (pushover and nonlinear time-history analysis) and compare with the previous experimental test results.

4) Investigate the influences of concrete strength, axial load ratio, and longitudinal reinforcement ratio on the yield displacement of RC bridge piers.

4.2 Proposed new yield displacement model for DDBD method

In the light of the critical literature review presented in Chapter 2, a robust model is needed to predict the yield displacement of circular RC bridge piers more accurately. Recently, a new plastic hinge method was proposed to modify the yield displacement of circular RC bridge piers (Goodnight *et al.*, 2016a). In this method, the strain penetration of reinforcement into the foundation towards plastic hinge was quantified to investigate the impact of load history for the RC bridge piers. Several parameters were considered in the model, such as axial load ratio and structural foundation strength.

Based on the literature review conducted in Chapter 2, for the development of the new yield displacement model the RC bridge pier is modelled as a single-degree-of-freedom (SDOF) system, as shown in Figure 4.2(a).
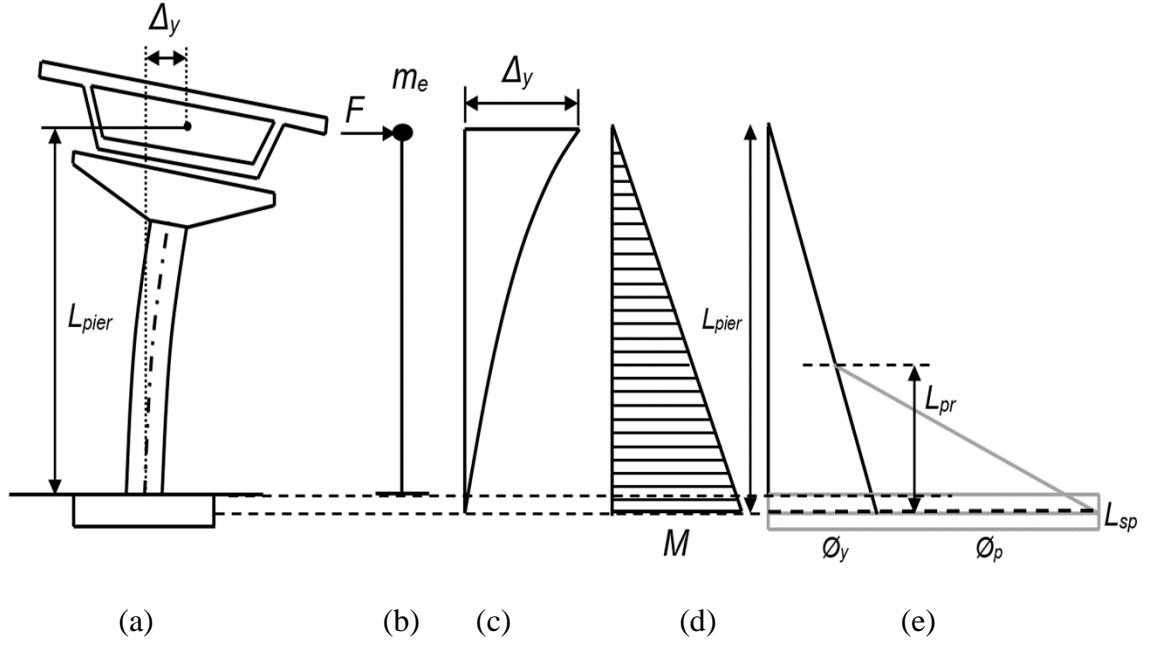
Figure 4.2 Concept of SDOF and modification of plastic hinge region used in this research: (a) SDOF system; (b) SDOF simulation; (c) Displacement shape; (d) Moment distribution; (e) Modification of equivalent curvature distributions

From Figure 4.2(c), the RC bridge pier can be considered as a cantilever column in an SDOF system. Hence, the yield displacement, Δ_y can be represented as:

$$\Delta_y = \frac{\phi_{yeff}(L_{pier})^2}{3} \tag{4.1}$$

where, ϕ_{yeff} is the effective yield curvature, and L_{pier} is the effective height of the RC bridge pier In the proposed model, the modification of equivalent curvature distribution shown in Figure 4.2(e) is adopted to predict the yield displacement of an RC bridge pier. This equivalent curvature distribution model were selected due to improved accuracy both separate tensile and compressive strain-displacement prediction and improved strain penetration length. To employ this model, critical RC bridge pier were selected. For example, for four-span RC bridge with three RC bridge pier, middle pier were considered as critical pier. In this figure, the displacement contributed by the strain penetration of longitudinal reinforcement into the foundation is considered. The displacement assigned to strain penetration is separated from the RC bridge pier. Based on the experimental testing, the proposed strain penetration length is considered as additional parameters. The accuracy of the equations is improved by considering the concrete strength of RC bridge pier and the expected concrete strength of the foundation.

61

Recent developments in the displacement-based design method have increased the need for improving the estimation of yield displacement to evaluate some critical parameters such as the target displacement, ductility demand, and the base shear of RC bridge piers. It is also needed to determine the proper response of RC bridge piers in the elastic and plastic regions and determine the displacement ductility for equivalent viscous damping in a DDBD method. Therefore, for the estimation of the yield displacement of an RC bridge pier, it is sensible to introduce several structural parameters including longitudinal reinforcement ratio, axial load ratio, concrete strength, the modified diameter of the RC bridge pier, and new equivalent curvature distribution.

4.2.1 Yield curvature and strain penetration concept

The concept of effective yield curvature and yield displacement used in this study is shown in Figure 4.3. The first yield point in the moment-curvature curve represents the effective yield curvature, where the yield displacement depends on effective yield curvature.
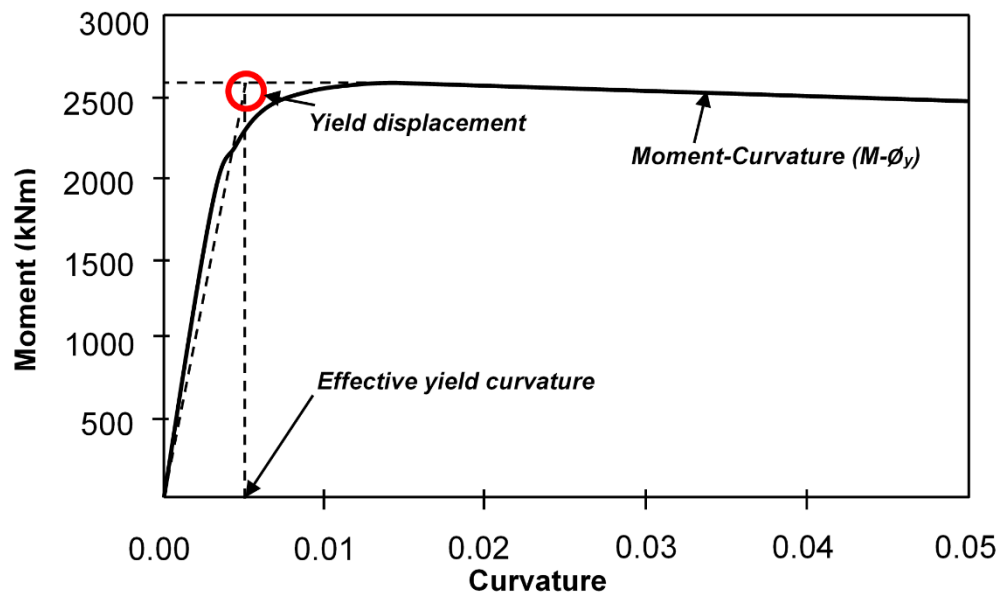
Figure 4.3 Effective yield curvature and yield displacement

In recent years, extensive research indicates that the yield curvature is likely to depend on yield strain, sectional diameter, as well as additional factors including axial load ratio, longitudinal reinforcement ratio, and the strength of concrete and concrete cover (Sheikh *et al.*, 2010). Sheikh *et al.* (2010) developed extensive expressions to estimate effective yield curvature for high- and normal-strength RC bridge piers. Influences of different

parameters were considered. Hence, the effective yield curvature, ϕ_{yeff} for the proposed model, is represented as:

$$\phi_{yeff} = \phi_y \times MF(f_c') \times MF(n) \times MF(p) \tag{4.2}$$

where

$$\phi_y = \frac{2.0 \times \varepsilon_y}{D^{1.1}} \tag{4.3}$$

The modification factor for the strength of concrete, $MF(f_c')$ is given as:

$$MF(f_c') = 1.25 \times f_c'^{-0.07} \tag{4.4}$$

where f_c' is the strength of concrete in the range of 30 to 100 MPa.

The modification factor for the consideration of axial load ratio, $MF(n)$ is given as:

$$MF(n) = 1 + (0.041 \times f_c' - 0.26) \times n - (0.043 \times f_c' + 0.85) \times n^2 \tag{4.5}$$

where n is the axial load ratio and f_c' is the strength of concrete. Eqn. (4.5) is suitable for higher diameter section ($D > 0.5$ m).

Based on the current design codes, the ratio of longitudinal reinforcement, p varies from 1–6%. The modification factor for longitudinal reinforcement ratio, $MF(p)$ is given as:

$$MF(p) = p^{0.16} \tag{4.6}$$

In this research, the model for calculating the yield displacement of an RC pier, Δ_y is based on the selected constraint base shear and the type of connection between RC bridge pier and deck, which is given as:

$$\Delta_y = \frac{\phi_{yeff} L_{eff}^2}{3} \tag{4.7}$$

Using Eqns. (4.2) to (4.7), the final expression of the yield displacement of an RC bridge pier, Δ_y is given as:

$$\Delta_y = \frac{2.0 \times \left(\dfrac{\varepsilon_y}{D^{1.1}}\right) \times MF(f_c') \times MF(n) \times MF(p) \times L_{eff}^2}{3} \tag{4.8}$$

where L_{eff} is the effective height of an RC bridge pier given by Eqn. (4.9):

$$L_{eff} = L_{pier} + L_{sp} \tag{4.9}$$

where L_{sp} is the modified strain penetration length defined as (see Figure 4.2 (e)):

$$L_{sp} = 0.152 \times (1 - \frac{P}{f_c' A_g} - \frac{L_{pier}}{16D}) \times \frac{f_{ye} d_{bl}}{\sqrt{f_{ce}'}} \tag{4.10}$$

where f_{ye} is the expected yield strength of longitudinal reinforcement, A_g is the gross area of concrete, P is a compressive axial load, f_c' are the RC bridge and pier concrete strength, f_{ce}' is the RC bridge and pier foundation concrete strength, d_{bl} is the diameter of the longitudinal reinforcement, L_{pier} is the height of the RC bridge pier, and D is the diameter of the RC bridge pier.

The modified strain penetration length highlighted in Eqn. (4.10) is based on the experimental studies conducted by (Goodnight *et al.*, 2016a). In the experiment conducted by Goodnight *et al.* (2016a), it was discovered that a proposed equation (Eqn. 4.10) considered numbers of parameters, helps to improved the estimation of strain penetration length, mainly for RC bridge. As to date, even though these equation has been developed recently, no implementation were consider in real or proposed design. Therefore, for this research, the implementation of this developed equation was proposed to be consider in estimation of yield displacement. The principle of this modified strain penetration lengths include new parameters such as the expected concrete strength of the foundation, the RC pier diameter, and compressive axial load ratio along with the existing parameters such as the diameter of the longitudinal reinforcement and the yield strength of the reinforcement. Because the RC bridge pier displacement is influenced by the consideration of strain penetration reinforcement into the foundation, so the modified strain penetration length is reasonable to determine the effective yield displacement for the proposed model. This is due to, the proposed yield displacement model are taken into account several parameters such as axial load ratio, concrete strength and longitudinal reinforcement ratio. To determine the limit of yield displacement, which is based on a structural performance level, the materials' strain limits for yield limit state are needed. In this study, the materials' strain limits for yield limit state used are shown in Table 4.1.

Table 4.1 Design parameters for RC bridge pier

Limit State	Steel Reinforcement Strain Limit
Yield	0.0021

4.3 Validations of the new yield displacement model

In order to validate the proposed new yield displacement model, the FEM developed in Chapter 3 is used. There are three validation stages. The first stage is to validate the yield displacements predicted by the FEM and the proposed model using a series of previous experimental pushover test results. The second stage is to validate the proposed yield displacement model with the Nonlinear Time–History Finite Element (NLTH-FE) analysis of a circular RC bridge pier subjected to various earthquake conditions. The third stage is to validate the proposed model with the NLTH-FE analysis of a completed RC bridge with circular piers under the Imperial Valley (USA) earthquake.

4.3.1 Validation using a series of the experimental pushover tests
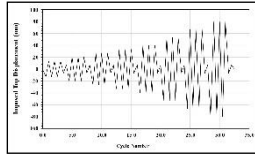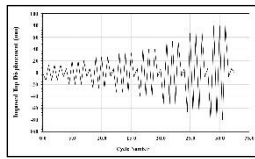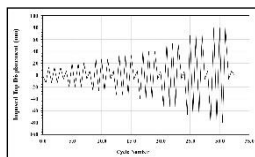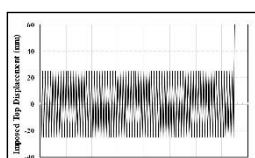
The details of the pushover tests used in this validation are summarised in Table 4.2. All the material properties and geometries of the specimens in the tests were used as input data for the proposed model and the FEM. In both experiment, the yield displacement results were determined based on yield limit state that depends on the longitudinal reinforcement strain. The displacement transducer were applied on the RC bridge pier in order to determine the longitudinal reinforcement strain.

Firstly, the tests conducted by Lehman *et al*. (2004) were employed. Lehman *et al.* (2004) conducted a series of experimental tests to evaluate the seismic performance of RC bridge piers. Two specimens: P415 and P430, were used. Figures 4.4(a) and 4.4(b) illustrated the comparisons between the experimental, FEM and proposed model's results. It can be seen from the figure that the two results are in good agreement.

Secondly, the tests carried out by Kunnath *et al.* (1997) were modelled. In these tests, two specimens: A2 and A3 were used. Figures 4.5(a) and 4.5(b) show the comparisons between the experimental, FEM and proposed model's results. From the figure, again, the yield displacements predicted by the FEM and proposed model are in good agreement with the test results. It is evident that the proposed model can be used to predict the yield

displacement of the pier with reasonable accuracy. Table 4.3 gives the yield displacements predicted by the FEM and proposed model, together with the test results.

Table 4.2 Details of the pushover tests

References	Specimens	Loading Condition	$f_c^{'}$ (MPa)	ρ	ρ_s	Axial Load
Lehman *et al.* (2004)	P415		30	22 H16 (1.5%)	0.70%	0.1
	P430		32	44 H16 (1.5%)	0.70%	0.1
Kunnath *et al.* (1997)	A2		29	21 H10	1%	0.1
	A3		29	21 H10	1%	0.1
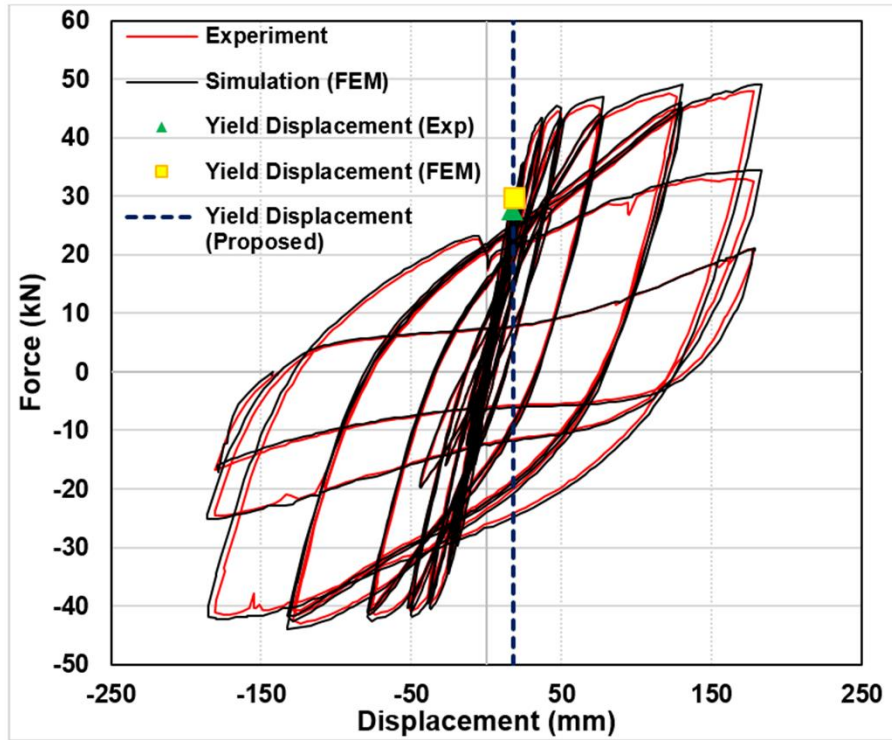
(a)
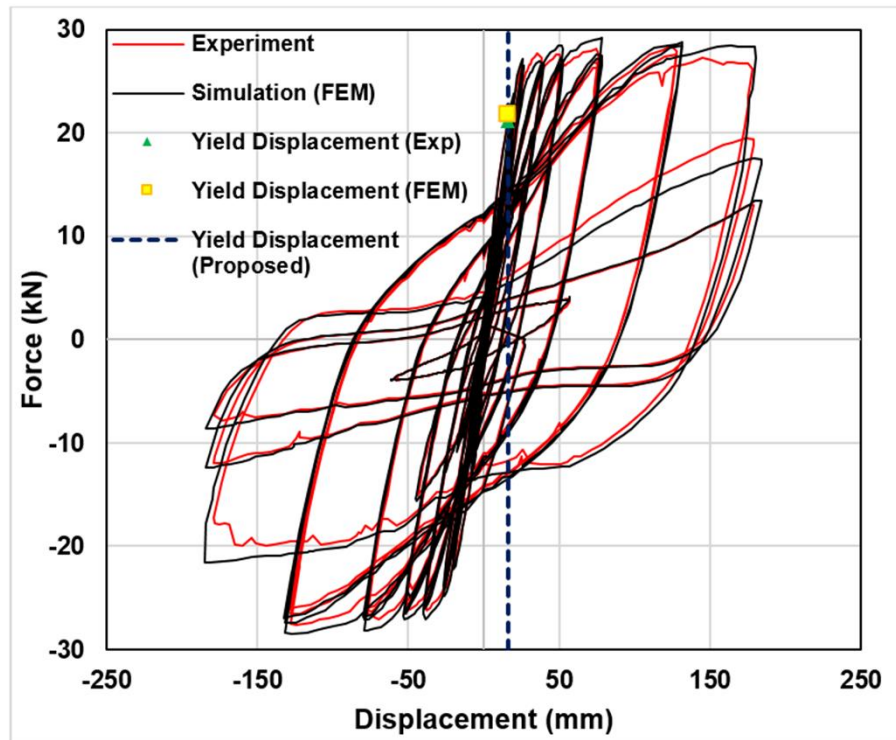
(b)

Figure 4.4 Comparisons of the experimental, FEM and test results (Lehman *et al.*, 2004): (a) P430 and (b) P415
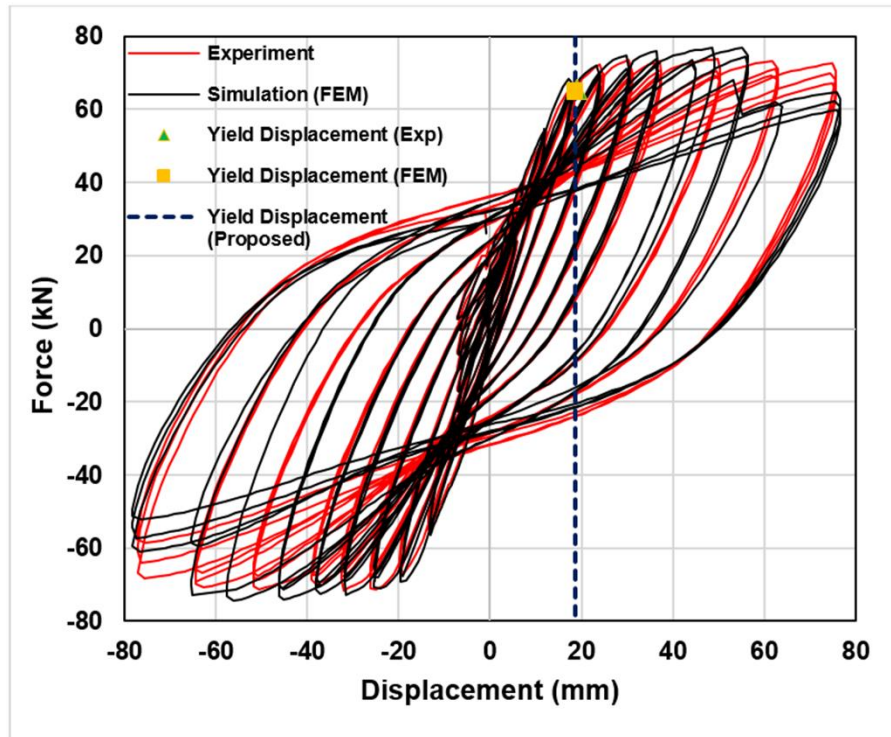
(a)
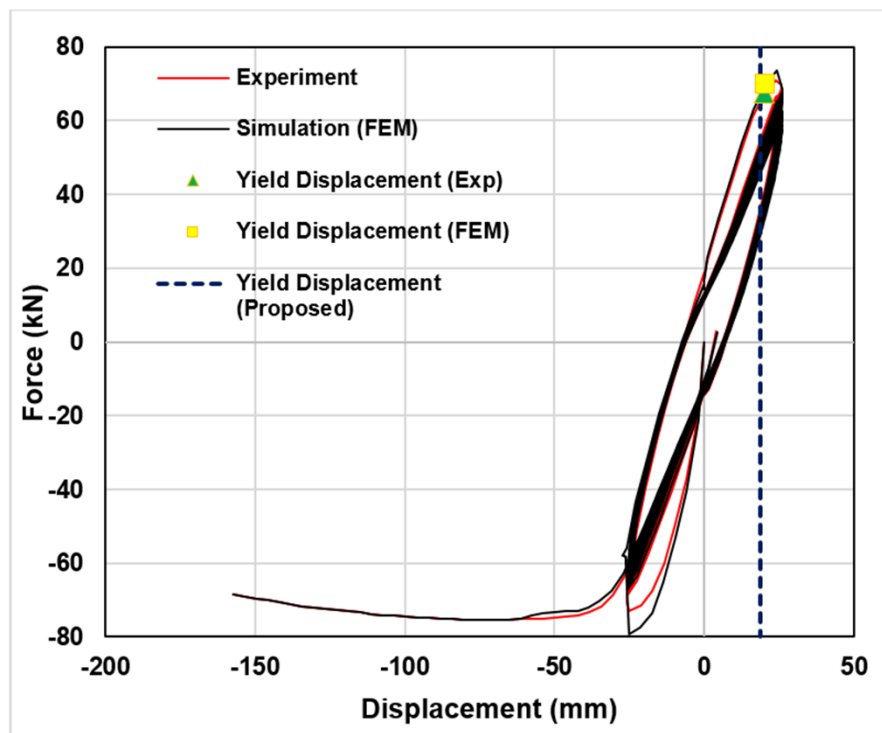
(b)

Figure 4.5 Comparisons of the experimental, FEM and test results (Kunnath *et al.*, 1997): (a) A2 and (b) A3

Table 4.3 The yield displacements predicted by the FEM and proposed model, together with the experimental test results.

References	Specimens	Experiment	FEM	Proposed model
Lehman *et al.* (2004)	P415	16.1 mm	16.65 mm	16.3 mm
	P430	16.8 mm	18.56 mm	18.1 mm
Kunnath *et al.* (1997)	A2	19.0 mm	18.36 mm	18.7 mm
	A3	19 mm	19.61 mm	18.7 mm

4.3.2 Validation using NLTH-FE analysis of a circular RC bridge pier

In this section, a circular RC bridge pier is established to study the responses of the pier subjected to different earthquake excitations. The RC bridge pier is subjected to different earthquakes ground motions records. The results from the NLTH-FE analysis are used to validate the proposed model's predictions. Table 4.4 highlights the details of the pier.

In this study, ground motions records from the 1989 Loma Prieta earthquake, 1999 Kocaeli earthquake, and the 1999 Chi-Chi earthquake were used in the simulation as the input ground motions for NLTH-FE analysis. The ground motions details and characteristics of the earthquakes used in this analysis are presented in Table 4.5.

The time-histories of the earthquake ground motions were converted to spectrum-compatible time-histories generated using SeismoArtif (Seismosoft, 2016) (available online) to make sure that the spectrum of the real accelerogram records is compatible with the EC8 design accelerogram spectrum (CEN, 2004b). The time-history data were scaled to generate the displacement spectra, which match type C with 5% damping with respect to EC8, as generally used in the DDBD method. Based on the DDBD method, the yield displacement of an RC bridge pier depends on the yield strain of longitudinal reinforcement. Hence, for NLTH-FE analysis, the yield displacement of the RC bridge pier is obtained when the longitudinal reinforcement bars reach the strain limit of 0.0021 ($\varepsilon_y = f_{ye}/E_s$), where E_s is the modulus of elasticity of longitudinal reinforcement.

Table 4.4 The details of the circular RC bridge pier

Parameter	Value	Remarks
Pier diameter (m)	1.0	-
Pier height (m)	3.50	-
Strain penetration length [L_{sp} (m)]	0.288	Eqn. (4.10)
Cover (mm)	50	-
Longitudinal Reinforcement (mm)	11 H32	1.12%
Axial load (kN)	5301	0.1
Concrete strength [$f_c^{'}$ (MPa)]	30	-
Longitudinal reinforcement yield strength [f_{ye} (MPa)]	420	-
Longitudinal reinforcement ultimate strength [f_{ye} (MPa)]	469	-

Table 4.5 The ground motions details and characteristics of the earthquakes used

Test	Earthquake	Year	Magnitude	Station	PGA (g)
EQ1	Loma Prieta (USA)	1989	6.9	090 CDMG Station	0.355
EQ2	Kocaeli (Turkey)	1999	7.6	YARIMCA (KOERI330)	-0.361
EQ3	Chi-Chi (Taiwan)	1999	7.6	TCU045	-0.349

Figure 4.6 shows the displacement–time responses of the RC bridge pier under different earthquake excitations: EQ1, EQ2, and EQ3. In EQ1, the RC pier reached a yield displacement of 21.14 mm, when the strain of the longitudinal reinforcement reached 0.0021. The corresponding yield displacement predicted by the proposed model was 22.70 mm, as highlighted in Figure 4.6(a). It is shown that the proposed model can reasonably predict the yield displacement of the pier on a moderate magnitude of the earthquake.

In EQ2, the NLTH-FE analysis predicted a yield displacement of 22.58 mm. This yield displacement was reached when the displacement–time response was at 7.16 s. The yield displacement occurred at the earlier stage of the earthquake when the acceleration of ground motions reached 0.0103 g. The corresponding yield displacement predicted by the proposed model was 22.70 mm, as highlighted in Figure 4.6(b). It is evident that the proposed model gives a reasonable prediction of the yield displacement of the pier for this type of earthquake.

In EQ3, the NLTH-FE analysis provided a yield displacement of 22.54 mm. This yield displacement was reached when the time of earthquake excitation was at 22.69 s. This phenomenon occurred due to the early stage of the Chi-Chi earthquake; the acceleration of ground motions was between 0.002 and 0.004 g. Therefore, the longitudinal reinforcement reached the strain of 0.021 when the acceleration of ground motions was −0.011 g. The corresponding yield displacement predicted by the proposed model was 22.70 mm, as highlighted in Figure 4.6(c). It is evident from the figures that the results generated by the proposed model agreed reasonably with the NLTH-FE analysis.

(a)

71
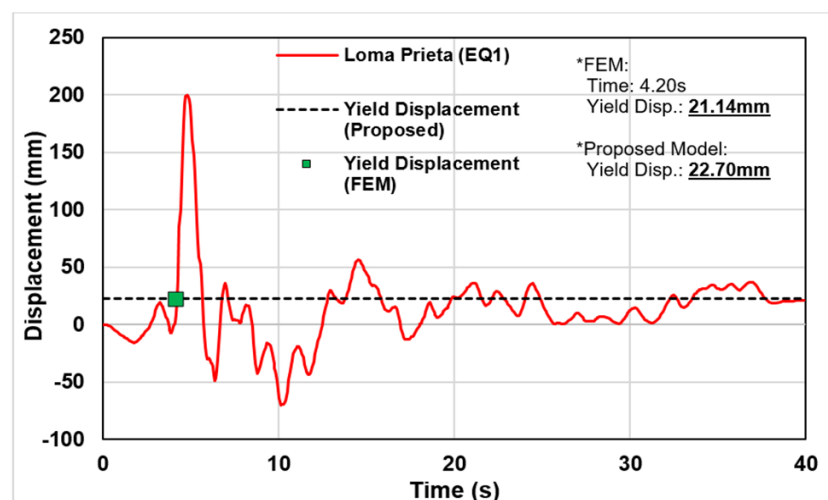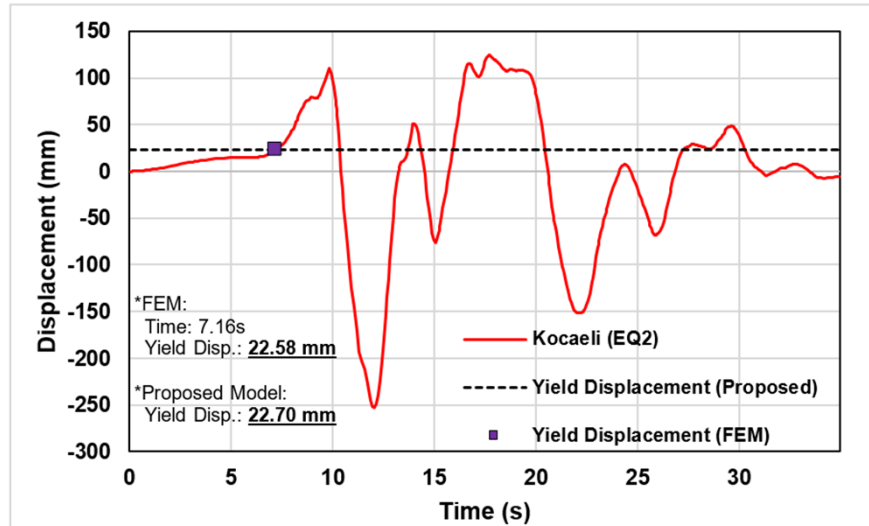
(b)
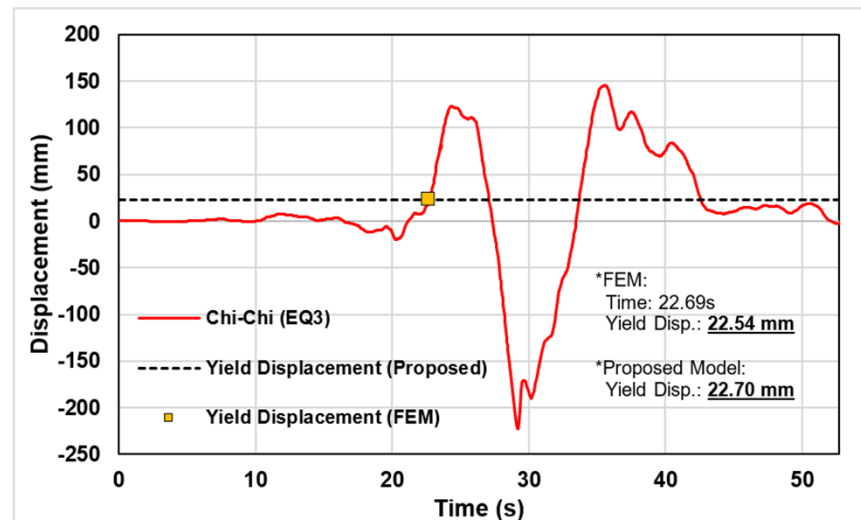
(c)

Figure 4.6 Displacement–time response of RC bridge pier subjected to the earthquake:

(a) EQ1; (b) EQ2; and (c) EQ3

4.3.3 Validation using NLTH-FE analysis of a completed RC bridge with circular pier

In this section, a four-span continuous RC bridge with circular piers was established to determine the yield displacements under the Imperial Valley (USA) earthquake. The detail of the Imperial Valley earthquake is highlighted in Figure 4.7. Figure 4.8 highlights the elevation view of a typical four-span (40-50-50-40 m) continuous RC bridge with an abutment at both ends. The RC bridge consists of three piers, where the height for Piers 1 and 3 was 10.0 m, and Pier 2 was 15.0 m. The RC bridge pier diameter was 1.5 m. The

diameter of the longitudinal reinforcement was 32 mm for all three piers. As to validate the proposed model, the details for concrete strength, axial load ratio, and longitudinal reinforcement ratio is required and presented in Table 4.6.
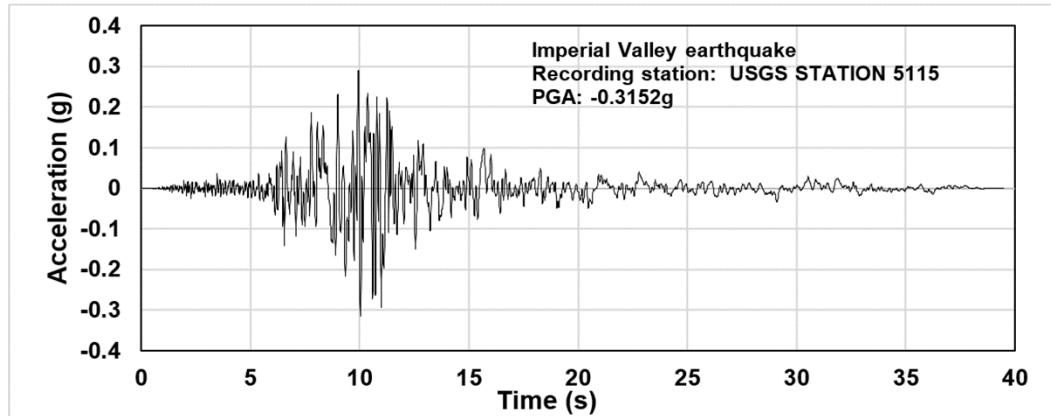
Figure 4.7 Imperial Valley ground motion
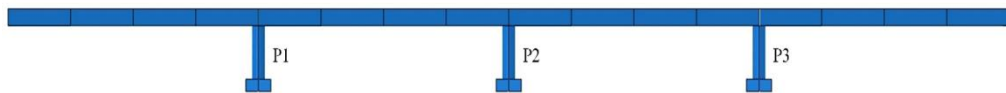
Figure 4.8 Elevation view of four-span RC continuous bridge (Not to scale)

The displacement–time responses for the RC bridge are presented in Figure 4.9. As observed, NLTH-FE analysis could predict the yield displacement subjected to the Imperial Valley earthquake for all three RC bridge piers with reasonable accuracy. According to Figure 4.9(a), the yield displacement for Pier 1 from NLTH-FE analysis was approximately 109.07 mm, when the time of the response reached 7.57 s. This prediction was determined based on the strain limit of the RC bridge pier, specifically longitudinal reinforcement strain limit reached 0.0022.

The corresponding yield displacement calculated from the proposed model was 110.70 mm, with a percentage difference of less than 1.5%. As shown in Figure 4.9(b) for Pier 2, the yield displacement from NLTH-FE analysis was approximately 244.15 mm, slightly higher compared to the proposed model, 243.10 mm. However, these outcomes are within an acceptable range of accuracy, where the percentage difference was less than 1%.

For Pier 3, the yield displacement from NLTH-FE analysis was approximately equal to Pier 1, which was 109.81 mm, as shown in Figure 4.9(c). Based on the same material

details, the yield displacement for the proposed model was similar to Pier 1, 110.70 mm. Again, a good agreement between the NLTH-FE analysis and the proposed model was achieved. It is evident that the proposed model can be used to predict a yield displacement for a range of parameters with reasonable accuracy.

Table 4.6 The details of the RC bridge

Parameter	Pier 1	Pier 2	Pier 3	Remarks
Pier diameter (m)	1.5	1.5	1.5	-
Pier height (m)	10.0	15.0	10.0	-
Strain penetration length [L_{sp} (m)]	0.213	0.136	0.213	Eqn. (4.10)
Cover (mm)	50	50	50	-
Longitudinal Reinforcement (mm)	44 H32	44 H32	44 H32	2%
Transverse Reinforcement (mm)	8mm	8mm	8mm	Spacing 100mm c/c
Axial load (kN)	Load from RC bridge decks			0.1
Concrete strength [$f_c^{'}$ (MPa)]	30	30	30	For pier and foundation
Longitudinal reinforcement yield strength [f_{ye} (MPa)]	420	420	420	-
Longitudinal reinforcement ultimate strength [f_{yeu} (MPa)]	469	469	469	-
Transverse reinforcement yield strength [f_{yh} (MPa)]	420	420	420	-
Transverse reinforcement ultimate strength [f_{yhu} (MPa)]	469	469	469	-
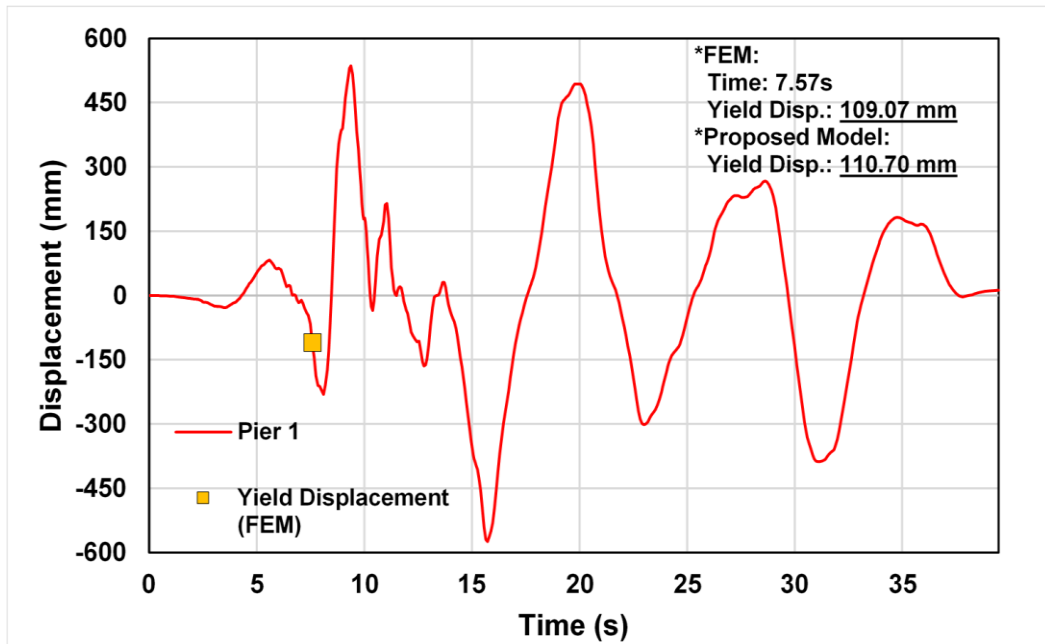
(a) Pier 1
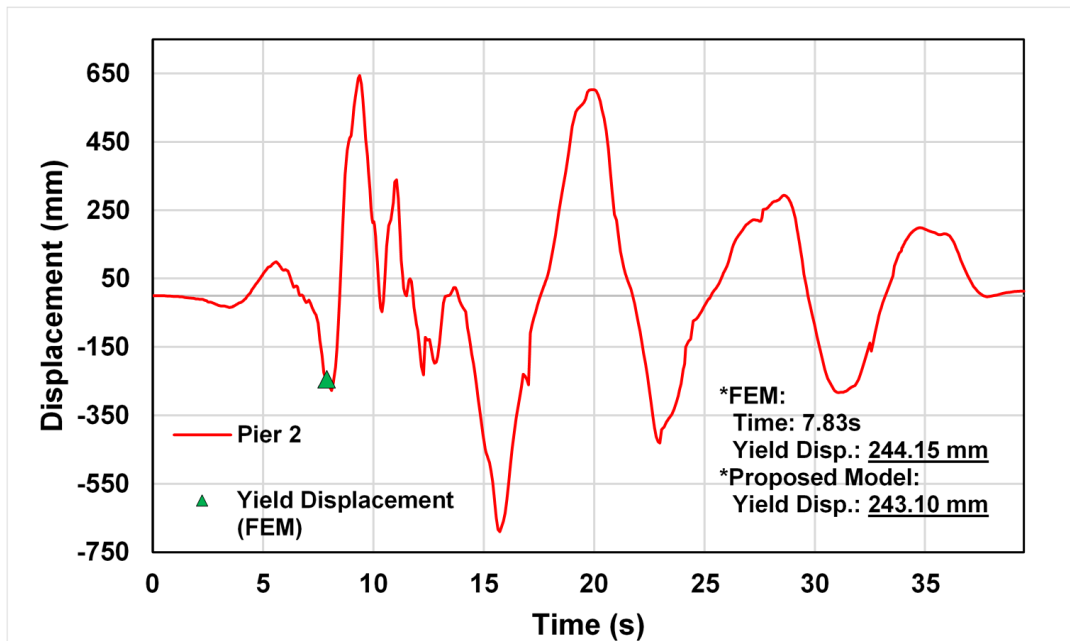
(b) Pier 2
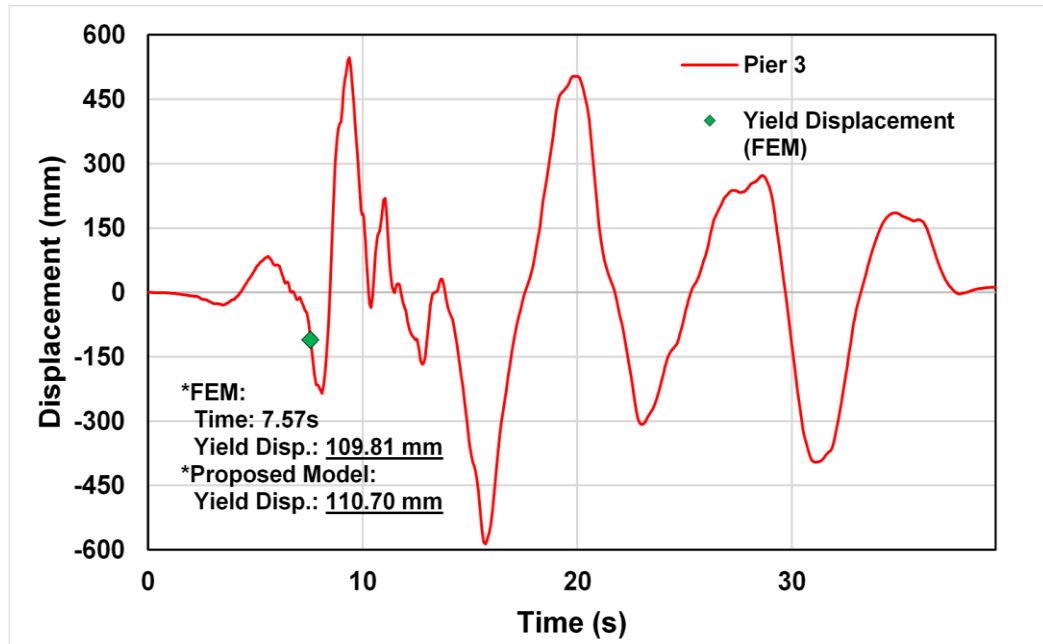
(c) Pier 3

Figure 4.9 Displacement–time response of RC continuous bridge subjected to earthquake, (a) Pier 1; (b) Pier 2 and (c) Pier 3

4.4 Parametric studies

In this section, the influences of different parameters, such as the RC bridge pier height, RC bridge pier diameter, concrete strength, longitudinal reinforcement ratio, and axial load ratio on the estimation of the yield displacement of circular RC bridge pier, are investigated. For this purpose, a simple SDOF cantilever circular RC bridge pier with the heights of 5–25 m, the diameters of 0.5–2.5 m, and reinforcement yield strain of 0.0021 were considered. The strain penetration length developed by Goodnight *et al.* (2016) was considered to determine the effective RC bridge pier height for the proposed model. Previous analytical model (Model A) (M.A) (Priestley *et al.*, 2007) and the currently developed model (Model B) (M.B) are used to predict the yield displacement of the circular RC bridge piers.

4.4.1 The influence of the sectional diameter and effective height

In the previous study, the previous researcher (Priestley *et al.*, 2007) had considered the effective height, including strain penetration for yield displacement estimation. Some researchers (Kowalsky *et al.*, 1995; Tecchio, 2013; Khan *et al.*, 2014) also reported that strain penetration into the foundation depends on the diameter and the yield strength of

76

longitudinal reinforcement, to estimate yield displacement. In this section, the influence of sectional diameter and the effective height of the RC pier on the predictions of yield displacement were examined using different values of section diameter and effective height of the RC piers. In this case, the concrete compressive strength of 30 MPa, axial load ratio of 0.1 (590 – 14727 kN varies depending on the diameter of the pier), and the longitudinal reinforcement ratio of 1% was considered. Figure 4.10 shows the predicted yield displacement of the pier against the pier heights and different pier sectional diameters. Based on the figures, the yield displacement predicted by the proposed model was slightly lower compared to that of the previous model. This phenomenon occurred due to the consideration of an improved strain penetration length. The yield curvature for the proposed model was slightly higher due to the consideration of additional parameters: concrete strength, axial load ratio, and longitudinal reinforcement ratio. Therefore, both strain penetration length and effective yield curvature contribute to the lower yield displacement. From Figure 4.10, it is evident that the new parameters introduced for yield curvature and strain penetration in Model B show considerable impacts for the diameter of 1.5 to 2.5 m. It can be seen that the effective pier height and sectional diameter have considerable influences on the predictions of the yield displacement of the pier. In general, the predictions of Model A are higher compared to the predictions of Model B.
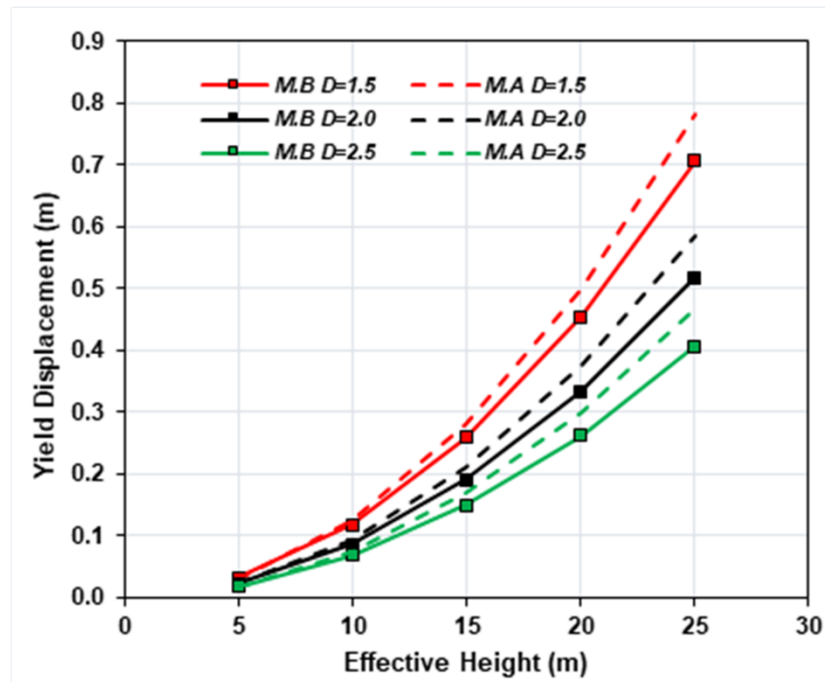
(a)
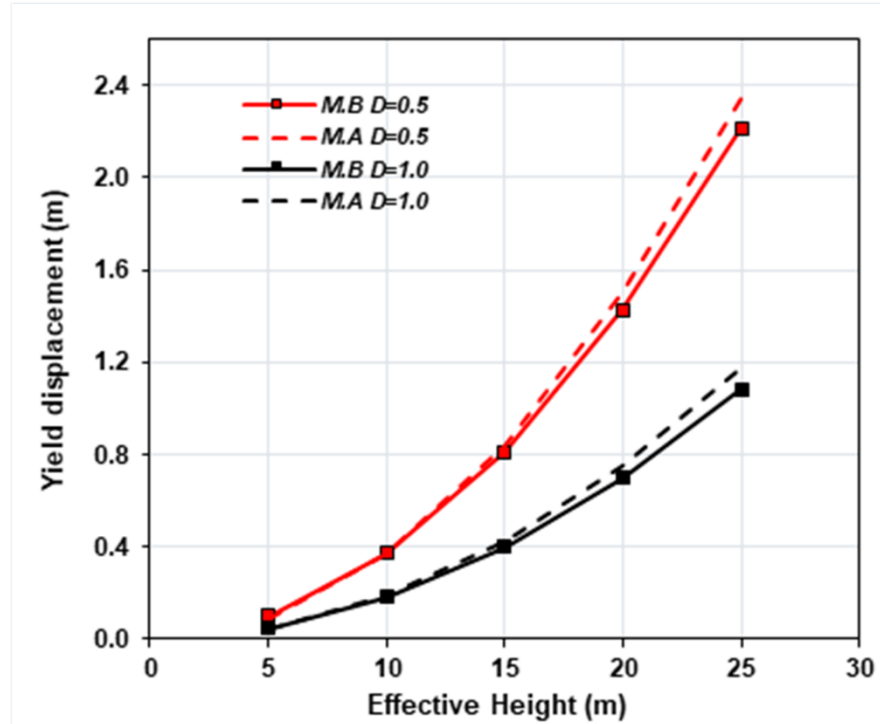
(b)

Figure 4.10 Influence of pier height and sectional diameter on the yield displacement:

(a) 1.5m ≤ D ≤ 2.5m; (b) 0.5m ≤ D ≤ 1.0m

4.4.2 The influence of concrete strength

The influence of concrete strength on the predicted yield displacement of the RC pier is investigated in this section. In this case, the sectional diameter and the height of the piers used were 1.0–2.0 m and 10–15 m, respectively. The axial load ratio of 0.1 (2357–31416 kN; varies depended on concrete strength) and the longitudinal reinforcement ratio of 1% were considered. The concrete strengths ranged from normal-strength concrete to high-strength concrete were considered for predicting the yield displacement.

As shown in Figure 4.11, the concrete strength has considerably influences on the prediction of yield displacement in Model B. However, the influence of concrete strength was ignored in Model A. From the figures, the yield displacement predicted by Model B increased with increasing concrete strength. By looking at this figures, it shows that previous model is not being critical, where the influence of concrete strength was ignored. Also, these results highlight that the concrete strength plays a vital role in determining yield displacement. Every type of concrete strength provides different types of compressive (inelastic strain) and tensile behaviour (cracking strain). By increasing the

78

concrete strength, the capacity of RC bridge pier can withstand more loads. Therefore, it will provide higher yield displacement. It is evident from the figures that the influence of concrete strength contributes significantly to determine the yield displacement. Hence, it is shows that previous model required further modification, as describe in current proposed model (Model B).
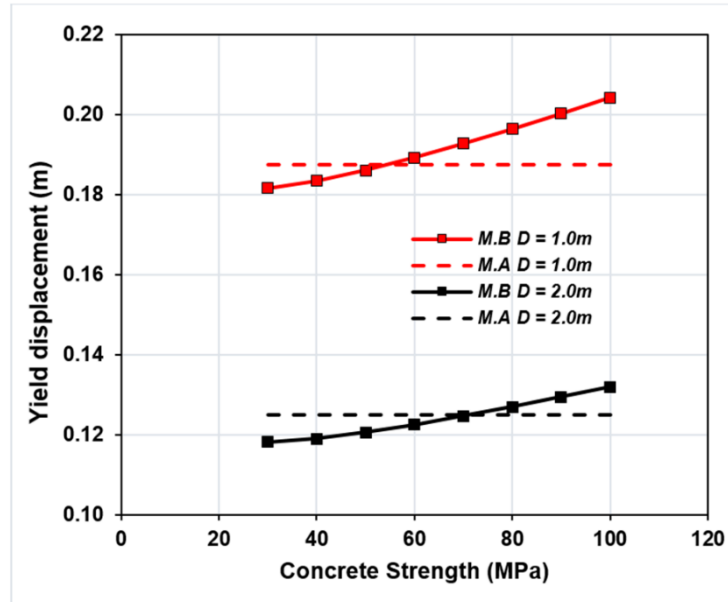
(a)
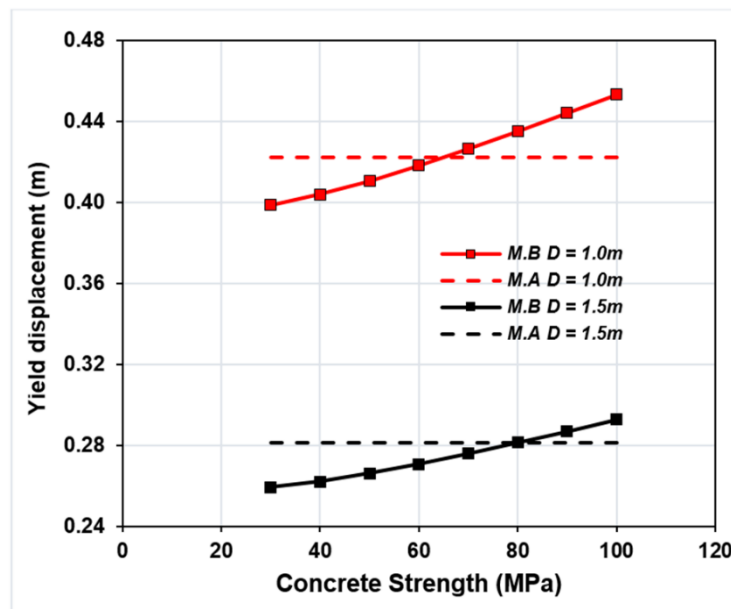
(b)

Figure 4.11 Influence of concrete strength, $f_c^{'}$ on yield displacement: (a) Pier height = 10m; (b) Pier height = 15m

4.4.3 The influence of axial load ratio

The influence of the axial load ratio on the prediction of yield displacement for the RC bridge pier is presented in this section. The other assumed parameters were pier height =10 m, sectional diameter D =1.5 m, and longitudinal reinforcement ratio = 1%. In this study, three concrete strengths of 30, 60, and 80 MPa were considered. The normal range of axial loads of 0.1 to 0.2 was considered based on common practices. However, high levels of axial load ratio were also considered to examine the impacts on the yield displacement. Many pieces of research considered high levels of axial load ratio even though it is unusual to be used in practice (Billah and Alam, 2016). Figure 4.12 shows the influences of the axial load ratio on the predictions of yield displacement of RC bridge piers.

In Model B, the influence of the axial load ratio on the predictions of yield displacement increased significantly, especially when the axial load ratio was less than 0.4. After the axial load ratio reached 0.4, the predicted yield displacement of the pier decreased significantly with increasing axial load ratio. A similar observation was found in previous research (EL-Attar *et al.*, 2016). This outcome is due to the effective yield curvature decreasing when the axial load increased. However, this phenomenon is related to the consideration of concrete strength. When normal strength concrete (30 MPa) was considered, the yield displacement started to decrease when the axial load ratio was at 0.2. Therefore, the yield displacement predicted by Model B was lower compared to that of the previous model.

For the high-strength concrete (80 MPa), the yield displacement predicted by the proposed model was higher compared to that of the previous model when 0.1–0.6 axial load ratio was considered. Therefore, the consideration of the axial load ratio along with concrete strength is significant to provide an accurate yield displacement for RC bridge piers. It is clear that the axial load ratio and concrete strength play a vital role in estimating the yield displacement.

(a)

(b)

81
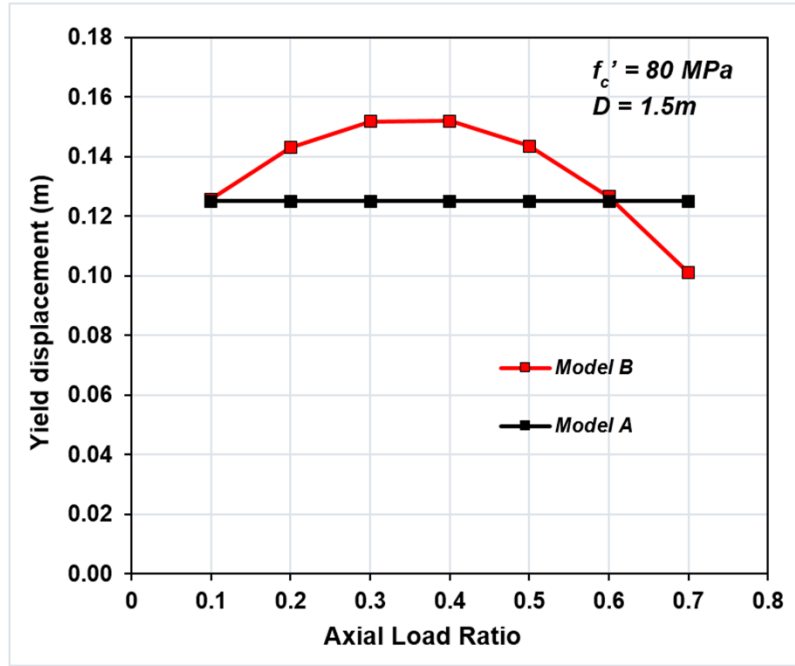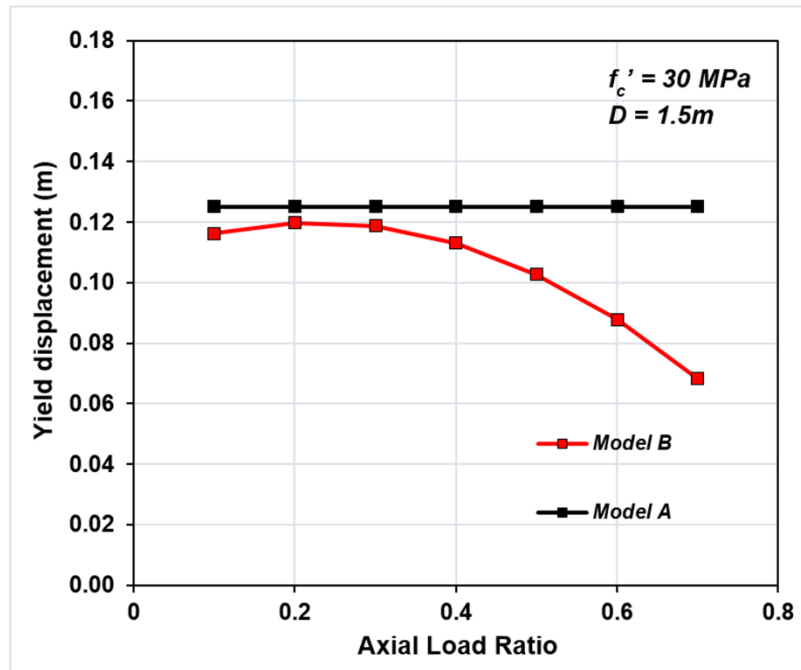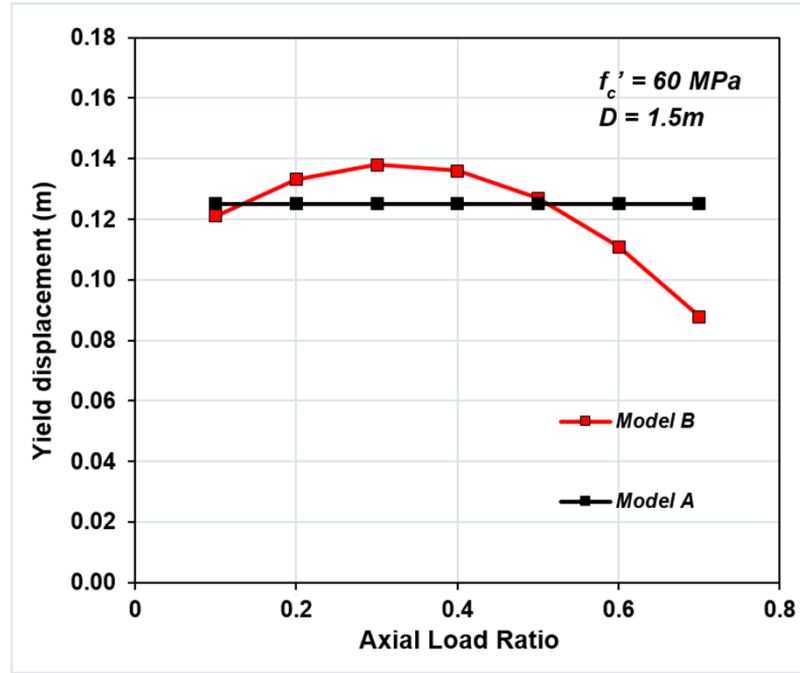
(c)

Figure 4.12 Influence of axial load ratio on yield displacement with $D = 1.5$ m: (a) $f_c' = 80\ MPa$; (b) $f_c' = 30\ MPa$; (c) $f_c' = 60\ MPa$

4.4.4　The influence of longitudinal reinforcement ratio

The impact of longitudinal reinforcement ratio on the yield displacement has been ignored in previous research. However, some recent research identified the influence of longitudinal reinforcement on determining the yield curvature of circular RC bridge piers (Sheikh *et al.*, 2010). In this section, the influence of the longitudinal reinforcement ratio on the prediction of the RC bridge pier was investigated. To explore the influence of the longitudinal reinforcement ratio on the yield displacement, six different ratios were considered (1%–6%). Other parameters used were: concrete strength = 30 MPa, axial load ratio = 0.1 (5302 kN), and pier height = 10 m. Figure 4.13 shows the influence of the longitudinal reinforcement ratio on the predicted yield displacement. From the figure, the yield displacement predicted by Model B increased considerably with increasing longitudinal reinforcement ratio. This is because by providing more longitudinal reinforcement, the strength of the RC bridge pier increased considerably. Furthermore, the reinforcement is good in tensile strength, and it provides enough ductility to prevent failure due to earthquakes.

82

(a)

(b)

83
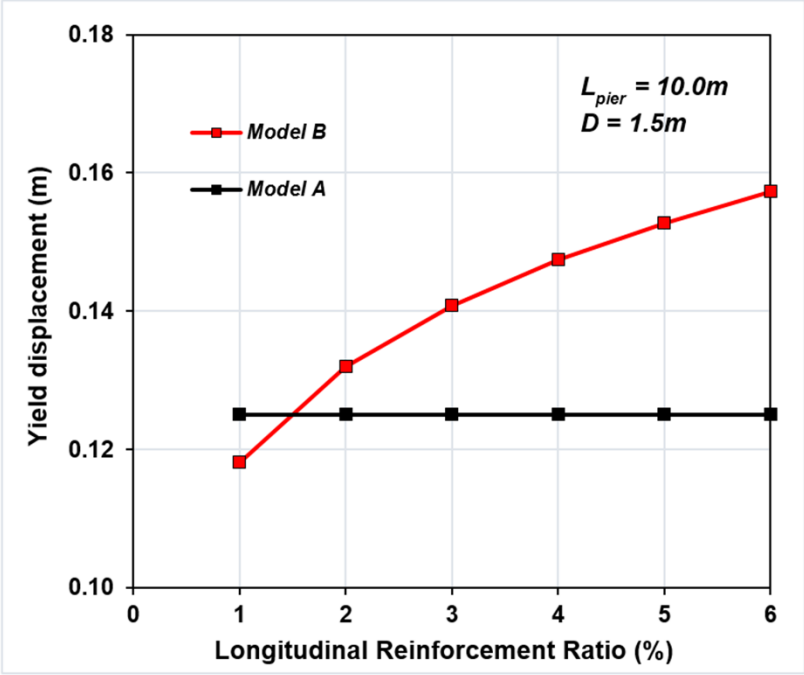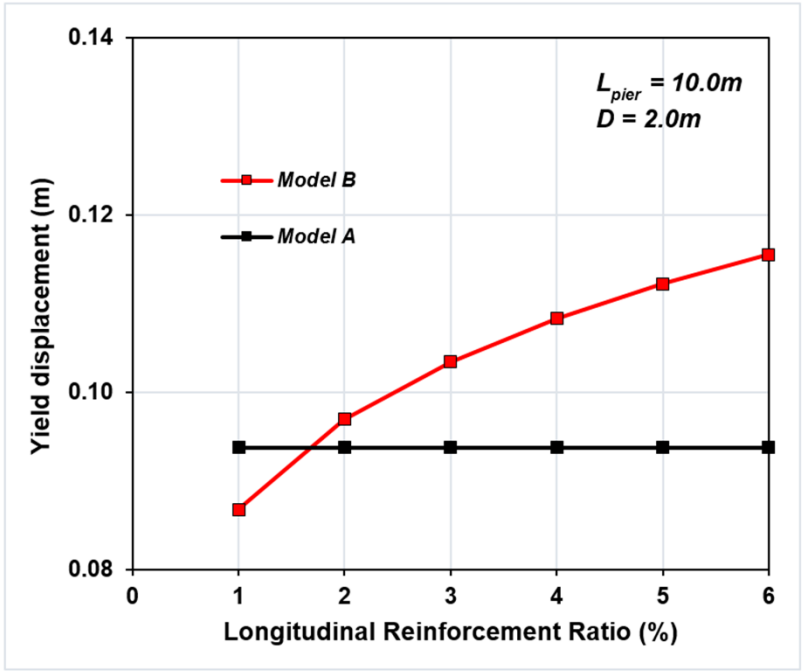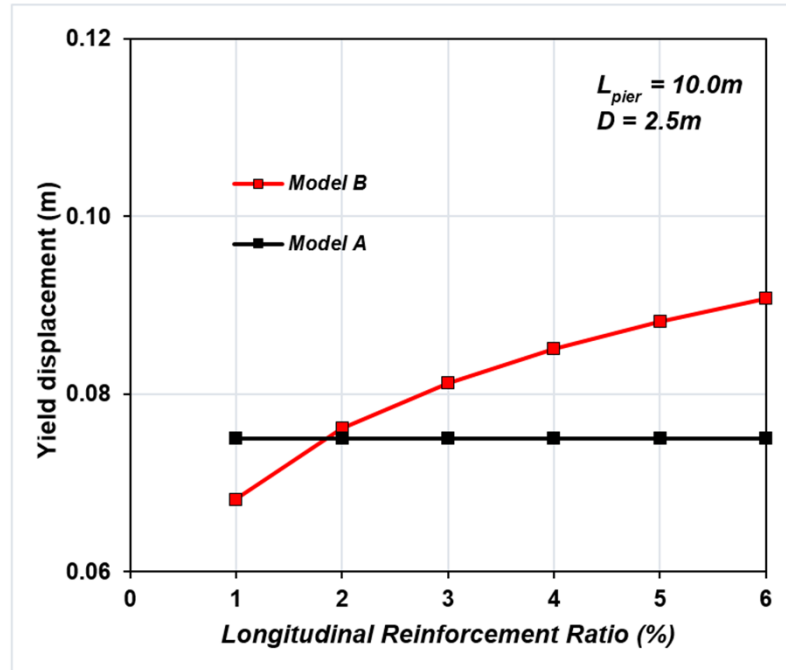
(c)

Figure 4.13 Influence of longitudinal reinforcement ratio on the yield displacement of the pier with pier height =10 m: (a) *D*=1.5 m; (b) *D*=2.0 m; (c) *D*=2.5

Hence, the yield displacement of the pier increased significantly. The combination with high concrete strength that holds more compressive forces ensures the structures can resist heavy loads and withstand earthquakes. Therefore, in real engineering practices, 1%–3% of the longitudinal reinforcement ratio is normally adopted to avoid the congestion of reinforcement in an RC bridge pier.

4.5 Conclusion

In this chapter, an analytical model has been developed for predicting the yield displacement of circular RC bridge piers for the DDBD method. The proposed model utilised effective yield curvature where new parameters are introduced: concrete strength, axial load ratio, and longitudinal reinforcement ratio. Moreover, a modified plastic hinge length region (strain penetration length) is considered to enhance the effective RC bridge pier height, thus estimated an accurate yield displacement. A series of RC bridge piers previously tested under cyclic loading (pushover test) were selected to validate the proposed model. The yield displacement was estimated through the force–displacement response and was compared with the proposed model. A series of validation subjected to a seismic loading were conducted to evaluate the proposed model of yield displacement.

Extensive parametric studies were conducted to evaluate the influence of several parameters on the prediction of the yield displacement of RC bridge pier. Some conclusions can be drawn as follows:

1) The proposed model predicts the reasonable values of the yield displacement of the pier under the cyclic loading. The values predicted by the proposed model were almost identical to the experimental results of the pushover tests. Therefore, the proposed model is able to predict the yield displacement for RC bridge piers under seismic loading condition.

2) The proposed model provides the reasonable values of the yield displacement of circular RC bridge pier subjected to earthquake loadings. Based on the displacement–time response figures, the influences of concrete strength, axial load ratio, longitudinal reinforcement ratio, and strain penetration length on the yield displacement of the RC bridge pier are significant. The yield displacement predicted by the NLTH-FE model subjected to earthquake loadings nearly equal to the proposed model.

3) The response of the RC bridge subjected to earthquake loadings provides a reasonable agreement between NLTH-FE results against the proposed model. For all three piers, the yield displacement estimated by the proposed model matched closely with the FEM results. It is evident that the proposed model can be used to estimate the yield displacement of the circular RC bridge pier.

4) The parametric studies were conducted, and the results are summarised as follows:
   - The effective pier height and sectional diameter have considerable influences on the predictions of the yield displacement.
   - It is crucial to consider concrete strength in the estimation of yield displacement. It shows that previous model is not being critical, where the influence of concrete strength was ignored. By considering and increasing the concrete strength, the capacity of the RC bridge pier increases, and the pier can survive more loads. Therefore, it will provide a significant value of the yield displacement. Hence, it is shows that previous model required further modification, as describe in current proposed model (Model B).
   - The consideration of axial load ratio along with concrete strength is essential to provide an accurate yield displacement for RC bridge pier.

- By increasing the longitudinal reinforcement, the yield displacement increases. This is because reinforced concrete has tensile and compressive strength, therefore manage to withstand the heavy load.

Chapter 5

A New Model to Predict the Damage-Control Target Displacement of RC Bridge Pier for DDBD Method

Based on the literature review presented in Chapter 2, there is a need to develop a new model to more accurately predict the damage-control target displacement of a circular RC bridge pier for DDBD method. The model needs to consider the influence of damage limit states and material strain limit on the damage-control target displacement.

5.1   Introduction

For seismic design of RC bridge, the displacement-based design method had been developed over the past decades in order to overcome the limitations of the force-based design (FBD) method (Kappos *et al.*, 2012; Samy Muhammad Reza, 2012; Calvi *et al.*, 2013; Sadan *et al.*, 2013; Reza *et al.*, 2014). The displacement-based design method relies on the design limit state and performance level (Priestley *et al.*, 2007). The fundamental theory of this method is to design the structures that are capable of achieving specific performance levels and design limit states under specific seismic intensity. As mentioned in Chapter 2, the structural performance levels can be classified into four categories (Priestley *et al.*, 2007). Recent researches indicate that for economic reasons, it is crucial to consider the "damage-control" performance level for seismic design structures (Priestley *et al.*, 2007; Suarez, 2008; Mackie *et al.*, 2010). At present, the "damage-control" performance level is not explicitly expressed in most seismic design codes; however, these criteria are presented in some design codes in terms of material strains, such as concrete compressive and steel reinforcement tensile strain limits.

In order to observe the "damage-control" performance level, understanding the relationship between structural performance level and limit state of a structure is crucial. In general, the structural performance is not limited to the life-safety level but is also focused on more restrictive limit states, such as damage-control limit state and serviceability limit state (Kowalsky, 2000; Kong, 2017). Damage-control represents the limit of the structure for economical repair or if the damage is repairable after seismic events. The damage-control limit state (DCLS) is significant to ensure the structures are in good condition, where if the structure's damage exceeds this limit state, the cost of

repair may be impracticable and uneconomical. To ensure the structural performance level can be controlled during an earthquake event, it is essential to consider DCLS as the design limit state. DCLS is used to ensure that the damage of structures is acceptable, and the repairable cost is less than the cost of building a new structure. For the RC bridge pier, the concrete spalling, buckling of longitudinal reinforcement, and breaking both transverse and longitudinal reinforcements should be avoided.

For direct displacement-based design (DDBD), the DCLS is used to determine the target displacement for damage-control. DCLS is governed by material strains, such as the ultimate concrete compression strain and ultimate reinforcement tensile strain. Currently, several models have been developed to investigate the material strains' limits for the RC bridge pier. By using the energy balance approach developed by Mander *et al.* (1988), the ultimate concrete reinforcement strain can be estimated (Goodnight, 2015; Abdul Halim *et al.*, 2018). However, presently, the models for prediction of the ultimate reinforcement limit strain for the RC bridge pier are still very limited (Kowalsky, 2000; Goodnight, 2015; Goodnight *et al.*, 2016b).

In the DDBD method, the seismic design of a bridge is performed by specifying the target displacement (Kowalsky *et al.*, 1995). The target displacement can be selected based on the material strain's limits that are correlated to the preferred damage level. To ensure the target displacement is based on the preferred damage level, a damage-control target displacement $\Delta_{T,DC}$ is required. Damage-control target displacement is determined based on the material strain's limits that are defined from DCLS. Previous research (Priestley *et al.*, 2007) indicated that $\Delta_{T,DC}$ could be defined as the "target displacement" when the damage-control concrete compression strain reaches 0.018, and the damage-control tension strain of flexural reinforcement reaches 0.06. Damage-control target displacement is then determined using the plastic hinge method (Priestley *et al.*, 2007), in which the yield displacement, yield curvature, and damage-control target curvature are required. The conventional approach for seismic bridge design relies on the plastic hinge region, where the formation of the plastic hinge dissipates the energy during seismic events. In an earthquake with higher magnitude, the enormous damage to the plastic hinge can lead to higher substantial repair costs and unrepairable structures.

In recent years, a series of studies on the reinforcement strain limit for single-degree-of-freedom (SDOF) RC bridge pier has been carried out. Goodnight *et al.* (2016b) conducted

a research to improve the steel reinforcement tensile strain limit. In that research, Goodnight *et al.* (2016b) developed a new strain-based bar buckling expression to evaluate the peak tension strain related to bar buckling that occurs on a longitudinal reinforcement bar. Several parameters have been introduced to enhance the reinforcement tensile strain limit estimation. Strain-based bar buckling is then used to evaluate the peak displacement when the bar buckling occurs. Therefore, the accurate displacement of the limit state can be defined based on the concrete compressive strain limit and the steel reinforcement tensile strain.

In this chapter, an attempt has been made to develop a more comprehensive model for predicting the damage-control target displacement, $\Delta_{T,DC}$, of a circular RC bridge pier. The model is based on the integration of the reinforcement strain limit proposed by Goodnight *et al.* (2016b), where the concrete compression strain limit is suggested by Mander *et al.* (1988) and the modified plastic hinge region (Goodnight *et al.*, 2016a). Hence, the main objectives of this chapter are to:

- Develop a new model to calculate the damage-control target displacement of a circular RC bridge pier. The proposed procedure is based on the damage-control limit state (DCLS), and it can be used for seismic design of circular RC bridge pier.
- Validate the proposed model using 3D FEM to model the pushover tests of the RC bridge piers and the NLTH-FE of the circular RC bridge piers subjected to seven earthquake ground motions.
- Conduct a series of parametric studies to investigate the influence of concrete strength and reinforcement ratio on the damage-control target displacement of the circular piers.

5.2   The model development

Previous researches (Goodnight *et al.*, 2013, 2016b; Goodnight, 2015) indicate that damage-control concrete compression strain $\varepsilon_{c,dc}$ and damage-control reinforcement tensile strain $\varepsilon_{s,dc}$ are dependent on the material strength of the concrete and reinforcing steel, reinforcement ratio and the axial load ratio of the RC bridge pier.

As highlighted by Goodnight et al. (2016b), numerous attempts (Hines and Seible, 2002; Moyer and Kowalsky, 2003) have been conducted in order to quantify $\varepsilon_{s,dc}$. Based on an extensive literature review, the model developed by Goodnight et al. (Goodnight, 2015; Goodnight et al., 2016b) is adopted in the proposed model to calculate $\varepsilon_{s,dc}$, that is:

$$\varepsilon_{s,dc} = 0.03 + 700\rho_s \frac{f_{yh}}{E_s} - 0.1\frac{P}{f_c' A_g} \tag{5.1}$$

where, ρ_s is the transverse reinforcement ratio, f_{yh} is the yield stress of transverse steel reinforcement, E_s is the elastic modulus of longitudinal reinforcement, and $\dfrac{P}{f_c' A_g}$ is the axial load ratio of the RC bridge pier. Eqn. (5.1) is based on the peak tension strain before bar buckling during a cyclic analysis of the RC bridge piers. As aforementioned, Goodnight et al. (2016b) had developed this model to determine the strain-based bar buckling in order to determine the peak displacement for the limit state. This equation is used to provide a refined reinforcement tensile strain for the damage-control limit state. This is to ensure, when RC bridges subjected to earthquakes, major damage such as bar buckling can be avoided.

Mander et al. (1988) suggested that the compression of confined concrete can be estimated using the dissipation energy balance approach. Hence, for the determination of $\varepsilon_{c,dc}$, the model developed by Mander et al. (1988) is adopted in the proposed model to calculate $\varepsilon_{c,dc}$, which can be expressed as:

$$\varepsilon_{c,dc} = 0.004 + 1.4\frac{\rho_s f_{yh} \varepsilon_{su}}{f'_{cc}} \tag{5.2}$$

where, ε_{su} is the ultimate strain of steel reinforcement in the transverse direction; and f'_{cc} is the compressive strength of confined concrete, which can be calculated as:

$$f'_{cc} = f'_{cun}\left(2.254\sqrt{1 + \frac{7.94 f_1}{f'_{cun}}} - 2\frac{f_1}{f'_{cun}} - 1.254\right) \tag{5.3}$$

where, f'_{cun} is the compressive strength of unconfined concrete; and f_1 is the confinement stress, which can be expressed as:

$$f_1 = 0.5 \rho_s f_{yh} \tag{5.4}$$

Priestley and Kowalsky (2000) believe that $\varepsilon_{c,dc}$ calculated based on Eqn. (5.2) is conservative. In this research, the proposed model to predict the damage-control target displacement, $\Delta_{T,DC}$, for an RC bridge pier can be expressed as:

$$\Delta_{T,DC} = \Delta_y + \left(\phi_{dc} - \phi_{y,eff} \right) L_{pr} \ L_{eff} \tag{5.5}$$

where, Δ_y is the yield displacement given by Eqn. (4.8), ϕ_{dc} is the damage-control target curvature highlighted in Eqn. (5.6), $\phi_{y,eff}$ is the yield curvature, L_{pr} is the triangular plastic hinge length, and L_{eff} is the effective pier height. The following subsections will give the details for the calculations of Δ_y, $\phi_{y,eff}$, L_{pr}, and L_{eff}.

$$\phi_{dc} = \min \left[\frac{\varepsilon_{c,dc}}{c}, \frac{\varepsilon_{s,dc}}{D-c} \right] \tag{5.6}$$

where, D is the diameter of the RC bridge pier; and c is the neutral axis depth that can be calculated as follows (Priestley *et al.*, 2007):

$$c = 0.2D \left(1 + 3.25 \frac{P}{f'_c A_g} \right) \tag{5.7}$$

where, P is the axial load of the RC bridge pier; f'_c is the concrete compressive strength, and A_g is the gross cross-sectional area of the RC bridge pier. Hence, $\dfrac{P}{f'_c A_g}$ is the axial load ratio of the RC bridge pier.

5.2.1 Effective yield curvature $\phi_{y,eff}$ and yield displacement Δ_y

In recent years, extensive research has indicated that the yield curvature is dependent on the yield strain, sectional diameter, and additional factors, such as axial load ratio, longitudinal reinforcement ratio and the strength of concrete and effective concrete cover (Sheikh *et al.*, 2010). To consider a single RC bridge pier bending in the current model, as shown in Figure 5.1, the effective yield curvature, $\phi_{y,eff}$, is calculated using Eqns. (4.2) to (4.6).

The yield displacement, Δ_y, used in the proposed model is given in Eqn. (4.8). The significant damage of the concrete covers occurs typically in the plastic hinge region. Reducing the damages in the plastic hinge region will avoid transverse bar buckling and reduce the displacement of the RC bridge piers that are subjected to cyclic loading and seismic acceleration.
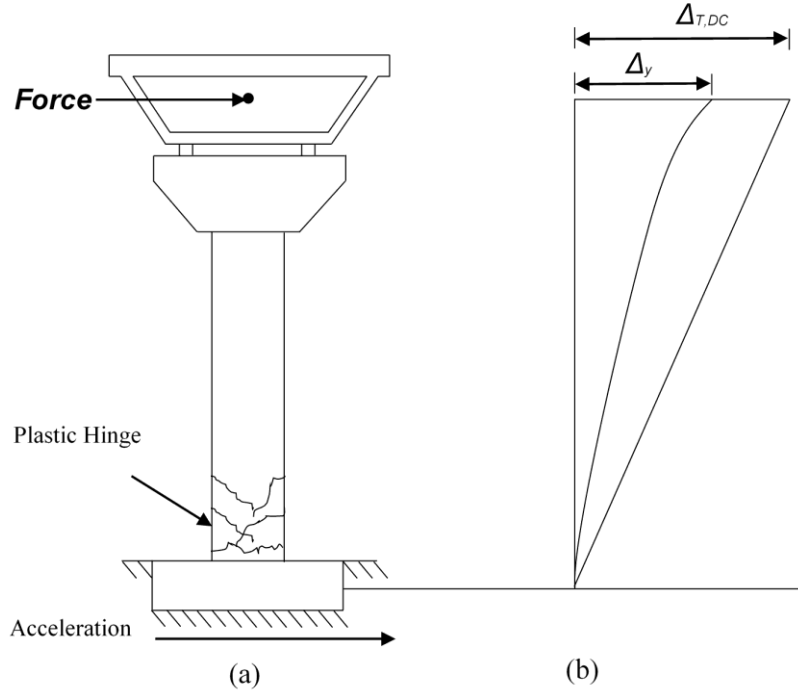
Figure 5.1 A single RC bridge pier.

5.2.2 Triangular plastic-hinge length L_{pr}

Based on the research conducted by Goodnight *et al.* (2016a), the triangular plastic hinge length, L_{pr}, is determined based on which strain limits ($\varepsilon_{c,dc}$ or $\varepsilon_{s,dc}$) govern the damage-control target curvature, ϕ_{dc}, as shown in Eqn. (5.6). If ϕ_{dc} is governed by $\varepsilon_{s,dc}$, then L_{pr} equals to the tensile plastic hinge length, $L_{pr,t}$. If ϕ_{dc} is governed by $\varepsilon_{c,dc}$, then L_{pr} equals to the compressive plastic hinge length, $L_{pr,c}$. $L_{pr,t}$ and $L_{pr,c}$ are represented as:

$$L_{pr,t} = 2kL_c + 0.75D \tag{5.8}$$

$$L_{pr,c} = 2kL_c \tag{5.9}$$

where:

$$k = 0.2\left(\frac{f_u}{f_y} - 1\right) \leq 0.08 \qquad (5.10)$$

$$L_c = L_{pier} \qquad (5.11)$$

where, f_u is the ultimate stress of the longitudinal reinforcement; and f_y is the yield stress of the longitudinal reinforcement. Figure 5.2 shows the flowchart of the proposed model to predict the damage-control target displacement, $\Delta_{T,DC}$ for an RC bridge pier. The proposed model is based on DCLS and several factors, such as the material's strength, stresses, reinforcement ratio, and axial load ratio, are considered.

The calculation steps of the proposed model can be summarised as follows:

(i)   Calculate the effective yield curvature, $\phi_{y,eff}$ (Eqn. (4.2));

(ii)   Calculate the effective length, L_{eff} (Eqn. (4.9)) and strain penetration length, L_{sp} (Eqn. (4.10));

(iii)   Calculate the yield displacement, Δ_y (Eqn. (4.8));

(iv)   Determine the damage-control reinforcement tensile strain limit, $\varepsilon_{s,dc}$ (Eqn. (5.1)) and damage-control concrete compression strain limit, $\varepsilon_{c,dc}$ (Eqn. (5.2));

(v)   Calculate the damage-control target curvature, ϕ_{dc} (Eqn. (5.6));

(vi)   Calculate the triangular plastic hinge length, L_{pr} (Eqns. (5.8) to (5.11)); and

(vii)   Calculate the damage-control target displacement, $\Delta_{T,DC}$ (Eqn. (5.5)).

Damage-Control Limit state

Damage-Control Material Strain

Damage-control concrete strain,

$$\varepsilon_{c,dc} = 0.004 + 1.4\,\frac{\rho_s\,f_{yh}\,\varepsilon_s}{f'_{cc}}$$

Damage-control steel strain,

$$\varepsilon_{s,dc} = 0.03 + 700\rho_s\frac{f_{yh}}{E_s} - 0.1\frac{P}{f'_c\,A_g}$$

Damage Control Curvature,

$$\phi_{dc} = \min\left[\frac{\varepsilon_{c,dc}}{c}, \frac{\varepsilon_{s,dc}}{D-c}\right]$$

Plastic Hinge Length (tensile),

$$L_{pr,t} = 2kL_c + 0.75D$$

Plastic Hinge Length (compression),

$$L_{pr,c} = 2kL_c$$

Strain Penetration Length,

$$L_{sp} = 0.152 \times (1 - \frac{P}{f'_c\,A_g} - \frac{L_{pier}}{16D}) \times \frac{f_y\,d_{bl}}{\sqrt{f'_{ce}}}$$

Plastic Hinge Length

$$L_{pr} \begin{cases} L_{pr,t} & \text{if govern by } \varepsilon_{s,dc} \\ L_{pr,c} & \text{if govern by } \varepsilon_{c,dc} \end{cases}$$

Effective Height,

$$L_{eff} = L_{pier} + L_{sp}$$

Yield Displacement,

$$\Delta_y = \frac{2.0 \times \left(\dfrac{\varepsilon_y}{D^{1.1}}\right) \times MF(f'_c) \times MF(n) \times MF(p) \times L_{eff}^2}{3}$$

Damage-control Target Displacement,

$$\Delta_{T,DC} = \Delta_y + \left(\phi_{dc} - \phi_y\right)L_{pr}\,L_{eff}$$

Figure 5.2 Flowchart of the proposed model for predicting $\Delta_{T,DC}$
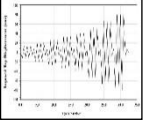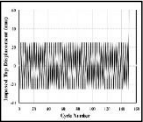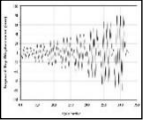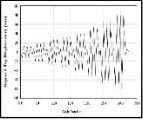
5.3 Validations of the proposed model

In this section, the proposed model in the above is validated using 3D FEM to model the pushover tests of the RC bridge piers and the NLTH-FE of the circular RC bridge piers subjected to seven earthquake ground motions.

5.3.1 Validations using 3D FEM to model the pushover tests

The pushover experimental tests of the RC piers were employed in this section. The details of the pushover test used are summarised in Table 5.1. All of the material characteristics, geometries and properties of the tested specimens in the experiments (Kunnath *et al.*, 1997; Lehman *et al.*, 2004) were used as input data for the validations.

Table 5.1 Details of pushover tests used for the validations

Reference	Specimen	Loading condition	Concrete strength (MPa)	Longitudinal reinforcement	ρ_s	Axial load
Kunnath *et al.* (1997)	A2		29	21 H10	1%	0.1
	A3		29	21 H10	1%	0.1
Lehman *et al.* (2004)	P415		30	22 H16 (1.5%)	0.70 %	0.1
	P430		32	44 H16 (1.5%)	0.70 %	0.1

The first test conducted by Kunnath *et al.* (1997) has two specimens: A2 and A3, which were subjected to a cyclic load. These two specimens were modelled to determine the damage-control target displacement and to observe the damage incurred. Figures 5.3(a) and 5.3(b) show the comparison between the results of FEM and the proposed model, together with the experimental results. Based on the observation in Figure 5.3(a), during the 15th cycle, initial spalling occurred at the concrete cover when the lateral displacement (damage-control target displacement for the experiment's result) was 42.3 mm. A similar observation is recorded for FEM, where the FEM experienced initial spalling of concrete at the 15th cycle, and the damage-control target displacement recorded was 44.9 mm.

Specimen A3 was subjected to a constant cyclic load, as shown in Table 5.1. As highlighted in Kunnath *et al.* (1997), the initial spalling and minor cracking had occurred in the first cycle. A similar observation can also be seen from the FEM, as shown in Figure 5.3(b). Based on the observation, the damage-control target displacements were 22.3 mm and 24.80 mm in the experiment and FEM, respectively. The damage-control target displacement predicted by the proposed model was 46.9 mm for both A2 and A3 since both tested specimens had similar material characteristics. Therefore, it can be seen from the figures that a good agreement between the FEM and experimental results. However, the proposed model produced the overestimation of the damage-control target displacements. As shown in Figure 5.4, minimal damage occurs on the tested specimens. It is shown in Figures 5.4(a) and 5.4(b) that the spalling of concrete and cracking had occurred on the tested specimen in the experimental test; a similar observation can be seen on the results of the FEM.

Red boxes indicate the spalling of concrete cover and yellow boxes indicate the cracking of concrete for both experimental and FEM, at the same position of RC bridge pier. A similar observation can be seen based on the results. It shows that, consideration of damage parameters on FEM, manage to capture damage accurately on the RC bridge pier. Both experimental and FEM results were determined using concrete strain in order to estimate the damage-control target displacement, for this section. Therefore, this validates that the proposed model can be used to ensure the damage is controllable and repairable.
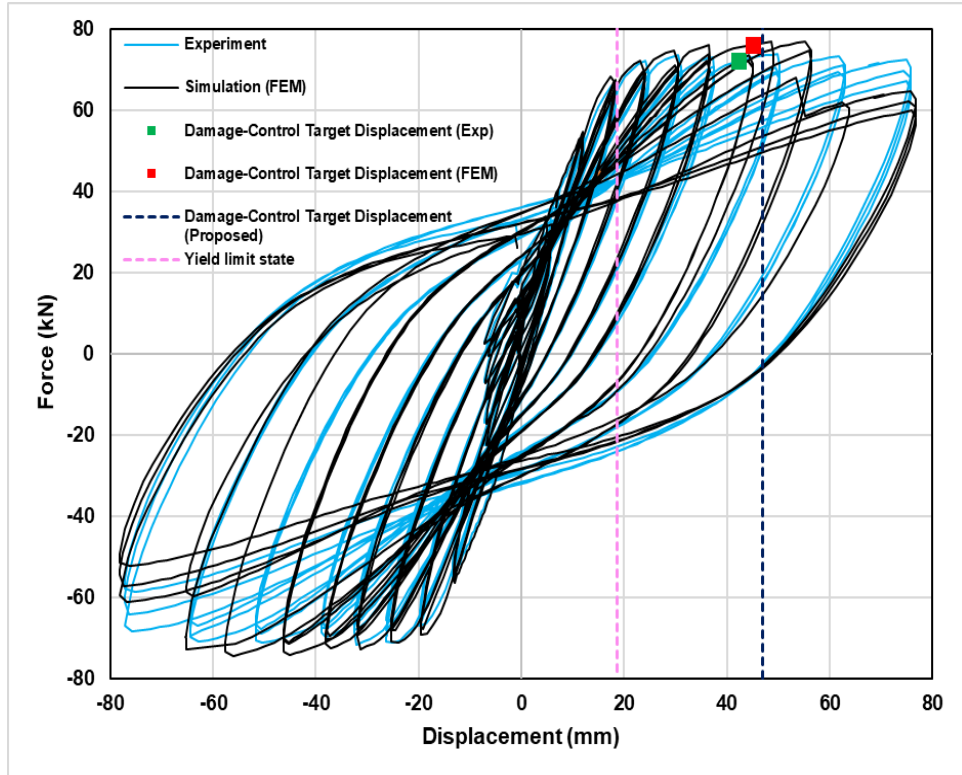
(a)
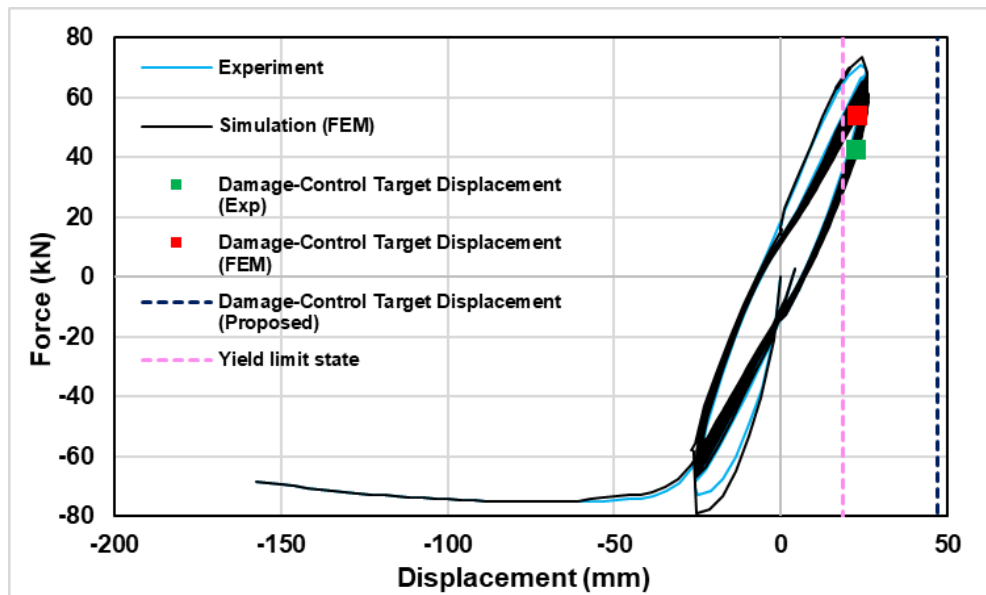
(b)

Figure 5.3 Comparison of the experimental (Kunnath *et al.*, 1997) and FEM results: (a) A2; and (b) A3
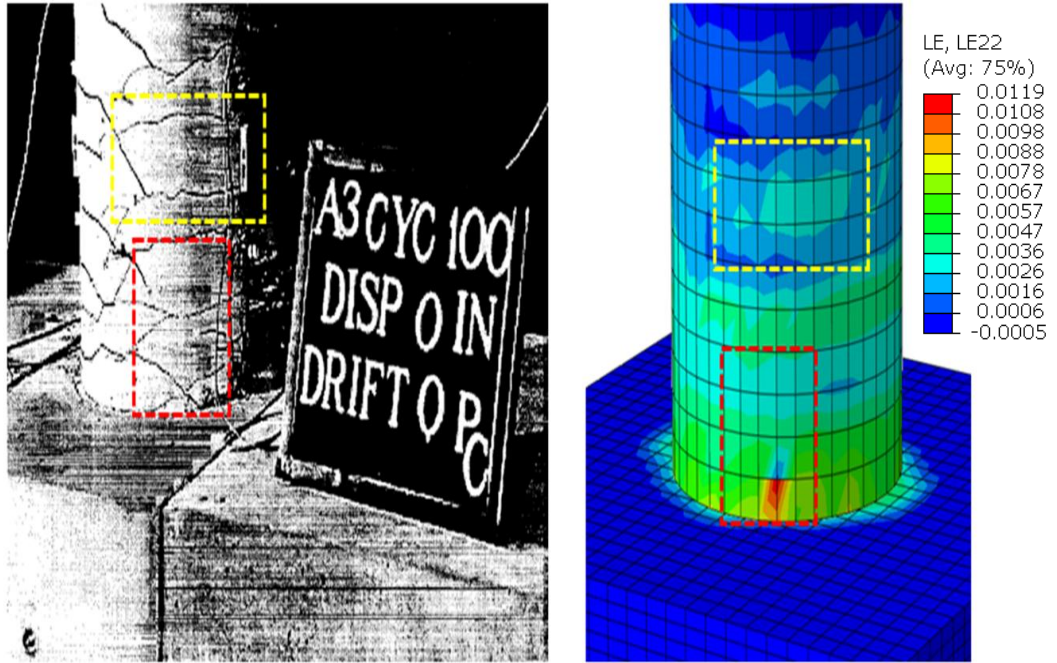
(a)
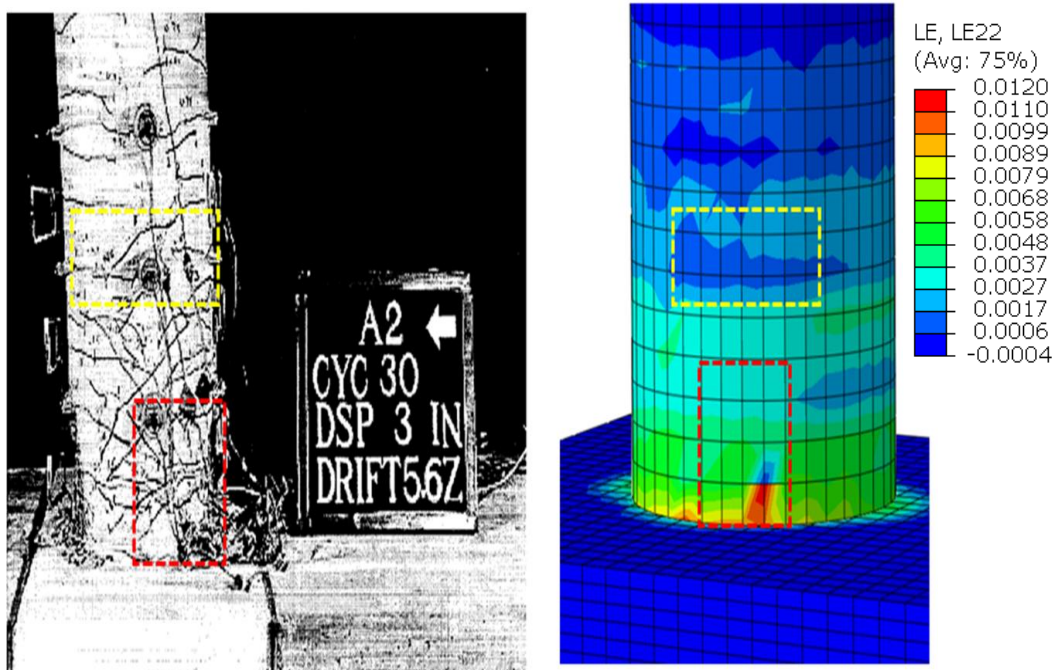
(b)

Figure 5.4 Damage observation of experimental (Kunnath *et al.*, 1997) and FEM
results: (a) A2 and (b) A3

The second test conducted by Lehman *et al.* (2004) has two specimens: P415 and P430. Similar to the first test, this test was modelled to determine the damage-control target displacement. Figures 5.5(a) and 5.5(b) show the comparison between the FEM and experimental results. Specimen P415 was subjected to a cyclic load. As reported by Lehman et al. (2004), the initial spalling of concrete was observed at lateral displacement (damage-control target displacement for the experiment's result) of 50.0 mm, as shown in Figure 5.5(a). The FEM confirmed that the initial spalling of concrete occurred in a similar cycle when the damage-control target displacement was 52.7 mm. The damage-control target displacement predicted by the proposed procedure was 102.24 mm. The final spalling of concrete was recorded at 124 mm, which is beyond the proposed model's results. This indicates that the RC bridge pier is repairable during the initial spalling until it reached 102.24 mm. Once it goes beyond that point, the RC bridge pier is no longer useable and needs to have the damaged section replaced.

Specimen P430 was subjected to a cyclic load. Initial spalling of concrete was observed at lateral displacements (damage-control target displacement for the experiment's result) of 71.3 mm and 79.9 mm in the experiment and FEM, respectively, as shown in Figure 5.5(b). The damage-control target displacement predicted by the proposed model was 109.57 mm. The final spalling of concrete was 178 mm. A similar conclusion can be made for P415, as the RC bridge pier was still repairable, and limited service was able to be provided during the initial spalling until it reached 109.77 mm. Beyond that limit, the RC bridge pier is no longer serviceable and needs to have the damaged section replaced. As shown in Figure 5.6, the spalling of concrete occurred on the tested specimens. Red boxes indicate the spalling of concrete cover and yellow boxes indicate the cracking of concrete for both experimental and FEM, at the same position of RC bridge pier. A similar observation can be seen based on the results. Both experimental and FEM results were determined using concrete strain in order to estimate the damage-control target displacement, for this section.

In the FEM simulation, the damage-control target displacement matches closely with the results from the experimental test results. Table 5.2 presents the damage-control target displacements predicted by the FEM and proposed model, together with the experimental test results.
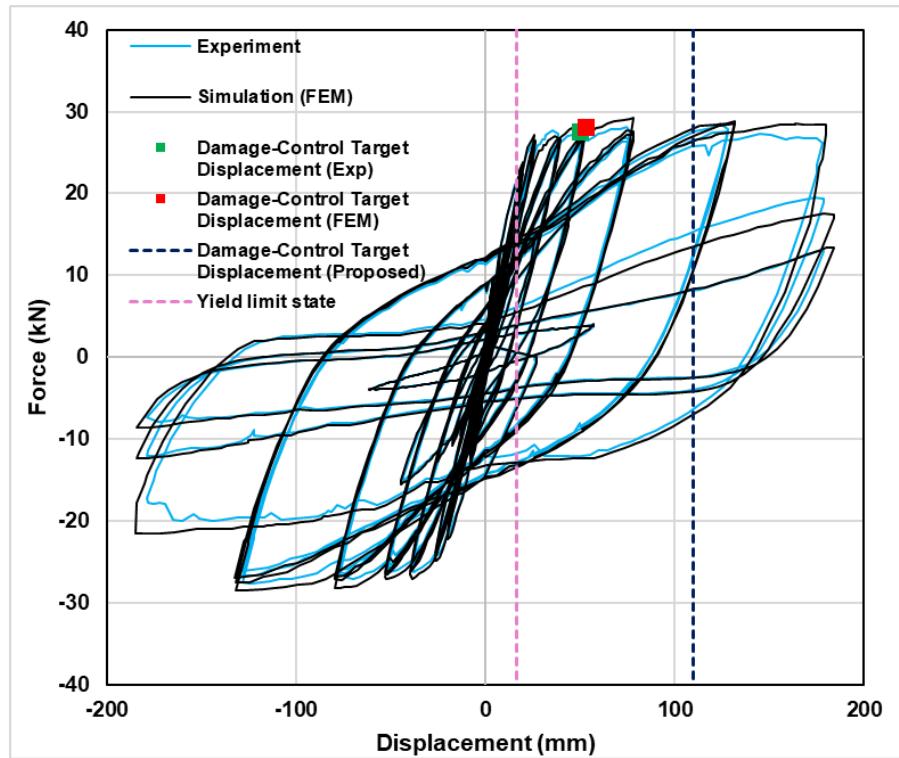
(a)
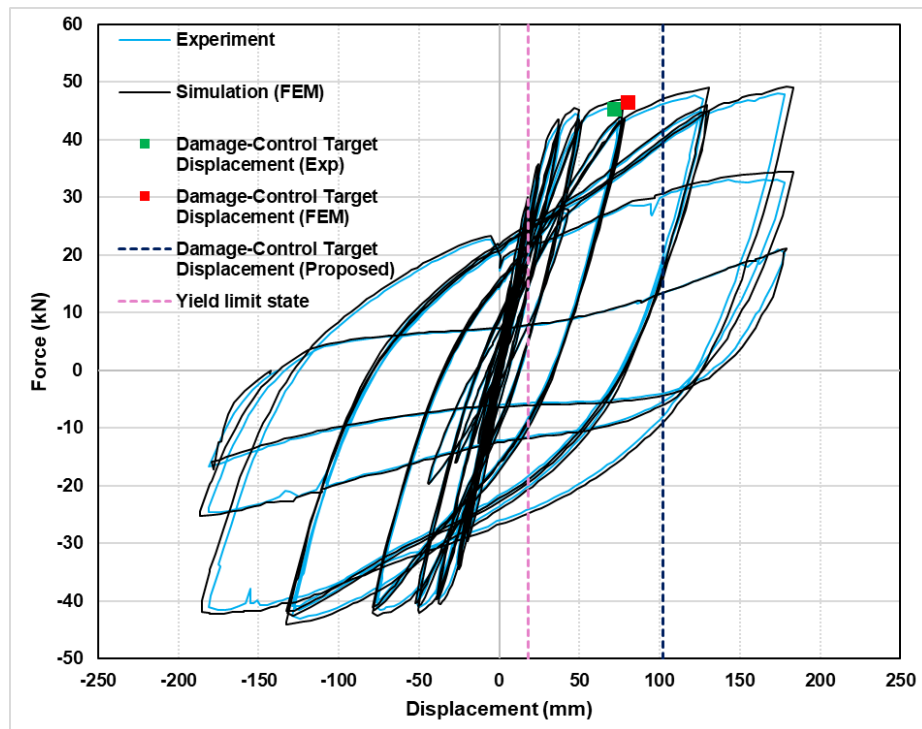
(b)

Figure 5.5 Comparison of the experimental (Lehman *et al.*, 2004) and FEM results: (a)
P415; and (b) P430
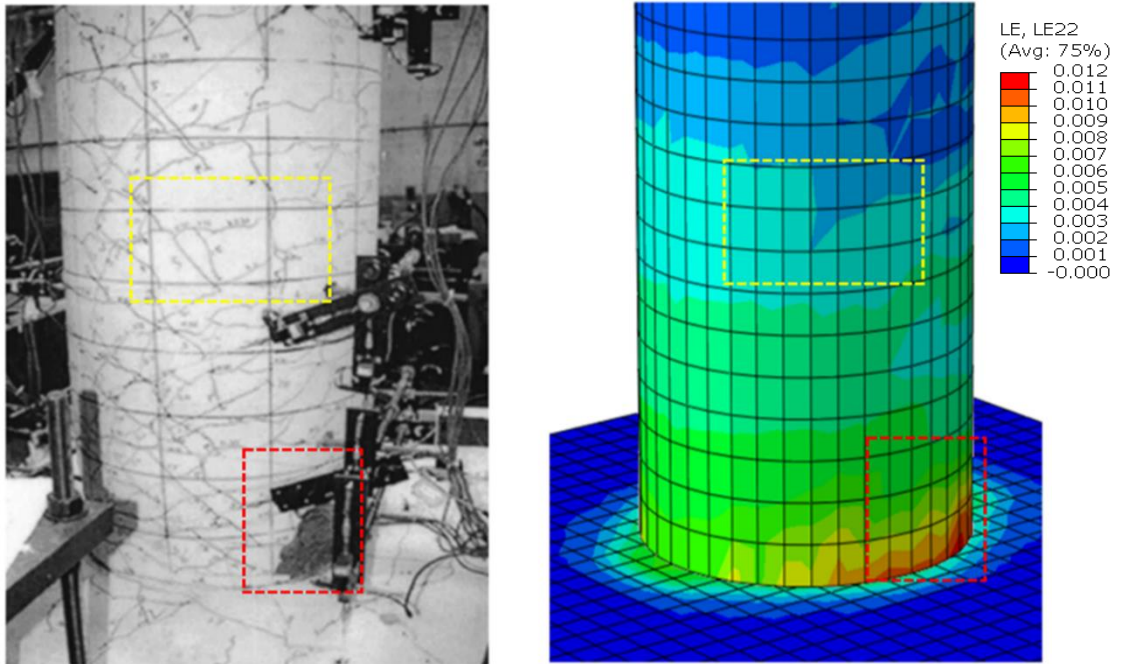
Figure 5.6 Damage observation of experimental (Lehman *et al.*, 2004) and FEM results for P430

Table 5.2 The damage-control target displacements predicted by the FEM and proposed model, together with the experimental test results.

Reference	Specimen	Proposed procedure	Experiment	FEM
Kunnath *et al.* (1997)	A2	46.90 mm	42.30 mm	44.90 mm
	A3	46.90 mm	22.30 mm	24.80 mm
Lehman *et al.* (2004)	P415	109.57 mm	71.30 mm	79.93 mm
	P430	102.24 mm	50.00 mm	52.70 mm

5.3.2 Validations using 3D FEM to model RC bridge pier subjected to different earthquakes

In this section, an RC bridge pier under different earthquakes is modelled by 3D FEM to predict the damage-control target displacement. The RC bridge pier was subjected to seven randomly ground motions. The main parameters considered in this section are the transverse reinforcement ratio, concrete strength, longitudinal reinforcement ratio, and axial load ratio. As highlighted in Section 5.2, these parameters are essential to determine the damage-control reinforcement tensile strain and damage-control concrete compression strain.

Three RC bridge piers used by Kong (2017) and Kowalsky (2000) were adopted for validation purposes. The details of the specimens are as follows: the diameter is 2.0 m, the concrete compressive strength is 30 MPa, the yield strength of reinforcement steel bars is 420 MPa, the longitudinal bar diameter, is 35 mm, and the transverse volumetric reinforcement ratio is 1%. The axial loads of the RC piers are calculated based on 8% axial load ratio for three piers with three difference longitudinal steel ratios (1%, 2% and 3%). Table 5.3 gives the details of the RC bridge piers used in this section.

Table 5.3 The details of the RC bridge piers used

Parameter	Kong (2017) and Kowalsky (2000)		
Pier	**Pier 1**	**Pier 2**	**Pier 3**
Pier diameter (m)	2.0		
Pier height (m)	7.0, 11.0 and 13.0		
Longitudinal Reinforcement (mm)	35		
Longitudinal Reinforcement Ratio (%)	1	2	3
Transverse Reinforcement Ratio (%)	1		

Axial load (kN) (%)	8
Concrete strength [$f_c^{'}$ (MPa)]	30
Longitudinal reinforcement yield strength [f_{ye} (MPa)]	420
Longitudinal reinforcement ultimate strength [f_{yeu} (MPa)]	469
Transverse reinforcement yield strength [f_{yh} (MPa)]	420
Transverse reinforcement ultimate strength [f_{yhu} (MPa)]	469

5.3.2.1 Seismic input ground motions for NLTH-FE analysis

In this section, seven randomly ground motions records: 1999 Chi-Chi earthquake, 1979 Imperial Valley earthquake, 1995 Kobe earthquake, 1989 Loma Prieta earthquake, 1994 Northridge earthquake, 1983 Trinidad earthquake, and 1940 El-Centro earthquake were used in the simulation as the input acceleration ground motions for NLTH-FE analysis. Details of the ground motions of the earthquakes are highlighted in Table 5.4. The details of seven randomly ground motions extracted from the Pacific Earthquake Engineering Research (PEER) Centre and SeismoArtif (Seismosoft, 2016) databases.

The time-histories of the earthquake ground motions were converted to spectrum-compatible time-histories generated using the SeismoArtif (available online) to make sure that the spectrum of the original accelerogram records is compatible with the EC8 design accelerogram spectrum (CEN, 2004b). The time-history data were scaled to generate the displacement spectra to match type C with 5% damping with respect to EC8, as generally used in the DDBD method.

The acceleration response spectra of the ground motions are presented in Figure 5.7. Based on the DDBD method, the damage-control target displacement of an RC bridge

pier depends on the damage-control limit states that are governed by damage-control reinforcement tensile strain and damage-control concrete compression strain. Hence, the damage-control target displacement for NLTH-FE was obtained based on the requirements of DDBD method governed by both strains. Damping can affect the structural response in the NLTH-FE analysis. In this study, modal damping is employed for NLTH-FE in order to determine the structural responses. The damping ratio of 5% was assumed and applied to the RC bridge pier model for each vibration mode.

Table 5.4 The ground motions details of the earthquakes

Test	Earthquake	Year	Station	PGA (g)	Magnitude
S1	Chi-Chi	1999	TCU045	-0.349	7.6
S2	Imperial Valley	1979	USGS STATION 5115	0.315	6.5
S3	Kobe	1995	KAKOGAWA(CUE90)	0.345	6.9
S4	Loma Prieta	1989	090 CDMG Station	0.355	6.9
S5	Northridge	1994	090 CDMG STATION 24278	0.568	6.7
S6	Trinidad	1983	090 CDMG STATION 1498	0.194	3.2
S7	EL-Centro	1940	USGS station 0117	0.349	6.9
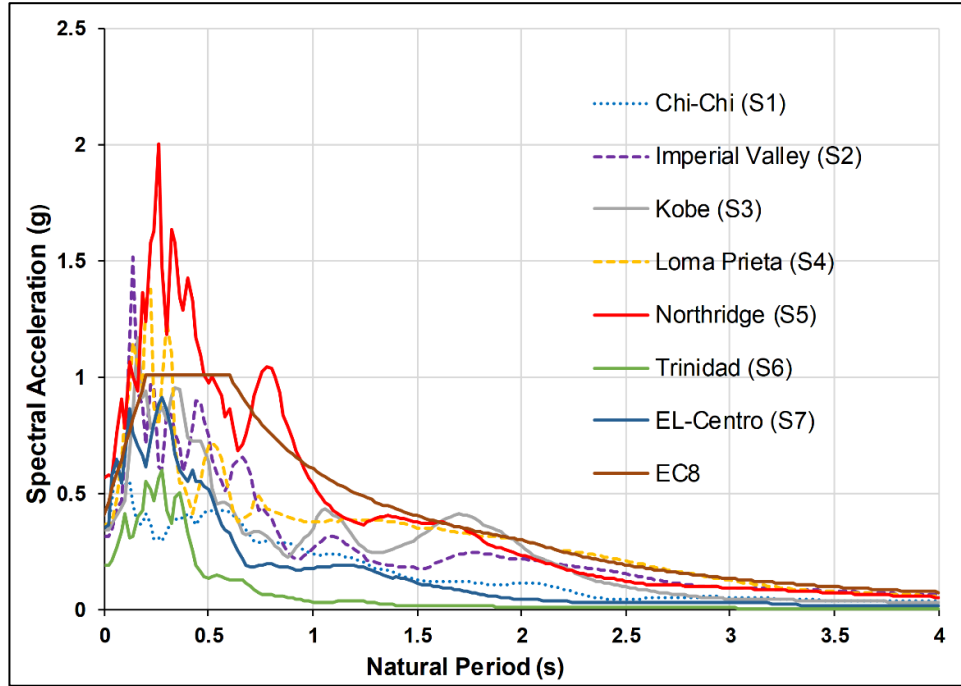
Figure 5.7 Acceleration response spectra with 5% damping

5.3.2.2 Determination of damage-control target displacement from FEM's results

As mentioned in the previous section, the damage-control target displacement of an RC bridge pier depends on the damage-control limit states that are governed by damage-control reinforcement tensile strain and damage-control concrete compression strain. Therefore, to determine the damage-control target displacement from NLTH-FE, the damage-control concrete compression strain limit, $\varepsilon_{c,dc}$, and damage-control reinforcement tensile strain limit, $\varepsilon_{s,dc}$, are calculated using Eqns. (5.2) and (5.1), respectively. Then, based on Eqn. (5.6), these two strain limits are used to determine the predicted $\Delta_{T,DC}$ from the NLTH-FE results. The step for this procedure is highlighted below:

1. Calculate the damage-control strain limit for concrete and reinforcement using Eqns. (5.2) and (5.1);

2. Check which strain limit governs the displacement of $\Delta_{T,DC}$ using Eqn. (5.6);

3. Compare the strain calculated in Step 2 with maximum strains at the plastic hinge region and base position of the RC bridge piers from NLTH-FE; and

4. Damage-control target displacement is determined at the top of the RC bridge pier when the strain from NLTH-FE matches closely with the calculated governed strain.

For example, the acceleration input of the 1989 Loma Prieta earthquake was considered to demonstrate the outcome of damage-control target displacement from the NLTH-FE results. According to Eqn. (5.6), the concrete compressive strain limit ($\varepsilon_{c,dc}$ = 0.0209) governs the condition to determine the damage-control target displacement. Based on the consideration of yield displacement and strain penetration length, as suggested in Eqns. (4.8) and (4.10), the predicted damage-control target displacement at the top of the bridge pier and maximum concrete compressive strain at the base of the RC bridge pier are shown in Figure 5.8. From the figure, the $\Delta_{T,DC}$ = 199.81 mm is determined.
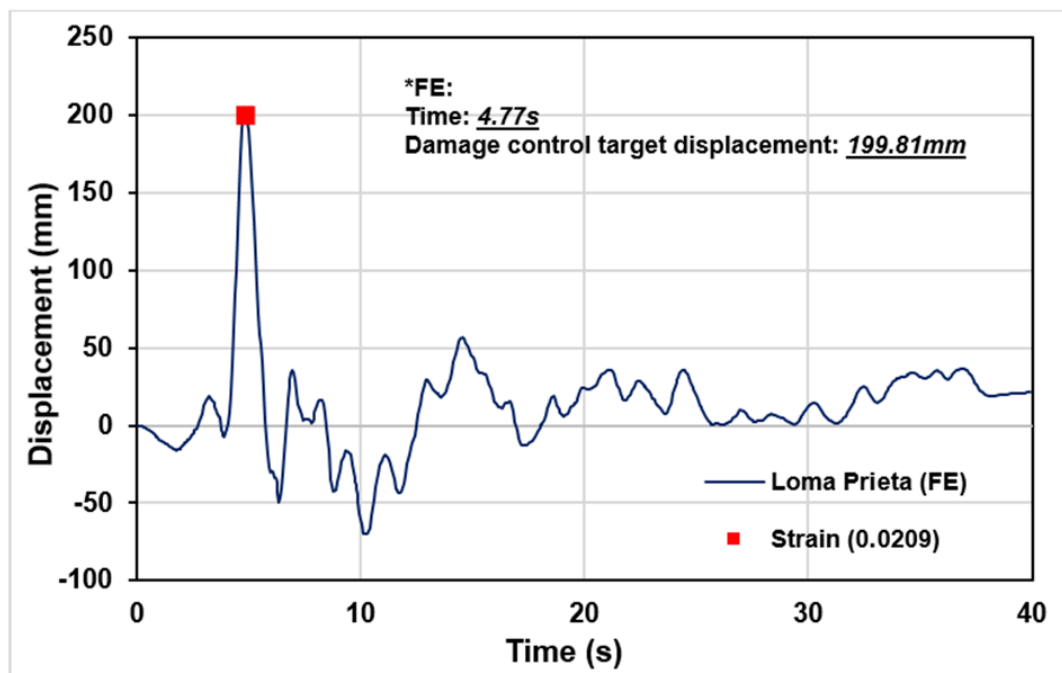
Figure 5.8 Damage-control target displacement prediction using NLTH-FE

5.3.2.3 3D FEM results

After successfully validating the proposed procedure against the experimental pushover test, this section's objective is to conduct a series of validation process using NLTH-FE analysis by 3D FEM. The proposed procedure results were compared with previous model results (Kowalsky, 2000; Kong, 2017), and the results generated from NLTH-FE

for all seven ground motions were recorded. Figure 5.9 shows the comparison of three different models' results with three different longitudinal reinforcement ratios for damage-control target displacement. Figure 5.9(a) shows the damage-control target displacement for 1% longitudinal reinforcement ratio. It can be seen that the proposed procedure matches closely with several earthquake ground motions, especially for lower and moderate earthquake magnitudes (S1, S2, S3, S4, and S7). Meanwhile, both previous models have overestimated the displacement, and they were even higher when compared with an S5 earthquake. Thus, it is clear that the proposed model can reasonably predict the damage-control target displacement of the RC bridge pier for the lower and moderate magnitudes of the earthquake.

Figure 5.9(b) highlights the damage-control target displacement for a 2% longitudinal reinforcement ratio for different RC bridge pier heights. A similar observation can be seen in this figure, where the proposed procedure predicts reasonable results that match closely with the NLTH-FE results for a lower and moderate earthquake magnitude. The result for three different RC bridge piers rose linearly; however, in this figure, one of the previous model's (Kowalsky, 2000) result was close with the higher magnitude earthquake (S5), while the other previous model had shown an overestimation compared with the NLTH-FE and proposed model's results. Therefore, it is evident that the proposed model can reasonably predict the damage-control target displacement for the lower and moderate magnitudes of the earthquake.

Figure 5.9(c) highlights the damage-control target displacement for a 3% longitudinal reinforcement ratio for different RC bridge pier height levels. It can be seen that the proposed model's results matches closely with several earthquake ground motions. Interesting outcomes can be seen for the RC bridge pier of 13 m height for the proposed model, where the damage-control target displacement was accurately predicted for the S3 and S7 earthquakes. The previous model had shown similar observation (Kowalsky, 2000), where it had accurately predicted the S5 earthquake for 13 m RC bridge pier height, while other previous models (Kong, 2017) had overestimated the outcomes for the three different RC bridge pier heights. Therefore, from Figure 5.9, it is clear that the results generated by the proposed model are in reasonable agreement with the NLTH-FE results.

These results were further demonstrated in Figure 5.10, where the average values of the seven ground motions used for NLTH-FE were plotted in different figures to avoid congestion in Figure 5.9. It can be seen that for all three different longitudinal reinforcement ratios, the damage-control target displacements predicted by the proposed model had matched closely with the NLTH-FE results. These results also indicate that the proposed model can be used to estimate the damage-control target displacement for RC bridge piers under the low and/or moderate magnitude of earthquakes.
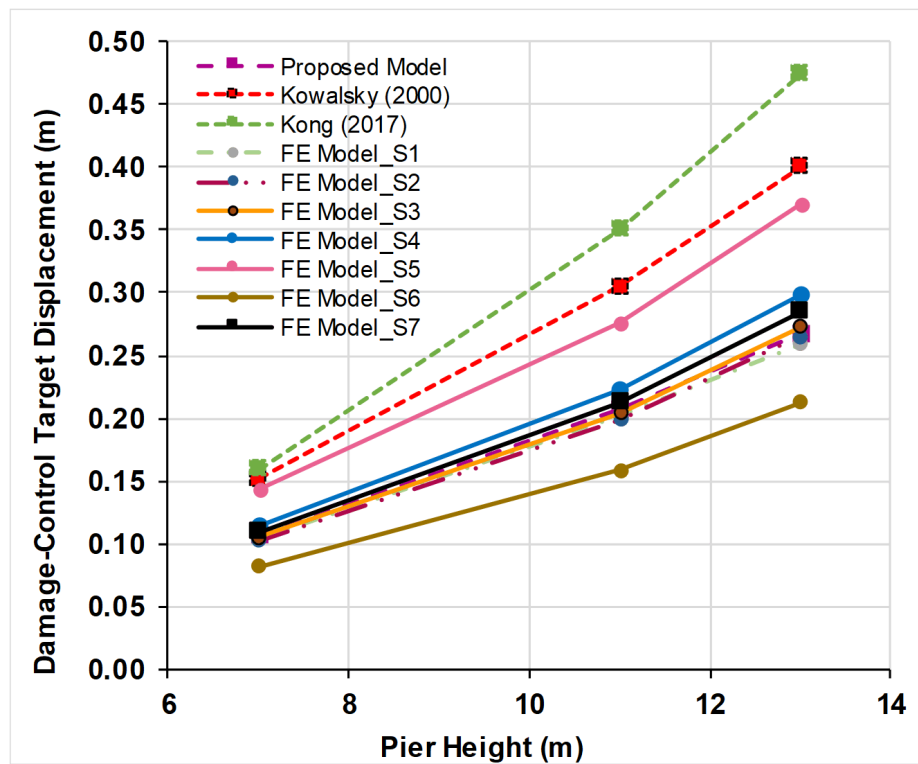
a) Longitudinal reinforcement ratio of 1%
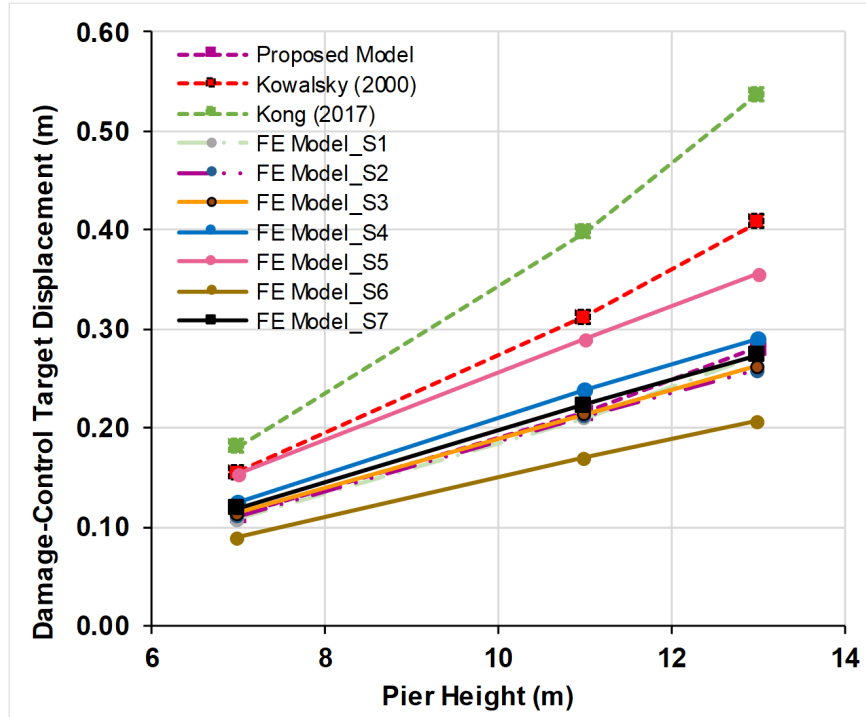
b) Longitudinal reinforcement ratio of 2%
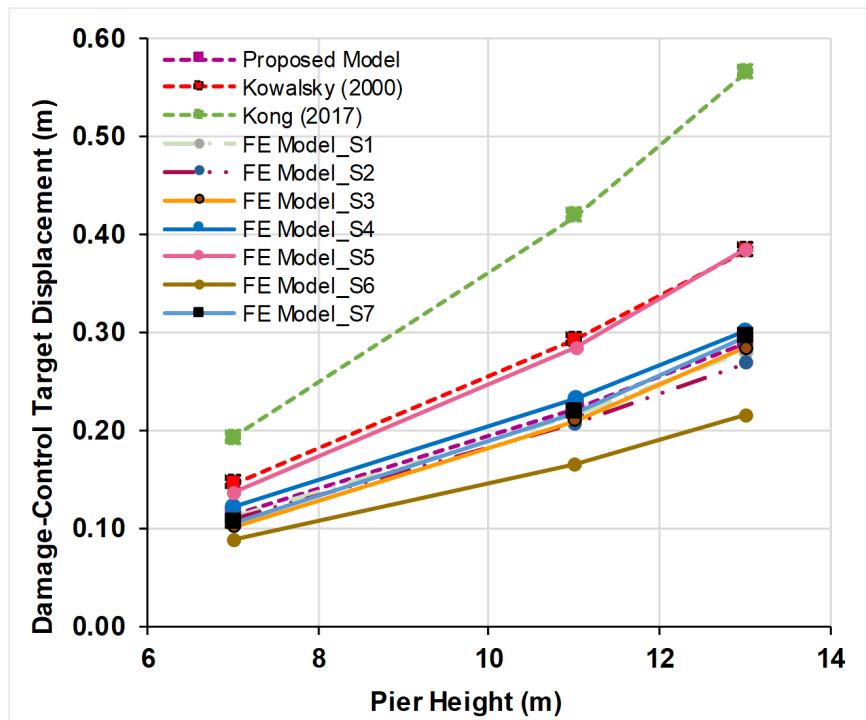
c) Longitudinal reinforcement ratio of 3%

Figure 5.9 Comparisons of the predicted damage-control target displacement by the proposed model, the NLTH-FE analyses, and the previous models (Kowalsky, 2000; Kong, 2017) under different earthquake ground motions
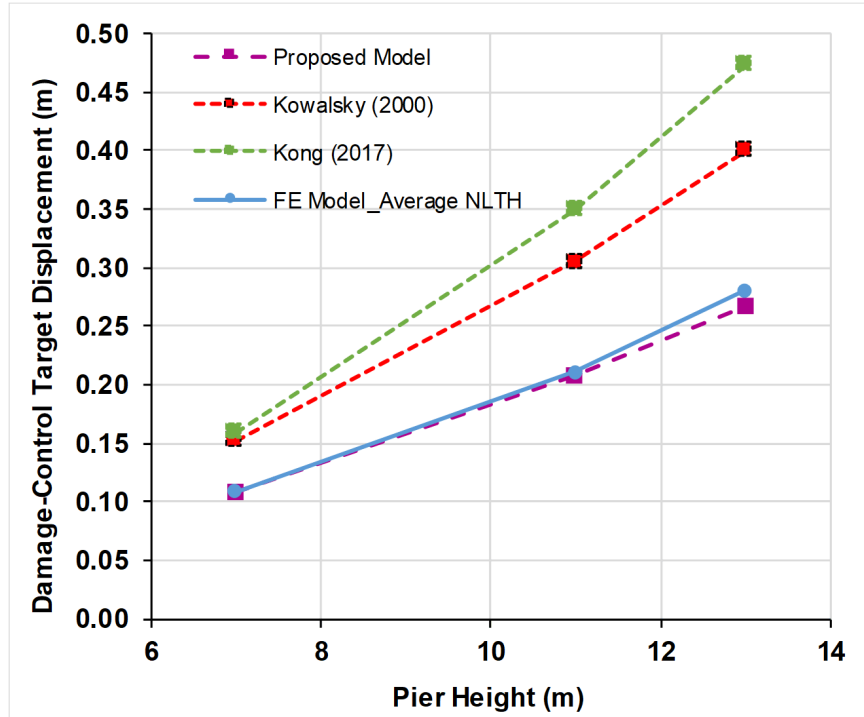
a) Longitudinal reinforcement ratio of 1%
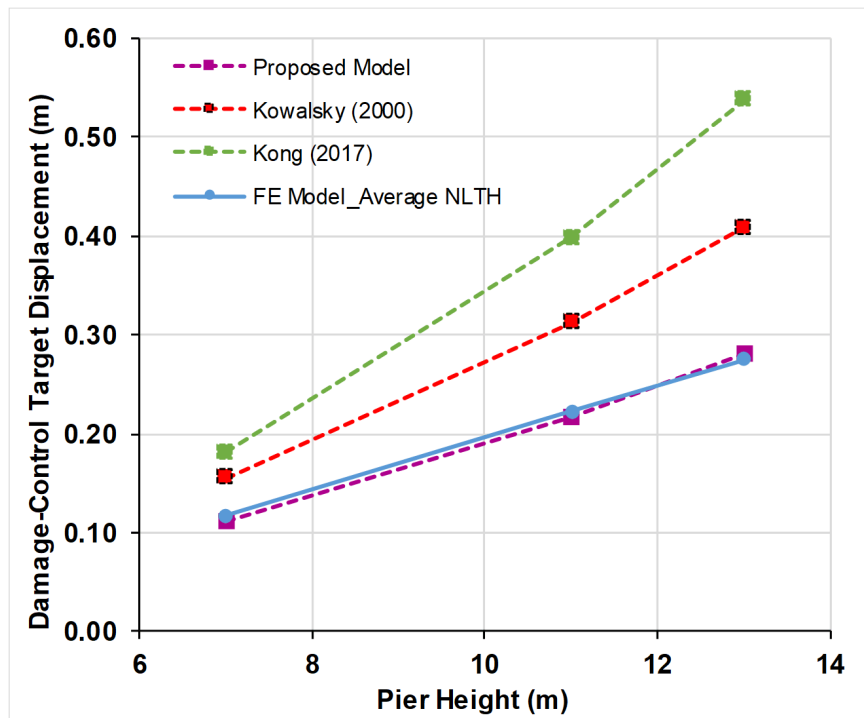
b) Longitudinal reinforcement ratio of 2%
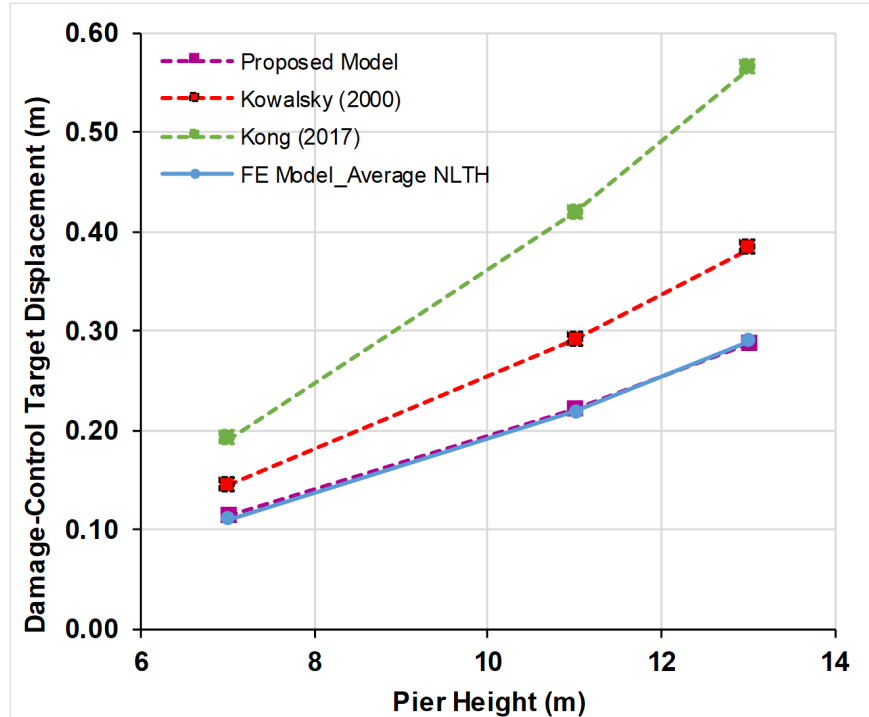
c) Longitudinal reinforcement ratio of 3%

Figure 5.10 Comparisons of the average predicted damage-control target displacement by the proposed model, the NLTH-FE analyses, and the previous models (Kowalsky, 2000; Kong, 2017) under different earthquake ground motions

5.4 Further validations

The proposed model is further validated in this section by NLTH-FE analyses of a circular RC bridge pier subjected to three different earthquake ground motions. Table 5.5 highlights the details of the RC bridge pier used in this section. Ground motion records from the 1989 Loma Prieta earthquake, 1999 Kocaeli earthquake, and 1999 Chi-Chi earthquake were used as the input ground motions for the NLTH-FE analysis. The characteristics of the ground motions used in this analysis are presented in Table 5.6.

Table 5.5 The details of the RC bridge pier used in this section

Parameter	Value	Remark
Pier diameter (m)	1.0	-
Pier height (m)	7.00	-
Strain penetration length [L_{sp} (m)]	0.288	Eqn. (4.10)
Cover (mm)	50	-
Longitudinal Reinforcement (mm)	11 H32	1.12%
Axial load (kN)	5301	0.1
Concrete strength [$f_c^{'}$ (MPa)]	30	-
Longitudinal reinforcement yield strength [f_{ye} (MPa)]	420	-
Longitudinal reinforcement ultimate strength [f_{ye} (MPa)]	469	-

Table 5.6 The ground motions details and characteristics

Test	Earthquake	Year	Magnitude	Station	PGA (g)
EQ1	Loma Prieta (USA)	1989	6.9	090 CDMG Station	0.355
EQ2	Kocaeli (Turkey)	1999	7.6	YARIMCA (KOERI330)	-0.361
EQ3	Chi-Chi (Taiwan)	1999	7.6	TCU045	-0.349

Figure 5.11 shows the displacement-time response of the RC bridge pier that was subjected to different earthquake ground motions: EQ1, EQ2, and EQ3. As shown in Figure 5.11(a), the yield and maximum displacements predicted by NLTH-FE were 21.14 and 199.85 mm, respectively. The damage-control concrete strain limit had governed the displacement; therefore, the damage-control target displacement estimated was 84.89 mm. The corresponding damage-control target displacement predicted by the proposed model was 80.34mm. This confirms the close matching of the damage-control target displacements predicted by the proposed model and NLTH-FE analysis.

For the case of EQ2, the estimated the damage-control target displacement of the NLTH-FE analysis was 80.41 mm, as highlighted in Figure 5.11(b). It matches closely with the prediction of the proposed model, which was 80.34 mm. In the NLTH-FE analysis, the damage-control target displacement was attained when the displacement-time response was at 9.31 s, which occurred at the earlier stage of the earthquake excitation at 0.0156 g. Therefore, it is clear from Figure 5.11(b) that the results generated by the proposed model have agreed reasonably with the prediction of the NLTH-FE analysis.

For EQ3, the damage-control target displacement estimated by the NLTH-FE analysis was 81.58 mm. For this earthquake, the damage-control target displacement was attained when the time of earthquake excitation was at 23.56 s. This NLTH-FE analysis shows that the damage-control tensile reinforcement strain had governed the displacement when the acceleration of ground motions was at -0.015 g. This phenomenon occurred at the middle stage of the earthquake when the earthquake excitation was between 0.02 and -0.017 g. Unlike in EQ1, the damage-control target displacement was attained at an early stage of the earthquake. This is because, at the early stage of EQ3, the acceleration of ground motions was between 0.002 and 0.004 g, whereby it did not cause the RC bridge pier to deflect. The corresponding damage-control target displacement predicted by the proposed model was 80.34 mm, as highlighted in Figure 5.11(c). It is evident that the proposed model is very robust to predict the damage-control target displacement for the circular RC bridge pier for this type of earthquake.

(a)

(b)

114
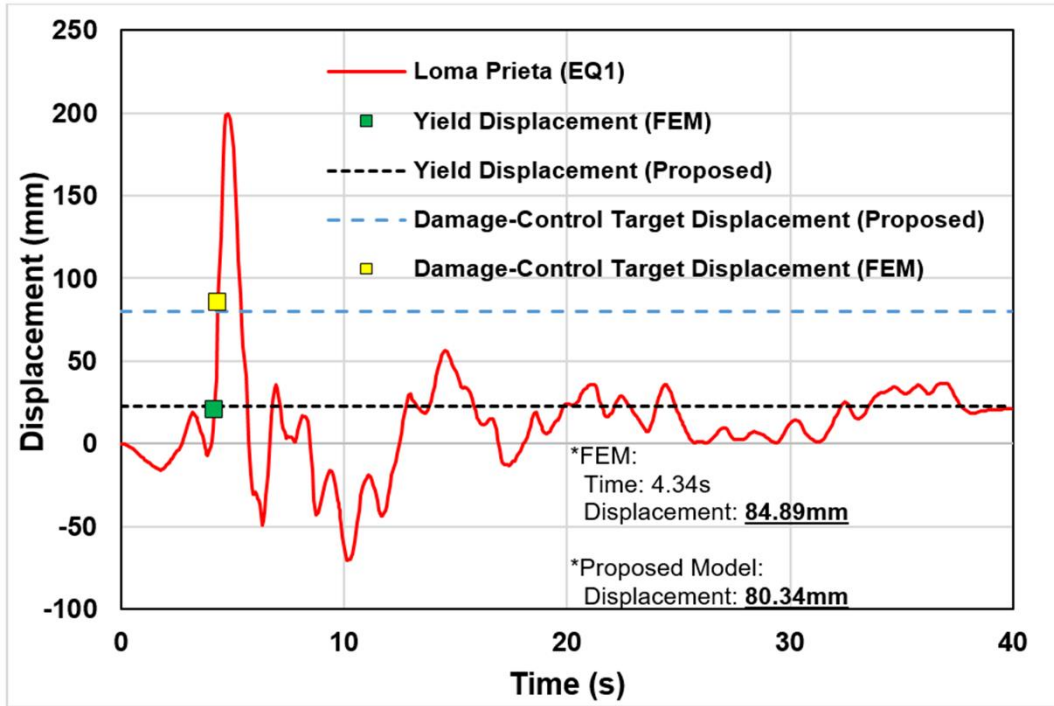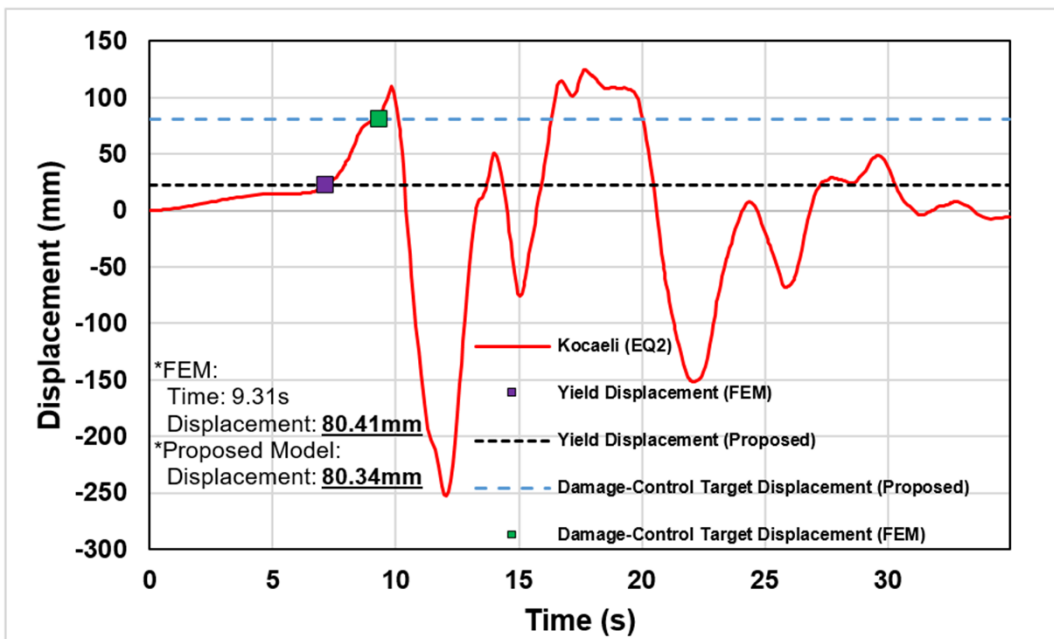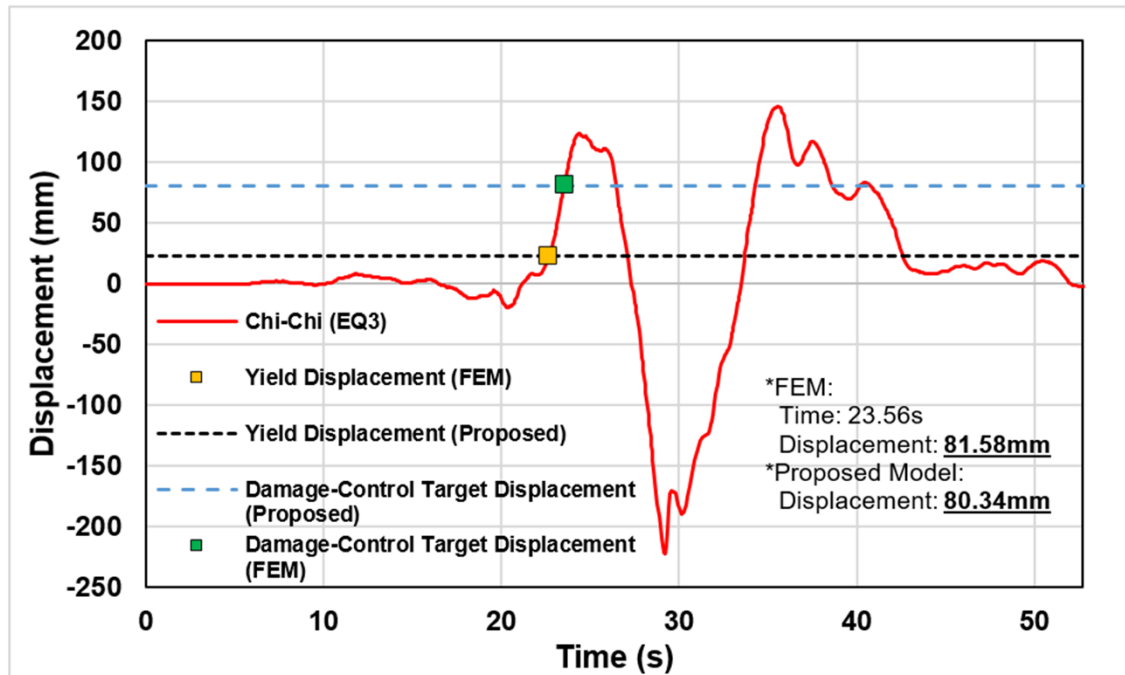
(c)

Figure 5.11 Displacement-time responses of the RC bridge pier subjected to the
earthquakes: (a) EQ1; (b) EQ2; and (c) EQ3

5.5 Parametric studies

In order to determine the influence of different parameters on the prediction of damage-control target displacement, the influence of concrete strength, transverse reinforcement ratio, and longitudinal reinforcement ratio were considered. In order to quantitatively investigate the effects of those factors on the prediction of damage-control target displacement, a series of parametric studies were conducted in this research. In this parametric study, an RC bridge pier with a diameter of 2.0 m was used. The mass from the RC bridge deck had acted upon the top part of the pier as an axial load. Approximately 10% of the axial load ratio was applied on the RC bridge pier, and seven ground motions were used for the NLTH-FE analysis.

5.5.1 The effect of concrete strength on damage-control target displacement

In order to investigate the influence of different concrete strengths on the prediction of damage-control target displacement, eight sets of concrete strengths, including normal- and high-strength concrete were applied in this section: 30, 40, 50, 60, 70, 80, 90, and

100 MPa. Constant longitudinal and transverse reinforcement ratio of 1% was applied in this section. Similar details were considered apart from the axial load ratio, as highlighted in Table 5.5. Figure 5.12 shows the influence of concrete strength on the predicted of the damage-control target displacement for an RC bridge pier with different pier heights under seven ground motions predicted by the proposed model, FEM, and previous studies. Based on Figure 5.12, the damage-control target displacement predicted by the proposed model shows that concrete strength has significant contribution to the proposed model, compared to the previous model. However, the proposed model's results have matched closely with several earthquakes (S1, S2, S3, S4, and S7). This phenomenon occurred due to the consideration of an improved DCLS.

Meanwhile, both previous models overestimated the displacements; in fact, they were higher compared with the S5 earthquake. The damage-control target displacements predicted by the proposed model and NLTH-FE analysis increase slightly with increasing concrete strength. However, the influence is almost similar for the piers with different heights and under different earthquake ground motions, as highlighted in Figures 5.12(a), 5.12(b), and 5.12(c).
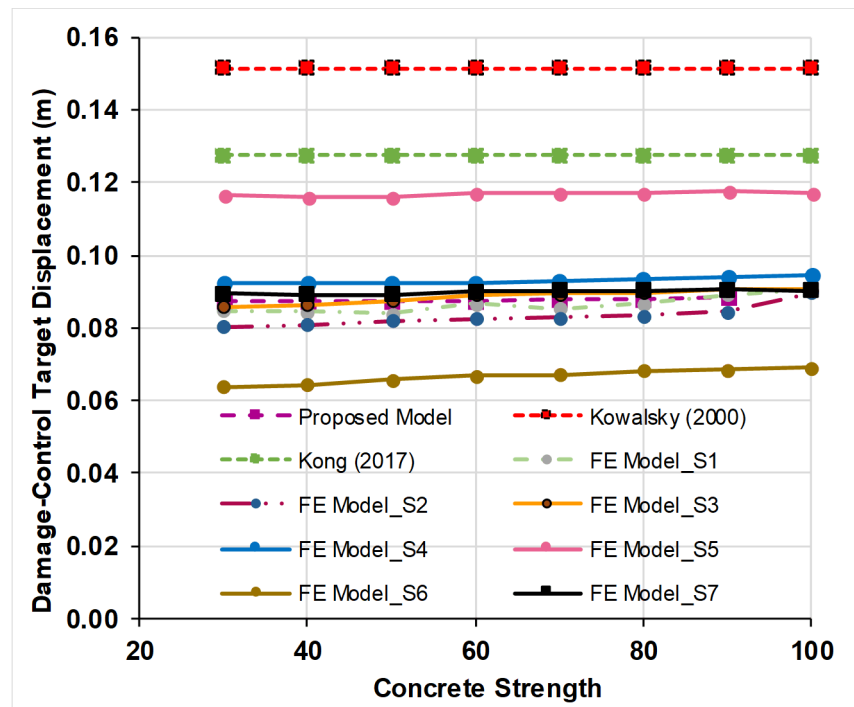
(a)
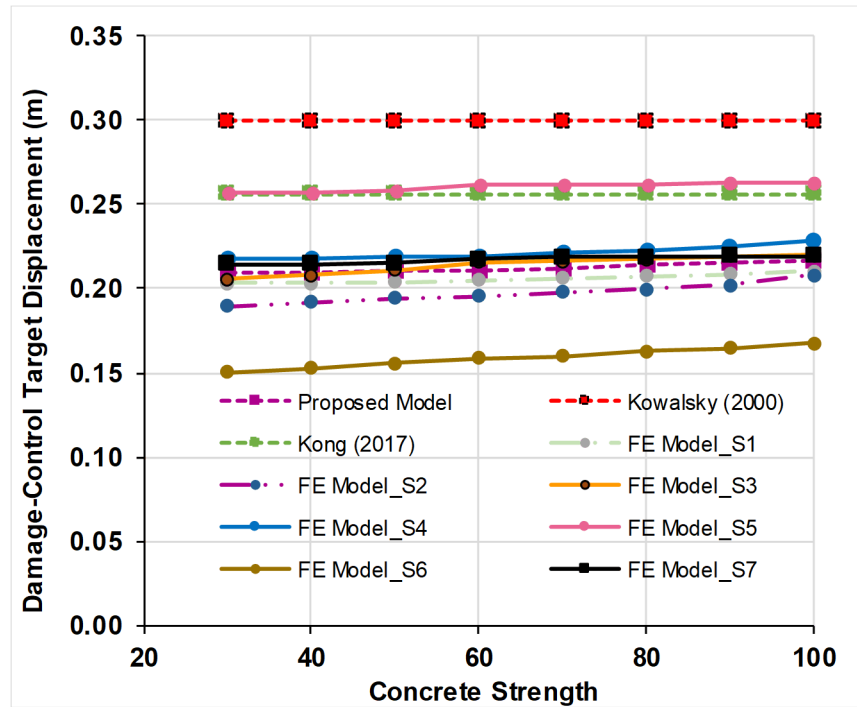
(b)
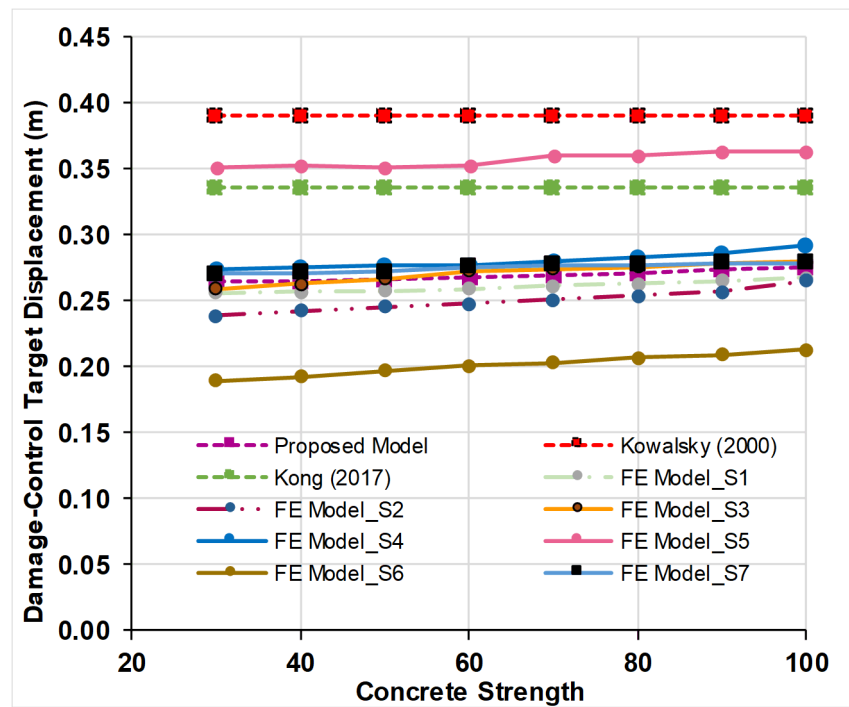
(c)

Figure 5.12 The influence of concrete strength on the damage-control target displacements of an RC bridge pier with different pier heights: (a) 7.0 m; (b) 11.0 m; and (c) 13.0 m

117

5.5.2 The effect of reinforcement ratio on damage-control target displacement

In this section, the influence of longitudinal and transverse reinforcement ratio on the prediction of damage-control target displacement of RC bridge pier was investigated. In order to explore the influence of these parameters on the prediction of damage-control target displacement, three longitudinal reinforcement ratios (1%, 2%, and 3%) and three transverse reinforcement ratios (0.7%, 0.8%, and 0.9%) were considered. Other parameters used in this section are similar to the ones used in the previous section, as highlighted in Table 5.5. Figure 5.13(a) shows the influence of the longitudinal reinforcement ratio on the prediction of damage-control target displacement for the RC bridge pier with three different transverse reinforcement ratios. Based on Figure 5.13(a), increasing the longitudinal reinforcement ratio for the three different transverse reinforcement applied has caused the damage-control target displacement to slightly increase. Figure 5.13(b) shows the influence of the transverse reinforcement ratio on the prediction of damage-control target displacement for the RC bridge pier with three different longitudinal reinforcement ratios. A similar observation can be seen from Figure 5.13(a), where the damage-control target displacement has slightly increased if a single parameter were considered.

The longitudinal and transverse reinforcement ratios have small influences on the prediction of damage-control target displacement for the RC bridge pier. However, with the increased axial load ratio and RC bridge pier height, the damage-control target displacement can vary, as shown in the validation section (Section 5.3.2). Therefore, this indicates that the seismic resistance of the RC pier improves with a higher reinforcement ratio, along with the consideration of other parameters. Apart from that, the RC pier with higher longitudinal and transverse reinforcement ratios can have a higher damage-control target displacement.
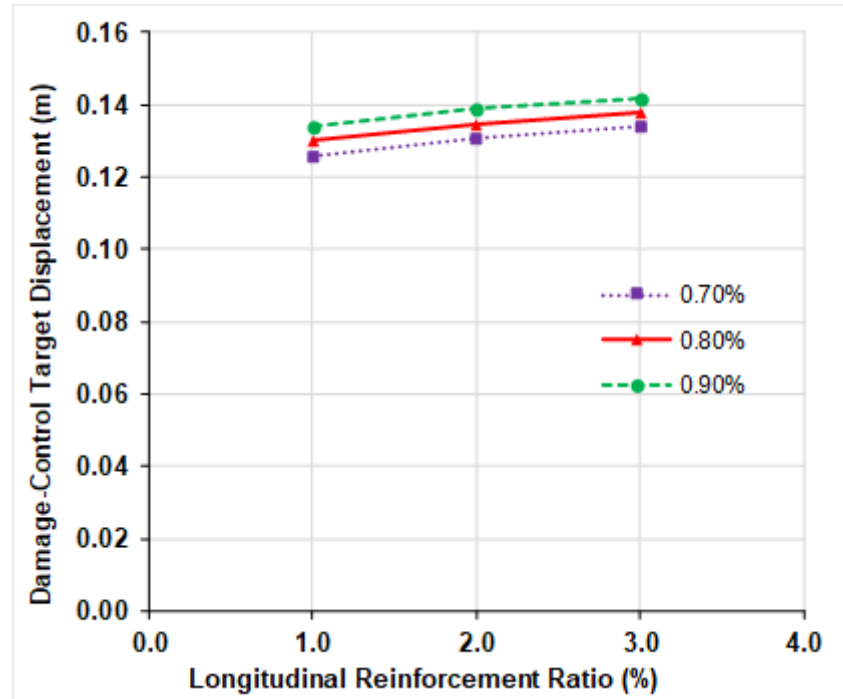
(a)
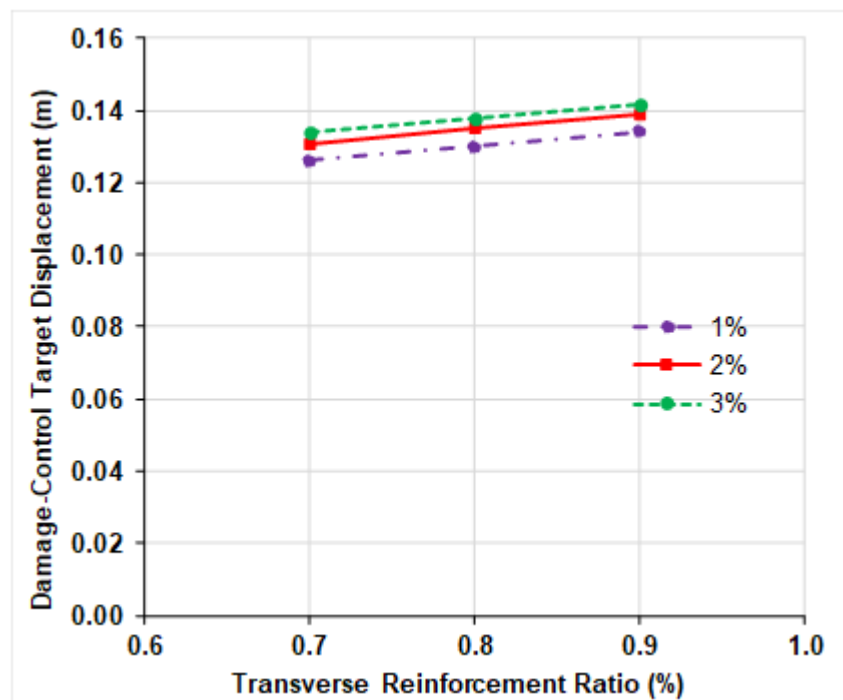
(b)

Figure 5.13 The influence of reinforcement ratio on the damage-control target displacement of the RC bridge pier: (a) transverse reinforcement ratio; and (b) longitudinal reinforcement ratio.

5.6   Implications on the seismic design of the RC bridge pier

The implication of the proposed model described in this chapter is essential for the seismic design of the RC bridge using the DDBD method. As highlighted previously, the estimation of target displacement is needed for the DDBD method to determine the equivalent viscous damping, ξ_{eq}, system effective mass, m_e, and displacement ductility, μ. Referring to Figure 5.14, the fundamental principle of the DDBD method procedure starts by determining the yield displacement and target displacement. As for the damage-control limit state design, the estimation of damage-control target displacement is required. From Figure 5.14(b), it can be seen that the damage-control target displacement is one of the critical parameters for engineers and designers to determine the level of damage within the damage-control limit states that are allowed according to the DDBD method guidelines (Dwairi and Kowalsky, 2006a; Priestley *et al.*, 2007).

Once the damage-control target displacement is obtained, the equivalent viscous damping for the RC bridge pier and effective mass of the system (Figure 5.14(a)) can be easily estimated. Displacement ductility is then determined from the ratio of damage-control target displacement and yield displacement, Δ_y in order to obtain equivalent viscous damping, as shown in Figure 5.14(c). Since the DDBD method utilises the concept of equivalent linearization, the equivalent viscous damping depends on elastic damping and hysteretic energy absorbed during the inelastic response (Calvi *et al.*, 2013). Thus, as shown in Figure 5.14(c), the equivalent viscous damping can be obtained based on the displacement ductility and ductility demand of structures. By using the $\Delta_{T,DC}$ at the maximum response and equivalent viscous damping, the effective time period, T_e, is then computed from the displacement spectra, as shown in Figure 5.14(d). Then, the effective secant stiffness, K_e for the structure is determined as below:

$$K_e = \frac{4\pi^2 m_e}{T_e^2} \tag{5.11}$$

Based on Figure 5.14(b), t base shear demand V (seismic lateral force, F), can be computed as:

$$F = V = K_e \Delta_{T,DC} \tag{5.12}$$

Finally, the base shear demand (seismic lateral force) will be used to design the RC bridge piers. The base shear force is used to estimate the longitudinal reinforcement ratio and transverse reinforcement to resist the moment and strain demands for the RC bridge pier. Hence, it is vital to predicting the damage-control target displacement accurately for the seismic design of the RC bridge. Further details of the implication of this proposed model are highlighted in Chapter 6, where the DCLS and damage-control target displacement is employed to design RC bridges, according to the DDBD method.
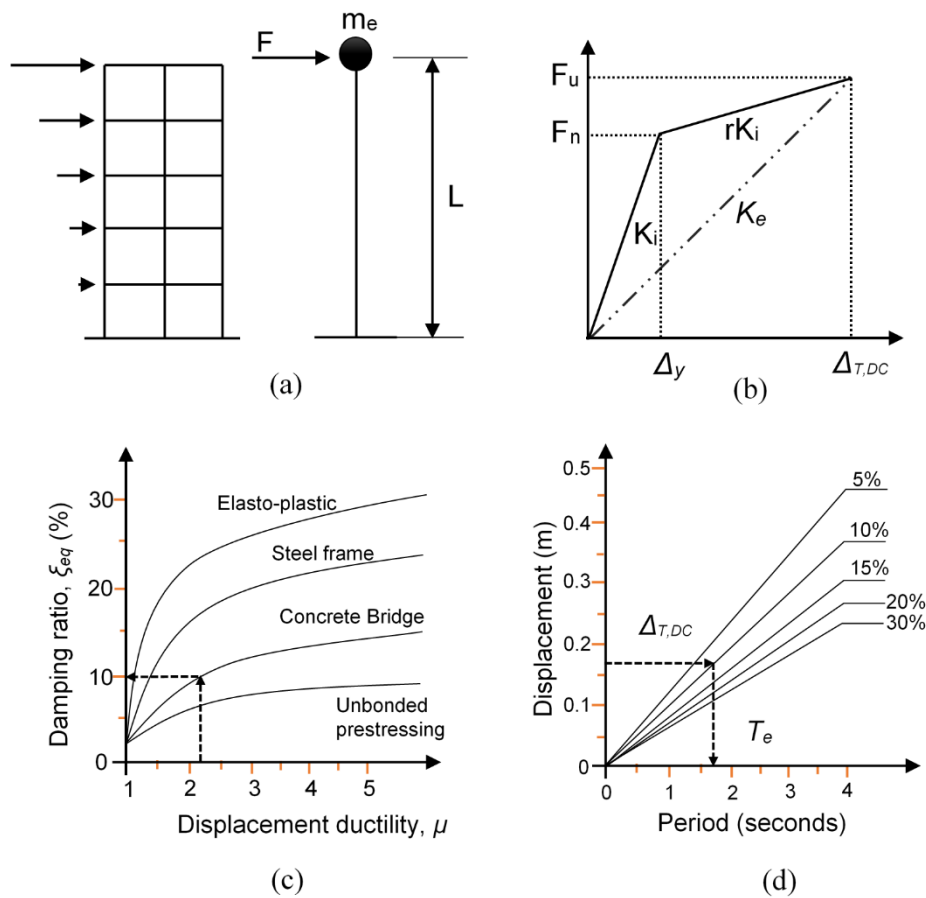
Figure 5.14 Fundamental principles of direct displacement-based design
(Priestley *et al.*, 2007)

5.7 Conclusion

In this chapter, a new model has been proposed for predicting the damage-control target displacement of circular RC bridge piers for the DDBD method. The proposed damage-control target displacement utilises the damage-control limit states, where new expressions are introduced in the model. Existing damage-control concrete compression strain and new expressions of damage-control reinforcement tensile strain are considered

in this model, along with the modified plastic hinge length, modified strain penetration length, and yield displacement. The model is proposed to improve the estimation of damage-control target displacement, mainly for the circular RC bridge pier. On the other hand, the FEM was employed to validate the proposed model. A series of RC bridge piers that were previously tested under cyclic loading (pushover tests) were selected to validate the proposed model by using the validated FEM. A series of validation was conducted using the RC bridge pier, which it was subjected to earthquake conditions. A parametric study was conducted to evaluate the influences of concrete strength and reinforcement ratio on the prediction of damage-control target displacement of the RC bridge pier. Some conclusions can be drawn as follows:

1) The proposed model presented in this chapter can predict the damage-control target displacement of circular RC bridge piers with reasonable accuracy. These results reveal the significant influence of improved damage-control reinforcement tensile strain and plastic hinge length to estimate the structural response based on DCLS.

2) The proposed model can be used to estimate the damage-control target displacement used in DDBD method for RC bridge piers under the lower and/or moderate magnitude of earthquakes.

3) The influence of concrete strength on the prediction of damage-control target displacement is not significant and can be ignored. However, the axial load ratio, pier height, and longitudinal and transverse reinforcement ratios have some influences on the prediction of damage-control target displacement for the RC bridge piers.

Chapter 6

The Seismic Design and Assessment of Multi-Span RC Bridge by using FE Analysis

Based on the literature review presented in Chapter 2, a comprehensive study to assess the behaviour of multi-span RC bridge with a circular pier (designed based on EC8 and DDBD methods) under different earthquake conditions is needed. Therefore, in this chapter, two multi-span RC bridges are designed based on EC8 and DDBD methods against earthquake. Then the two RC bridges under different earthquake conditions are modelled using developed full-scale 3D FEM for assessing the seismic resistances of both bridges.

6.1   Introduction

Significant damage or collapse of bridges during earthquake events cause loss of life and incur repairing cost. In some cases, some part of the bridge component needs replacement due to extensive damage or collapse. Most of the seismic design codes provide guidelines, focusing on minimising damage and preventing the bridge from collapse under earthquake events. However, reflecting on the number of previous earthquakes that occurred around the world, structures such as RC bridges were collapsed or faced damages significantly under the moderate and strong earthquakes (Hu *et al.*, 2017; Li *et al.*, 2017). It is well known that the repair of the RC bridge after an earthquake is an extremely challenging task. During an earthquake, several components of the RC bridge may fail, including the pier, decks, connection, foundation, bearings, and girders. However, it should be noted that failure of the RC bridge pier might result in extreme damage, including the collapse of the whole RC bridge.

It should be noted that the most common failure substructure of an RC bridge is the RC bridge pier. The RC bridge piers are the essential parts of overall RC bridge structures to support the bridge deck and load from the traffic. During an earthquake, RC bridge piers can suffer several damages, including damages towards concrete cover and buckling of the longitudinal reinforcement. Li *et al.* (2017) reported that during an earthquake, the damage could occur towards an RC bridge pier. Due to insufficient in the ductility of RC bridge piers, flexural-shear failure can occur. Similar observation reported by Zhang and

Unjoh (2008) indicated that the typical damage of RC bridge piers subject to the earthquake was a flexural-shear failure. Further extensive damage to the RC bridges and bridge piers during an earthquake can be presented as buckling of longitudinal reinforcement, crushing of core concrete, and total collapse.

The research on the seismic-resistant of RC bridge structures has been conducted for decades to prevent the severe damage and total collapse of RC bridges in the event of an earthquake. In seismic design, Eurocode 8 - Part 1 (EC8-1) (CEN, 2004b) and Eurocode 8 - Part 2 (EC8-2) (CEN, 2004c) are the codes that provide a method and guideline for researchers and engineers to design the structures to withstand a minor and major earthquake. Traditionally, bridges were designed using the force-based design (FBD) method. FBD method has been adopted by most of the current design codes (Kappos *et al.*, 2012), including EC8-2. FBD method uses force as design criteria; however, it is not explicitly connected with the damage to the RC bridges. In recent research, Davi (2015) conducted the seismic analysis and design of bridges using EC8-2 and the direct displacement-based design (DDBD) method. Also, the finite element (FE) nonlinear time-history analysis (NLTH) was conducted, using FE software SAP2000. A five-span RC bridge with four bridge piers was adopted in this study. The results indicated that the structures designed using the DDBD method performed better than EC8-2.

Previous research has shown that the displacement is a key factor to cause severe damage to the RC bridges. FBD method has many uncertainties and weaknesses based on the performance of structures in the previous earthquake events. In the past events, it was reported that RC bridges designed by FBD method failed to control and minimise the damage towards the structures in the major earthquakes (Ghobarah, 2001), including the 1995 Kobe earthquake, 1989 Loma Prieta earthquake and 2008 Wenchuan earthquake. During recent years, the displacement-based design method has been developed to overcome the limitations of the FBD method. The DDBD method has evolved as a new way to implement the displacement-based design method for RC bridge design. The fundamental of DDBD method is to ensure the structures are designed to achieve specific target displacement and damage level under different levels of earthquake intensities (Kowalsky *et al.*, 1995; Priestley and Kowalsky, 2000; Priestley and Calvi, 2007; Priestley *et al.*, 2007; Calvi *et al.*, 2013), based on a substitute structure approach pioneered by Shibata and Sozen (1976). The DDBD method has been proved to be one of the most effective design approaches, among other displacement-based design methods

(Kowalsky, 2002; Restrepo, 2006; Suarez, 2008; Suarez and Kowalsky, 2011). Bardakis and Fardis (2011) identified that EC8-2 design is less cost-effective and less rational compared with the displacement-based design. In EC8-2, the seismic design is specified through the analysis without any consideration of the structural performance under an earthquake (Lehman *et al.*, 2004).

In recent years several researchers use the FE method to analyse the seismic failure of the RC bridge. Some studies on the seismic performance of RC bridge by using FE method have been conducted to assess the seismic performance of RC bridges design based on the FBD method and DDBD method (Bardakis and Fardis, 2011; Reza *et al.*, 2014; Zhang *et al.*, 2015). The general findings are that the RC bridge designed based on the FBD method, suffers too much damage, and increases the cost of repair. However, the RC bridge designed using the displacement-based method has less damage, but it is too conservative. Many researchers used a simplified FEM to model the RC bridge in order to reduce the high computation cost. However, more comprehensive three-dimensional (3D) finite element models (FEM) are needed for profoundly understanding the damage mechanism of the RC bridge under different earthquake conditions. Therefore, the main objectives of this chapter are:

- To assess the seismic performances of RC bridges designed based on EC8-2 (FBD) method and recently improved DDBD method by using the developed 3D FEM model.

- To propose some design recommendations on how to enhance the seismic performance of RC bridges under multiple earthquake conditions.

6.2 Design of RC bridges according to EC8-2 and DDBD method

6.2.1 RC bridge information

Two RC bridges with circular piers consisting of four-spans shown in Figure 6.1 are adopted in this research. The RC bridge considered in this chapter is used widely in engineering practice (Botero, 2004; Restrepo, 2006; Montoya, 2008). As shown in Figure 6.1(a), the span between abutment and Piers 1 and 3 is 40.0 m. The span between each pier is 50.0 m. The cross-section of the circular RC bridge pier and deck is shown in Figure 6.1(b). As shown in Figure 6.1(b), the width and height of the box girder are 12.0 m and 2.0 m, respectively. The RC bridge has four-span and three circular RC bridge

piers. The three circular RC bridge piers have an equal height of 10.0 m and a diameter of 2.0 m. It is assumed that the RC bridge is subjected to seismic loading in the longitudinal and transverse directions. Based on the current design practice, the RC bridge deck in this study is considered to behave as elastic during an earthquake. The connection of the RC bridge deck with the pier is assumed to be pinned connection. Hence, the inelastic behaviour of the bridge is mainly focused on the RC bridge pier. The RC bridge deck sectional properties are presented in Table 6.1. Two RC bridges have the same properties and configurations of the RC bridge deck. It is assumed that the circular RC bridge piers have a rigid connection at the bottom and pinned connection at the top (cantilever RC bridge pier).
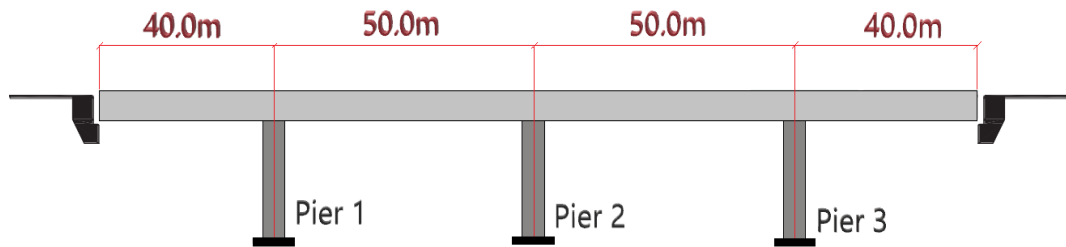
(a)
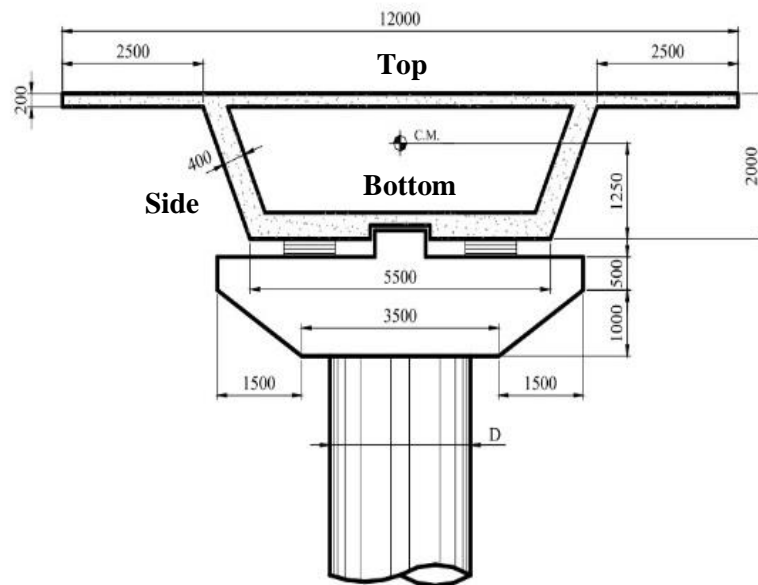
(b)

Figure 6.1 (a) Elevation view of the RC bridge; (b) RC bridge pier transverse section

Table 6.1 RC bridge deck properties

Parameter	Deck Properties		
Deck position	Top	Bottom	Side
Thickness (mm)	200	400	400
Concrete strength [$f_c^{'}$ (MPa)]	30		
Concrete elastic modulus (GPa)	35000		
Poisson's ratio	0.2		
Longitudinal Reinforcement (mm)	H20-200	H16-150	H16-150
Reinforcement elastic modulus (GPa)	210		
Longitudinal reinforcement yield strength [f_{ye} (MPa)]	420	420	420
Longitudinal reinforcement ultimate strength [f_{yeu} (MPa)]	469	469	469

6.2.2 Design of RC bridge pier according to EC8-2 method

According to EC8, the seismic design of the ductile circular RC bridge pier aims to ensure a relatively uniform distribution of inelastic displacement demand at specified dissipating zones. The regularity of circular RC bridge piers is affected by the minimum longitudinal reinforcement ratio. In EC8-2 (CEN, 2004c), the minimum longitudinal reinforcement ratio is not directly specified (Gkatzogias and Kappos, 2016). Therefore, EC2 (CEN, 2004a) is used to determine the minimum longitudinal reinforcement ratio for the RC bridge pier. The concrete compressive strength is 30 MPa. The circular RC bridge is designed based on EC8-2 'Type-1' elastic spectrum corresponding to soil type C (medium-stiff soil) and 0.5g peak ground acceleration (PGA) with a 5% damped displacement response (damping). The assumption is made in order to estimate the structural stiffness which will be used to determine the natural period of the structures and distribution of the forces to different structural members.

In this approach, the effective cracked stiffness of the piers is evaluated from design ultimate moment, using EC8 Annex C method no. 2, EC8-2 requirements. The effective stiffness for the cracked section has been calculated by multiplying stiffness reduction factors to the initial bending of circular RC bridge pier stiffness, according to the uncracked moment of inertia. For all piers, the stiffness is assumed to be 40 % of the uncracked stiffness. The design base shear force is obtained and dividing to each pier by the force-reduction factors. The strength of the circular RC bridge pier is reduced by inelastic displacement capacity (ductility), in which the level of required ductility is depended on force reduction factor, displacement ductility, and time period. Therefore, by considering the force-reduction factor, there are some issues to define and determine the exact position of yield and ultimate (maximum) displacement. The base shear is then distributed between RC bridge piers proportions to the elastic stiffness of each pier. In this case, all piers will have a similar reinforcement ratio (Calvi *et al.*, 2013). The same approach is applied for a regular RC bridge with a fixed abutment at both sides, and the odd number of piers, the middle pier, will have a higher longitudinal reinforcement ratio. For this research, the design flowchart of the circular RC bridge pier, according to EC8-2, is shown in Figure 6.2.
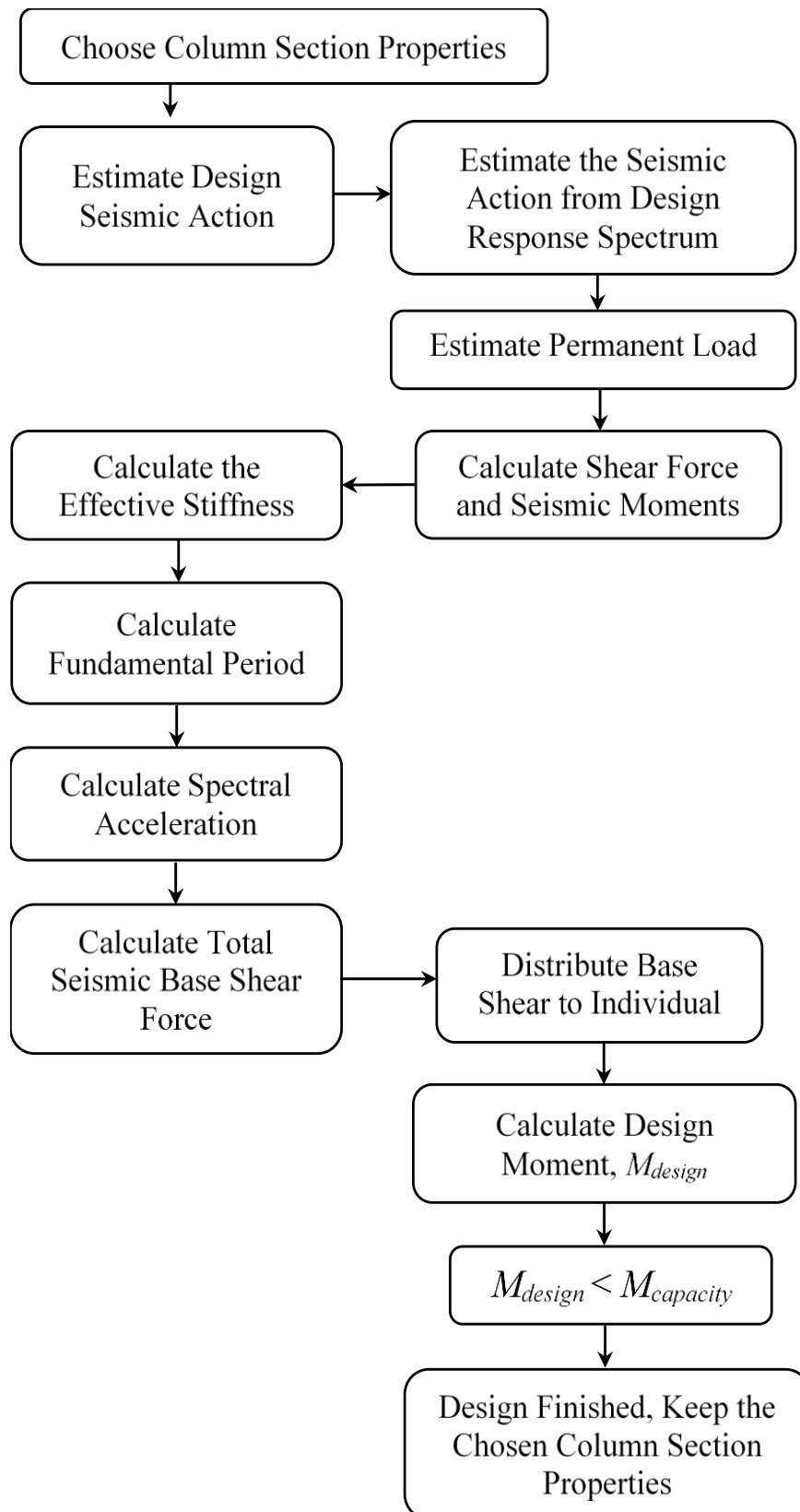
Figure 6.2 Design flowchart of RC bridge pier according to EC8-2

Step 1: Estimating the design seismic action

Figure 6.3 shows the design response spectrum of EC8-2, in which T_B and T_C are the limits of the constant spectra acceleration and T_D is the period indicating the beginning of the constant displacement response range of the spectrum. The design seismic action is calculated by considering a response spectrum type 1 and ground type C. Therefore, the characteristic period is $T_B = 0.20$ s, $T_C = 0.60$ s, and $T_D = 2.50$ s, and the soil factor is $S = 1.15$. The seismic action in the horizontal direction $a_g S$ is 0.40 g.
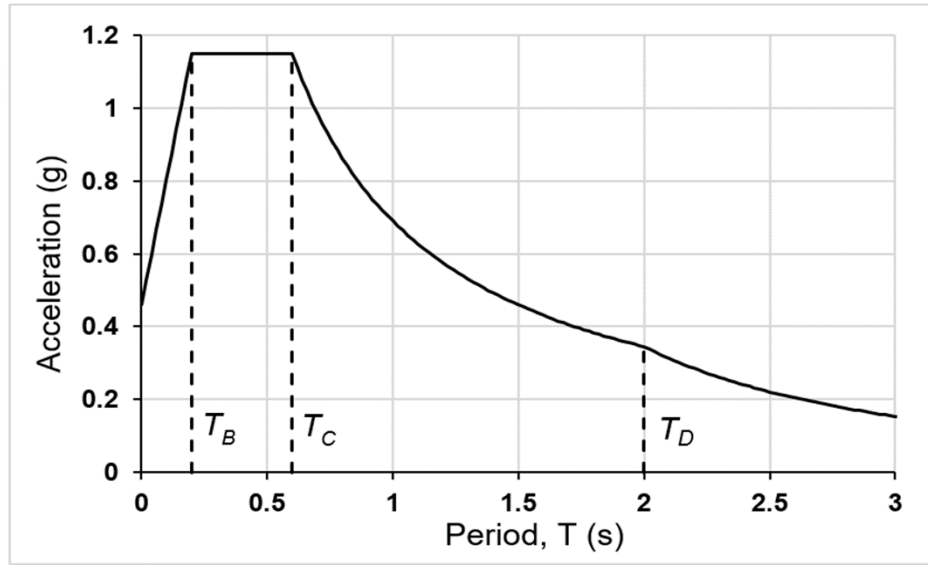
Figure 6.3 Design response spectrum of EC8.

Step 2: Estimating the permanent load

Based on the information on the RC bridges used in this study, the weight W_E of the RC bridge is 33940 kN, including the self-weight, additional traffic load, and 20% of the effective seismic load.

Step 3: Estimating the shear force and seismic moments

For the circular RC bridge pier of diameter $D = 2.0$ m, the uncracked moment of inertia J_{un} is:

$$J_{un} = \frac{\pi \times D^4}{64} \tag{6.1}$$

$$J_{un} = \frac{\pi \times 2.0^4}{64} = 0.7853 \, m^4$$

The assumed effective moment of inertia of circular RC bridge piers is $J_{eff}/J_{un} = 0.40$. J_{eff} is an effective moment of inertia. Based on the circular RC bridge pier fixed at the bottom and pinned at the top and for the concrete grade of C30/37 with Young modulus, $E_{cm} = 33,000$ MPa, the effective stiffness, K_i for individual RC bridge pier in the longitudinal direction is:

$$K_i = \frac{3E_{cm}J_{eff}}{L_{pier}^3} \tag{6.2}$$

$$K_{1,2,3} = \frac{3(33000)\times(0.40\times0.7835)}{10^3} = 31.0MN/m$$

where L_{pier} is the pier height of circular RC bridge pier. The total stiffness K_T of three circular RC bridge piers is 93.0 MN/m. The fundamental period T can be calculated as:

$$T = 2\pi\sqrt{\frac{m}{K_T}} \tag{6.3}$$

$$T = 2\pi\sqrt{\frac{33940/9.81}{93000}} = 1.21s$$

where m is the mass of the RC bridge deck. Once the fundamental period is established, the spectral acceleration, S_e in a longitudinal direction, can be calculated as:

$$S_e = a_g S \times \frac{2.5}{q} \times \frac{T_C}{T} \tag{6.4}$$

where q is the seismic behaviour factor.

$$S_e = 0.4\times1.15\times\frac{2.5}{3.5}\times\frac{0.60}{1.21} = 0.162g$$

The total seismic shear force, V_E, for RC bridge piers is given as:

$$V_E = S_e W_E \tag{6.5}$$

where W_E is the weight of the RC bridge in unit kN/g

$$V_E = 0.162\times33,940 = 5499kN$$

Therefore, the total seismic shear force is distributed to circular RC bridge pier 1, 2, and 3 proportionally to their stiffness:

$$V_i = \frac{K_i}{K_T} \times V_E \qquad (6.6)$$

where V_i is the individual seismic shear force.

$$V_1 = \frac{31.0}{93.0} \times 5499 = 1833 kN ; \; V_1 = V_2 = V_3$$

The individual seismic moment demands, M_i for circular RC bridge piers, are:

$$M_i = V_i L_{pier,i} \qquad (6.7)$$

$$M_1 = V_1 L_{pier,1} = 1833 \times 10 = 18330 kNm ; \; M_1 = M_2 = M_3$$

Based on the seismic moments demands which are less than moment capacity, the longitudinal reinforcement provided for all piers is 1.3%. The longitudinal reinforcement selected is 50 H32. The transverse reinforcement is provided based on the minimum requirement stated in EC2. Thus, 10 mm – 150 mm center to center (c/c) is provided, as shown in Table 6.2.

6.2.3 Design of RC bridge pier according to DDBD method

In the DDBD method, a yield displacement and target displacement are determined based on a selected performance level. For this research, the damage-control limit state (DCLS) is selected in order to design the RC bridge pier subjected to an earthquake. The RC bridge piers are designed to meet the requirement of DCLS. Since the circular RC bridge piers are equal height, all the RC bridge piers will govern the design. Figure 6.4 shows the design flowchart of the RC bridge pier, according to the DDBD method. The detailed procedure is described as follow:

Step 1: Evaluating the yield displacement for the RC bridge pier

Based on the information on the RC bridge adopted in this study, the axial load ratio is approximately 10%. The longitudinal reinforcement is estimated at approximately 2%. The pier height is 10.0 m for all piers. For calculating the yield displacement of the RC bridge pier, Δ_y the model developed in Chapter 4 is used and Δ_y = 97.7 mm. Also, the

model developed in Chapter 5 is adopted to compute the damage-control target displacement $\Delta_{T,DC}$ and the $\Delta_{T,DC} = 242$ mm.
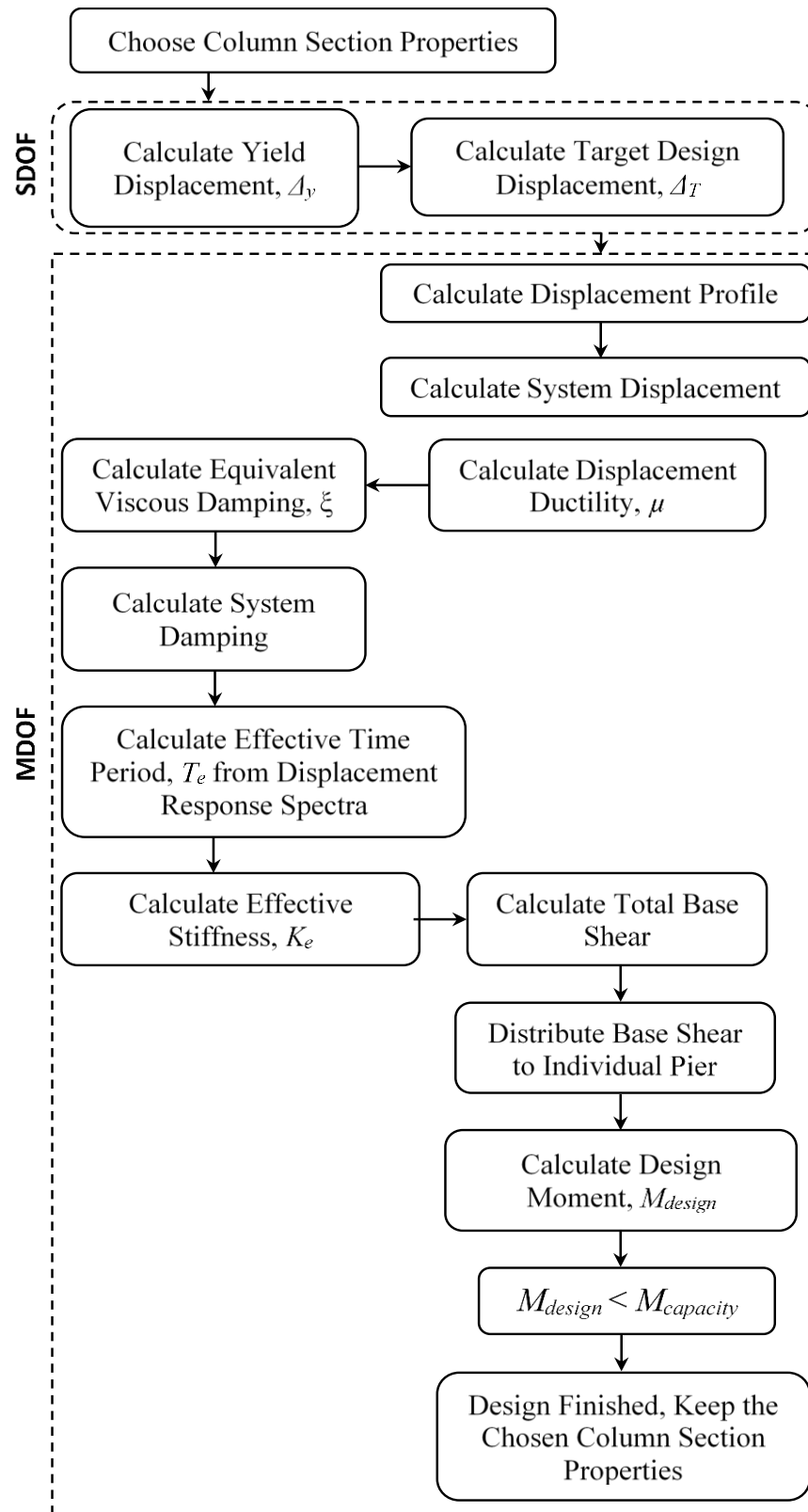
Figure 6.4 Design flowchart of RC bridge according to DDBD method

Step 2: Evaluate the equivalent properties for the RC bridge

The system damage-control target displacement $\Delta_{T,DC,sys}$ based on DCLS and circular RC bridge pier equivalent damping $\xi_{eq,i}$ are computed according to Eqn. (6.8) and Eqn. (6.9), respectively (Kowalsky, 2002; Priestley *et al.*, 2007).

$$\Delta_{T,DC,sys} = \sum_{i=1}^{n}\left(m_i\Delta_i^2\right) \bigg/ \sum_{i=1}^{n}\left(m_i\Delta_i\right) \tag{6.8}$$

$$\xi_{eq,i} = 0.05 + 0.444\left(\frac{\mu_i - 1}{\mu_i\pi}\right) \tag{6.9}$$

where m_i is mass from bridge deck acting on individual circular RC bridge pier, Δ_i is the displacement subjected to displacement profile (displaced shape), and μ_i is displacement ductility for each circular RC bridge pier.

The system equivalent damping, ξ_{eq} is assumed of 50% of the total shear carried by the superstructure and abutment and given by Eqn. (6.10) (Restrepo, 2006; Priestley *et al.*, 2007).

$$\xi_{eq} = \frac{0.025\Delta_{T,DC,sys} + 0.5\left(\sum_{i=1}^{n}\frac{1}{L_{pier}}\Delta_i\xi_{eq,i}\right) \bigg/ \sum_{i=1}^{n}\frac{1}{L_{pier}}}{0.5\Delta_{T,DC,sys} + 0.5\left(\sum_{i=1}^{n}\frac{1}{L_{pier}}\Delta_i\right) \bigg/ \sum_{i=1}^{n}\frac{1}{L_{pier}}} \tag{6.10}$$

where $\Delta_{T,DC,sys}$ is the system displacement based on DCLS, L_{pier} is the pier height and $\xi_{eq,i}$ is the equivalent damping for each circular RC bridge pier. From Step 1, the $\Delta_{T,DC}$ is 0.242 m (242 mm) for the RC bridge pier with a height of 10 m and approximately 2% of the longitudinal reinforcement ratio. Therefore, the displacement profile under transverse response, δ_i for the circular RC bridge pier shown in Figure 6.5 is given by Eqn. (6.11) (Kong, 2017).

$$\delta_i = a_i \sin\left(\frac{x_i}{x_{total}}\pi\right) \tag{6.11}$$

where a_i is the modified relative circular RC bridge pier stiffness coefficient based on half-sine displaced shape; x_i is the span from the abutment to the RC bridge pier and x_{total}

134

is the total span of the RC bridge. In this case, both abutment were assumed to be restrained transversely and free to move longitudinally, as usual design practice of the RC bridge for gravity loads.
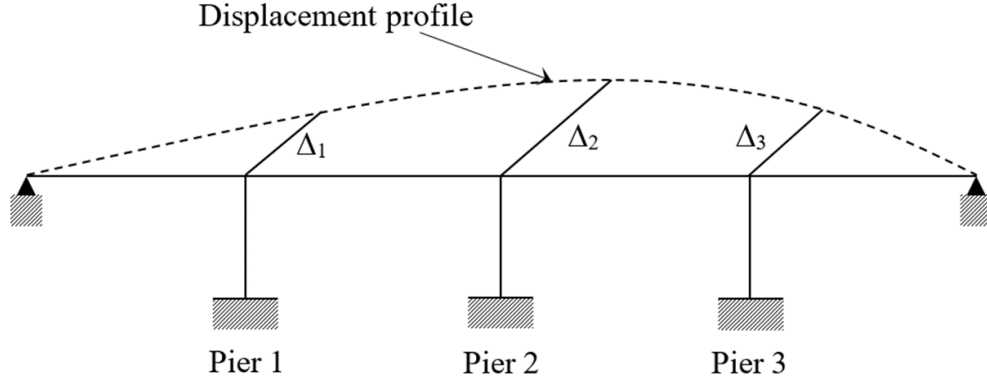
Figure 6.5 Displacement profile under transverse response

Then, the individual target displacement based on the displacement profile $\Delta_{T,i}$ is given by Eqn. (6.12), where $\Delta_{T,DC}$ is the design damage-control target displacement.

$$\Delta_{T,i} = \delta_i \times \Delta_{T,DC} \tag{6.12}$$

Pier 1: $x_1 = 40$ m, $\delta_1 = 1 \times \sin\left(\dfrac{40}{180}\pi\right) = 0.642$; $\Delta_1 = 0.642 \times 0.242 = 0.155\,m$

Pier 2: $x_2 = 90$ m, $\delta_2 = 1 \times \sin\left(\dfrac{90}{180}\pi\right) = 1$; $\Delta_2 = 1 \times 0.242 = 0.242\,m$

Pier 3: $x_3 = 140$ m, $\delta_3 = 1 \times \sin\left(\dfrac{140}{180}\pi\right) = 0.642$; $\Delta_3 = 0.642 \times 0.242 = 0.155\,m$

The system damage-control target displacement is computed using Eqn. (6.13). The mass m_i from RC bridge deck added on the RC bridge pier 1, 2, and 3 are 11000 kN, 11940 kN, and 11000 kN, respectively.

$$\Delta_{T,DC,sys} = \frac{m_1\Delta_1^2 + m_2\Delta_2^2 + m_3\Delta_3^2}{m_1\Delta_1 + m_2\Delta_2 + m_3\Delta_3}\,; 0.195 \text{ m.} \tag{6.13}$$

The displacement ductility, μ_i for each pier, is given by Eqn. (6.14), where Δ_y is the yield displacement for Pier 1, 2, and 3.

$$\mu_i = \frac{\Delta_i}{\Delta_y} \tag{6.14}$$

$$\mu_1 = \mu_2 = \frac{0.155}{0.097} = 1.59 \; ; \; \mu_3 = \frac{0.242}{0.097} = 2.49$$

The circular RC bridge pier equivalent damping for each pier is:

$$\xi_{eq,1} = \xi_{eq,3} = 0.05 + 0.444 \left(\frac{1.59-1}{1.59\pi} \right) = 0.102$$

$$\xi_{eq,2} = 0.05 + 0.444 \left(\frac{2.49-1}{2.49\pi} \right) = 0.134$$

Therefore, the system damping for the RC bridge calculates using Eqn. (6.10), was approximately 5.5 %.

$$\xi_{eq} = \frac{0.025(0.195) + 0.5 \left(\left[\frac{1}{10} \times 0.155 \times 0.102 \times 2 \right] + \left[\frac{1}{10} \times 0.242 \times 0.134 \right] \right) \Big/ \frac{3}{10}}{0.5(0.195) + 0.5 \left(\left[\frac{1}{10} \times 0.155 \times 2 \right] + \left[\frac{1}{10} \times 0.242 \right] \right) \Big/ \frac{3}{10}}$$

$$\xi_{eq} = 0.055 = 5.5\%$$

Once the system damping is calculated, the effective time period T_e is determined from the displacement spectra. The displacement spectra are based type C with 5% damping, 0.4 PGA with respect to EC8-2. The displacement spectra were derived using SeismoArtif software (Seismosoft, 2016), as shown in Figure 6.6.
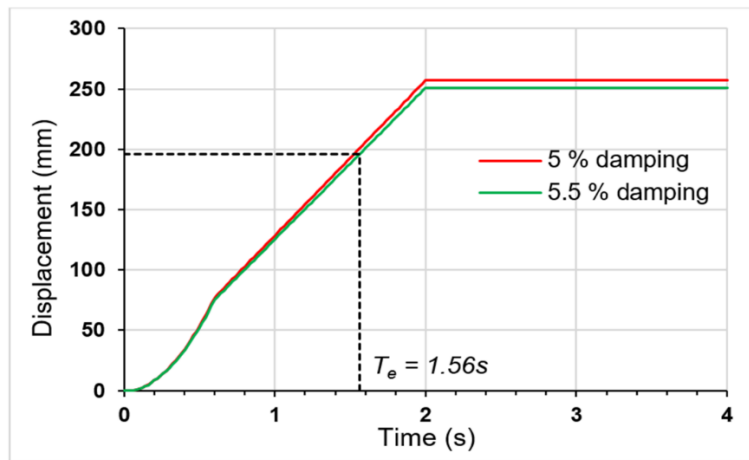
Figure 6.6 Displacement response spectra based on type C, 0.4 PGA with according to EC8

136

As shown in Figure 6.6, the effective time period of the system for the target displacement of 195 mm is 1.56 s. The effective weight of the RC bridge is 33940 kN. Therefore, the effective secant stiffness K_e is given by Eqn. (6.15).

$$K_e = \frac{4\pi^2 m_e}{T_e^2} ; \tag{6.15}$$

$$K_e = \frac{4\pi^2 (33940)}{9.81 \times 1.56^2} = 56,125 \, kN/m$$

Where m_e is the system effective mass. Total base shear demand, V is calculated by multiplying the effective secant stiffness, and the system damage-control target displacement using Eqn. (6.16).

$$V = K_e \Delta_{T,DC,sys} \tag{6.16}$$

$$V = 56125 \times 0.195 = 10944 \, kN$$

The base shear is distributed to each circular RC bridge pier in inverse proportion to the height of the circular RC bridge pier. Therefore, the circular RC bridge piers have equal bending moments and subjected to an equal longitudinal reinforcement ratio. The design base shear for individual circular RC bridge pier, V_i is calculated using Eqn. (6.17).

$$V_i = \frac{1/L_{pier,1}}{1/L_{pier,1} + 1/L_{pier,2} \ldots\ldots 1/L_{pier,n}} V \tag{6.17}$$

$$V_{1,2,3} = \frac{1/10}{1/10 + 1/10 + 1/10} 10944 = 3648 \, kN$$
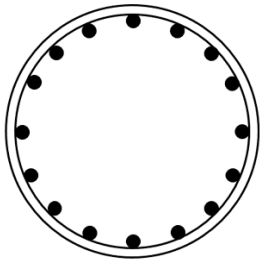
Therefore, the individual seismic moment demands, M_i for circular RC bridge pier 1, 2, and 3 are:

$$M_1 = V_1 L_{pier,1} = 3648 \times 10 = 36480 kNm ; \quad M_1 = M_2 = M_3$$

Based on the DDBD method, the circular RC bridge pier was subjected to an equal bending moment. Therefore an equal longitudinal reinforcement ratio is provided to meet the requirements of system damage-control target displacement of 0.195 m. By using this moment demand, the area of reinforcement required is 62000 mm². The longitudinal

reinforcement ratio provided is 2 %, equivalent to 50 H40. The transverse reinforcement provided was 12 mm – 150 mm c/c, as shown in Table 6.2. Based on Table 6.2, it is clear that RC bridge design using EC8 were unconservative and provide less reinforcement.

Table 6.2 Design reinforcement in RC bridge pier

Cross-Section*	Pier	DDBD	EC8
	Pier 1	50 H40 mm Link bar 12 mm - 150 c/c	50 H32 mm Link bar 10 mm – 150 mm c/c
	Pier 2	50 H40 mm Link bar 12 mm – 150 c/c	50 H32 mm Link bar 10 mm – 150 mm c/c
	Pier 3	50 H40 mm Link bar 12 mm – 150 c/c	50 H32 mm Link bar 10 mm – 150 mm c/c

*Cross-section contains reinforcement is not to scale

6.3   Evaluation methods

In order to assess seismic performance and to compare both design methods, two evaluation methods are used, including maximum displacement and damage level indicated by Damage Index (DI). The maximum displacement is the primary indicator of the RC bridge assessment subjected to an earthquake. RC bridge with lower displacement is expected to perform much better compared with the higher displacement under an earthquake. DI indicates the level of damages associated with the RC bridge subjected to an earthquake. The DI is related to damage level to represent the cracking of the concrete cover, buckling of longitudinal reinforcement bar, or collapse. The higher number of DI indicates the more severe damage of the RC bridge.

6.3.1   Maximum displacement

As aforementioned, the maximum displacement is one of the leading indicators of the RC bridge assessment subjected to an earthquake. As suggested by the DDBD method, the displacement is a crucial parameter to indicate the damage potential of the circular RC bridge pier. Due to this relation, by understanding the maximum displacement, the engineer and designer can be able to design the RC bridge to ensure the damage towards the structure is within the allowable limit proposed by the DDBD method. To evaluate

the RC bridge, subjected to multiple earthquakes, the maximum displacements predicted by FEM for both RC bridges designed using DDBD and EC8-2 are compared with system target displacement specified during the design (Dwairi and Kowalsky, 2006b). As for this research, the RC bridge was design to meet damage-control requirements. Therefore, the maximum displacement's result from FEM was compared with system damage-control target displacement for circular RC bridge under the DDBD limit states, as described in the previous section.

6.3.2 Damage Level

It is essential to assess the level of damage to the RC bridge following earthquake events. One of the objectives of this chapter is to assess the level of damage to the RC bridge. For instance, damage index (DI) is an advanced tool to quantify the level of damage for a range of types of structures, particular bridges. The circular RC bridge pier is easily damaged under earthquake conditions. Therefore, it is essential to determine the DI in order to assess the severity of damages. Many researchers have proposed numbers of DI depends on several numbers of a parameter such as energy dissipation, deformation, ductility, time period, and stiffness. In general, DI is based on structural performance parameters such as displacement, drift, and forces. Many DI that have been developed have their advantages. The damage index proposed by Su *et al.* (2017) was employed in this chapter to assess the RC bridges.

6.3.2.1 Damage indices and quantification of damages

In this research, five damages states were considered to assess the RC bridge and bridge pier subjected to earthquakes or seismic loading. Combining the damage states proposed by several researchers (Kunnath *et al.*, 1997; Hindi and Sexsmith, 2001; Priestley *et al.*, 2007), the damage index classification is highlighted in Table 6.3. In Table 6.3, the damage-control performance was considered to describe moderate damage, where beyond this performance level, the circular RC bridge pier is no longer repairable. It is essential to define the section damage for circular RC bridge pier as described in Section 2.3.1.1, in order to determine the damage states of the RC bridges. In this research, the damage index (DI) is calculated using material strain extracted from NLTH-FE analysis. The material strains during analysis, subjected to earthquakes, are extracted for each second of the earthquake for both concrete and reinforcement material. The damage index

can be calculated using equations explained as followed. Figure 6.7 highlights the flowchart to determine the damage index for circular RC bridges.

Table 6.3 Damage index and damage states for circular RC bridge pier

| Damage Index (*DI*)	Damage States	Damage Description	Performance Level
$DI < 0.1$	No damage	No visual of damage	Fully operational
$0.1 \leq DI < 0.2$	Slight damage	First cracking of the concrete, yielding of the longitudinal bar	Operational
$0.2 \leq DI < 0.4$	Moderate damage	Spalling of concrete cover	Damage-control
$0.40 \leq DI < 0.6$	Major damage	Significant spalling, some buckling of longitudinal bars	Life safety
$0.6 \leq DI < 1.0$	Collapse	Crushing of concrete core	Collapse
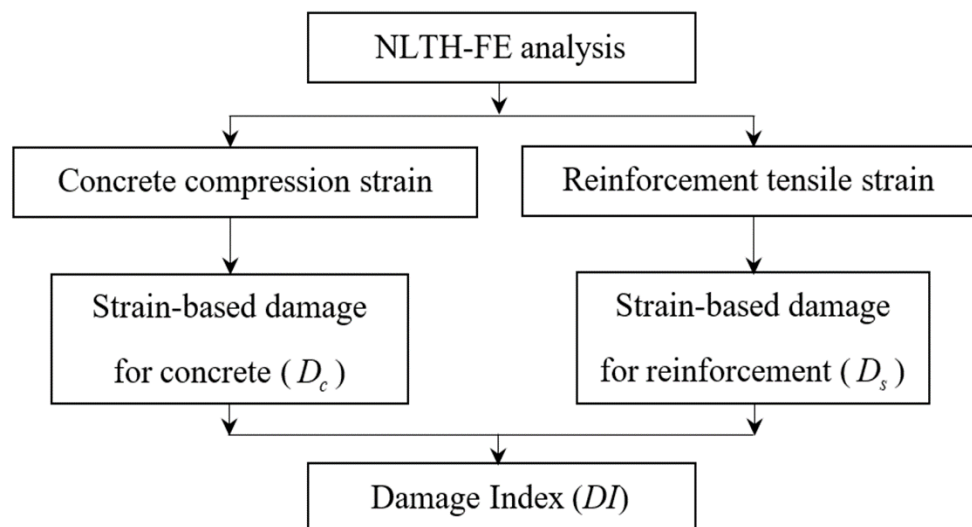
Figure 6.7 Flowchart to estimate damage index for RC bridge

Strain-based damage for reinforcement, D_s can be calculated using Eqn. (6.18) (Su *et al.*, 2017).

$$D_s = \begin{cases} \left(\varepsilon_{s,FE}/\varepsilon_y\right) \times D_{s1}, \varepsilon_s < \varepsilon_y \\ D_{s1} + \left(\left(\varepsilon_{s,FE} - \varepsilon_y\right)/\left(\varepsilon_{s,c1} - \varepsilon_y\right)\right) \times \left(D_{s2} - D_{s1}\right), \varepsilon_y \leq \varepsilon_{s,FE} < \varepsilon_{s,c1} \\ D_{s2} + \left(\left(\varepsilon_{s,FE} - \varepsilon_{s,c1}\right)/\left(\varepsilon_{s,c2} - \varepsilon_{s,c1}\right)\right) \times \left(D_{s3} - D_{s2}\right), \varepsilon_{s,c1} \leq \varepsilon_{s,FE} < \varepsilon_{s,c2} \\ D_{s3} + \left(\left(\varepsilon_{s,FE} - \varepsilon_{s,c2}\right)/\left(\varepsilon_{s,dc} - \varepsilon_{s,c2}\right)\right) \times \left(D_{s4} - D_{s3}\right), \varepsilon_{s,c2} \leq \varepsilon_{s,FE} < \varepsilon_{s,dc} \\ D_{s4} + \left(\left(\varepsilon_{s,FE} - \varepsilon_{s,dc}\right)/\left(\varepsilon_u - \varepsilon_{s,dc}\right)\right) \times \left(D_{s5} - D_{s4}\right), \varepsilon_{s,dc} \leq \varepsilon_{s,FE} < \varepsilon_u \\ D_{s5}, \varepsilon_{s,FE} \geq \varepsilon_u \end{cases} \quad (6.18)$$

In Eqn. (6.18), ε_y is the yield strain of the longitudinal reinforcement, $\varepsilon_{s,c1}$ and $\varepsilon_{s,c2}$ is representing the strain of longitudinal bar corresponding to 1 mm and 2 mm crack widths on the concrete cover. Based on previous research (Goodnight *et al.*, 2016b), $\varepsilon_{s,c1}$ and $\varepsilon_{s,c2}$ are 0.01 and 0.02, respectively. Reinforcement strain from NLTH-FE analysis, $\varepsilon_{s,FE}$ was extracted from the NLTH-FE results, as highlighted before. ε_u is the ultimate strain of longitudinal reinforcement defined as 0.1 and $\varepsilon_{s,dc}$ is the damage-control tensile reinforcement strain corresponding to the bar buckling, given by Eqn. (6.19) (Goodnight *et al.*, 2016a).

$$\varepsilon_{s,dc} = 0.03 + 700\rho_s \frac{f_{yh}}{E_s} - 0.1\frac{P}{f_c' A_g} \quad (6.19)$$

where ρ_s is the transverse reinforcement ratio, f_{yh} is the yield stress of transverse reinforcement and $P/f_c' A_g$ is the RC bridge pier axial load ratio. Based on the parameter used in Section 6.3, $\varepsilon_{s,dc}$ is defined as 0.0340. Damage reinforcement measure, D_{s1} to D_{s5} corresponding to performance level are equal to 0.1, 0.2, 0.4, 0.6 and 1.0.

Strain-based damage for concrete, D_c can be calculated using Eqn. (6.20) (Su *et al.*, 2017).

$$D_c = \begin{cases} \left(\varepsilon_{c,FE}/\varepsilon_{c,25}\right) \times D_{c1}, \varepsilon_{c,FE} \leq \varepsilon_{c,25} \\ D_{c1} + \left(\left(\varepsilon_{c,FE} - \varepsilon_{c,25}\right)/\left(\varepsilon_{c,65} - \varepsilon_{c,25}\right)\right) \times \left(D_{c2} - D_{c1}\right), \varepsilon_{c,25} < \varepsilon_{c,FE} \leq \varepsilon_{c,65} \\ D_{c2} + \left(\left(\varepsilon_{c,FE} - \varepsilon_{c,65}\right)/\left(\varepsilon_{c,100} - \varepsilon_{c,65}\right)\right) \times \left(D_{c3} - D_{c2}\right), \varepsilon_{c,65} < \varepsilon_{c,FE} \leq \varepsilon_{c,100} \end{cases} \tag{6.20}$$

In Eqn. (6.20), $\varepsilon_{c,FE}$ is the concrete strain extracted from the NLTH-FE results. Babazadeh *et al.* (2015) suggested that 0.005 is the strain limit for the spalling of concrete cover, based on 3D FEM analysis and experimental validation. A compressive strain of 0.005 is adopted in this study to predict the full spalling of concrete cover. Therefore, a concrete strain for 25% spalling on the concrete cover, $\varepsilon_{c,25}$ was assigned as 0.005. $\varepsilon_{c,100}$ and $\varepsilon_{c,65}$ are the concrete strain value corresponding to 100% and 65% of spalling of concrete cover, defined as 0.027 and 0.018, respectively. Mander *et al.* (1988) suggest that 0.018 is the limit for economical repair. Beyond the 0.018, the concrete is no longer repairable or not economical to be repaired. Figure 6.8 highlights the spalling of concrete definitions used in this research.

Onset of spalling (25%)   Significant spalling (65%)   Full spalling (100%)

■ Spalling of concrete   □ Concrete cover   ▨ Core concrete
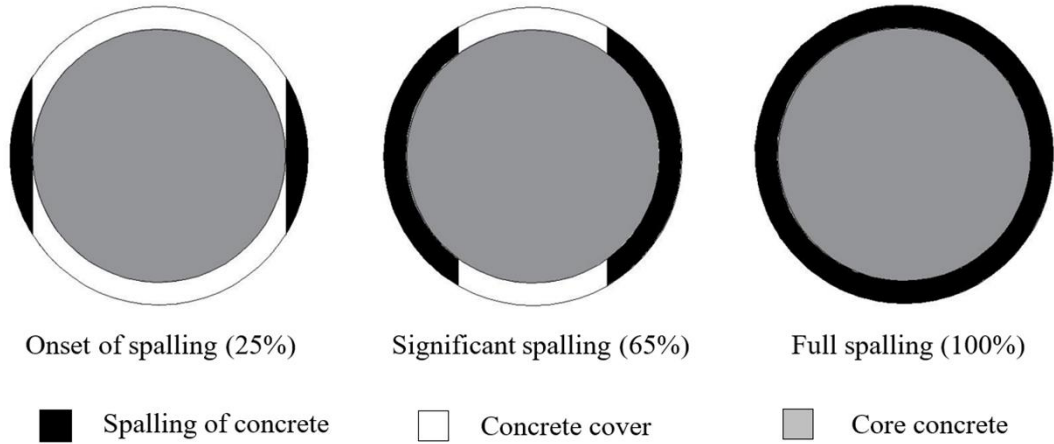
Figure 6.8 Type of spalling of concrete cover

Both strain-based damages were determined using Eqns. (6.18) and (6.20). Therefore, as suggested by Su *et al.* (2017), the damage index to represents the RC bridge pier section consists of concrete, and reinforcement is taken as the bigger one between both strain-based damage, using Eqn. (6.21).

$$DI = \max\{D_s, D_c\} \tag{6.21}$$

6.4 Nonlinear time-history finite element analysis

In this section, the comprehensive 3D FEM using ABAQUS developed in Chapter 3 is employed to conduct the Nonlinear Time-History Finite Element (NLTH-FE) analysis for the two bridges designed according to EC8-2 and DDBD method. The seismic performances of the RC bridges subjected to different seismic loading conditions are details investigated.

6.4.1 Seismic loading and ground motions

In this study, the RC bridges were subjected to different earthquakes ground motions records. Five randomly ground motion records were generated from the Pacific Earthquake Engineering Research Centre and SeismoArtif (Seismosoft, 2016) database. The details of five ground motions and characteristics used in this analysis were presented in Table 6.4. The time-histories of the earthquake ground motion were converted to spectrum-compatible time-histories generated using SeismoArtif (available online) (Seismosoft, 2016) to make sure that the spectrum of the original accelerogram records is compatible with the EC8-1 design accelerogram spectrum (CEN, 2004b). Since the RC bridges were designed for the UK and Europe purposes, the time-history data were scaled to generate the displacement spectra in order to match with type C with 5% damping with respect to EC8-1, as mostly used in DDBD approach. The scaled was conducted by using SeismoArtif software. The acceleration response spectra of the ground motions are presented in Figure 6.9.

Table 6.4 Selected ground motion records

No.	Earthquake	Recording station	Year	PGA (g)	Magnitude
S1	Chi-Chi	TCU045	1999	0.361	7.6
S2	Imperial Valley	USGS Station 5115	1979	0.315	6.5
S3	Kobe	KAKOGAWA (CUE90)	1995	0.345	6.9
S4	Loma Prieta	090 CDMG Station 47381	1989	0.367	6.9
S5	Friuli	TOLMEZZO(000)	1976	0.323	6.5
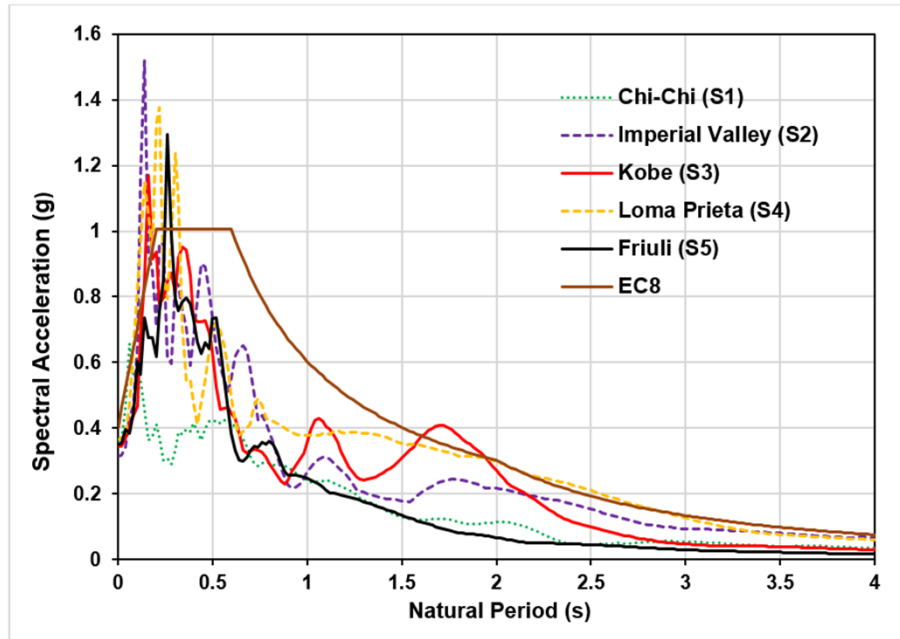
Figure 6.9 Acceleration spectra with 5% damping

6.5 Performances of the two RC bridges subjected to multiple earthquakes

This section provides a detailed comparison of the NLTH-FE analysis's results of the two RC bridges under different earthquakes. Due to the two bridges are a regular type of RC bridge with the same pier height, the comparisons of the results presented in this section are made using Pier 2 (middle pier).

6.5.1 Maximum transverse displacement

Figure 6.10 shows the comparison of the transverse displacement-time responses at the top of the Pier 2 for the RC bridges. As can be seen from the figure, the bridge designed by the DDBD method (DDBD bridge) has the lowest transverse displacement compared with the bridge designed using EC8-2 (EC8-2 bridge). The positive and negative displacements indicate that the RC bridge moves in the left and right direction during an earthquake event.

Figure 6.10(a) shows the transverse displacement-time response of the bridges subjected to the Chi-Chi earthquake (S1). It can be seen that the maximum transverse displacement of the EC8-2 bridge is higher than the one of the DDBD bridge. It is noticed that at the early stage of the earthquake, the displacements for both bridges show a similar pattern. However, after the response time of 20 s, the displacement differences of two bridges

144

increased with time. This is mainly attributed to the influences of a higher longitudinal reinforcement ratio of the DDBD bridge compared to the EC8-2 bridge. Due to the major damage on the concrete cover and part of core concrete in the EC8-2 bridge, the higher maximum transverse displacement has resulted in the maximum transverse displacement of the DDBD bridge was -223.8 mm (-ve indicate the transverse displacement in the left direction of the bridge) at 29.19 s. In this case, the maximum transverse displacement is higher than the damage-control target displacement $\Delta_{T,DC,sys} = 195$ mm, estimated by the DDBD method. Therefore, the bridge, designed according to the DDBD method, could not sustain the Chi-Chi earthquake (0.361 g). Meanwhile, the maximum transverse displacement of EC8 bridge was -273.2 mm in a similar direction. Figure 6.11(a) shows the transverse displacement profiles with the maximum transverse displacement for both bridges at 29.19 s of S1 earthquake.

Figure 6.10(b) shows the transverse displacement-time response of the bridges under the Imperial Valley (S2) earthquake. It is noticed that at the early stage of the earthquake, the transverse displacements of both bridges were approximately similar until 7.0 s, but after that, the displacement differences of the bridges increased with time. However, at 8 s, the displacement of the DDBD bridge was slightly higher than the EC8-2 bridge. As observed in Figure 6.10(b), the maximum transverse displacement (211.1 mm) of the EC8 bridge occurred at 9.37 s, and the maximum transverse displacement of the DDBD bridge was -179.6 mm at 15.72 s. In this case, the maximum transverse displacement of the DDBD bridge is lower than the damage-control target displacement ($\Delta_{T,DC,sys} = 195$ mm). Therefore, the DDBD bridge could sustain a moderate earthquake of 0.315 g. Due to the influences of spalling concrete cover in the EC8-2 bridge, this led to higher maximum transverse displacement compared with the DDBD bridge. The transverse displacement profiles with the maximum transverse displacement for both bridges are shown in Figure 6.11(b).

Figures 6.10(c) to 6.10(e) show the transverse displacement-time responses of the two bridges under Kobe (S3), Loma Prieta (S4), and Friuli (S5) earthquakes, respectively. For S3, the maximum transverse displacements of the DDBD bridge and EC8-2 bridge were 189.4 mm and 227.1 mm, respectively, at 11.39 s. The maximum transverse displacements of the DDBD bridge and EC8-2 bridge under Loma Prieta (S4) earthquakes were 228.4 mm and 264.0 mm, respectively, at 4.77 s. Under the Friuli (S5) earthquake,

the maximum transverse displacements of the DDBD bridge and EC8-2 bridge were -157.7 mm and -189.3 mm, respectively, at 3.98 s.

It is evident that in all three cases, the maximum transverse displacements of the EC8-2 bridge are higher than the one of the DDBD bridge. It is interesting to note that the maximum transverse displacements of the DDBD bridge under Kobe (S3) and Friuli (S5) earthquakes are lower than the damage-control target displacement ($\Delta_{T,DC,sys}$ = 195 mm). Hence, the DDBD bridge could sustain the moderate earthquakes of 0.315 g and 0.323 g. However, under the Loma Prieta (S4) earthquake, the maximum transverse displacement of DDBD bridge was higher than the damage-control target displacement ($\Delta_{T,DC,sys}$ = 195 mm). Therefore, the bridge, designed according to DDBD, could not sustain the Loma Prieta (S4) earthquake (0.367 g). Figures 6.11(c) to 6.11(e) show the transverse displacement profiles with the maximum transverse displacement for both bridges under Kobe (S3), Loma Prieta (S4), and Friuli (S5) earthquakes, respectively.
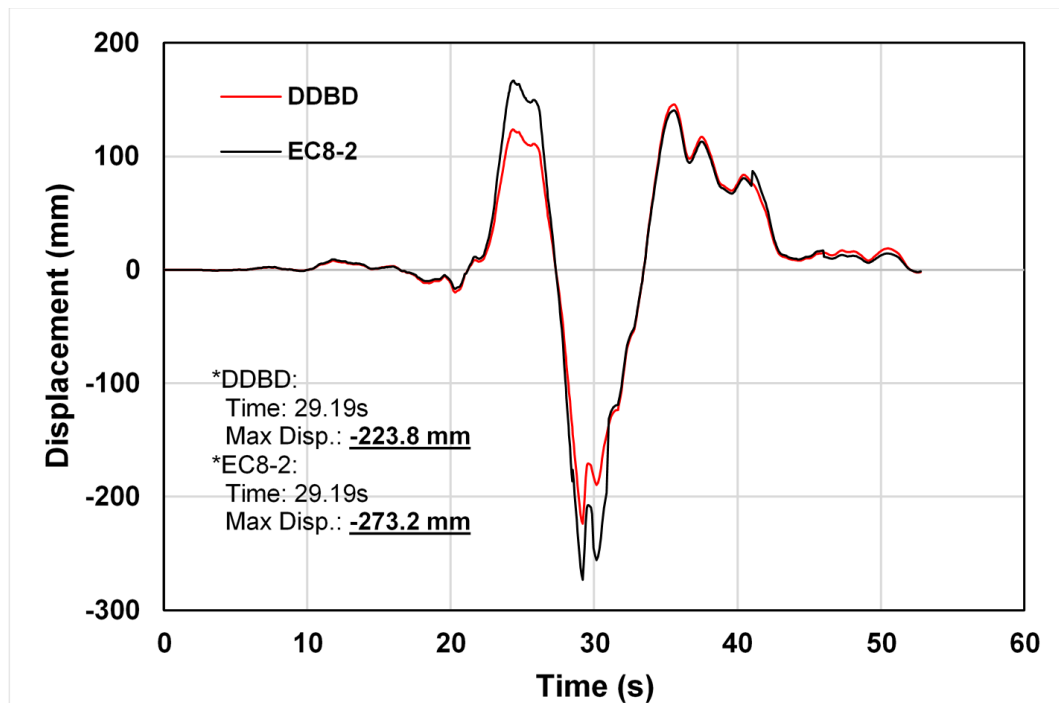
(a)
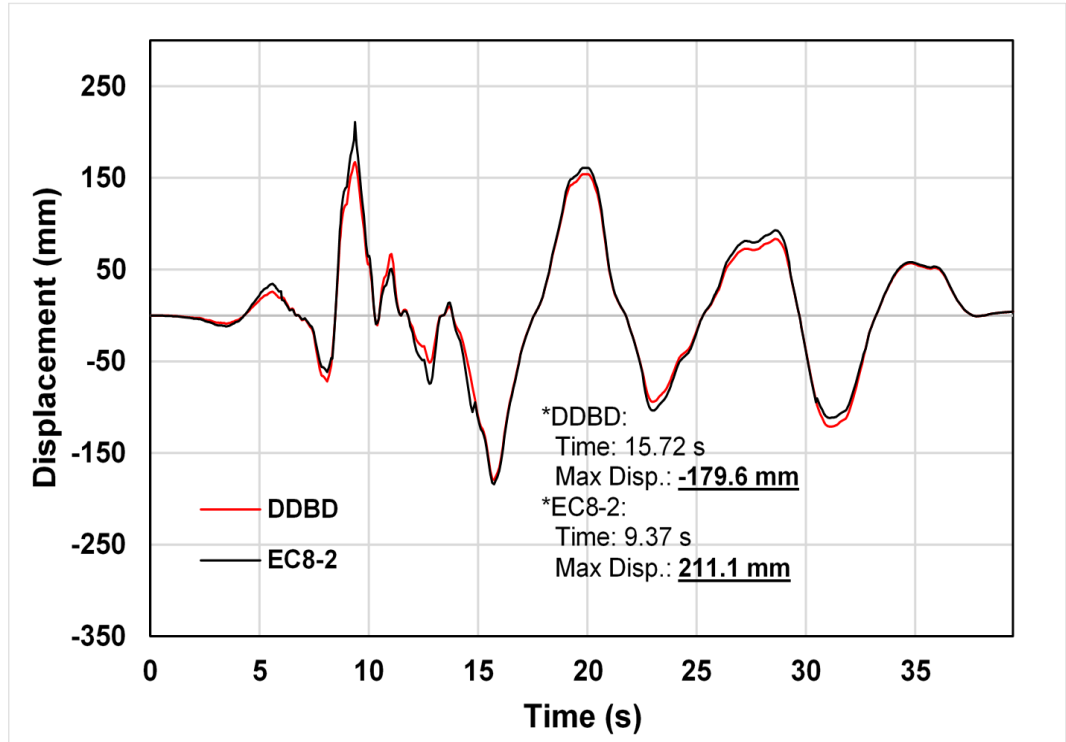
(b)
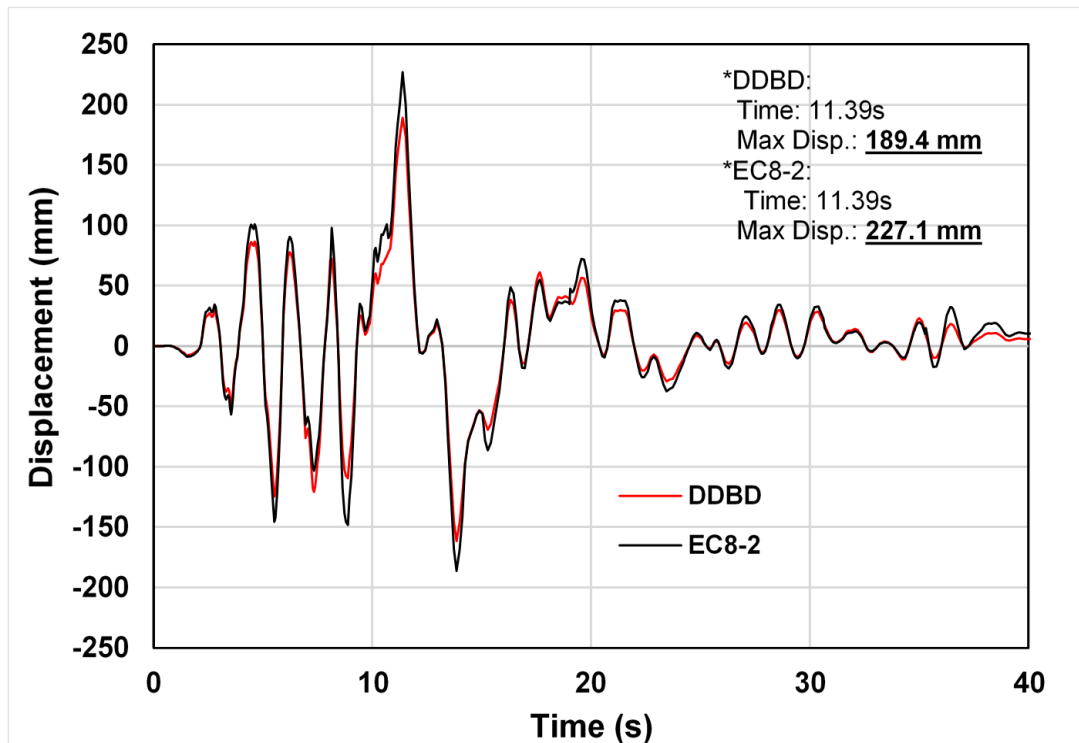
(c)
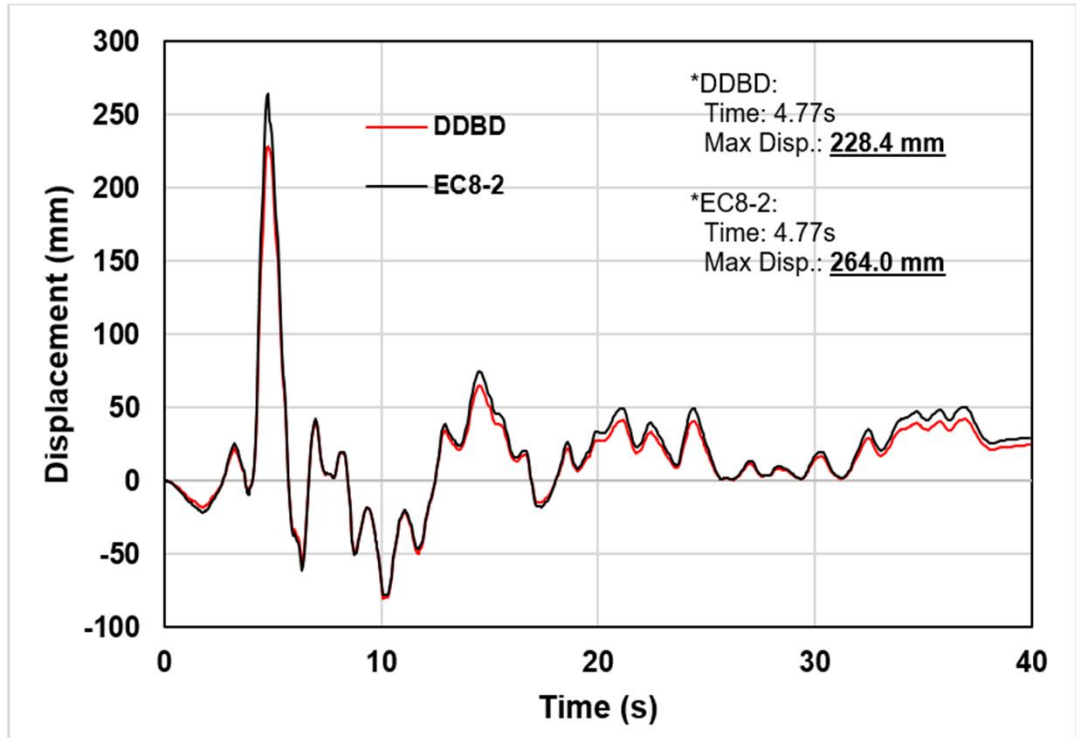
(d)
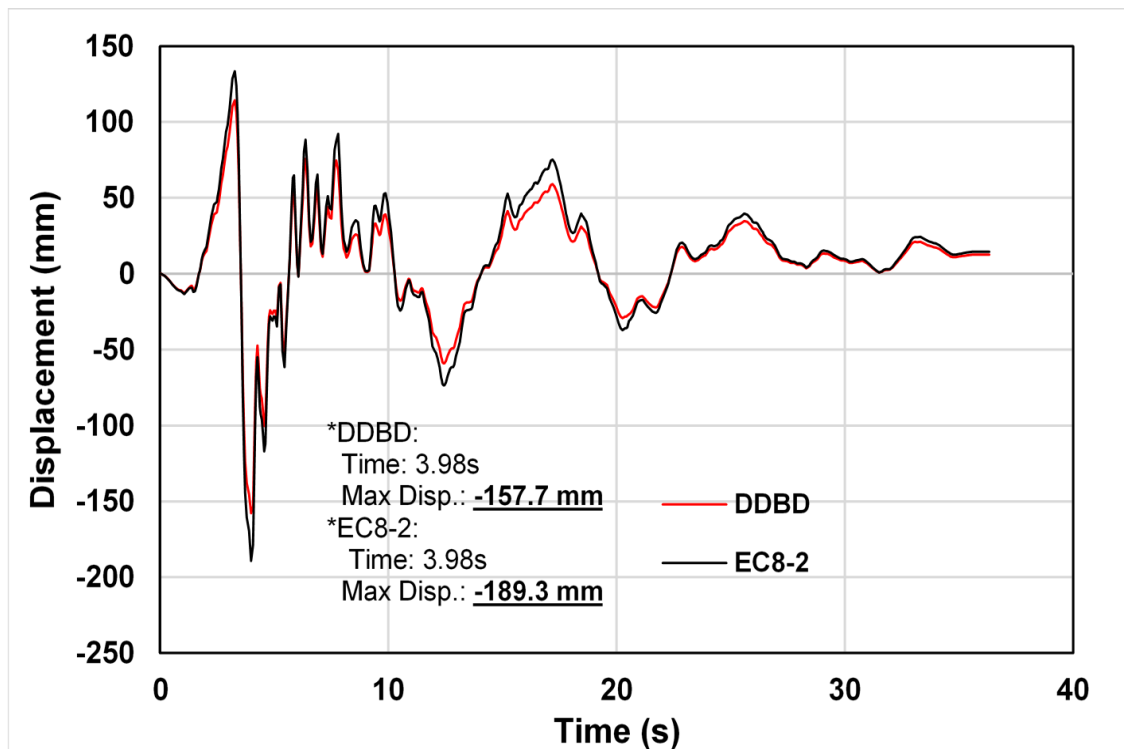
(e)

Figure 6.10 The displacement-time responses of DDBD and EC8-2 RC bridge; (a) S1; (b) S2; (c) S3; (d) S4; and (e) S5 earthquakes

148

DDBD
Maximum
displacement:
-223.8mm

EC8-2
Maximum
displacement:
-273.2mm
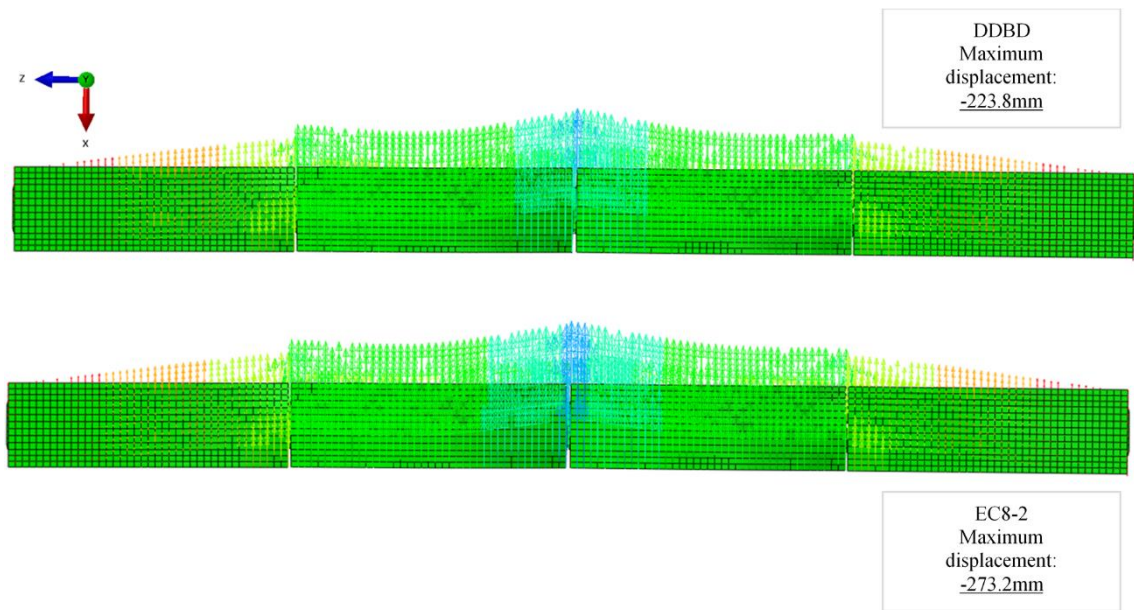
(a) Transverse displacement profile at maximum displacement for both RC bridge at 29.19 s of S1 earthquake

DDBD
Maximum
displacement:
-179.6 mm

EC8-2
Maximum
displacement:
211.1 mm
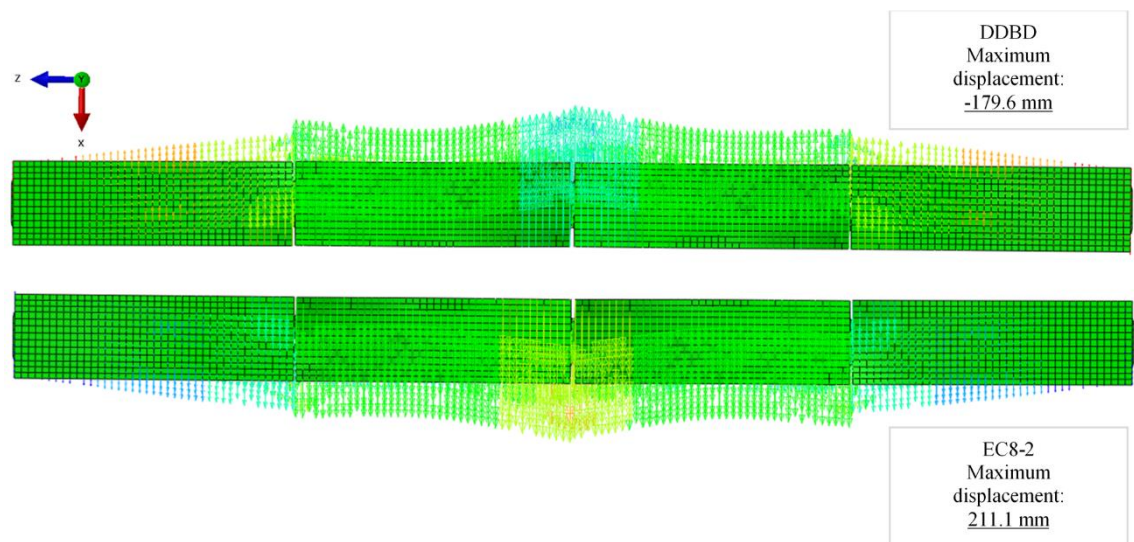
(b) Transverse displacement profile at maximum displacement for both RC bridge of S2 earthquake: DDBD at 15.72 s and EC8-2 at 9.37 s
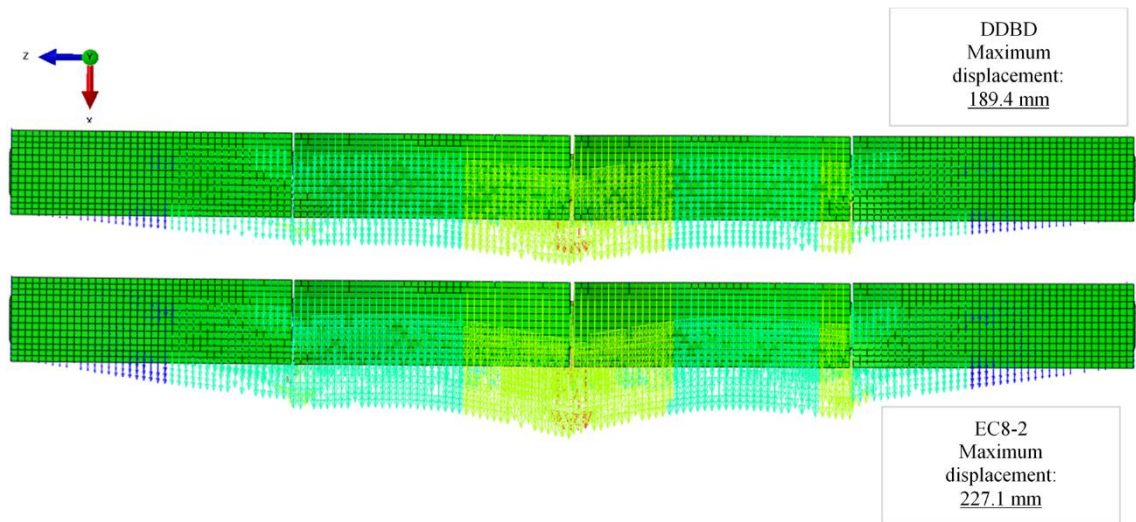
(c) Transverse displacement profile at maximum displacement for both RC bridge at 11.39 s of S3 earthquake
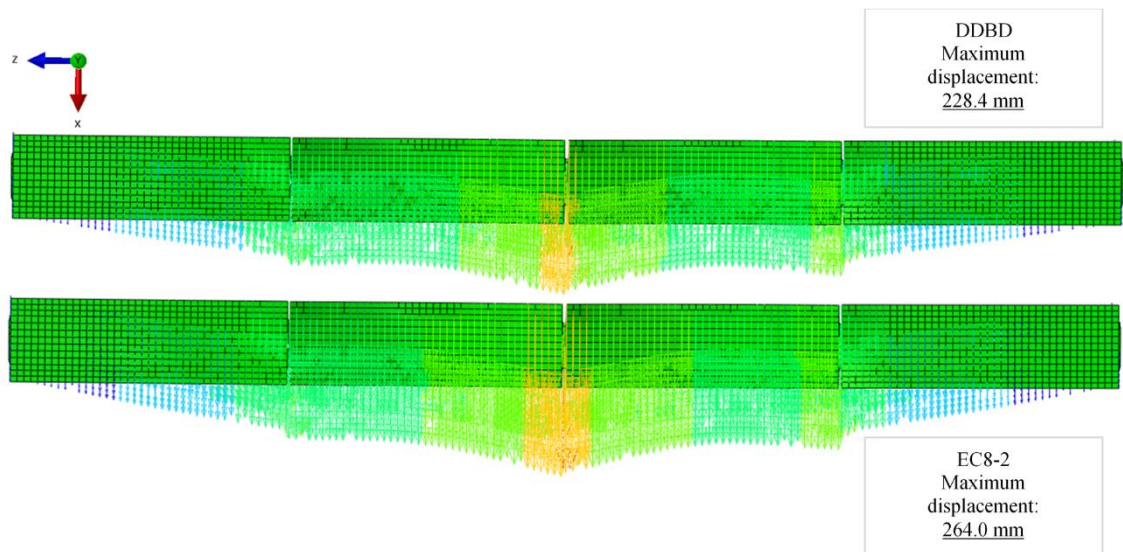
(d) Transverse displacement profile at maximum displacement for both RC bridge at 4.77 s of S4 earthquake
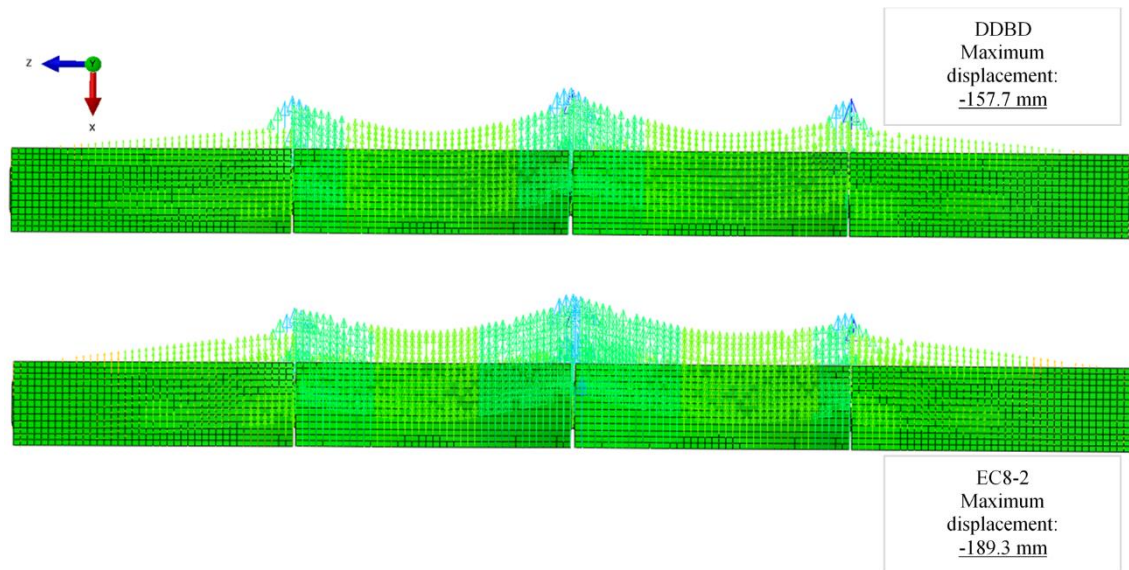
(e) Transverse displacement profile at maximum displacement both RC bridge at 3.98 s of S5 earthquake

Figure 6.11 Transverse displacement profile at maximum displacement of the DDBD and EC8-2 RC bridge; (a) S1; (b) S2; (c) S3; (d) S4; and (e) S5 earthquakes

6.5.2 Damage state level and progression

The damage progression associated with maximum displacement was investigated and compared for both RC bridge, presented in this section. Figure 6.12 shows the comparison damage index and state, and Figure 6.13 shows the comparison damage progression of the RC bridge pier design using DDBD and EC8-2. The outcomes for damage state and progression are from NLTH-FE results. Table 6.3 was used to provide details description for damage associated with the damage index, state, and progression, as shown in Figures 6.12 and 6.13. In Figure 6.12, the concrete damage progression was expressed by concrete strain distribution along pier height and can be represented as the distribution of longitudinal concrete strain (LE, LE22) (Babazadeh *et al.*, 2015).

Figure 6.12(a) shows the damage progression response for the Chi-Chi earthquake (S1). As observed from the figure, based on NLTH-FE results, the first cracking of concrete cover occurs when the displacement was approximately -19.3 mm for the DDBD bridge and -16.2 mm for the EC8-2 bridge, and the first longitudinal bar yielded at a displacement of 22.5 mm for the DDBD bridge and 19.5 mm for the EC8-2 bridge after 22.6 s. The damage indices of the RC bridge pier for the DDBD and EC8-2 bridges at these damage levels were 0.10. As suggested in Table 6.3, 0.10 indicates that first

151

cracking occurs on the concrete cover. At this stage, both RC bridge design using DDBD and EC8-2 methods experience similar damage. As the loading continues, the onset spalling of the concrete cover was observed in the EC8-2 bridge after 24.2 s, while the DDBD bridge was observed similar damage approximately at 25.6 s. The damage indices at this stage for the DDBD and EC8-2 bridges were 0.28 and 0.32, respectively. When the maximum displacement takes place around 29.19 s, the EC8-2 bridge suffers more damage than the DDBD bridge. This indicates that significant spalling and extended cracks occurred. The damage indices at this stage for the DDBD and EC8-2 bridges were 0.45 and 0.50, respectively, and the RC bridge was in the major damage state. As observed, at the final state of the damage states, the circular RC bridge design using EC8-2 method suffers more damage than DDBD method. The corresponding damage index for the DDBD and EC8-2 bridges were 0.53 and 0.57, respectively. At this stage, the concrete strain is 0.0242 for the DDBD bridge and 0.0259 for the EC8-2 bridge. The reinforcement tensile recorded at the final stage of damage was 0.0291 for the DDBD bridge and 0.0322 for the EC8-2 bridge. Figure 6.13(a) shows the damage progression distribution indicates the final concrete damage of the circular RC bridge (Pier 2).

Figure 6.12(b) shows the damage progression response for Imperial Valley (S2) earthquake. The damage indices for the first cracking of concrete cover for the DDBD and EC8-2 bridges were approximately 0.10 and 0.11, respectively. The yielding of the longitudinal bar was at 0.17 for both bridges. The circular RC bridge pier was experiencing a slight damage state. Onset spalling of concrete cover occurred at 9.37 s when the displacement of the circular RC bridge pier was at a peak for the EC8-2 bridge. The corresponding damage index for EC8-2 bridges was 0.25, indicating that the spalling of the concrete cover occurred. However, at a similar time, DDBD bridges damage index is 0.19. At this stage, RC bridges for DDBD and EC8-2 suffered minor and moderate damage, respectively. When the displacement of the circular RC bridge pier reached -179.6 mm at 15.72 s for the DDBD bridge, the damage index was 0.35, while the EC8-2 bridge at a similar time was approximately 0.46. At this stage, the RC bridge designed according to EC8-2 suffers major damage, while the RC bridge designed using DDBD were experienced moderate damage, as shown in Figure 6.13(b). It is indicated that the DDBD bridge is still repairable compared to the EC8-2 bridge. The concrete compression strains at this stage for the DDBD and EC8-2 bridges were 0.0160 and 0.0212,

respectively. While the reinforcement tensile strains at this stage for the DDBD and EC8-2 bridges were 0.0184 and 0.0241, respectively.

The damage progression response of the Kobe (S3) earthquake is shown in Figure 6.12(c). In the S3 earthquakes NLTH-FE results, the first concrete cracking initiated at a displacement approximately 24 mm. As observed in Figure 6.12(c), the damage index corresponding with the first cracking for the DDBD and EC8-2 bridges were 0.10 and 0.11, respectively. When the RC bridges reached 9.76 s, maximum displacement occurred for both bridges. In this stage, the RC bridge designed using EC8-2 suffers major damage, where the significant spalling of concrete cover occurred and, the corresponding damage index was 0.54. With respect to Figure 6.12(c), the damage index calculated for the RC bridge designed using DDBD at the maximum displacement was 0.37, where the onset spalling of concrete cover occurred. It can be concluded that the DDBD bridge suffers moderate damage, where repair is applicable, while the EC8-2 bridge suffers major damage. The concrete compression strains at this stage for the DDBD and EC8-2 bridges was 0.0156 and 0.0251, respectively. While the reinforcement tensile strains at this stage for the DDBD and EC8-2 bridges were 0.0188 and 0.0298, respectively. This damage index also indicates that the RC bridge designed using the DDBD method was capable of withstanding this type of earthquake. Figure 6.13(c) shows the concrete damage state occurred on both the circular RC bridge pier (Pier 2).

In Loma Prieta (S4) NLTH-FE results, the first cracking of concrete initiated at the displacement of 21 mm and 24 mm for the DDBD and EC8-2 bridges, respectively. As observed in the damage progression response (S4), as shown in Figure 6.12(d), the damage index of both bridges corresponding to the first cracking state was 0.11 at 4.64 s for the DDBD bridge and 0.15 at 4.43 s for the EC8-2 bridge. As can be seen, the RC bridge designed using EC8-2 was started to suffer slight damage (first cracking) early than the DDBD bridge. As the circular RC bridge pier reached the maximum displacement for the EC8-2 bridge at 4.77 s, the bar buckling and core concrete crushing occurred, and the corresponding damage index was 0.64. This damage index indicates that the circular RC bridge designed using EC8-2 suffers local failure (collapse). Within the same time period, circular RC bridge designed using DDBD where suffers significant spalling of concrete cover, with the value of the damage index was 0.56, at the maximum displacement of 228.4 mm. At this stage, the DDBD bridge suffers major damage. The concrete compression strains at this stage for the DDBD and EC8-2 bridges were 0.0251

and 0.0291, respectively. While the reinforcement tensile strains at this stage for the DDBD and EC8-2 bridges were 0.0327 and 0.0491, respectively. This damage can be further described in Figure 6.13(d), where the concrete damage progression was highlighted for both RC bridges.

The damage progression response of the Friuli (S5) earthquake is shown in Figure 6.12(e). The first damage state occurred when displacement at 64 mm and 75 mm at 2.75s for the DDBD and EC8-2 bridges, respectively. At this stage, no damage was observed. When the maximum displacement occurred for both RC bridges, the damage indices were 0.09 and 0.11 for the DDBD and EC8-2 bridges, respectively. The damage indices indicate that the onset spalling of concrete cover occurred. At the final stage, the corresponding damage indices were 0.10 and 0.12 for the DDBD and EC8-2 bridges. This damage index indicates that both RC bridges suffer moderate damage. The concrete compression strains at this stage for the DDBD and EC8-2 bridges were 0.0025 and 0.0028, respectively. While the reinforcement tensile strains at this stage for the DDBD and EC8-2 bridges were 0.0101 and 0.0109, respectively. This damage can be further described in Figure 6.13(e), where the concrete damage progression for both circular RC bridges faced an approximately similar pattern of damage. Therefore, based on Figures. 6.12(e) and 6.13(e), it can be concluded that the DDBD bridge was experienced less damage than the EC8-2 bridge. However, both bridges are repairable.

(a)

(b)

(c)

155
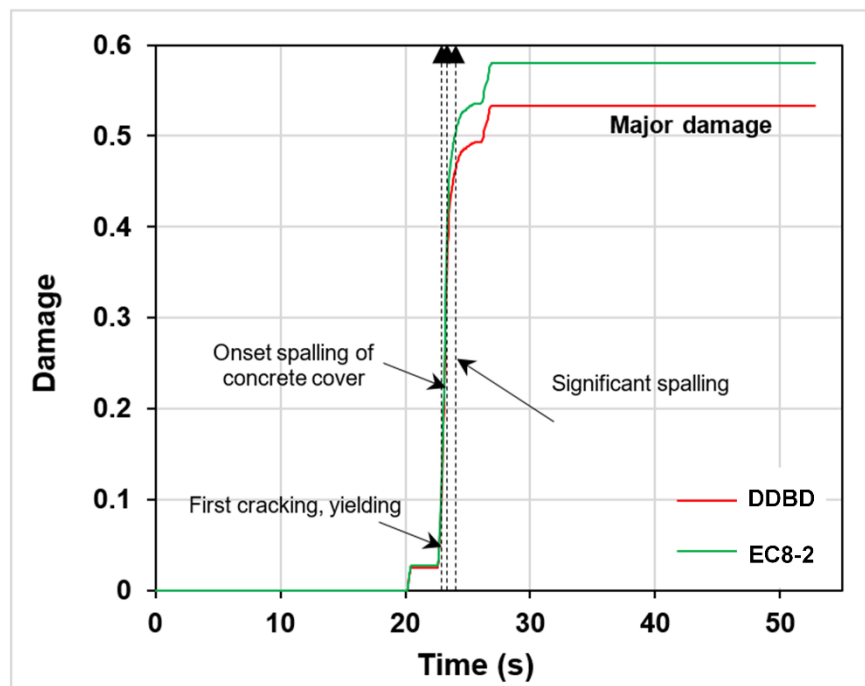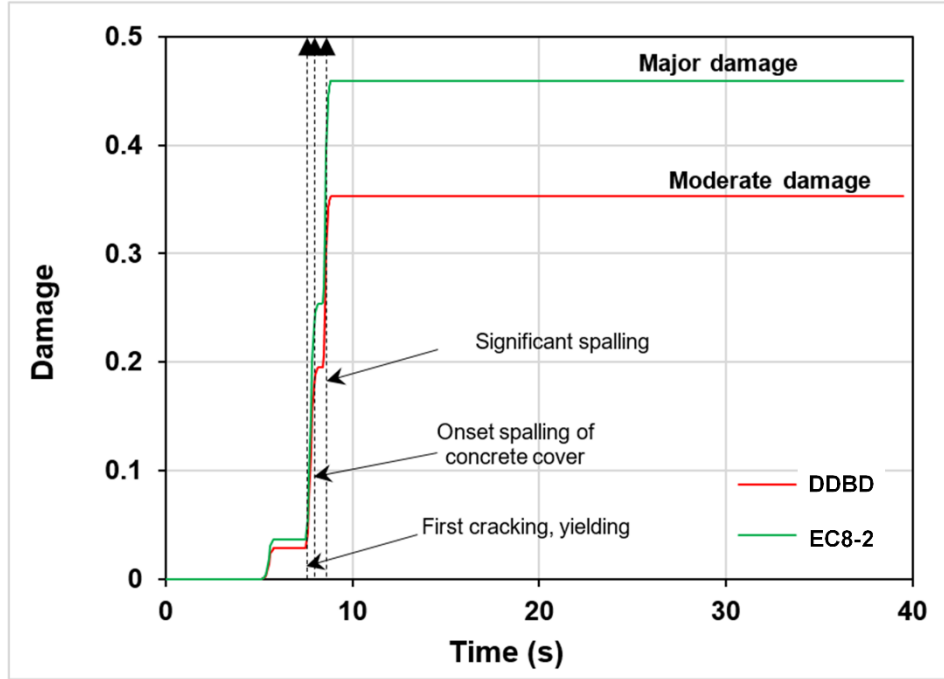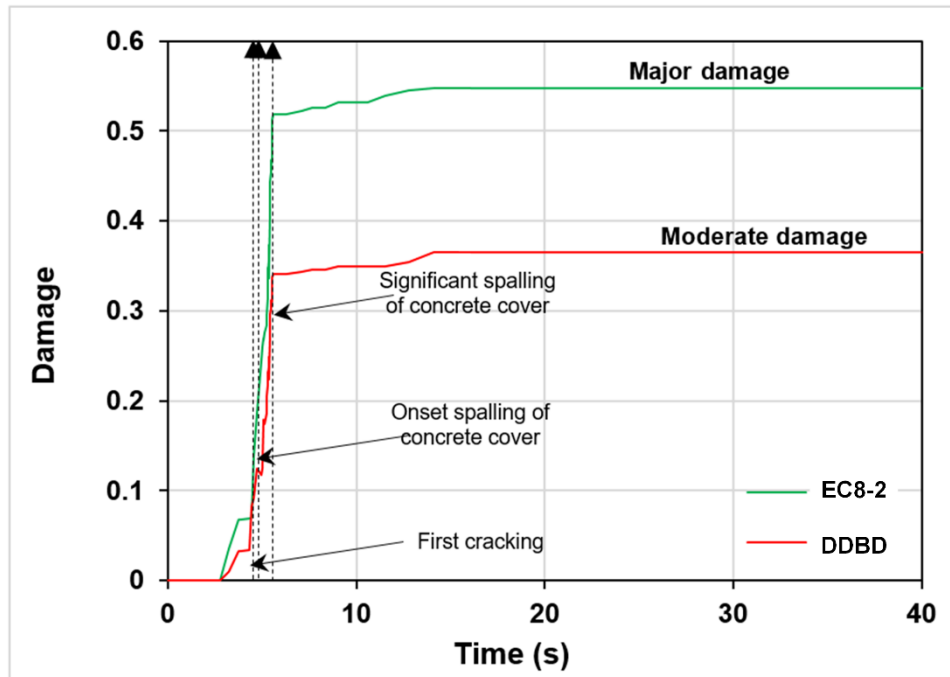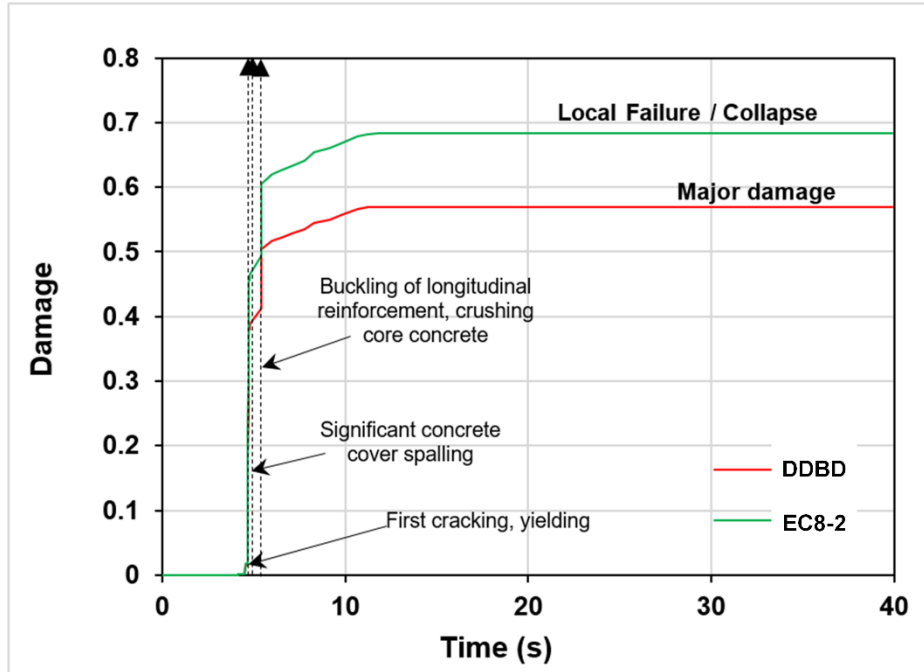
(d)
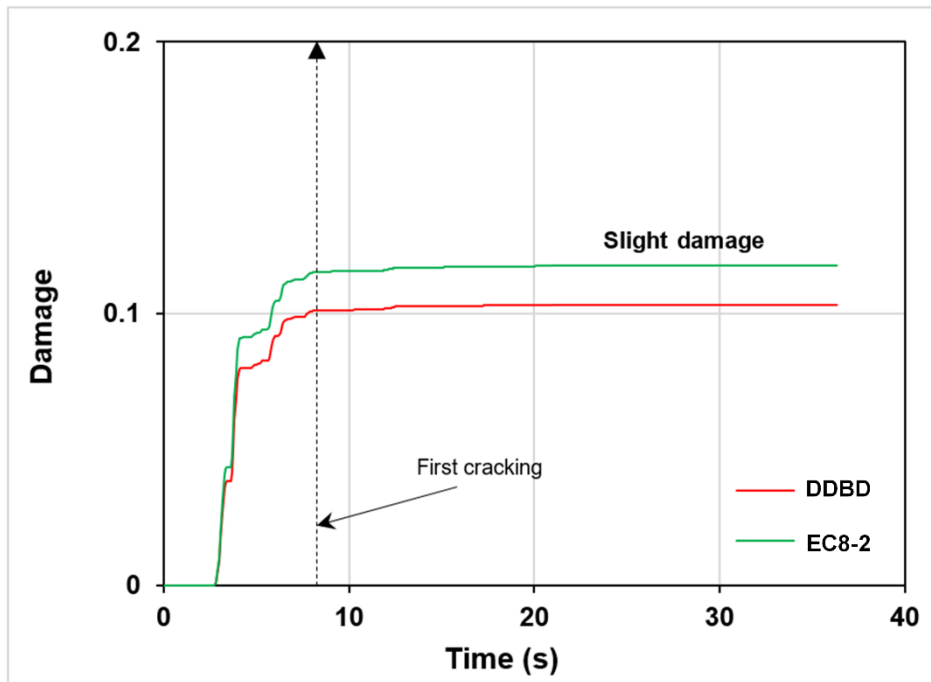
(e)

Figure 6.12 Damage state for the DDBD and EC8-2 RC bridges: (a) S1; (b) S2; (c) S3; (d) S4; and (e) S5 earthquakes

(a)

(b)

(c)

(d)

158

(e)
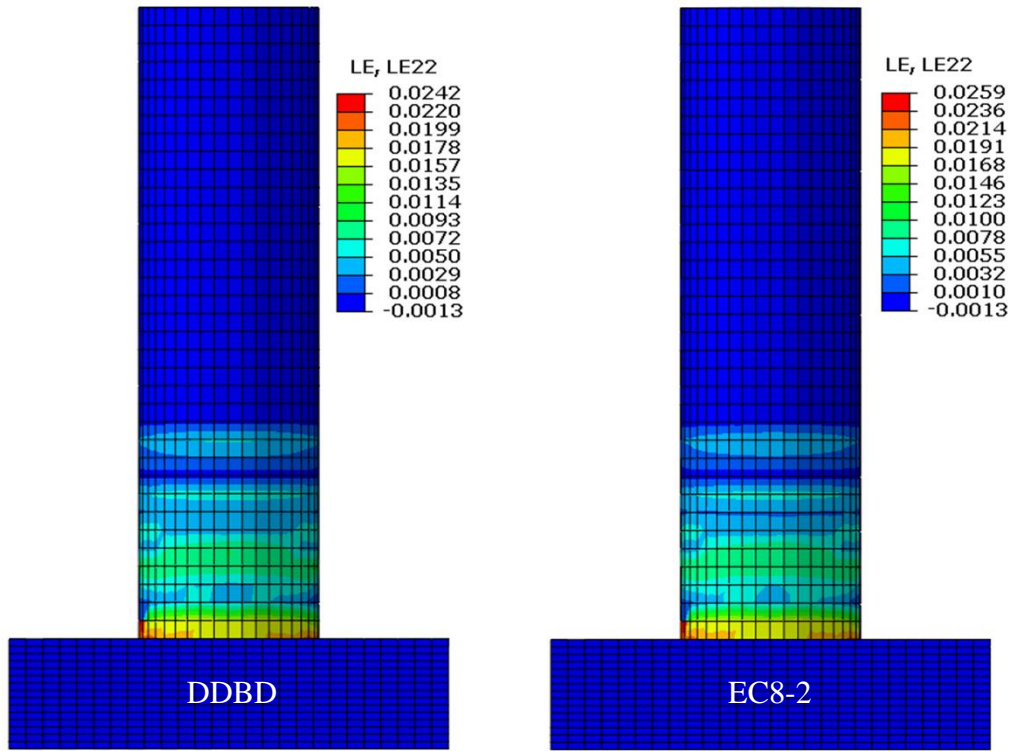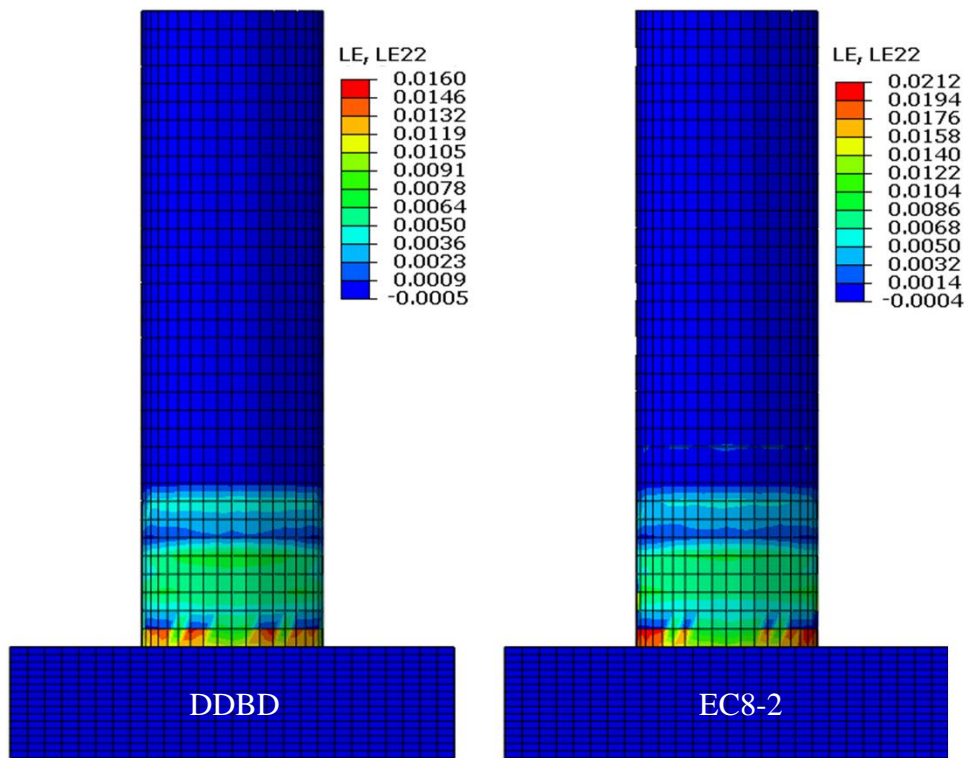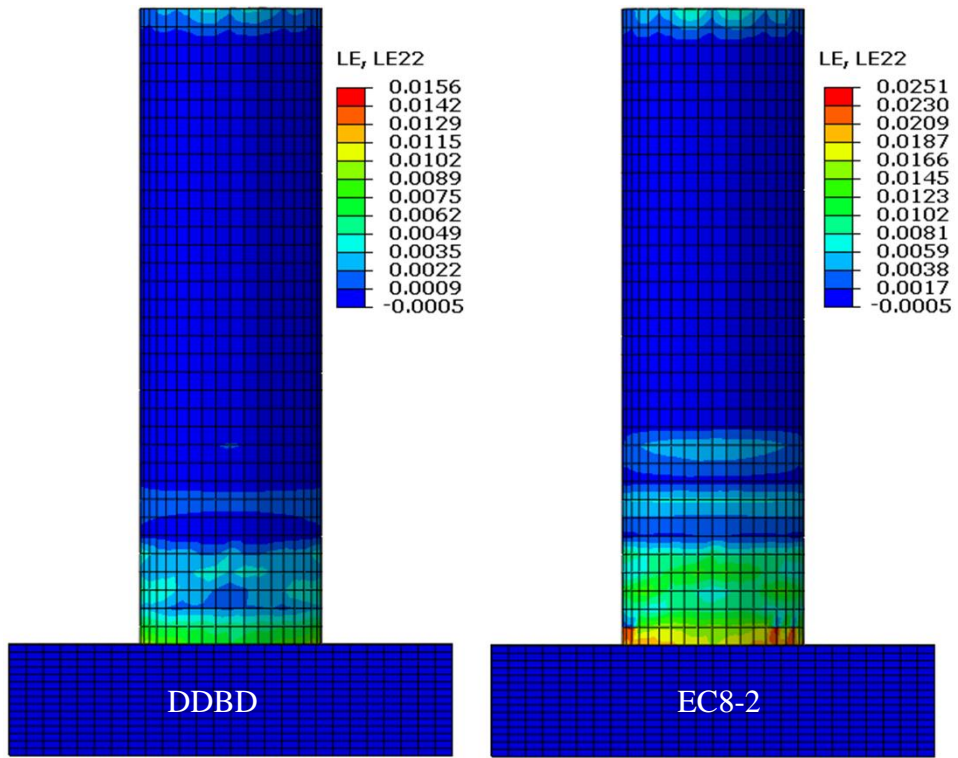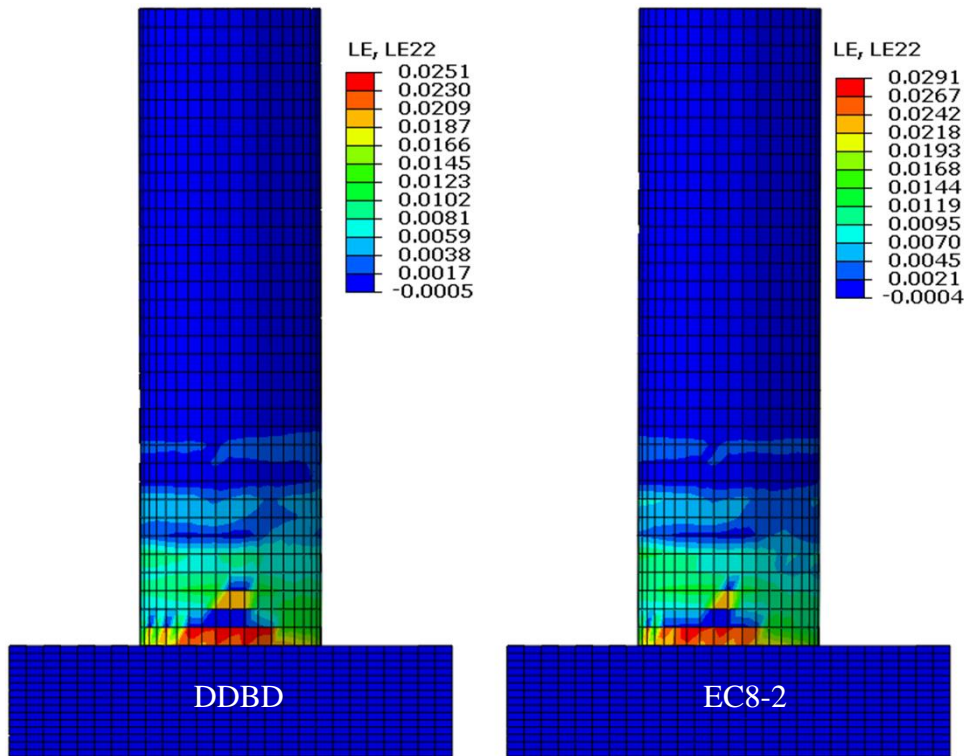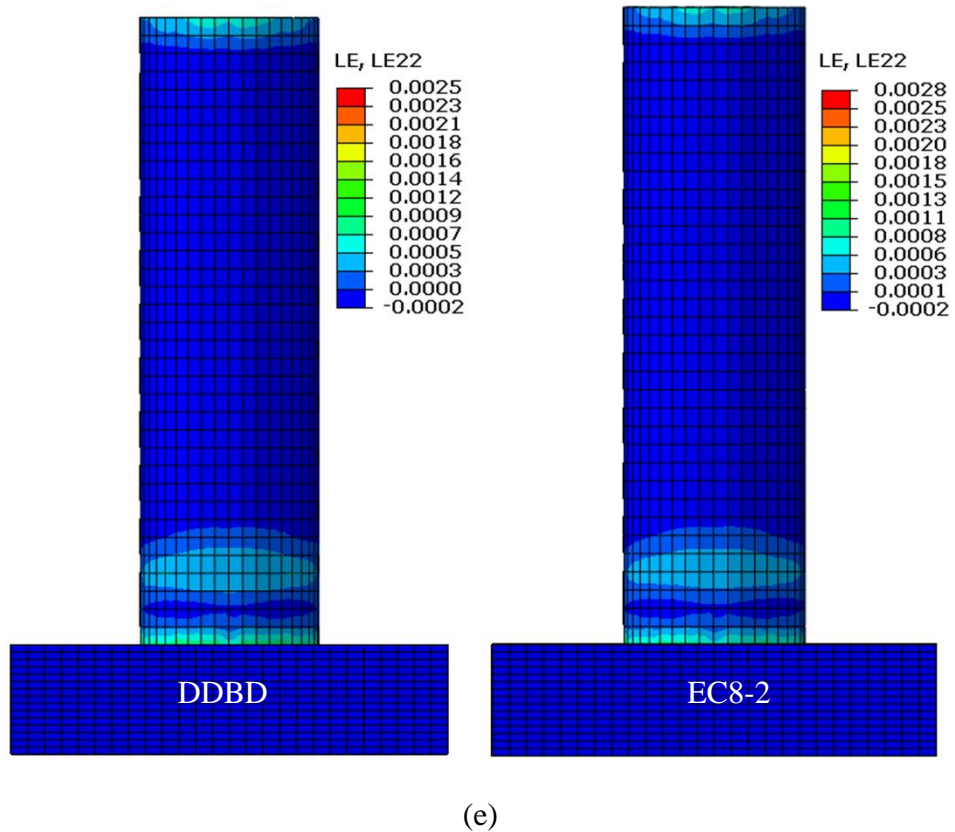
Figure 6.13 Concrete damage progression distribution of the DDBD and EC8 bridges (Pier 2): (a) S1; (b) S2; (c) S3; (d) S4; and (e) S5 earthquakes

6.6 Discussion and recommendation for the EC8-2 and DDBD design methods

The NLTH-FE results of the EC8-2 and DDBD bridges were discussed in the above sections. It is evident that the EC8-2 bridge suffered higher maximum displacement and more significant damages compared to the DDBD bridge under different earthquakes. This reveals some weaknesses of the current EC8-2 design method. In the EC8-2 design method, the RC bridge is designed based on seismic forces rather than to achieve specific target displacement, as proposed in the DDBD design method. Also, the bridge is designed based on initial stiffness, and the initial stiffness of the bridge piers was calculated based on an assumed effective moment of inertia and pier height without taking any considerations of the strain penetration length at the base of the piers. Another issue for EC8-2 design method is the utilisation seismic behaviour factor in determining spectral acceleration. As highlighted in Eqn. (6.4), the seismic behaviour factor will reduce original seismic action in the horizontal direction. Therefore, the estimation of the total seismic shear force is relatively lower. Hence, the individual seismic shear force and

the seismic moment demand of each RC bridge pier are relatively lower. This resulting in the longitudinal reinforcement ratio provided based on the EC8-2 design method is relatively lower compared to the DDBD design method.

Another issue for EC8-2 design method is that a minimum longitudinal reinforcement ratio is not directly specified in the method. Due to insufficient longitudinal reinforcement ratio of the RC bridge piers, the bridge designed using EC8-2 method will suffer severe damage and higher maximum displacement compared to the RC bridge designed according to the DDBD method. Also, EC8-2 bridge was designed based on serviceability limit states, as highlighted in Clause 2.2.3 EC8-1. The bridge should remain operational, even though some parts may suffer minimal damage. The damage might occur due to the bridge experiences higher maximum displacement, which is resulted from insufficient longitudinal reinforcement ratio.

For the DDBD method, it is suggested that to restrain the structures from extensive damage, the damage-control limit state is required. If beyond the damage-control limit state, the repair of the RC bridge pier is no longer cost-effective. In this research, the DDBD bridge was designed to achieve a damage-control limit state, where all RC bridge piers governed the yield and target displacement of the bridge. Thus, the longitudinal reinforcement provided for all piers will be in the same ratio. However, reflecting from Section 6.5, under S1 and S4 earthquakes, the maximum displacements of the DDBD bridge were exceeded the damage-control target displacement. Therefore, the improvement of the DDBD method should be considered.

Therefore, based on the results generated from this research, the following recommendations are proposed for improving EC8 and DDBD design methods:

1) For EC8-2 design method, it is suggested that the secant stiffness of the bridge pier needs to be considered for estimating the stiffness of the RC bridge. By considering secant stiffness, the maximum target displacement can be determined; thus, the equal RC bridge moment demand is provided. Also, it is suggested that the seismic behaviour factor should not be considered, which will reduce the stiffness and the total seismic shear force of the bridge pier. Therefore, by considering these two factors, a reasonable longitudinal reinforcement ratio can be provided for all RC bridge piers.

2) Implementation more refined limit states are needed for EC8-2 design method, such as the damage-control limit state. The damage-control is essential to avoid extensive damage occurred on the RC bridge structures. By considering this limit state, the RC bridge will be explicitly designed to avoid major damage. Therefore, the suitable longitudinal reinforcement provided will help to reduce the damage on the RC bridge pier, significantly.

3) The bridge designed based on the DDBD method proposed in this research was failed and suffered major damage under some more severe earthquakes. Therefore, it is suggested that the estimation of yield displacement of RC bridge pier should take into account the influence of the confining (transverse) reinforcement ratio. At present DDBD method, the yield displacement of the bridge pier is based on the yield curvature, which depends on axial load ratio, concrete strength, and longitudinal reinforcement ratio. Additionally, further research is needed in order to estimate damage-control target displacement. Adequate transverse reinforcement and transverse reinforcement strain limit in the estimation of damage-control limit states should be improved to provide better ductility and to reduce damage on the RC bridge pier.

6.7 Conclusion

In this chapter, the 3D FEM developed in Chapter 3 was used to predict the behaviours of two RC bridges designed using EC8-2 and DDBD methods. The FE modelling results were used to investigate the seismic performances of the two RC bridges under five different earthquakes. Based on the results generated in this research, some conclusions can be drawn as follows:

1) The 3D FEM developed in Chapter 3 can be used to accurately predict the behaviour of the RC bridge under different earthquake conditions. Also, the FEM results can be used to assess the different design methods.

2) Overall, the maximum displacement of the RC bridge designed according to the DDBD method is lower compared with the bridge design based on EC8-2 method. This is primarily attributed to the lower longitudinal reinforcement ratio provided from the EC8-2 design method compared to the DDBD design method. For the moderate and high intensive earthquake conditions, the bridge designed using

EC8-2 is unconservative. The RC bridge design, according to the current proposed DDBD design method, is only suitable for moderate earthquake condition.

3) It is recommended that for EC8-2 design method, the secant stiffness of the bridge pier needs to be considered for estimating the stiffness of the RC bridge. Also, the seismic behaviour factor should not be considered. More refined limit states, such as damage-control limit state, need to be introduced into the EC8-2 design method. The damage-control is essential to avoid extensive damage occurred on the RC bridge structures.

4) The bridge designed based on the DDBD method proposed in this research suffer major damage under some more severe earthquakes. Therefore, it is suggested that the influence of the confining (transverse) reinforcement ratio on the estimation of the yield displacement of RC bridge pier needs to be considered for determination of the yield displacement of the bridge pier in the future development of DDBD design method.

Chapter 7

Conclusions and Recommendations for Future Works

For many decades, considerable progress has been made in order to understand the seismic design and assessment of RC structures, particularly RC bridge. A review of the literature revealed that the current seismic design of structures in most design codes, including Eurocode 8, is based on the FBD method. Previous research indicated that the current design codes have some weaknesses, and the RC bridges designed based on those codes did not perform well in the previous earthquake events. To overcome the limitations of the FBD method, a performance-based seismic design (PBSD) method has been developed in order to prevent the structure from collapse, loss of life, and extensive economic losses. In recent years, a number of PBSD methods have been developed in order to overcome the limitations of the FBD method. Among them, the direct displacement-based design (DDBD) method is known as one of the reliable methods in the PBSD method.

A comprehensive literature review on the current seismic design and assessment of RC bridge have been presented in Chapter 2. It is clear that the yield displacement and damage-control target displacement are the key factors for the seismic design using the DDBD method. It is evident from the review that 3D FEM is an essential tool for the analysis of RC bridges with circular pier under different earthquakes conditions. Based on the comprehensive literature review, four research gaps, as presented in Chapter 1, are identified. Five objectives of this PhD research presented in Chapter 1 are also proposed to address these research gaps.

7.1 Summary of thesis contribution

7.1.1 Development of a comprehensive full-scale 3D FEM

One of the research gaps identified in the literature review is that a comprehensive 3D FEM for analysis of RC bridge with circular pier subjected to an earthquake is needed. The FEM can be used for the full-scale modelling of RC bridge and assess the earthquake resistance of RC bridge with a circular pier. Hence in this PhD research, a full-scale 3D FEM has been developed to consider full interaction between circular RC bridge pier,

deck, and steel reinforcement. The developed FEM can accurately predict the structural responses of the RC bridge with circular pier subjected to an earthquake in terms of displacement, strain, and damage. In this 3D FEM, the concrete damage plasticity (CDP) material model is considered to capture the nonlinear behaviour of concrete. A bilinear stress-strain relationship is adopted for reinforcing steel. Also, full implementation of damage parameters is considered where compressive and tensile damage parameters for unconfined and confined concrete are taken into account to accurately capture the damage of the circular RC bridge pier and bridge subjected to an earthquake.

The 3D FEM has been validated against the experimental results with good agreements between the FEM and experimental results. The developed FEM is used to validate the proposed models developed in Chapters 4 and 5, which predict the yield displacement and damage-control target displacement of the circular RC bridge pier. Also, the FEM is used to conduct a comprehensive study for assessing the behaviour of multi-span RC bridge with a circular pier (designed based on EC8-2 and DDBD methods) under different earthquake conditions (see Chapter 6).

7.1.2 Development of a new model to predict the yield displacement of RC bridge pier for the DDBD method

At present, for DDBD method, the estimation of the yield displacement of the circular RC bridge pier solely depends on the yield curvature and strain penetration of the pier. Also, the yield curvature of the pier is independent of the reinforcement and axial load contributions. The yield curvature solely depends on the yield strain of longitudinal reinforcement and the sectional diameter of the pier. Therefore, the estimation of yield displacement of circular RC bridge pier should consider the influences of concrete strength, longitudinal reinforcement ratio and axial load ratio of the pier. The research gap identified in the literature review is that there is a need to develop a new analytical model to calculate the yield displacement of circular RC bridge piers more accurately.

Hence, an analytical model has been developed for predicting the yield displacement of circular RC bridge piers for the DDBD method. The model is based on the improved yield curvature estimation by introducing new essential parameters, including concrete strength, longitudinal reinforcement ratio, and axial load ratio. Also, the model incorporates a modified plastic hinge region with equivalent curvature distribution for strain penetration length to predict the yield displacement of the RC bridge pier. A series

of RC bridge piers previously tested under cyclic loading (pushover tests) were selected to validate the proposed model. The yield displacement was estimated through the force–displacement response and was compared with the proposed model. A series of validation subjected to a seismic loading were conducted to evaluate the proposed model of yield displacement. Extensive parametric studies were conducted to evaluate the influence of several parameters on the prediction of the yield displacement of RC bridge pier.

7.1.3 Development of a new model to predict the damage-control target displacement of RC bridge pier for DDBD method

At present, for DDBD method, the damage-control target displacement of the pier was based on the design damage-control limit states, which is governed by the material's strain. However, the prediction of the reinforcement tensile strain limit for damage-control limit states is still very limited. Besides, to estimate the damage-control target displacement, it is important to have more accurate estimations of the yield displacement, strain penetration length, and the plastic hinge region. Therefore, it is needed to develop a new model to calculate the damage-control target displacement of a circular RC bridge pier for the DDBD method.

In this PhD research, a new model has been developed for predicting the damage-control target displacement of circular RC bridge piers for the DDBD method. The proposed model is based on the damage-control limit states, where new expressions are introduced in the model. Existing damage-control concrete compression strain and new expressions of damage-control reinforcement tensile strain are considered in this model, along with the modified plastic hinge length, modified strain penetration length, and yield displacement. The model improves the estimation of damage-control target displacement, mainly for the circular RC bridge pier. Also, the FEM was employed to validate the proposed model. The developed model has been validated using a series of RC bridge piers that were previously tested under cyclic loading (pushover tests). A series of validations were conducted using the RC bridge pier, which it was subjected to earthquake conditions and simulated by the validated FEM. A parametric study was conducted to evaluate the influences of concrete strength and reinforcement ratio on the prediction of damage-control target displacement of the RC bridge pier.

7.1.4 The seismic design and assessment of multi-span RC Bridge by using FE analysis

The literature review conducted in Chapter 2 indicated that a comprehensive study to assess the behaviour of multi-span RC bridge with a circular pier (designed based on EC8-2 and DDBD methods) under different earthquake conditions is needed. Therefore, the 3D FEM developed in Chapter 3 was used to predict the behaviours of two RC bridges designed using EC8-2 and DDBD methods. The FE modelling results were used to investigate the seismic performances of the two RC bridges under five different earthquakes. The results indicate that the bridge designed based on EC8-2 suffered higher maximum displacement and more significant damages compared to the bridge designed by the DDBD method under different earthquakes. This reveals some weaknesses of the current EC8-2 design method.

For the DDBD method, it is suggested that to restrain the structures from extensive damage, the damage-control limit state is required. If beyond the damage-control limit state, the repair of the RC bridge pier is no longer cost-effective. The bridge designed based on the DDBD method proposed in this research was failed and suffered major damage under some more severe earthquakes. Therefore, it is suggested that the estimation of yield displacement of RC bridge pier should take into account the influence of the confining (transverse) reinforcement ratio. Adequate transverse reinforcement and transverse reinforcement strain limit in the estimation of damage-control limit states should be improved to provide better ductility and to reduce damage on the RC bridge pier.

7.2 Conclusions

Based on the results for the validations of the developed comprehensive 3D FEM for analysis of RC bridge with circular pier subjected to earthquake and the developed models for predicting the yield displacement and damage-control target displacement of the circular RC bridge pier; the parametric studies and the assessment of the multi-span circular RC bridges under different earthquakes, the following conclusions can be drawn:

1) The developed full-scale 3D FEM with the concrete damaged plasticity model can simulate the RC bridge subjected to multiple earthquakes. The 3D FEM can capture the yield displacement, damage-control target displacement, and damage progression of the RC bridge pier under different earthquake conditions with

reasonable accuracy. The 3D FEM can be used to conduct a comprehensive study for the seismic design and assessment of multi-span RC bridge with circular pier under different earthquake conditions.

2) The model developed to predict the yield displacement of RC bridge pier for the DDBD method is robust. The values predicted by the proposed model were almost identical to the experimental results of the pushover tests. Therefore, the proposed model is able to predict the yield displacement for RC bridge piers under seismic loading condition.

3) Based on the displacement–time response results, the influences of concrete strength, axial load ratio, longitudinal reinforcement ratio, and strain penetration length on the yield displacement of the RC bridge pier are significant. The yield displacement predicted by the NLTH-FE model subjected to earthquake loadings agreed well with the proposed model's predictions.

4) Based on the results of the parametric studies, the effective pier height and sectional diameter have considerable influences on the predictions of the yield displacement. It is crucial to consider concrete strength in the estimation of yield displacement. By increasing the concrete strength, the capacity of the RC bridge pier increases, and the pier can survive more loads. The consideration of axial load ratio along with concrete strength is essential to provide an accurate yield displacement for RC bridge pier. By increasing the longitudinal reinforcement, the yield displacement increases. This is because reinforced concrete has tensile and compressive strength, therefore manage to withstand the heavy load.

5) The developed model to predict the damage-control target displacement of RC bridge pier for the DDBD method is also robust. The model can predict the damage-control target displacement of circular RC bridge piers with reasonable accuracy. The model can be used to estimate the damage-control target displacement used in the DDBD method for RC bridge piers under the lower and/or moderate magnitude of earthquakes.

6) The influence of concrete strength on the prediction of damage-control target displacement is not significant and can be ignored. However, the axial load ratio, pier height, and longitudinal and transverse reinforcement ratios have some

influences on the prediction of the damage-control target displacement for the RC bridge piers.

7) Overall, the maximum displacement of the RC bridge designed according to the DDBD method is lower compared with the bridge design based on EC8-2 method. This is primarily attributed to the lower longitudinal reinforcement ratio provided from the EC8-2 design method compared to the DDBD design method. For the moderate and high intensive earthquake conditions, the bridge designed using EC8-2 is unconservative. The RC bridge design, according to the current proposed DDBD design method, is only suitable for moderate earthquake condition.

8) It is recommended that for EC8-2 design method, the secant stiffness of the bridge pier needs to be considered for estimating the stiffness of the RC bridge. Also, the seismic behaviour factor should not be considered. More refined limit states, such as damage-control limit state, need to be introduced into the EC8-2 design method. The damage-control is essential to avoid extensive damage occurred on the RC bridge structures.

9) The bridge designed based on the DDBD method proposed in this research suffer major damage under some more severe earthquakes. Therefore, it is suggested that the influence of the confining (transverse) reinforcement ratio on the estimation of the yield displacement of RC bridge pier needs to be considered for determination of the yield displacement of the bridge pier in the future development of the DDBD design method.

7.3 Recommendations for future research

It is clear from this PhD research that there are questions to be further addressed regarding the yield displacement, damage-control target displacement, and the assessment of circular RC bridge pier and bridges for the DDBD method. In summary, it is recommended that the following areas should be considered for further works:

1) The development of FEM subjected to earthquakes is highly demanded. Therefore, to analyse circular RC bridges subjected to earthquakes, full implementation of full-scale 3D FEM requires further research. This current state of FEM can be improved, where the solid section can be modelled and implementing the damage parameters on the RC bridge deck.

2) The developed models in this research can be further extended to cover different sections of RC bridge piers such as square or rectangular RC bridge piers.

3) The developed models in this research consider axial load ratio, longitudinal reinforcement ratio, and concrete strength. However, the current proposed models can be further extended and developed to consider the transverse reinforcement ratio for predicting the yield displacement for circular RC bridge pier, subjected to seismic loading conditions.

4) Experimental data on the damage-control target displacement subjected to seismic loading are minimal. An extension of research to produce more experiments data is necessary for the validations and improvements of the new models.

5) More experiments are needed to assess the influence of longitudinal reinforcement ratio, concrete strength, and axial load ratio. The further tested data can be used to compare the results generated from the parametric studies of yield displacement and damage-control target displacement using current developed models.

6) A further numerical study is needed to assess the circular RC bridges for different configurations, such as irregular pier height subjected to multiple earthquakes. Further research is necessary to optimize the improved DDBD method for seismic design of RC bridges.

References

Abdul Halim, N. H. F., Alih, S. C. and Vafaei, M. (2018) 'Structural behavior of RC columns transversely reinforced with FRP strips', *International Journal of Civil Engineering and Technology*, 9(4), pp. 1572–1583.

Adhikari, R. K., Bhagat, S. and Wijeyewickrema, A. C. (2015) 'Damage scenario of reinforced concrete buildings in the 2015 Nepal earthquakes', *Proceeding of 14th International Symposium on New Technologies for Urban Safety of Mega Cities in Asia*. Kathmandu, Nepal.

Alhaddad, M. S., Wazira, K. M., Al-Salloum, Y. A. and Abbas, H. (2015) 'Ductility damage indices based on seismic performance of RC frames', *Soil Dynamics and Earthquake Engineering*, 77, pp. 226–237.

Aschheim, M. (2002) 'Seismic design based on the yield displacement', *Earthquake Spectra*, 18(4), pp. 581–600.

Babazadeh, A., Burgueno, R. and Silva, P. F. (2015) 'Use of 3D finite-element models for predicting intermediate damage limit states in RC bridge columns', *Journal of Structural Engineering*, 141(10), pp. 1–11.

Bardakis, V. G. and Fardis, M. N. (2011) 'A displacement-based seismic design procedure for concrete bridges having deck integral with the piers', *Bulletin of Earthquake Engineering*, 9(2), pp. 537–560.

Belarbi, A., Zhang, L. X. and Hsu, T. T. C. (1996) 'Constitutive laws of reinforced concrete membrane elements', *Proceeding of 11th World Conference on Earthquake Engineering*. Acapulco, Mexico.

Billah, A. H. M. M. and Alam, M. S. (2015) 'Seismic fragility assessment of highway bridges: a state-of-the-art review', *Structure and Infrastructure Engineering*, 11(6), pp. 804–832.

Billah, A. H. M. M. and Alam, M. S. (2016) 'Plastic hinge length of shape memory alloy (SMA) reinforced concrete bridge pier', *Engineering Structures*, 117, pp. 321–331.

Billah, A. H. M. M and Alam, M. S. (2016b) 'Performance-based seismic design of shape memory alloy–reinforced concrete bridge piers. II: methodology and design example',

Journal of Structural Engineering, 141(10), pp. 1–5.

Botero, J. C. A. (2004) *Displacement-based design of continuous concrete bridges under transverse seismic excitation*. M.Sc. Thesis, Universita degli Studi di Pavia.

Broglio, S., Crowley, H. and Pinho, R. (2010) 'Simplified capacity curves for RC bridges', *Proceeding of 14th European Conference on Earthquake Engineering (14ECEE)*. Ohrid, Macedonia.

Calvi, G. M., Pinho, R., Magenes, G., Bommer, J. J., Retsrepo-Velez, L. F. and Crowley, H. (2006) 'Development of seismic vulnerability assessment methodologies over the past 30 years', *ISET Journal of Earthquake Technology*, 43(3), pp. 75–104.

Calvi, G. M., Priestley, M. J. N. and Kowalsky, M. J. (2008) 'Displacement–based seismic design of structures', *Proceeding of 3rd Greek Conference on Earthquake Engineering and Engineering Seismology*. Athens, Greece.

Calvi, G. M., Priestley, M. J. N. and Kowalsky, M. J. (2013) 'Displacement-based seismic design of bridges', *Structural Engineering International: Journal of the International Association for Bridge and Structural Engineering (IABSE)*, 23(2), pp. 112–121.

Calvi, G. M. and Kingsley, G. R. (1995) 'Displacement based seismic design of multi-degree-of-freedom bridge structures', *Earthquake Engineering & Structural Dynamics*, 24(9), pp. 1247–1266.

Calvi, G. M. and Sullivan, T. (2009) 'Development of a model code for direct displacement based design', *The state of Earthquake Engineering Research in Italy: the ReLUIS-DPC 2005-2008 Project*, pp. 141–171.

Cao, V. V., Ronagh, H. R., Ashraf, M. and Baji, H. (2014) 'A new damage index for reinforced concrete structures', *Earthquake and Structures*, 6(6), pp. 581–609.

Cardone, D., Dolce, M. and Palermo, G. (2008) 'Force-based vs. direct displacement-based design of buildings with seismic isolation', *Proceeding of 14th World Conference on Earthquake Engineering (14WCEE)*. Beijing, China.

Cashell, K. A., Elghazouli, A. Y. and Izzudin, B. A. (2010) 'Experimental and analytical assessment of ductility in lightly reinforced concrete members', *Engineering Structures*, 32(9), pp. 2729–2743.

CEN (2004a) *Eurocode 2: Design of concrete structures - Part 1-1 : General rules and*

rules for buildings, *European Committee for Standardization*.

CEN (2004b) *Eurocode 8: Design of structures for earthquake resistance - part 1: General rules, seismic actions and rules for buildings (EN1998-1)*, *European Committee for Standardization*. Brussels.

CEN (2004c) *Eurocode 8 - Design of structures for earthquake resistance - Part 2: Bridges (EN1998-2)*, *European Committee for Standardization.* Brussels.

CEN (2008) *Eurocode 2: Design of concrete structures - Part 1-1 : General rules and rules for buildings*, *European Committee for Standardization.* Brussels.

Chopra, A. K. and Goel, R. K. (2001) 'Direct displacement-based design: use of inelastic vs. elastic design spectra', *Earthquake Spectra*, 17(1), pp. 47–64.

Darwash, H. (2017) *Effect of load path and failure modes on seismic response of regular bridges*. Ph.D. Thesis, University of Central Florida.

Davi, D. (2015) 'Seismic analysis and design of bridges according to EC8-2 : comparison of different analysis methods on a theoretical case-study', *Proceeding of SECED 2015 Conference: Earthquake Risk and Engineering towards a Resilient World*. Cambridge, UK.

Dwairi, H. and Kowalsky, M. (2006) 'Implementation of inelastic displacement patterns in direct displacement-based design of continuous bridge structures', *Earthquake Spectra*, 22(3), pp. 631–662.

Dwairi, H. M. (2004) *Equivalent damping in support of direct displacement-based design*. Ph.D. Thesis, North Carolina State University.

Dwairi, H. M. and Kowalsky, M. J. (2004) 'Inelastic displacement patterns in support of displacement-based design for multi-span bridges', *Proceeding of 13th World Conference on Earthquake Engineering (13WCEE)*. Vancouver, Canada.

EL-Attar, M. M., EL-Karmoty, H. Z. and EL-Moneim, A. A. (2016) 'The behavior of ultra-high-strength reinforced concrete columns under axial and cyclic lateral loads', *HBRC Journal*, 12(3), pp. 284–295.

Elwood, K. J. and Eberhard, M. O. (2009) 'Effective stiffness of reinforced concrete columns', *ACI Structural Journal*, 106(4), pp. 1–5.

Fardis, M. N. (2007) *Guidelines for Displacement-based Design of Buildings and*

Bridges, IUSS Press.

Fedak, L. K. (2012) *Evaluation of plastic hinge models and inelastic analysis tools for performance-based seismic design of RC bridge columns*. MSc Thesis, Michigan State University.

Fischinger, M., Fajfar, P., Dolsek, M., Zamfirescu, D. and Stratan, A. (1997) 'General methodologies for evaluating the structural performance under exceptional loadings', *Improvement of Buildings' Structural Quality by New Technologies: Proceedings of the International Seminar*, pp. 113–126.

Florides, M. M. and Cashell, K. A. (2017) 'Numerical modelling of composite floor slabs subject to large deflections', *Structures*, 9, pp. 112–122.

Ghobarah, A. (2001) 'Performance-based design in earthquake engineering: state of development', *Engineering Structures*, 23(8), pp. 878–884.

Gkatzogias, K. I. and Kappos, A. J. (2016) 'Seismic design of concrete bridges : Some key issues to be addressed during the evolution of Eurocode 8 - Part 2', in *Concrete Structures Conference*. Thessaloniki, Greece.

Goel, R. K. and Chopra, A. K. (2001) 'Improved direct displacement-based design procedure for performance-based seismic design of structures', *Structures,* 510, pp. 53–53.

Goodnight, J. C., Kowalsky, M. J. and Nau, J. M. (2013) 'Effect of load history on performance limit states of circular bridge columns', *Journal of Bridge Engineering*, 18, pp. 1383–1396.

Goodnight, J. C. (2015) *The effects of load history and design variables on performance limit states of circular bridge columns*. Ph.D. Thesis, North Carolina State University.

Goodnight, J. C., Kowalsky, M. J. and Nau, J. M. (2016a) 'Modified plastic-hinge method for circular RC bridge columns', *Journal of Structural Engineering*, 142(11), pp. 1–12.

Goodnight, J. C., Kowalsky, M. J. and Nau, J. M. (2016b) 'Strain limit states for circular RC bridge columns', *Earthquake Spectra*, 32(3), pp. 1627–1652.

Hernández-Montes, E. and Aschheim, M. (2017) 'An estimate of the yield displacement of coupled walls for seismic design', *International Journal of Concrete Structures and Materials*, 11(2), pp. 275–284.

Hernández-Montes, E. and Aschleim, M. (2003) 'Estimates of the yield curvature for design of reinforced concrete columns', *Magazine of Concrete Research*, 55(4), pp. 373–383.

Hindi, R. A. and Sexsmith, R. G. (2001) 'A proposed damage model for RC bridge columns under cyclic loading', *Earthquake Spectra*, pp. 261–290.

Hines, E. M. and Seible, F. (2002) 'Experimental spread of plasticity in reinforced concrete bridge piers', *Structural systems research project 2001/08*. University of California.

Hose, Y., Silva, P. and Seible, F. (2000) 'Development of a performance evaluation database for concrete bridge components and systems under simulated seismic loads', *Earthquake Spectra*, 16(2), pp. 413–442.

Hu, M., Han, Q., Du, X. and Liang, X. (2017) 'Seismic collapse analysis of RC highway bridges based on a simplified multiscale FE modeling approach', *Shock and Vibration*, 2017, pp. 1–19.

Hwang, H., Liu, J. B. and Chiu, Y. H. (2001) 'Seismic fragility analysis of highway bridges', *Technical Report MAEC RR-4 Project*. Tennessee, Center for Earthquake Research and Information, The University of Memphis.

Jankowiak, T. and Lodygowski, T. (2005) 'Identification of parameters of concrete damage plasticity constitutive model', *Foundations of Civil and Environmental Engineering*, 6, pp. 53–69.

Kappos, A., Gkatzogias, K. I. and Gidaris, I. G.(2011) 'An improved displacement-based seismic design methodology for bridges accounting for higher mode effects', *Proceeding of 3rd International Conference on Computational Methods in Structural Dynamics and Earthquake Engineering (COMPDYN 2011)*. Corfu, Greece.

Kappos, A. J., Gidaris, I. G. and Gkatzogias, K. I. (2012) 'Problems associated with direct displacement-based design of concrete bridges with single-column piers, and some suggested improvements', *Bulletin of Earthquake Engineering*, 10(4), pp. 1237–1266.

Kappos, A. J. (2015) 'Performance-based seismic design and assessment of bridges', in *Perspectives on European earthquake and engineering seismology*, pp. 163–205.

Kawashima, K., Takahashi, Y., Ge, H., Wu, Z. and Zhang, J. (2009) 'Reconnaissance

report on damage of bridges in 2008 Wenchuan, China, earthquake', *Journal of Earthquake Engineering*, 13(7), pp. 965–996.

Khan, E., Sullivan, T. J. and Kowalsky, M. J. (2014) 'Direct displacement-based seismic design of reinforced concrete arch bridges', *Journal of Bridge Engineering*, 19(1), pp. 44–58.

Khan, E. (2015) *Direct displacement based seismic design of continuous curved bridges.* Ph.D. Thesis, North Carolina State University.

Kim, T. -H., Lee, K. -M., Chung, Y. -S. and Shin, H. M. (2005) 'Seismic damage assessment of reinforced concrete bridge columns', *Engineering Structures*, pp. 576–592.

Kong, C. (2017) *Rapid direct displacement-based assessment approach for bridge structures.* Ph.D. Thesis, North Carolina State University.

Kowalsky, M. J., Priestley, M. J. N. and Macrae, G. A. (1995) 'Displacement-based design of RC bridge columns in seismic regions', *Earthquake Engineering & Structural Dynamics*, 24(12), pp. 1623–1643.

Kowalsky, M. J. (2000) 'Deformation limit states for circular reinforced concrete bridge columns', *Journal of Structural Engineering*, 126(8), pp. 869–878.

Kowalsky, M. J. (2002) 'A displacement-based approach for the seismic design of continuous concrete bridges', *Earthquake Engineering & Structural Dynamics*, 31, pp. 719–747.

Kunnath, S. K., EL-Bahy, A., Taylor, A. W. and Stone, W. C. (1997) *Cumulative seismic damage of reinforced concrete bridge piers*, *Technical Report NCEER 97-0006*. Buffalo, NY: US National Center for Earthquake Engineering Research.

Laulusa, A., Bauchau, O. A., Choi, J. Y., Tan, V. B. C. and Li, L. (2006) 'Evaluation of some shear deformable shell elements', *International Journal of Solids and Structures*, 43(17), pp. 5033–5054.

Lee, D. H., Choi, E. and Zi, G. (2005) 'Evaluation of earthquake deformation and performance for RC bridge piers', *Engineering Structures*, 27(10), pp. 1451–1464.

Lee, J. and Fenves, G. L. (1998) 'Plastic-damage model for cyclic loading of concrete structures', *Journal of Engineering Mechanics*, 124(8), pp. 892–900.

Lehman, D., Moehle, J., Mahin, S., Calderone, A. and Henry, L. (2004) 'Experimental

evaluation of the seismic performance of reinforced concrete bridge columns', *Journal of Structural Engineering*, 130(6), pp. 869–879.

Li, Z., Yu, C. and Yundong, S. (2017) 'Numerical failure analysis of a continuous reinforced concrete bridge under strong earthquakes using multi-scale models', *Earthquake Engineering and Engineering Vibration*, 16(2), pp. 397–413.

Liu, L., Zong, H. and Li, M. H. (2018) 'Numerical study of damage modes and assessment of circular RC pier under noncontact explosions', *Journal of Bridge Engineering*, 23(9), pp. 1-16.

Lubliner, J., Oliver, J., Oller, S. and Onate, E. (1989) 'A plastic-damage model for concrete', *International Journal of Solids and Structures*, 25(3), pp. 299–326.

Mackie, K., Suarez, V. and Kwon, O. S. (2011) 'Seismic performance assessment of concrete bridges', *Proceeding of 27th US - Japan Bridge Engineering Workshop*. Tsukuba, Japan.

Mackie, K. R., Wong, J. M. and Stojadinovic, B. (2010) 'Post-earthquake bridge repair cost and repair time estimation methodology', *Earthquake Engineering & Structural Dynamics*, 39, pp. 281–301.

Mahboubi, S. and Shiravand, M. R. (2019) 'Proposed input energy-based damage index for RC bridge piers', *Journal of Bridge Engineering*, 24(1), pp. 1–19.

Malekpour, S. and Dashti, F. (2013) 'Application of the direct displacement based design methodology for different types of RC structural systems', *International Journal of Concrete Structures and Materials*, 7(2), pp. 135–153.

Mander, J. B., Priestley, M. J. N. and Park, R. (1988) 'Theoretical stress-strain model for confined concrete', *Journal of Structural Engineering*, 114(8), pp. 1804–1826.

Massena, B., Bento, R. and Degee, H. (2012) 'Assessment of direct displacement-based seismic design of reinforced concrete frames', *Proceeding of 15th World Conference on Earthquake Engineering (15WCEE)*. Lisboa, Portugal.

Montoya, R. A. Z. (2008) *Direct displacement based design on bridges with foundation flexibility*, MSc. Thesis, Università degli Studi di Pavia.

Moyer, M. J. and Kowalsky, M. J. (2003) 'Influence of tension strain on buckling of reinforcement in concrete columns', *ACI Structural Journal*, 100(1), pp. 75–85.

176

Muljati, I., Asisi, F. and Willyanto, K. (2015) 'Performance of force based design versus direct displacement based design in predicting seismic demands of regular concrete special moment resisting frames', *Procedia Engineering*, 125, pp. 1050–1056.

Nguyen, V. B. (2006) *Numerical modelling of reinforced concrete bridge pier under artificially generated earthquake time-histories*. Ph.D. Thesis, University of Birmingham.

Paraskeva, T. S. and Kappos, A. J. (2010) 'Further development of a multimodal pushover analysis procedure for seismic assessment of bridges', *Earthquake Engineering and Structural Dynamics*, 39(2), pp. 211–222.

Parghi, A. M. (2016) *Seismic performance evaluation of circular reinforced concrete bridge piers retrofitted with fibre reinforced polymer*. Ph.D. Thesis, The University of British Columbia.

Prakash, S. S. and Belarbi, A. (2010) 'Towards damage-based design approach for RC bridge columns under combined loadings using damage index models', *Journal of Earthquake Engineering*, 14(3), pp. 363–389.

Priestley, M. J. N. (1993) 'Myths and fallacies in earthquake engineering – conflicts between design and reality', *Bulletin, NZ National Society for Earthquake Engineering*, 26(3), pp. 329–341.

Priestley, M. J. N., Seible, F. and Calvi, G. M. (1996) *Seismic design and retrofit of bridges*, *John Wiley & Sons*. New York: John Wiley & Sons.

Priestley, M. J. N., Calvi, G. M. and Kowalsky, M. J. (2007) *Displacement-based seismic design of structures*. Pavia, Italy: IUSS Press.

Priestley, M. J. N. and Kowalsky, M. J. (2000) 'Direct displacement-based seismic design of concrete buildings', *Bulletin of the New Zealand National Society for Earthquake Engineering*, 33(4), pp. 421–444.

Priestley, N. and Calvi, G. M. (2007) 'Displacement-based seismic design of bridges', *Proceeding of 1st US-Italy Seismic Bridge Workshop*. Pavia, Italy.

Restrepo, J. C. O. (2006) *Displacement-based design of continuous concrete bridges under transverse seismic excitation*. MSc Thesis, Università degli Studi di Pavia.

Reza, S. M., Alam, M. S. and Tesfamariam, S. (2014) 'Seismic performance comparison

between direct displacement-based and force-based design of a multi-span continuous reinforced concrete bridge with irregular column heights.', *Canadian Journal of Civil Engineering*, 41(5), pp. 440–449.

Saatcioglu, M. and Bingo, D. (1999) 'Circular high-strength concrete columns under simulated seismic loading', *Journal of Structural Engineering*, 125(3), pp. 272–280.

Sadan, O. B., Petrini, L. and Calvi, G. M. (2013) 'Direct displacement-based seismic assessment procedure for multi-span reinforced concrete bridges with single-column piers', *Earthquake Engineering & Structural Dynamics*, 42, pp. 1031–1051.

Safar, M. and Ghobarah, A. (2006) 'Constant ductility response spectrum based on constant yield displacement concept', *Proceeding of First European Conference on Earthquake Engineering and Seismology*. Geneva, Switzerland.

Samy Muhammad Reza (2012) *Seismic performance of multi-span RC bridges with irregular column heights*, MSc Thesis, The University of British Columbia.

Segovia, V. A. and Ruiz, S. E. (2017) 'Direct displacement-based design for buildings with hysteretic dampers, using best combinations of stiffness and strength ratios', *Journal of Earthquake Engineering*, 21, pp. 752–775.

Seismosoft (2016) *SeismoArtif - A computer program for generating artificial earthquake accelerograms matched to a specific target response spectrum*. Available at: www.seismosoft.com.

Sheikh, M. N., Tsang, H. H. and Lam, N. T. K. (2008) 'Estimation of yield curvature for direct displacement-based seismic design of RC columns', *Proceeding of Australian Earthquake Engineering Conference (AEES)*. Ballarat, Australia.

Sheikh, M. N., Tsang, H. H., McCarthy, T. J. and Lam, N. T. K. (2010) 'Yield curvature for seismic design of circular reinforced concrete columns', *Magazine of Concrete Research*, 62(10), pp. 741–748.

Shibata, A. and Sozen, M. (1976) 'Substitute structure method for seismic design in R/C', *Journal of the Structural Division*, 102(1), pp. 1–18.

Simao, M. R. (2017) *Seismic performance evaluation of reinforced concrete structures using multi-directional polygonal 3D lattice model*. Ph.D. Thesis, Kobe University.

Simulia (2016) *Abaqus Analysis User's Manual*, *Abaqus Documentation*. Providence, RI,

USA.

Sortis, A. De and Petrangeli, M. (1998) 'Seismic response by pseudodynamic tests of RC bridges designed to Eurocode 8 and Italian seismic code', *Proceeding of 11th World Conference on Earthquake Engineering (11WCEE)*. Acapulco, Mexico.

Su, J., Dhakal, R. P. and Wang, J. (2017) 'Fiber-based damage analysis of reinforced concrete bridge piers', *Soil Dynamics and Earthquake Engineering*, 96, pp. 13–34.

Suarez, V. A. (2008) *Implementation of direct displacement-based design for highway bridges*. Ph.D. Thesis, North Carolina State University.

Suarez, V. A. and Kowalsky, M. J. (2011) 'A stability-based target displacement for direct displacement-based design of bridge piers', *Journal of Earthquake Engineering*, 15(5), pp. 754–774.

Suarez, V. and Kowalsky, M. J. (2007) 'Displacement-based seismic design of drilled shaft bents with soil-structure interaction', *Journal of Earthquake Engineering*, 11(6), pp. 1010–1030.

Suarez, V. R. (2014) *Evaluation of displacement-based seismic design of reinforced concrete building frames*. Ph.D. Thesis, North Carolina State University.

Sullivan, T. J., Calvi, G. M. and Priestley, M. J. N. (2004) 'Initial stiffness versus secant stiffness in displacement based design', *Proceeding of 13th World Conference on Earthquake Engineering (13WCEE)*. Vancouver, Canada.

Sun, Z., Wang, D., Guo, X., Si, B. and Huo, Y. (2012) 'Lessons learned from the damaged Huilan interchange in the 2008 Wenchuan earthquake', *Journal of Bridge Engineering*, 17(1), pp. 15–24.

Tecchio, G. (2013) *Simplified displacement-based approaches for seismic design and vulnerability assessment of multi-span RC bridges*. Ph.D. Thesis, University of Padova.

Tecchio, G., Dona, M. and Modena, C. (2015) 'Direct displacement - based design accuracy prediction for single - column RC bridge bents', *Earthquakes and Structures,* 9(3), pp. 455–480.

Tjhin, T. N., Aschheim, M. A. and Wallace, J. W. (2004) 'Yield displacement estimates for displacement-based seismic design of ductile reinforced concrete structural wall buildings', *Proceeding of 13th World Conference on Earthquake Engineering*

(13WCEE). Vancouver, Canada.

Tjhin, T. N., Aschheim, M. A. and Wallace, J. W. (2007) 'Yield displacement-based seismic design of RC wall buildings', *Engineering Structures*, (29), pp. 2946–2959.

Wang, D. S., Ai, Q. H., Li, H. N., Si, B. J. and Sun, Z. G. (2008) 'Displacement based seismic design of RC bridge piers: method and experimental evaluation', *Proceeding of 14th World Conference of Earthquake Engineering (14WCEE)*. Beijing, China.

Wang, Z. and Padgett, J. E. (2014) 'Toward a uniform seismic risk design of reinforced concrete bridges: A displacement-based approach', *Structural Safety*, 50.

Yen, W-H. P., Chen, G., Yashinsky, M., Hashash, Y., Holub, C., Wang, K. and Guo, X. (2011) 'China earthquake reconnaissance report: performance of transportation structures during the May 12, 2008, M7.9 Wenchuan Earthquake', *FHWA-HRT-11-029*. Federal Highway Administration.

Zhang, G. and Unjoh, S. (2008) 'Inelastic seismic response analyses of reinforced concrete bridge piers with three-dimensional FE analysis method', *Proceeding of 24th US-Japan Bridge Engineering Workshop*. Minnesota, USA.

Zhang, Q., Alam, M. S., Khan, S. and Jiang, J. (2015) 'Seismic performance comparison between force-based and performance- based design of a highway bridge', *Proceeding of 11th Canadian Conference on Earthquake Engineering (11CCEE)*. Victoria, Canada.

Zhao, L., Hao, H., Bi, K. and Li, X. (2018) 'Numerical study of the seismic responses of precast segmental column bridge under spatially varying ground motions', *Journal of Bridge Engineering*, 23(12), pp. 1–18.